

AD-A103 487

NORTH CAROLINA UNIV AT CHAPEL HILL

F/G 8/3

THE GULF STREAM MEANDERS EXPERIMENT. CURRENT METER AND ATMOSPHE--ETC(U)

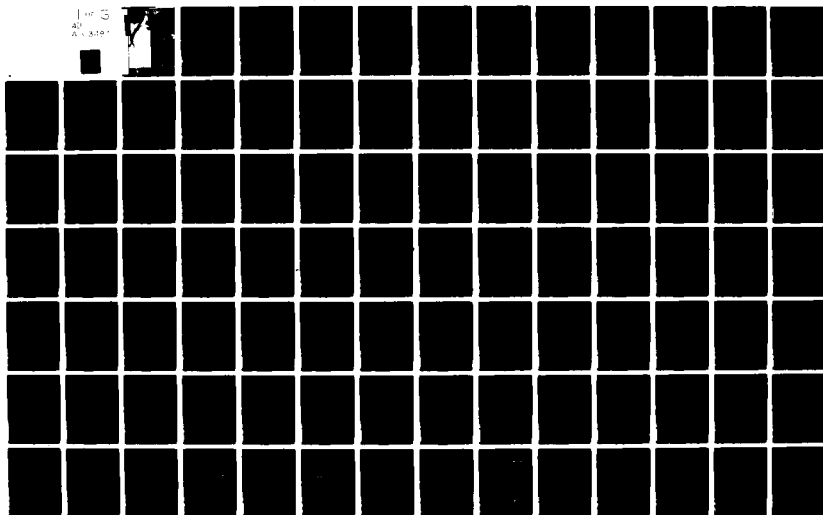
MAY 81 D A BROOKS, J M BANE, R L COHEN

N00014-77-C-0354

NL

UNCLASSIFIED

1 of 3
40
GPO 5-79



AD A103487

LEVEL

12

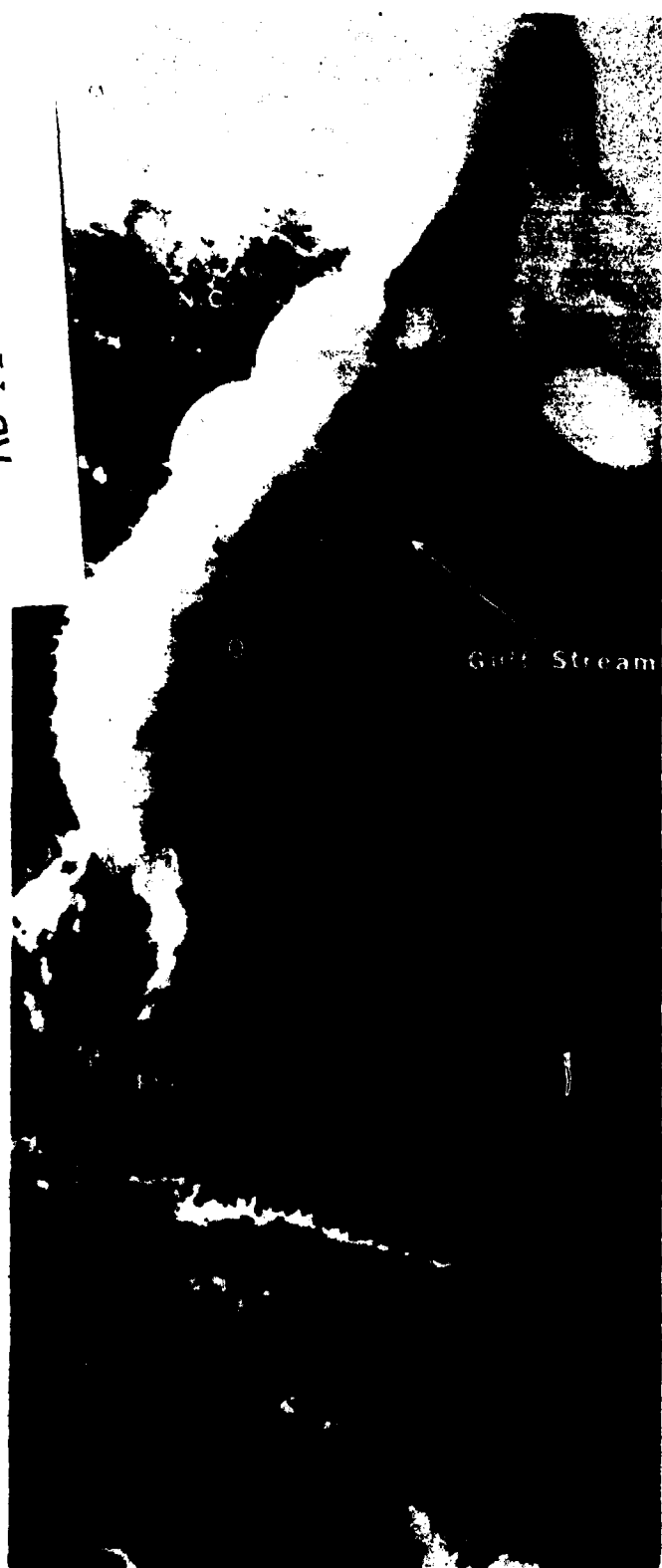
**THE GULF STREAM
MEANDERS
EXPERIMENT.**

Current Meter and Atmospheric

Data Report

for the August to November, 1979

Mooring Period



Gulf Stream

DTIC
ELECTE
AUG 26 1981

10

by

David A./Brooks

John M./Bane

Robert L./Cohen

Paul/Blankinship

H

15

12/194

NAVAL-77-C-0354 VNS
100-77-256

Texas A&M University

-Reference-81-3-T

May 1981

11

DISTRIBUTION STATEMENT A

Approved for public release;
Distribution Unlimited

81 8 26 038 259500

200

DTIC

THE GULF STREAM MEANDERS EXPERIMENT

12

Current Meter and Atmospheric
Data Report for the
August to November, 1979 Mooring Period

by

David A. Brooks

John M. Bane¹

Robert L. Cohen

Paul Blankinship²

DTIC
SELECTED
AUG 26 1981
H

Texas A&M University

Reference 81-3-T

May 1981

¹ University of North Carolina at Chapel Hill.

² North Carolina State University at Raleigh

DISTRIBUTION STATEMENT A

Approved for public release;
Distribution unlimited

FOREWORD

This is the last in a sequence of data reports from the Gulf Stream Meanders Experiment. The field phases of the experiment were implemented as a joint project of principal investigators at Texas A&M University (DAB), and at the University of North Carolina at Chapel Hill (JMB). The complete set of reports is:

1. Hydrographic Data Report, EN-031 (Jan 79) and EN-037 (May 79). TAMU Technical Report 80-1-T, January 1980, 145 pp.
2. Current Meter, Atmospheric, and Sea Level Data Report for the January to May 1979 Mooring Period. TAMU Technical Report 80-7-T, July 1980, 264 pp.
3. Hydrographic Data Report, EN-040 (Aug 79) and EN-045 (Nov 79) TAMU Technical Report 80-10-T, September 1980, 170 pp.
4. Current Meter and Atmospheric Data Report for the August to November 1979 Mooring Period. TAMU Technical Report 81-3-T, May 1981.
5. AXBT/PRT Data Report, 9-18 February 1979. UNC Technical Report CMS-80-2, December 1980, 213 pp.
6. AXBT/PRT Data Report, 21-29 November 1979 UNC Technical Report CMS-81-2, April 1981.

Accession For	
NTIS GRA&I	<input checked="checked" type="checkbox"/>
DTIC TAB	<input type="checkbox"/>
Unannounced	<input type="checkbox"/>
Justification	<i>Per</i>
<i>from SO on file</i>	
By	
Distribution/	
Availability Codes	
and/or	
Dist	Special
<i>A</i>	

Contents

	<i>page</i>
FOREWORD	ii
SECTION 1. Setting and Design of the Experiment	1
1.1. Historical Aspects	1
1.2. The Moored Instrument Array	3
1.3. Supporting Observations	9
SECTION 2. Data Sources, Processing, and Basic Statistics	10
2.1. Transcription of Aanderaa Data Tapes	10
2.2. Instrument Calibration	10
2.3. Aanderaa Data Editing	19
2.4. Ancillary Data Sources	19
2.5. Data Processing	19
2.6. Basic Statistics of the Current Meter Data Set	22
2.7. Data Presentation Formats	36
SECTION 3. Raw and 40 HRLP Data for Each Instrument	37
SECTION 4. 3-40 HRBP Data for Each Instrument	69
SECTION 5. 40 HRLP Data for Each Mooring	101
SECTION 6. 40 HRLP Current Vector "Stick" Plots for Each Mooring	118
SECTION 7. 40 HRLP Atmospheric Data from Cape Hatteras and NDBO Buoy 41002	135
SECTION 8. Comparison of 40 HRLP Wind Stress and Current Vector "Sticks"	142
SECTION 9. Spectrum Calculations for Various Combinations of 40 HRLP Data Sets	147
Acknowledgments	181
References	182

List of Tables

<i>Table</i>		<i>page</i>
1.	Instrument identification, start and stop times, depths, and mooring locations.	8
2.	Aanderaa-supplied (Aa) and calibration-produced (Cal) coefficients for the conversion of recorded binary numbers to scientific units. The general formula $V = A + BN + CN^2 + DN^3$ was used, where V is the variable, and N is decimal equivalent (0 - 1023) of the recorded binary number.	14
3.	First-order and variance statistics of temperature (T) and velocity components (u, v) from each instrument, shown from 3 HRLP, 3-40 HRLP, and 40 HRLP filtered data sets.	23
4.	Sub-band variance ratios for temperature (T) and velocity components (u, v) from each instrument. The sub-bands approximately divide the principal tidal and inertial spectrum (3-40 HRLP) for the low frequency spectrum (40 HRLP).	26

List of Figures

<i>Figure</i>		<i>page</i>
1.	Map of the South Atlantic Bight, showing the location of the Gulf Stream Meanders Experiment (inset box). Atmospheric data from moored NOAA buoys NDBO-2 and NDBO-4 and from Cape Hatteras are shown in this report.	2
2.	Cross-shelf section of the Gulf Stream off Cape Fear, showing two-month mean summer isotachs. The position of the A and B mooring current meters have been projected about 10 km upstream onto this section.	4
3.	Detailed map of the experiment area (the inset box Fig. 1), showing the locations of moorings "A" through "D," with the record-long mean current vectors at the top (T), middle (M), and bottom (B) instruments. The mooring "D" position is shown displaced (inset box) for clarity.	5
4.	Typical mooring design, showing the position of Aanderaa current meters (Aa) in the wire held taut by a large main float and a train-wheel anchor. AMF (now EG&G) sea-link acoustic releases were used.	7
5.	Calibration curves for compass direction, based on coefficients supplied by Aanderaa (-) and coefficients based on directly measured calibration data (---). The latter were used for calibration of all instruments.	15
6.	Response function for the 40 hour low pass Lanczos filter.	21
7.	Polar histogram for instrument A-top showing the normalized magnitude distribution of the 3 HRLP velocity, accumulated vectorially in ten degree sectors. The downstream (+ v) direction of the rotated coordinate system is shown by the radial tick mark.	28
8.	Polar histogram for instrument A-bot showing the normalized magnitude distribution of the 3 HRLP velocity, accumulated vectorially in ten degree sectors. The downstream (+ v) direction of the rotated coordinate system is shown by the radial tick mark.	29

9. Polar histogram for instrument B-top showing the normalized magnitude distribution of the 3 HRLP velocity, accumulated vectorially in ten degree sectors. The downstream (+ v) direction of the rotated coordinate system is shown by the radial tick mark. 30
10. Polar histogram for instrument B-bot showing the normalized magnitude distribution of the 3 HRLP velocity, accumulated vectorially in ten degree sectors. The downstream (+ v) direction of the rotated coordinate system is shown by the radial tick mark. 31
11. Polar histogram for instrument C-top showing the normalized magnitude distribution of the 3 HRLP velocity, accumulated vectorially in ten degree sectors. The downstream (+ v) direction of the rotated coordinate system is shown by the radial tick mark. 32
12. Polar histogram for instrument C-mid showing the normalized magnitude distribution of the 3 HRLP velocity, accumulated vectorially in ten degree sectors. The downstream (+ v) direction of the rotated coordinate system is shown by the radial tick mark. 33
13. Polar histogram for instrument C-bot showing the normalized magnitude distribution of the 3 HRLP velocity, accumulated vectorially in ten degree sectors. The downstream (+ v) direction of the rotated coordinate system is shown by the radial tick mark. 34
14. Polar histogram for instrument D-top showing the normalized magnitude distribution of the 3 HRLP velocity, accumulated vectorially in ten degree sectors. The downstream (+ v) direction of the rotated coordinate system is shown by the radial tick mark. 35
15. Raw and 40HRLP salinity, velocity component, and temperature data from instrument A-top. The positive (v, u) directions are (downstream, offshore). 38
16. Raw and 40HRLP salinity, velocity component, and temperature data from instrument A-bot. The positive (v, u) directions are (downstream, offshore). 42
17. Raw and 40HRLP salinity, velocity component, and temperature data from instrument B-top. The positive (v, u) directions are (downstream, offshore). 46
18. Raw and 40HRLP salinity, velocity component, and temperature data from instrument B-bot. The positive (v, u) directions are (downstream, offshore). 50

19.	Raw and 40HRLP salinity, velocity component, and temperature data from instrument C-top. The positive (v, u) directions are (downstream, offshore).	54
20.	Raw and 40HRLP salinity, velocity component, and temperature data from instrument C-mid. The positive (v, u) directions are (downstream, offshore).	58
21.	Raw and 40HRLP salinity, velocity component, and temperature data from instrument C-bot. The positive (v, u) directions are (downstream, offshore).	62
22.	Raw and 40HRLP salinity, velocity component, and temperature data from instrument D-top. The positive (v, u) directions are (downstream, offshore).	65
23.	3 to 40 HRBP salinity, velocity component, and temperature data for instrument A-top.	70
24.	3 to 40 HRBP salinity, velocity component, and temperature data for instrument A-bot.	74
25.	3 to 40 HRBP salinity, velocity component, and temperature data for instrument B-top.	78
26.	3 to 40 HRBP salinity, velocity component, and temperature data for instrument B-bot.	82
27.	3 to 40 HRBP salinity, velocity component, and temperature data for instrument C-top.	86
28.	3 to 40 HRBP salinity, velocity component, and temperature data for instrument C-mid.	90
29.	3 to 40 HRBP salinity, velocity component, and temperature data for instrument C-bot.	94
30.	3 to 40 HRBP salinity, velocity component, and temperature data for instrument D-top.	97
31.	Pressure, salinity, velocity component, and temperature data shown jointly for all instruments on the "A" mooring. All data shown are 40 HRLP filtered except for the pressure (topmost instrument only), which is unfiltered.	102
32.	Pressure, salinity, velocity component, and temperature data shown jointly for all instruments on the "B" mooring. All data shown are 40 HRLP filtered except for the pressure (topmost instrument only), which is unfiltered.	106

33.	Pressure, salinity, velocity component, and temperature data shown jointly for all instruments on the "C" mooring. All data shown are 40 HRLP filtered except for the pressure (topmost instrument only), which is unfiltered.	110
34.	Pressure, salinity, velocity component, and temperature data shown jointly for all instruments on the "D" mooring. All data shown are 40 HRLP filtered except for the pressure (topmost instrument only), which is unfiltered.	114
35.	Vector or "stick" plots of 40 HRLP currents shown jointly for all instruments on the "A" mooring. The downstream direction is toward the top of the figure.	119
36.	Vector or "stick" plots of 40 HRLP currents shown jointly for all instruments on the "B" mooring. The downstream direction is toward the top of the figure.	123
37.	Vector or "stick" plots of 40 HRLP currents shown jointly for all instruments on the "C" mooring. The downstream direction is toward the top of the figure.	127
38.	Vector or "stick" plots of 40 HRLP currents shown jointly for all instruments on the "D" mooring. The downstream direction is toward the top of the figure.	131
39.	Wind stress vectors, atmospheric pressure, and temperature at Cape Hatteras and at the NDBO-4 buoy. The NDBO sea surface temperature is also shown.	136
40.	Comparison of the NDBO wind stress vector "sticks" with the current vector "sticks" at the top instruments.	143
41.	Spectrum, phase, and coherence calculations for $E_T V$ / $C_T V$ Summer 40 HRLP	148
42.	Spectrum, phase, and coherence calculations for $B_T V$ / $D_T V$ Summer 40 HRLP	149
43.	Spectrum, phase, and coherence calculations for $B_T V$ / $B_B V$ Summer 40 HRLP	150
44.	Spectrum, phase, and coherence calculations for $B_T U$ / $B_T V$ Summer 40 HRLP	151
45.	Spectrum, phase, and coherence calculations for $A_B U$ / $B_B U$ Summer 40 HRLP	152
46.	Spectrum, phase, and coherence calculations for $C_T V$ / $D_T V$ Summer 40 HRLP	153
47.	Spectrum, phase, and coherence calculations for $C_T U$ / $D_T U$ Summer 40 HRLP	154

48.	Spectrum, phase, and coherence calculations for V-Stress _{HAT} / V-Stress _{NDBO-2} Summer 40 HRLP	155
49.	Spectrum, phase, and coherence calculations for U-Stress _{HAT} / U-Stress _{NDBO-2} Summer 40 HRLP	156
50.	Spectrum, phase, and coherence calculations for V-Stress _{NDBO-2} / V-Stress _{NDBO-4} Summer 40 HRLP	157
51.	Spectrum, phase, and coherence calculations for U-Stress _{NDBO-2} / U-Stress _{NDBO-4} Summer 40 HRLP	158
52.	Spectrum, phase, and coherence calculations for V-Stress _{HAT} / V-Stress _{NDBO-4} Summer 40 HRLP	159
53.	Spectrum, phase, and coherence calculations for U-Stress _{HAT} / U-Stress _{NDBO-4} Summer 40 HRLP	160
54.	Spectrum, phase, and coherence calculations for V-Stress _{NDBO-2} / B _T U Summer 40 HRLP	161
55.	Spectrum, phase, and coherence calculations for V-Stress _{NDBO-2} / B _T V Summer 40 HRLP	162
56.	Spectrum, phase, and coherence calculations for V-Stress _{NDBO-2} / C _T U Summer 40 HRLP	163
57.	Spectrum, phase, and coherence calculations for V-Stress _{NDBO-2} / C _T V Summer 40 HRLP	164
58.	Spectrum, phase, and coherence calculations for V-Stress _{NDBO-2} / C _M U Summer 40 HRLP	165
59.	Spectrum, phase, and coherence calculations for V-Stress _{NDBO-2} / C _M V Summer 40 HRLP	166
60.	Spectrum, phase, and coherence calculations for V-Stress _{NDBO-2} / D _T U Summer 40 HRLP	167
61.	Spectrum, phase, and coherence calculations for V-Stress _{NDBO-2} / D _T V Summer 40 HRLP	168
62.	Spectrum, phase, and coherence calculations for V-Stress _{NDBO-2} / A _B U Summer 40 HRLP	169
63.	Spectrum, phase, and coherence calculations for V-Stress _{NDBO-2} / A _B V Summer 40 HRLP	170
64.	Spectrum, phase, and coherence calculations for V-Stress _{NDBO-2} / B _B U Summer 40 HRLP	171
65.	Spectrum, phase, and coherence calculations for V-Stress _{NDBO-2} / B _B V Summer 40 HRLP	172

66.	Spectrum, phase, and coherence calculations for U-Stress _{NDBO-2} / B _T U Summer 40 HRLP	173
67.	Spectrum, phase, and coherence calculations for U-Stress _{NDBO-2} / B _T V Summer 40 HRLP	174
68.	Spectrum, phase, and coherence calculations for U-Stress _{NDBO-2} / C _T U Summer 40 HRLP	175
69.	Spectrum, phase, and coherence calculations for U-Stress _{NDBO-2} / C _T V Summer 40 HRLP	176
70.	Spectrum, phase, and coherence calculations for U-Stress _{NDBO-2} / A _B U Summer 40 HRLP	177
71.	Spectrum, phase, and coherence calculations for U-Stress _{NDBO-2} / A _B V Summer 40 HRLP	178
72.	Spectrum, phase, and coherence calculations for U-Stress _{NDBO-2} / B _B U Summer 40 HRLP	179
73.	Spectrum, phase, and coherence calculations for U-Stress _{NDBO-2} / B _B V Summer 40 HRLP	180

SECTION 1

Setting and Design of the Experiment

1.1 HISTORICAL ASPECTS

The principal objective of the Gulf Stream Meanders Experiment was to kinematically and dynamically describe the nature of meanders. The upper continental slope region off Onslow Bay, North Carolina (~~inset box, Fig. 1~~) was chosen for the experiment site because several previous investigations in that area provided a baseline data set giving some ideas about time and space variability scales within and a several-month mean view of the Stream, (Webster, 1961a, b; Richardson, *et al.*, 1969). In addition, earlier observations ranging from reports in centuries-old ship logs to recent satellite infrared imagery made it apparent that Gulf Stream meandering was more intense between Charleston, South Carolina and Cape Hatteras, North Carolina.

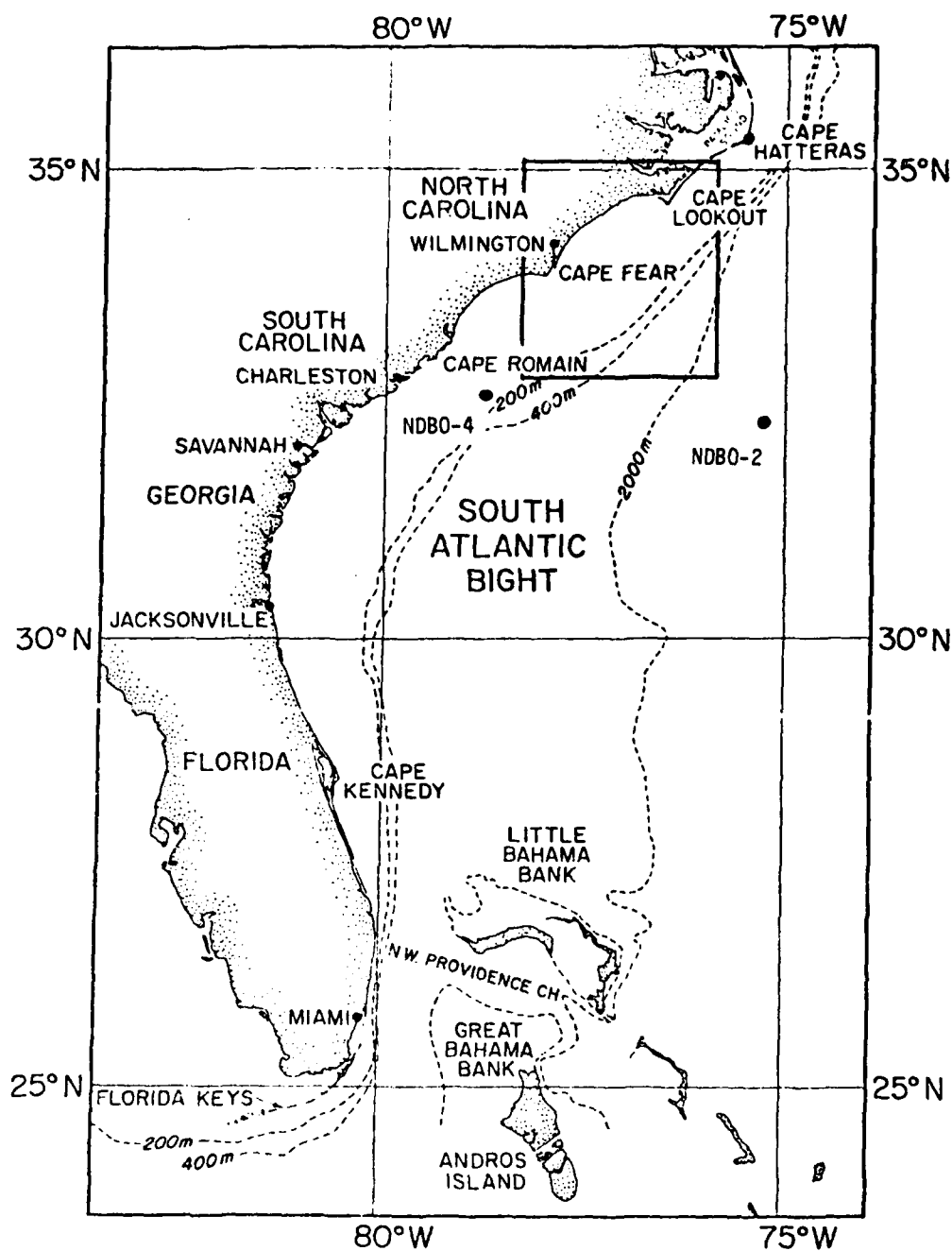


Figure 1. Map of the South Atlantic Bight, showing the location of the Gulf Stream Meanders Experiment (inset box). Atmospheric data from moored NOAA buoys NDBO-2 and NDBO-4 and from Cape Hatteras are shown in this report.

1.2 THE MOORED INSTRUMENT ARRAY

Averaged over two months, the Gulf Stream current speed on a section perpendicular to the topography off Cape Fear shows a broad, surface-intensified core (Richardson, *et al.*, 1969) extending over most of the upper continental slope (Fig. 2). Viewed on shorter time scales, however, the Stream core may be much narrower, with surface speeds considerably higher than those shown in Fig. 2. The Stream core wanders laterally over the upper slope with excursions of tens of kilometers (Webster, 1961a). Such a dynamically active region poses severe practical constraints on an experiment employing moored instruments, because the intense and highly variable current forces tend to push moorings over in the water column. Drawing on previous mooring experience in the Florida Current (Düing, 1973), we decided to deploy an L-shaped array consisting of four high-tension, subsurface moorings, each supporting two or three Aanderaa RCM-4 current meters in the lower half of the water column. The array was aligned with the local topography, with the long (75 km) leg of the "L" on the 400 m isobath. For perspective, the two moorings forming the short (15 km) leg of the "L" are shown projected about 10 km upstream onto Fig. 2. The plan view of the array is shown in Fig. 3, which is a more detailed map of the region in the inset box of Fig. 1. Mooring "D" is shown displaced for clarity. Due to instrument malfunctions, no data were recorded by meters number 3345 and 3324 which were at the D MID and D BCT positions, respectively.

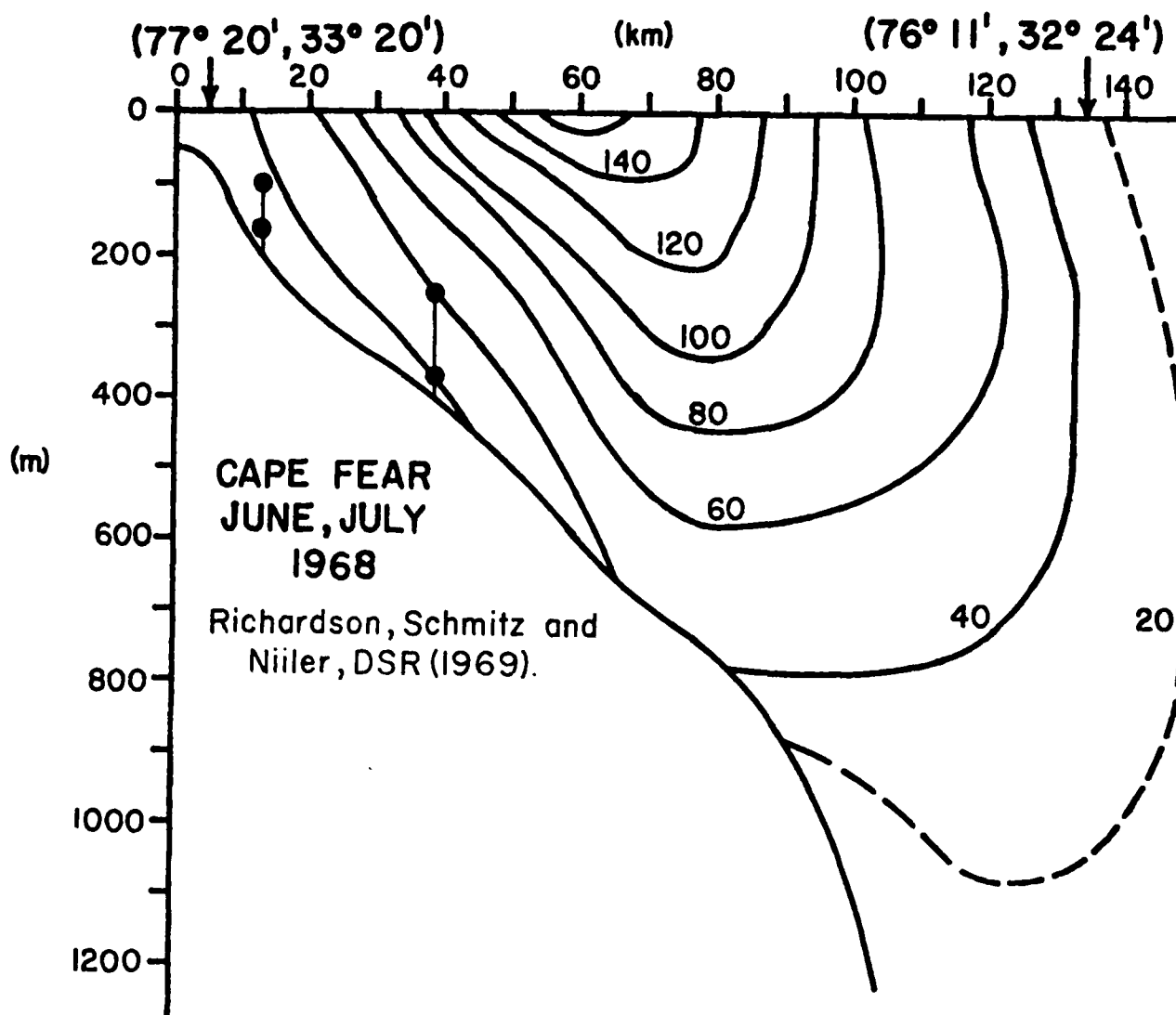


Figure 2. Cross-shelf section of the Gulf Stream off Cape Fear, showing two-month mean summer isotachs. The position of the A and B mooring current meters have been projected about 10 km upstream onto this section.

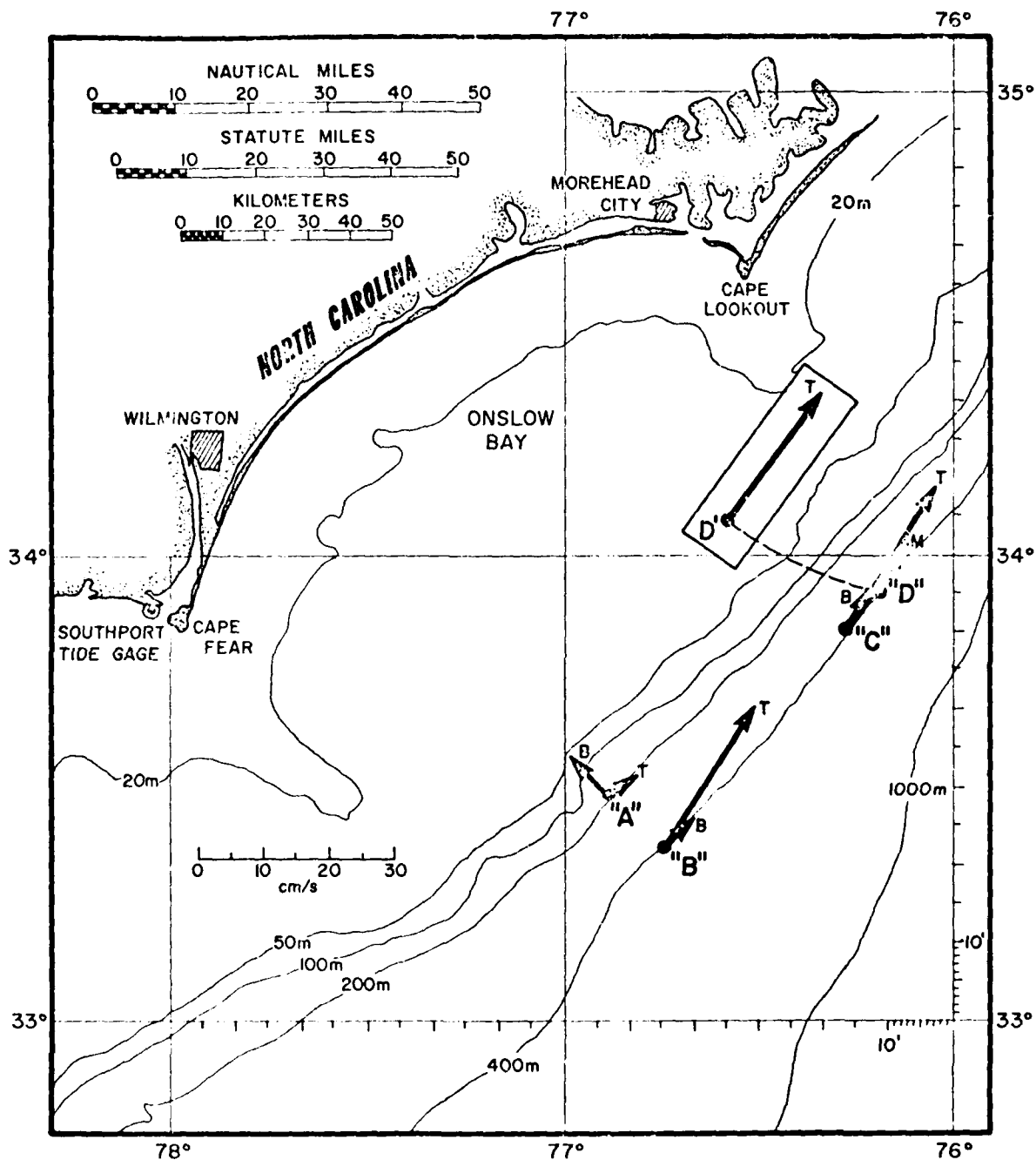


Figure 3. Detailed map of the experiment area (the inset box Fig. 1), showing the locations of moorings "A" through "D," with the record-long mean current vectors at the top (T), middle (M), and bottom (B) instruments. The mooring "D" position is shown displaced (inset box) for clarity.

Each mooring was supported by a single 37" (0.94m) diameter ORE float, yielding buoyancy in excess of 200 kg. The A and B moorings each supported two current meters, and the C and D moorings each supported three current meters. The vertical mooring design was similar to that given by Lee and Schutts (1977); a typical arrangement is shown in Fig. 4. The mooring coordinates, instrument start and stop times, instrument depths, and water depths are given in Table 1. The "summer" data set reported here spans the period from 03 August to 18 November 1979, or 107 days. Data from a similar experiment in the winter of 1979 are presented in Brooks, *et al.* (1980b).

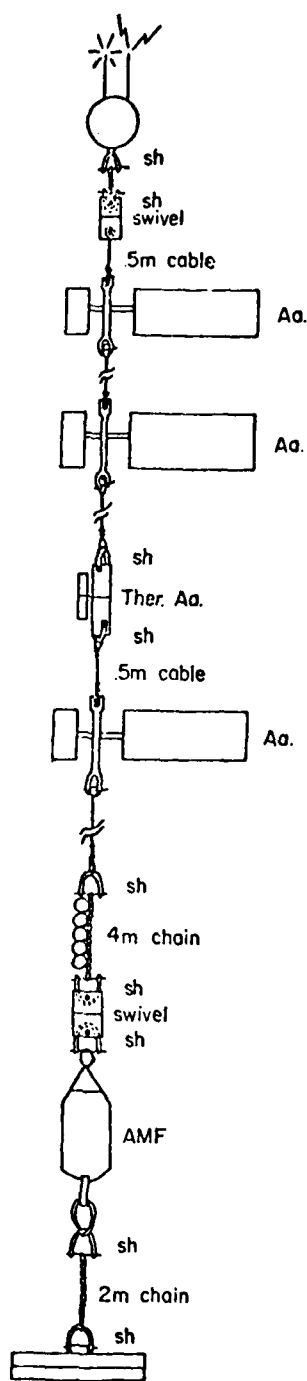


Figure 4. Typical mooring design, showing the position of Aanderaa current meters (Aa) in the wire held taut by a large main float and a train-wheel anchor. AMF (now EG&G) sea-link acoustic releases were used.

Table 1. Instrument identification, start and stop times, depths, and mooring locations.

Mooring no.	Instrument no.	Instrument type	Reference no.	Coordinates	Water depth (m)	Instr. depth (m)	Sample interval (min)	Anchor deployment (1979) Day-No.-Hr. (GMT)	Anchor release (1979) Day-No.-Hr. (GMT)	Initial cycle (GMT) (1979)	Final cycle (GMT) (1979)
A TOP	3425	AA	655	Lat 33°28.2' Long 76°52.1'	200	100	20	06 AUG 1732	18 NOV 1345	31 JUL 1740	18 NOV 1419
A BOT	3343	AA	41			180	20			31 JUL 1740	18 NOV 1419
B TOP	3426	AA	622	Lat 33°21.9' Long 76°41.3'	410	270	20	03 AUG 0647	18 NOV 1150	31 JUL 1740	18 NOV 1242
B BOT	3423	AA	286			390	20			01 AUG 1620	18 NOV 1238
C TOP	3332	AA	500	Lat 33°51.1' Long 76°14.7'	400	260	20	03 AUG 1036	18 NOV 1657	31 JUL 1740	18 NOV 1811
C MID	3427	AA	733			320	20			31 JUL 1740	18 NOV 1800
C BOT	2244	AA	624			380	20			31 JUL 1740	18 NOV 1758
D TOP	3337	AA	67	Lat 33°55.1 Long 76°11.1	390	250	20	03 AUG 1556	17 NOV 2130	31 JUL 1710	17 NOV 2315
D MID	3345	AA	30			310	20			31 JUL 1740	*
D BOT	3424	AA	840			370	20			31 JUL 1740	*

* Failed, no data.

1.3 SUPPORTING OBSERVATIONS

Hydrographic and other observations collected during the summer array launch and recovery operations were reported by Bane *et al.* (1980). The at-sea operations were conducted in R/V *Endeavor*.

SECTION 2

Data Sources, Processing, and Basic Statistics

2.1 TRANSCRIPTION OF AANDERAA DATA TAPES

The raw data on Aanderaa magnetic tapes consist of a sequence of pulse width modulated (PCM) binary numbers. Two binary words are recorded for each sensor sampled, plus two words for an internal reference number. The binary PCM data tapes were read by a reel-to-reel tape deck, then transcribed to computer-compatible binary words by a hardware interface device built by Mr. Lawrence Ives of North Carolina State University. The decoded raw data consist of time series of numbers in the range of 0 to 1023 (decimal equivalent).

2.2 INSTRUMENT CALIBRATION

The ten Aanderaa RCM-4 recording current meters used in the Gulf Stream Meanders Experiment were calibrated for direction and temperature. The four meters which were positioned at the top of the moorings contained pressure sensors, which were also calibrated. The calibration values supplied by the manufacturer for speed and conductivity were used; no other laboratory calibration was performed for these variables. In this section the calibration procedures and results are presented, along with the manufacturer's calibration information. The calibration data, either measured or supplied by Aanderaa, were used to convert from the internally recorded binary number, N, which ranges in decimal equivalent from 0 to 1023, into scientific units. With the exception of direction, the winter experiment calibration coefficients

were also used for the summer experiment. Only the new direction calibration curves are shown in this report; for other calibration curves, see TAMU technical report number 80-7-T.

Speed

The conversion from N to speed, in cm/sec, was accomplished with the linear formula

$$\text{Speed} = 1.5 + 0.14 N.$$

The values 1.5 and 0.14 were supplied by Aanderaa.

Conductivity

Aanderaa calibration values for conductivity were used for all meters. The coefficients in the linear formula

$$\text{Conductivity (mmho/cm)} = A + BN$$

are listed in Table 2.

Direction

Each RCM-4 compass was calibrated as follows: The instrument was mounted on a non-magnetic bracket located away from known magnetic interference. With the internal digitizing and recording mechanisms set to continuously record, the instrument was turned through 360°, indexing by ten degrees, allowing the compass to stabilize at each position and to record at least six cycles of the direction reading. A cubic equation of the form

$$\text{Direction (magnetic)} = A + BN + CN^2 + DN^3$$

was fitted to the 36 calibration values. The coefficients A through D for each meter are listed in Table 2. The direction values from the cubic equation differed by less than one degree from the measured calibration values. Graphs of the calibration curve and the Aanderaa curve for the eight meters which operated successfully are shown in Fig. 5.

Temperature

All temperature sensors were calibrated as follows: With all meters sealed and recording at 15 minute intervals, they were immersed in an icewater bath. The ice was allowed to slowly melt, and the water to warm to room temperature (~25°C). Stirring was provided throughout the warming period by two small pumps. Four independent Hewlett-Packard quartz-crystal thermometers were placed around the bath for temperature measurement. A continuous record (strip chart) of the temperature measured by one of the quartz sensors was made and used as the calibration standard. Temperature readings around the bath using the other three sensors showed the temperature differences to be always less than 0.05°C,¹ insuring that all meters were recording essentially the same temperature. Calibration temperatures at known times of RCM-4 recordings were compared with the corresponding recorded values of N. A number (ca. 15 to 19) of Temperature-N pairs were used to determine the best fit to the cubic equation:

$$\text{Temperature } (^\circ\text{C}) = A + BN + CN^2 + DN^3$$

The coefficients A through D are listed for each meter in Table 2, along with the coefficients supplied by Aanderaa. The difference between the temperature calibration values computed from the cubic equation and those directly measured was in all cases less than the stated accuracy of the temperature sensor (0.15 °C).

Pressure

The pressure transducers on instruments 3425, 3426, 3332 and 3337 were calibrated using a manual hydraulic pump. Calibration data were collected in the range 0 to 500 PSIG at intervals of 50 PSIG, covering the approximate depth range of 0 to 350 m. These points were fitted to the cubic equation

¹ After all ice had melted.

$$\text{Pressure (PSIG)} = A + BN + CN^2 + DN^3.$$

The coefficients in the cubic equation for each meter are listed in Table 2, along with the Aanderaa coefficients.

Salinity

Salinity values were calculated from the temperature and conductivity time series in scientific units as follows: The conductivity that seawater with a salinity of 35 ‰ would have at the measured temperature was calculated using the formula

$$\begin{aligned} \text{Cond (T, 35)} &= 29.01067 + 0.8677579 T \\ &+ 0.4074545 \times 10^{-2} T^2 - \\ &0.1437152 \times 10^{-4} T^3, \end{aligned}$$

where T is the measured temperature (°C) and Cond is in mmho/cm. This formula is the best-fit cubic equation calculated from information presented by Weyl (1964). The conductivity ratio at the measured temperature was calculated by

$$R_T = \text{Cond (meas)} / \text{Cond (T, 35)},$$

where Cond (meas) is the measured conductivity in mmho/cm. The difference, Δ_{15} , between the conductivity ratio at 15°C and R_T was calculated with the formula (National Institute of Oceanography of Great Britain and Unesco, 1971)

$$\begin{aligned} \Delta_{15} &= 10^{-5} R_T (R_T - 1) (T - 15) [96.7 - 72.0 R_T \\ &+ 37.3 R_T^2 - (0.63 + 0.21 R_T^2) (T - 15)]. \end{aligned}$$

The salinity in parts per thousand was then calculated using the formula (*ibid.*)

$$\begin{aligned} S(\text{‰}) &= -0.08996 + 28.29720 R_{15} + 12.80832 R_{15}^2 \\ &- 10.67869 R_{15}^3 + 5.98624 R_{15}^4 \\ &- 1.32311 R_{15}^5, \end{aligned}$$

where $R_{15} = R_T + \Delta_{15}$.

Table 2. Aanderaa-supplied (Aa) and calibration-produced (Cal) coefficients for the conversion of recorded binary numbers to scientific units. The general formula $V = A + BN + CN^2 + DN^3$ was used, where V is the variable, and N is decimal equivalent (0 - 1023) of the recorded binary number.

Meter No.	Variable	Speed (cm sec ⁻¹)		Direction (degrees mag)		Conductivity (mmho cm ⁻¹)		Temperature (°C)		Pressure (kg cm ⁻²) (PSI)	
		Aa	Cal	Aa	Cal	Aa	Cal	Aa	Cal	Aa	Cal
3332	A	1.5		1.5	-5.1395	0		-0.885	-0.4144	-4.30507	-53.4979
	B	0.14		0.349	0.3218	0.07593		0.03587	0.0361	0.0770611	1.1150
	C				0.7794×10^{-4}			-0.8388×10^{-5}	-0.8734×10^{-5}		-0.2201×10^{-3}
	D				-0.5684×10^{-7}			0.4300×10^{-8}	0.4470×10^{-8}		0.3127×10^{-6}
3337	A	1.5		1.5	-5.0853	0.076		-0.0905	-0.3128	-3.78849	-67.9111
	B	0.14		0.349	0.3478	0.07607		0.03587	0.0375	0.0758634	1.3185
	C				0.8150×10^{-5}			-0.8388×10^{-5}	-0.1230×10^{-5}		-0.8994×10^{-3}
	D				-0.9962×10^{-8}			0.4300×10^{-8}	0.6655×10^{-8}		0.9220×10^{-6}
3343	A	1.5		1.5	-8.5998	-0.084		-0.9103	-0.3176		
	B	0.14		0.349	0.3519	0.07593		0.03587	0.0375		
	C				0.2027×10^{-4}			-0.8388×10^{-5}	-0.1260×10^{-5}		
	D				-0.2458×10^{-7}			0.4300×10^{-8}	0.6858×10^{-8}		
3344	A	1.5		1.5	-7.4634	-0.084		-0.0905	-0.2421		
	B	0.14		0.349	0.3561	0.07593		0.03587	0.0372		
	C				0.1300×10^{-4}			-0.8388×10^{-5}	-0.1226×10^{-5}		
	D				-0.2292×10^{-7}			0.4300×10^{-8}	0.7004×10^{-8}		
3345	A	1.5		1.5	No	0.076		-0.0773	-0.2877		
	B	0.14		0.349	calibration	0.07597		0.03587	0.0367		
	C				data			-0.8388×10^{-5}	-0.1044×10^{-5}		
	D							0.4300×10^{-8}	0.5516×10^{-8}		
3423	A	1.5		1.5	-9.7707	0		-0.9511	No		
	B	0.14		0.349	0.3946	0.07574		0.03587	calibration		
	C				-0.7497×10^{-4}			-0.8388×10^{-5}	data		
	D				0.2784×10^{-7}			0.4300×10^{-8}			
3424	A	1.5		1.5	No	0		-0.8781	-0.079		
	B	0.14		0.349	calibration	0.07650		0.03587	0.0386		
	C				data			-0.8388×10^{-5}	-0.1790×10^{-5}		
	D							0.4300×10^{-8}	1.1579×10^{-8}		
3425	A	1.5		1.5	-4.2754	0.07574		-0.8651	-0.2713	-3.92054	-65.2533
	B	0.14		0.349	0.3842	0.07574		0.03587	0.0377	0.0757081	1.2346
	C				-0.9950×10^{-4}			-0.8388×10^{-5}	-1.3034×10^{-5}		-0.5164×10^{-3}
	D				0.6525×10^{-7}			0.4300×10^{-8}	0.7184×10^{-8}		0.5034×10^{-6}
3426	A	1.5		1.5	-0.8219	0		-0.8827	-0.2922	-4.20812	-72.1725
	B	0.14		0.349	0.3886	0.07598		0.03587	0.0375	0.0761238	1.3555
	C				-0.8587×10^{-4}			-0.8388×10^{-5}	-1.2131×10^{-5}		-1.0077×10^{-3}
	D				0.4428×10^{-7}			0.4300×10^{-8}	0.6462×10^{-8}		1.0679×10^{-6}
3427	A	1.5		1.5	-6.2256	0.07612		-0.9121	-0.3606		
	B	0.14		0.349	0.3736	0.07612		0.03587	0.0380		
	C				-0.7050×10^{-4}			-0.8388×10^{-5}	-1.3525×10^{-5}		
	D				0.4491×10^{-7}			0.4300×10^{-8}	0.7438×10^{-8}		

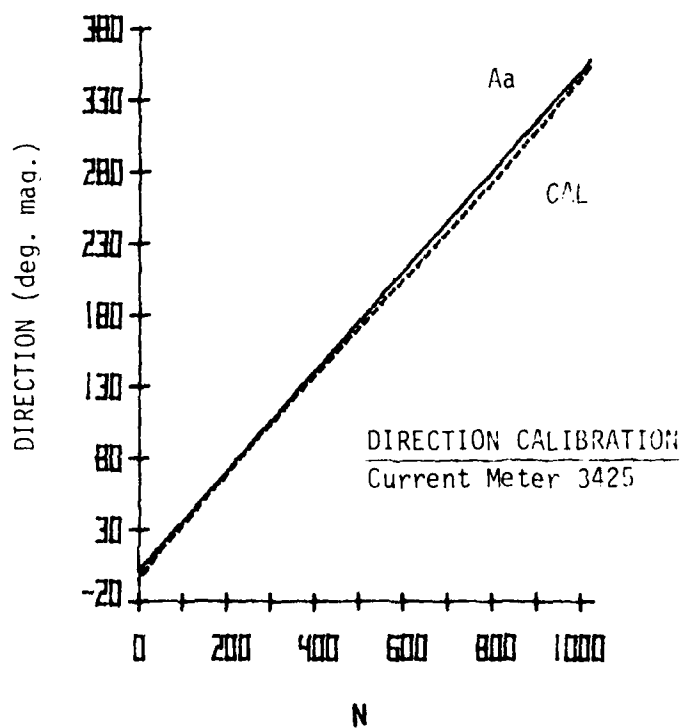
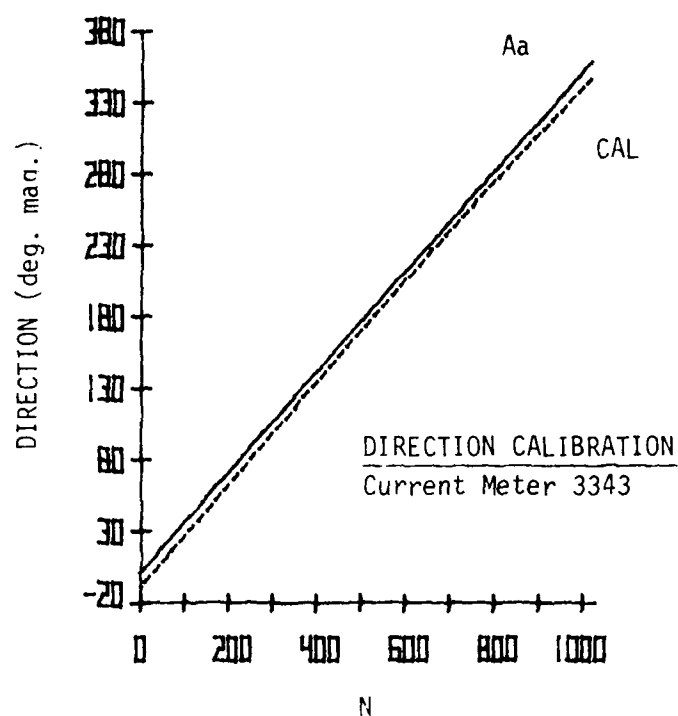
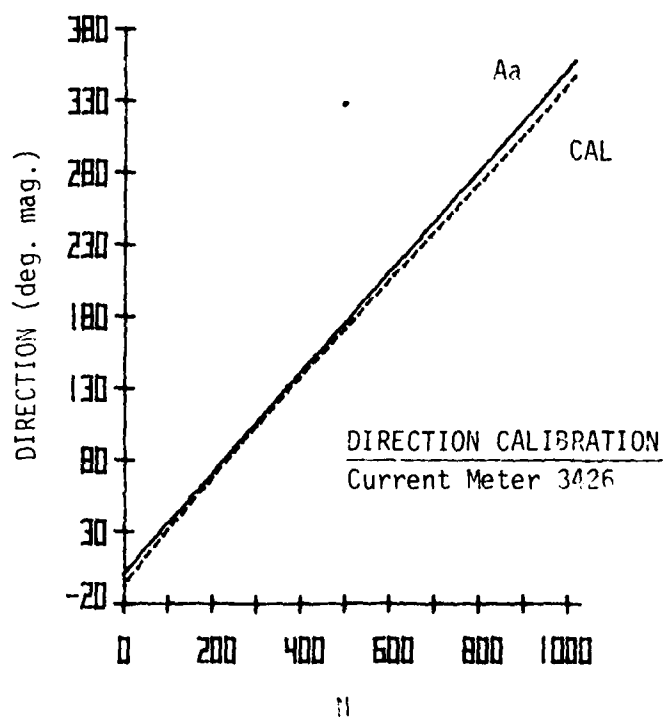
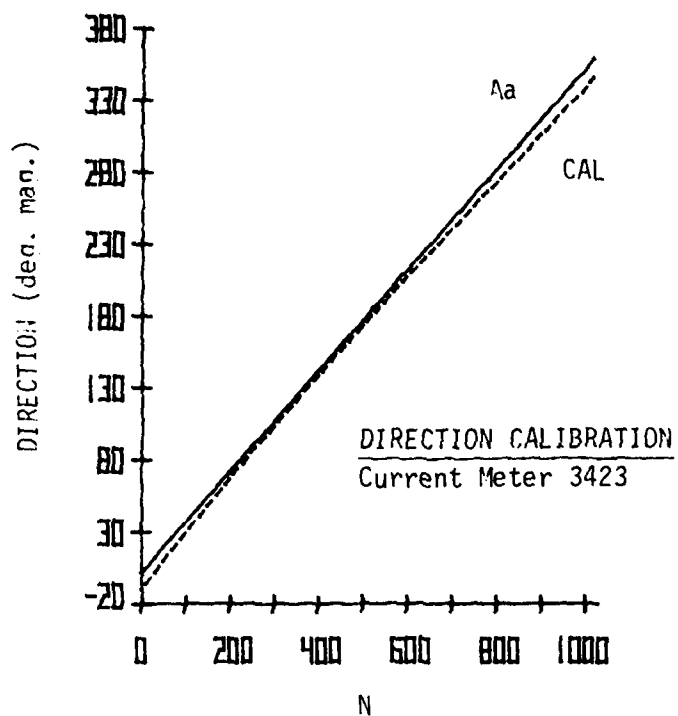
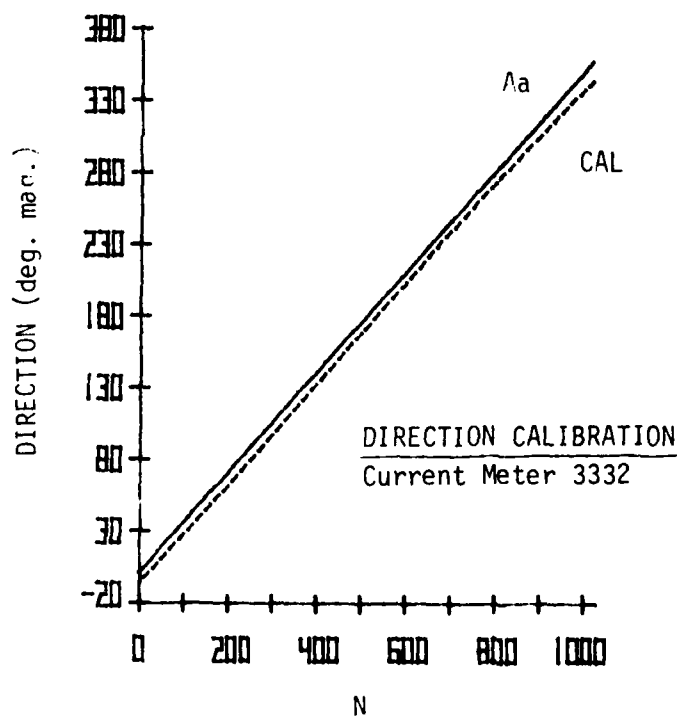
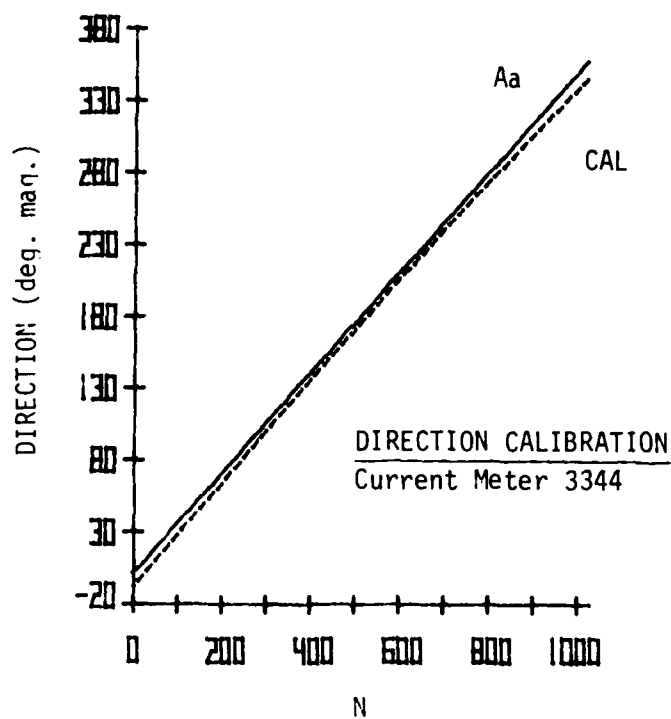
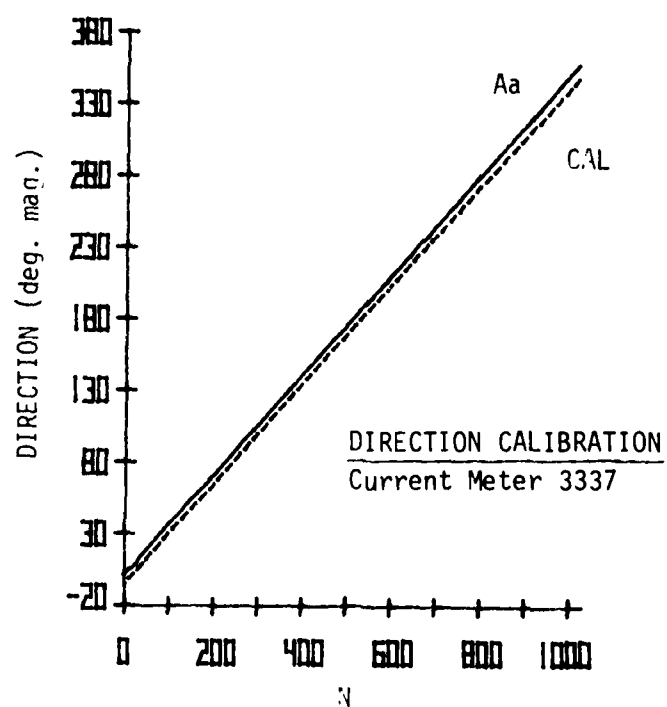
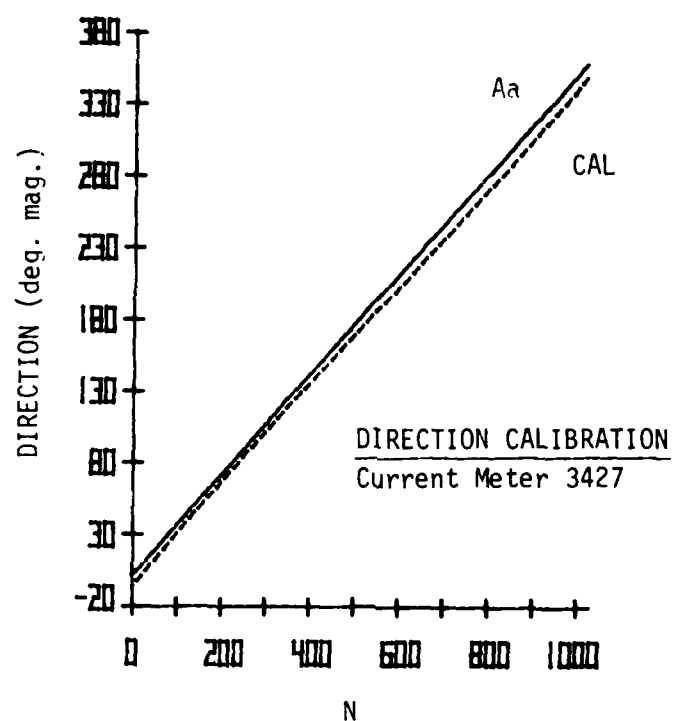


Figure 5. Calibration curves for compass direction, based on coefficients supplied by Aanderaa (-) and coefficients based on directly measured calibration data (----). The latter were used for calibration of all instruments.







2.3 AANDERAA DATA EDITING

The calibrated Aanderaa data files were machine-edited for extreme values exceeding reasonable upper and lower bounds on each variable. Bad points were replaced by values linearly interpolated between the preceding and succeeding good points. The data were then plotted, and further editing of unreasonable values was done by operating on the data files interactively using a computer terminal. All edited points were replaced by interpolated values, as in the machine-edited case.

2.4 ANCILLARY DATA SOURCES

Atmospheric surface observations at Cape Hatteras and at NDBO moored buoys number 41004 and 41002, Fig. 1, were obtained from the National Archives for the summer array period. The Hatteras atmospheric data shown here are air temperature and atmospheric pressure. In addition, the wind stress vector components were computed, using a constant drag coefficient $C_D = 1.5 \times 10^{-3}$. The shallow NDBO buoy (NDBO-4 on Fig. 1) was located at 32.6°N, 78.7°W, approximately on the 100 m isobath, and the offshore buoy (NDBO-2 on Fig. 1) was located at 32.3°N, 75.3°W, approximately on the 3800 m isobath. The NDBO data presented are air and sea surface (water) temperatures and atmospheric pressure. The NDBO wind stress components are also shown.

2.5 DATA PROCESSING

The raw, calibrated data from the current meters consisted of time series of current speed and direction, temperature, salinity, and (only for top instruments) pressure. The basic sampling interval for all current meters was 20 minutes. Current speed and direction were converted to (u, v) vector velocity components in an (offshore, downstream) coordinate frame rotated

clockwise 34 degrees from true north to align with the 400 m isobath. The same coordinate frame was used for all vector data sets, which facilitates direct comparison between them.

Standard digital filtering techniques based on the FESTSA time series analysis system (Brooks, 1976) were used to subdivide the frequency domain of the data sets. First, a 3-hour low pass filter (3 HRLP) was applied to reduce sampling noise and possible aliasing. Then a 40-hour low pass filter (40 HRLP) was applied to separate the daily and semidaily tidal and inertial motions from those with periods of several days and longer. For both filters, the specified cutoff period is the period at which the filter energy response is 0.25 times its long period response (-6db point). A Lanczos taper was used in each case, and the smoothed response function of the 40 HRLP filter is shown in Fig. 6. The response at the semidaily (dominant) tidal period is less than 10^{-7} . In addition, a 3 to 40 hours bandpass (3-40 HRBP) data set was obtained by subtracting the 40 HRLP set from the 3 HRLP set. The final sample interval was 1 hour for the 3 HRLP and 3-40 HRBP sets and 6 hours for the 40 HRLP set.

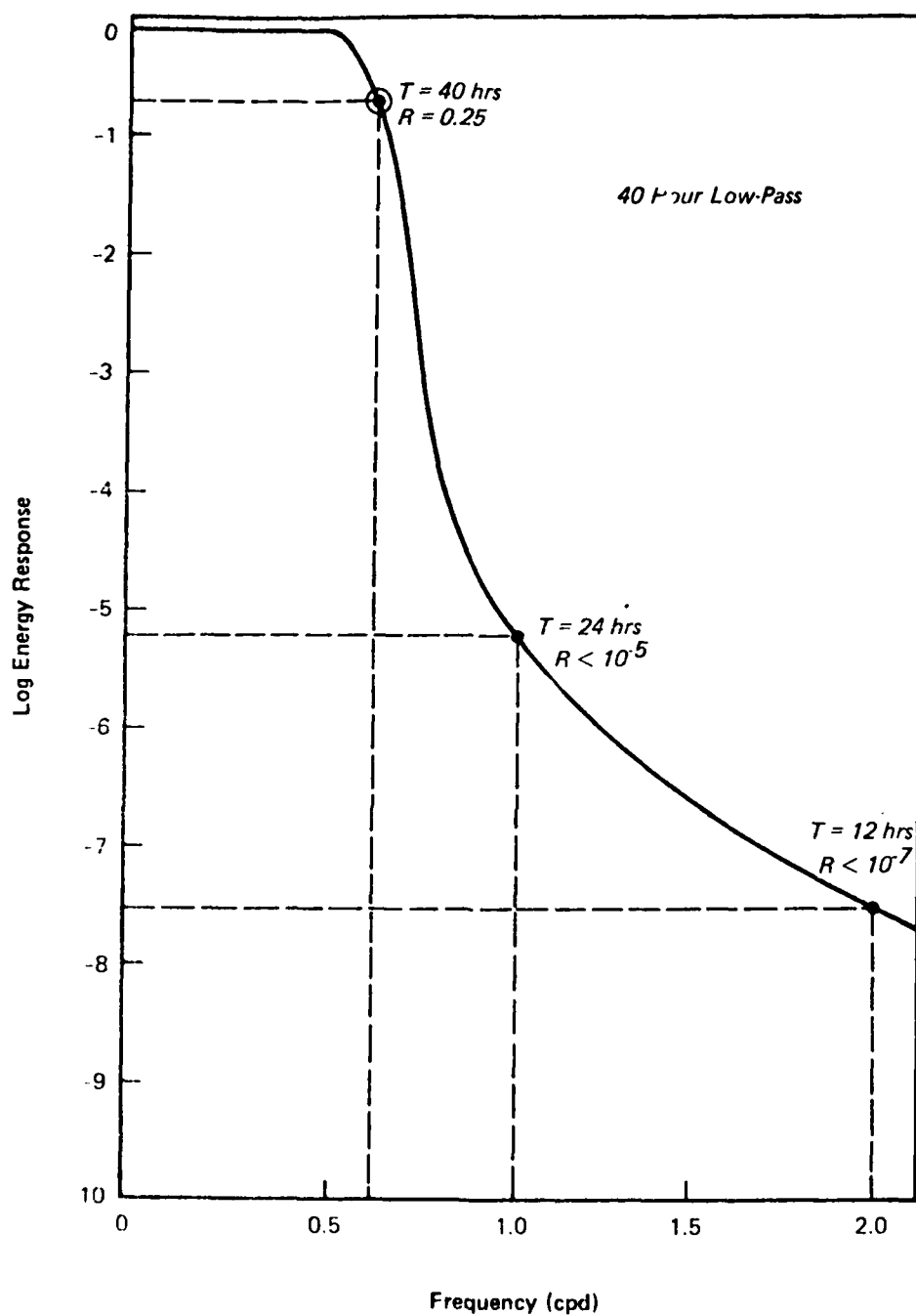


Figure 6. Response function for the 40 hour low pass Lanczos filter.

2.6 BASIC STATISTICS OF THE CURRENT METER DATA SET

First order and variance statistics for u , v , and T (temperature) from each current meter are shown in Table 3. No data are presented for instruments number 3345 and 3424, which failed. These instruments were located at the D MID and D BOT positions, respectively. Table 4 shows the variance ratios 3-40 HRBP/3 HRLP and 40 HRLP/3 HRLP, which approximately represent the division of total spectrum energy between the tidal-inertial band and the long period band, respectively. Departure of their sum from unity for each variable is a measure of filtering imperfection. The tidal-inertial band motions were strongest in the cross-shelf (u) component, particularly at the deepest instruments. The downstream (v) component fluctuations predominantly had periods of several days and longer.

Table 3. First-order and variance statistics of temperature (T) and velocity components (u, v) from each instrument, shown from 3 HRLP, 3-40 HRLP, and 40 HRLP filtered data sets.

3 HRLP

Current meter	Parameter	N	Min	Max	Mean	SD	Var
A TOP	T	2472	12.1	24.3	17.7	2.3	5.2
	S	2472	35.2	36.6	36.0	0.3	0.1
	U	1210	-37.4	50.2	2.1	12.5	155.8
	V	1210	-86.1	126.1	5.4	44.2	1951.9
A BOT	T						
	S						
	U	2472	-50.8	31.3	-7.8	10.2	103.4
	V	2472	-65.6	75.5	1.5	19.6	384.2
B TOP	T	2470	8.5	17.4	11.9	2.3	5.1
	S	2470	34.8	36.2	35.3	0.3	0.1
	U	2470	-59.2	48.3	-0.7	16.4	270.6
	V	2470	-40.7	126.1	25.8	30.4	921.7
B BOT	T	2470	5.7	12.2	8.2	1.2	1.5
	S	2470	35.6	36.2	35.8	0.1	0.0
	U	2471	-35.8	41.4	1.1	10.0	100.0
	V	2471	-41.1	66.7	6.4	19.1	363.3
C TOP	T	2475	8.7	17.2	12.0	1.9	3.6
	S	2475	35.1	36.4	35.5	0.3	0.1
	U	2475	-37.9	35.8	-1.4	10.1	101.6
	V	2475	-57.4	139.0	25.1	34.4	1182.7
C MID	T	2475	7.7	16.0	10.5	1.5	2.3
	S	2475	34.7	35.9	35.0	0.2	0.0
	U	2401	-30.3	36.5	0.2	8.5	72.9
	V	2401	-56.2	113.1	16.6	26.9	725.2
C BOT	T	2054	6.1	13.4	8.8	1.1	1.2
	S	2054	34.7	35.5	34.9	0.1	0.0
	U	2054	-24.4	29.4	-0.7	7.6	57.3
	V	2054	-49.5	63.1	7.6	19.2	370.6
D TOP	T	2456	8.9	17.1	12.3	1.8	3.2
	S	2456	34.9	36.2	35.4	0.3	0.1
	U	2456	-40.9	38.9	0.7	9.7	93.7
	V	2456	-47.7	141.6	23.9	34.0	1154.0

Current meter	Parameter	N	Min	Max	Mean	SD	Var
A TOP	T	2280	-2.1	1.8	0.0	0.5	0.2
	S	2280	-0.3	0.4	0.0	0.1	0.0
	U	1018	-34.2	25.3	0.0	7.3	52.7
	V	1018	-29.8	23.7	0.0	7.1	50.3
A BOT	T						
	S						
	U	2280	-23.4	27.5	0.0	6.1	37.3
	V	2280	-29.7	32.6	0.0	6.3	39.2
B TOP	T	2278	-1.3	1.3	0.0	0.4	0.1
	S	2278	-0.2	0.2	0.0	0.1	0.0
	U	2278	-21.3	21.3	0.0	6.2	38.1
	V	2278	-31.2	30.2	0.0	7.3	53.4
B BOT	T	2278	-1.8	1.9	0.0	0.3	0.1
	S	2278	-0.2	0.2	0.0	0.0	0.0
	U	2279	-21.6	24.8	0.0	5.7	32.5
	V	2279	-21.4	17.6	0.0	5.1	26.3
C TOP	T	2283	-1.9	1.6	0.0	0.4	0.2
	S	2283	-0.3	0.3	0.0	0.1	0.0
	U	2283	-22.5	22.4	0.0	5.6	31.0
	V	2283	-32.4	40.1	0.0	7.7	58.8
C MID	T	2283	-1.8	1.7	0.0	0.4	0.1
	S	2283	-0.3	0.3	0.0	0.1	0.0
	U	2209	-27.5	18.8	0.0	5.7	32.1
	V	2209	-23.3	33.4	0.0	6.3	39.3
C BOT	T	1862	-1.4	1.8	0.0	0.3	0.1
	S	1862	-0.3	0.3	0.0	0.0	0.0
	U	1862	-23.3	21.8	0.0	5.9	34.8
	V	1862	-17.3	19.7	0.0	5.2	27.0
D TOP	T	2264	-1.7	1.8	0.0	0.4	0.2
	S	2264	-0.3	0.3	0.0	0.1	0.0
	U	2264	-33.5	19.9	0.0	5.3	28.0
	V	2264	-36.7	43.2	0.0	8.0	64.2

Current meter	Parameter	N	Min	Max	Mean	SD	Var
A TOP	T	380	12.6	23.1	17.6	2.2	5.0
	S	380	35.2	36.4	36.0	0.3	0.1
	U	170	-21.0	34.3	2.3	9.9	98.6
	V	170	-75.1	115.9	4.8	45.0	2026.8
A BOT	T						
	S						
	U	380	-45.7	25.2	-7.9	8.3	68.7
	V	380	-55.4	61.2	1.1	18.4	336.7
B TOP	T	380	8.5	17.2	11.9	2.3	5.1
	S	380	34.8	36.2	35.3	0.3	0.1
	U	380	-49.2	33.9	-0.5	14.8	218.2
	V	380	-28.8	120.7	26.5	29.3	856.7
B BOT	T	380	5.9	11.8	8.2	1.2	1.4
	S	380	35.6	36.2	35.8	0.1	0.0
	U	380	-24.2	19.3	1.1	7.8	61.0
	V	380	-31.7	57.9	6.8	18.2	330.1
C TOP	T	381	8.7	17.0	12.0	1.9	3.5
	S	381	35.1	36.3	35.5	0.3	0.1
	U	381	-27.1	20.2	-1.6	8.1	65.9
	V	381	-53.0	124.1	25.2	33.1	1093.0
C MID	T	381	8.0	15.1	10.5	1.4	2.1
	S	381	34.7	35.8	35.0	0.2	0.0
	U	369	-15.8	19.9	0.1	6.1	37.2
	V	369	-49.9	87.4	16.5	26.1	682.3
C BOT	T	311	6.3	12.5	8.8	1.0	1.0
	S	311	34.8	35.4	34.9	0.1	0.0
	U	311	-17.2	12.9	-0.7	4.6	21.3
	V	311	-42.7	51.0	7.6	18.9	356.8
D TOP	T	378	9.0	17.3	12.3	1.8	3.1
	S	378	34.9	36.2	35.4	0.3	0.1
	U	378	-24.2	32.5	0.6	8.1	65.3
	V	378	-45.1	118.1	24.7	33.0	1087.0

Table 4. Sub-band variance ratios for temperature (T) and velocity components (u, v) from each instrument. The sub-bands approximately divide the principal tidal and inertial spectrum (3-40 HRBP) for the low frequency spectrum (40 HRLP).

Current meter	Parameter	Variance ratio	
		$\frac{3-40 \text{ HR BP}}{3 \text{ HRLP}}$	$\frac{40 \text{ HRLP}}{3 \text{ HRLP}}$
A TOP	T	0.04	0.96
	U	0.34	0.63
	V	0.03	1.04
A BOT	T	---	---
	U	0.36	0.66
	V	0.10	0.88
B TOP	T	0.02	1.00
	U	0.14	0.81
	V	0.06	0.93
B BOT	T	0.67	0.93
	U	0.33	0.61
	V	0.07	0.91
C TOP	T	0.06	0.97
	U	0.31	0.65
	V	0.05	0.92
C MID	T	0.04	0.91
	U	0.44	0.51
	V	0.05	0.94
C BOT	T	0.08	0.83
	U	0.61	0.37
	V	0.07	0.96
D TOP	T	0.06	0.97
	U	0.30	0.70
	V	0.06	0.94

The 3 HRLP mean velocity vectors are shown on the mooring array plan view. (Fig. 3). The largest mean departure from the downstream direction occurred for the A-bottom instrument, possibly indicating bottom boundary layer effects.

Polar histograms giving the distribution of the normalized, cumulative 3 HRLP vector magnitude are shown in Figs. 7 through 14. The coordinate rotation angle is shown in Figs. 7 through 14 by the radial tick mark at 34° clockwise from north.

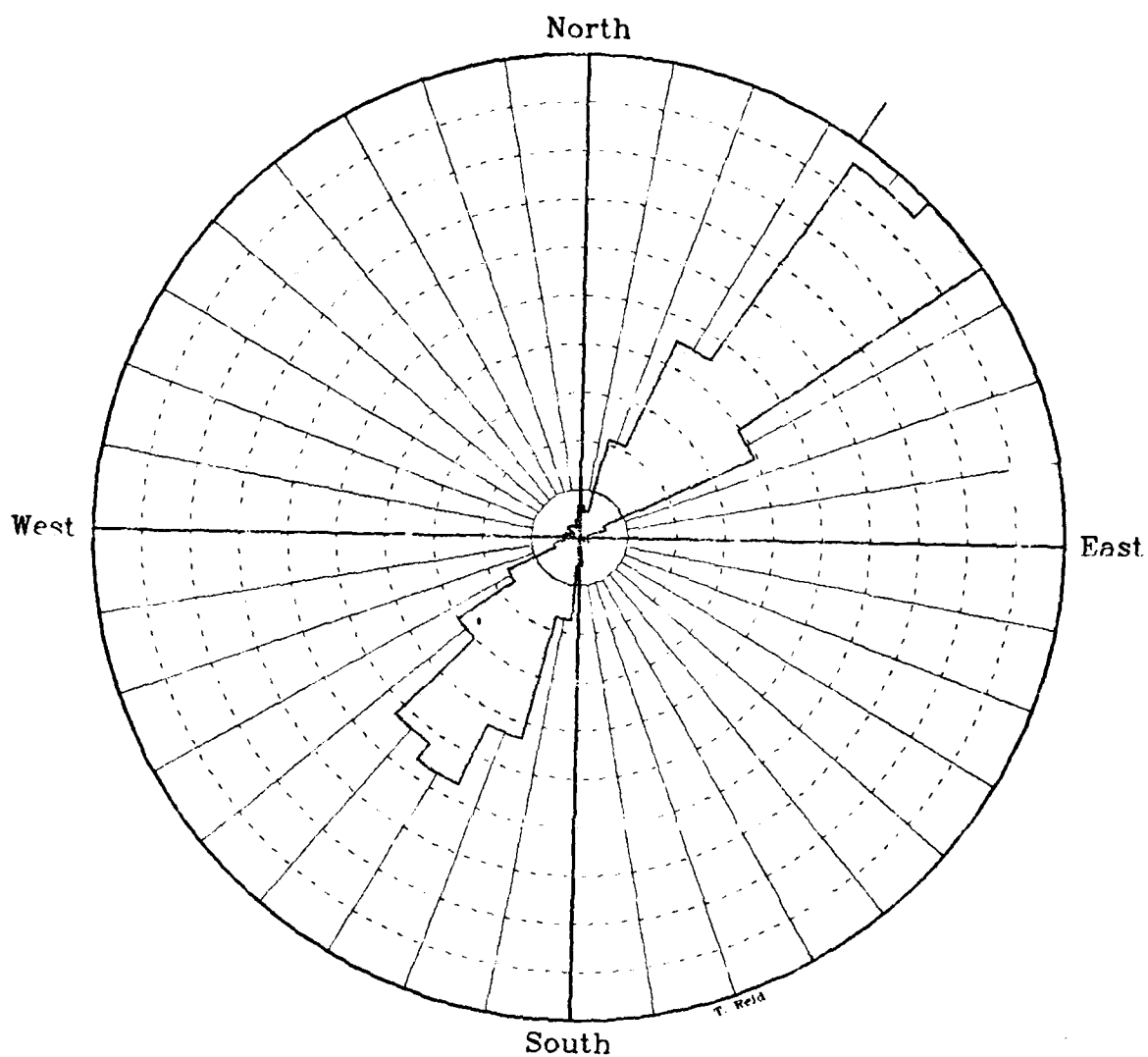
A_T 3 HRLP

Figure 7. Polar histogram for instrument A-top showing the normalized magnitude distribution of the 3 HRLP velocity, accumulated vectorially in ten degree sectors. The downstream (+v) direction of the rotated coordinate system is shown by the radial tick mark.

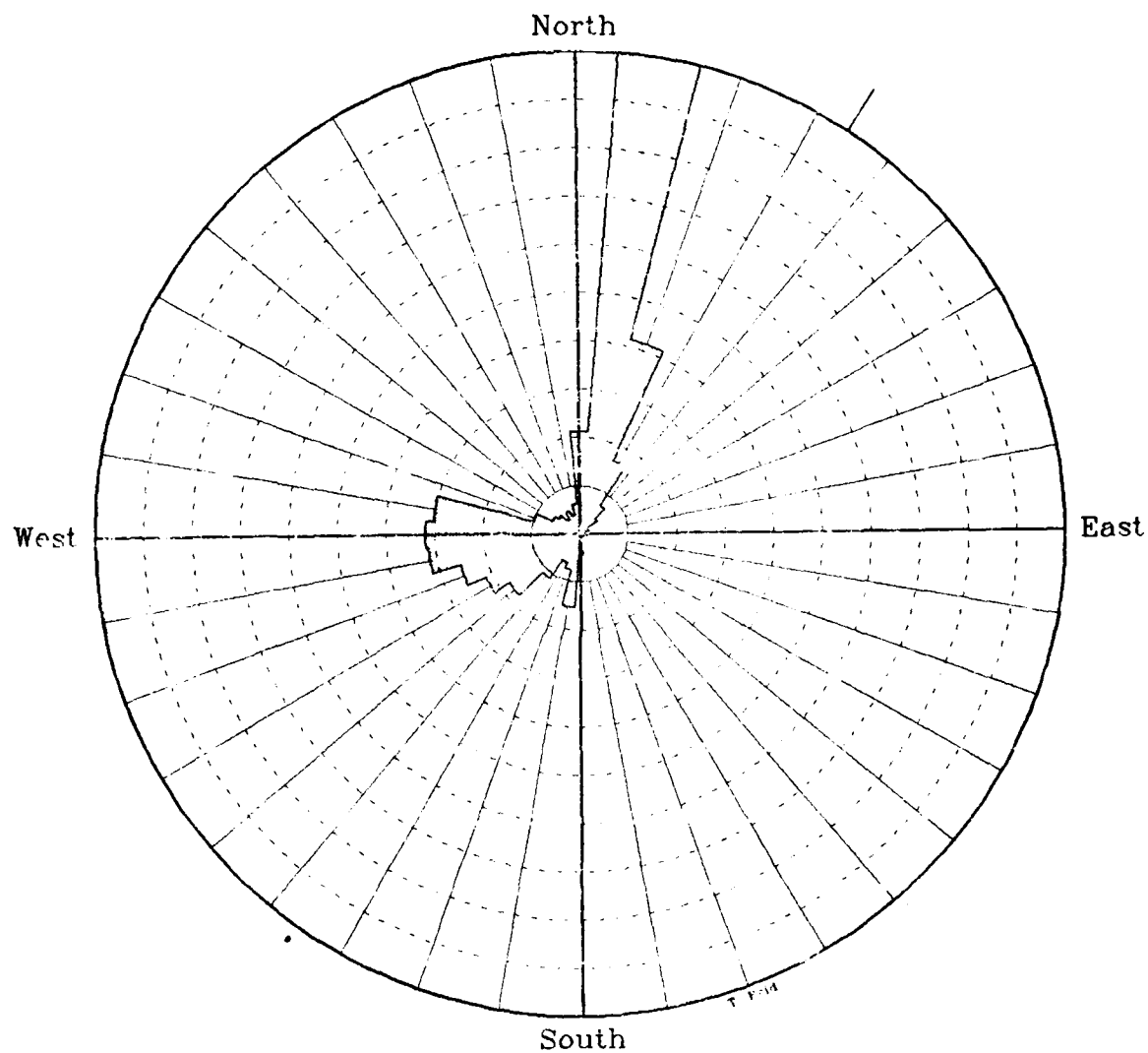
A_B 3 HRLP

Figure 8. Polar histogram for instrument A-bot showing the normalized magnitude distribution of the 3 HRLP velocity, accumulated vectorially in ten degree sectors. The downstream (+ v) direction of the rotated coordinate system is shown by the radial tick mark.

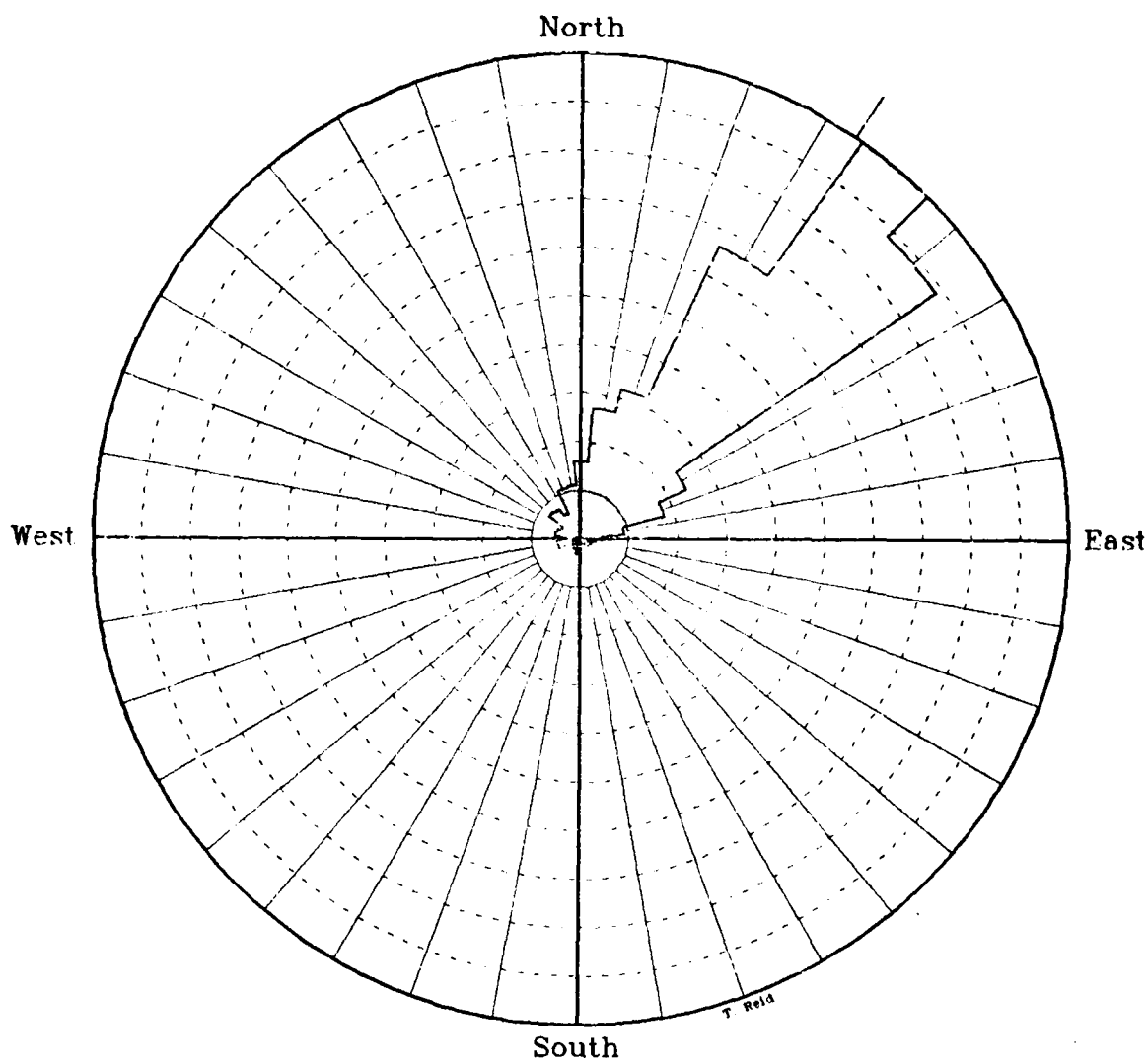
B_T 3 HRLP

Figure 9. Polar histogram for instrument B-top showing the normalized magnitude distribution of the 3 HRLP velocity, accumulated vectorially in ten degree sectors. The downstream (+ v) direction of the rotated coordinate system is shown by the radial tick mark.

B_B 3 HRLP

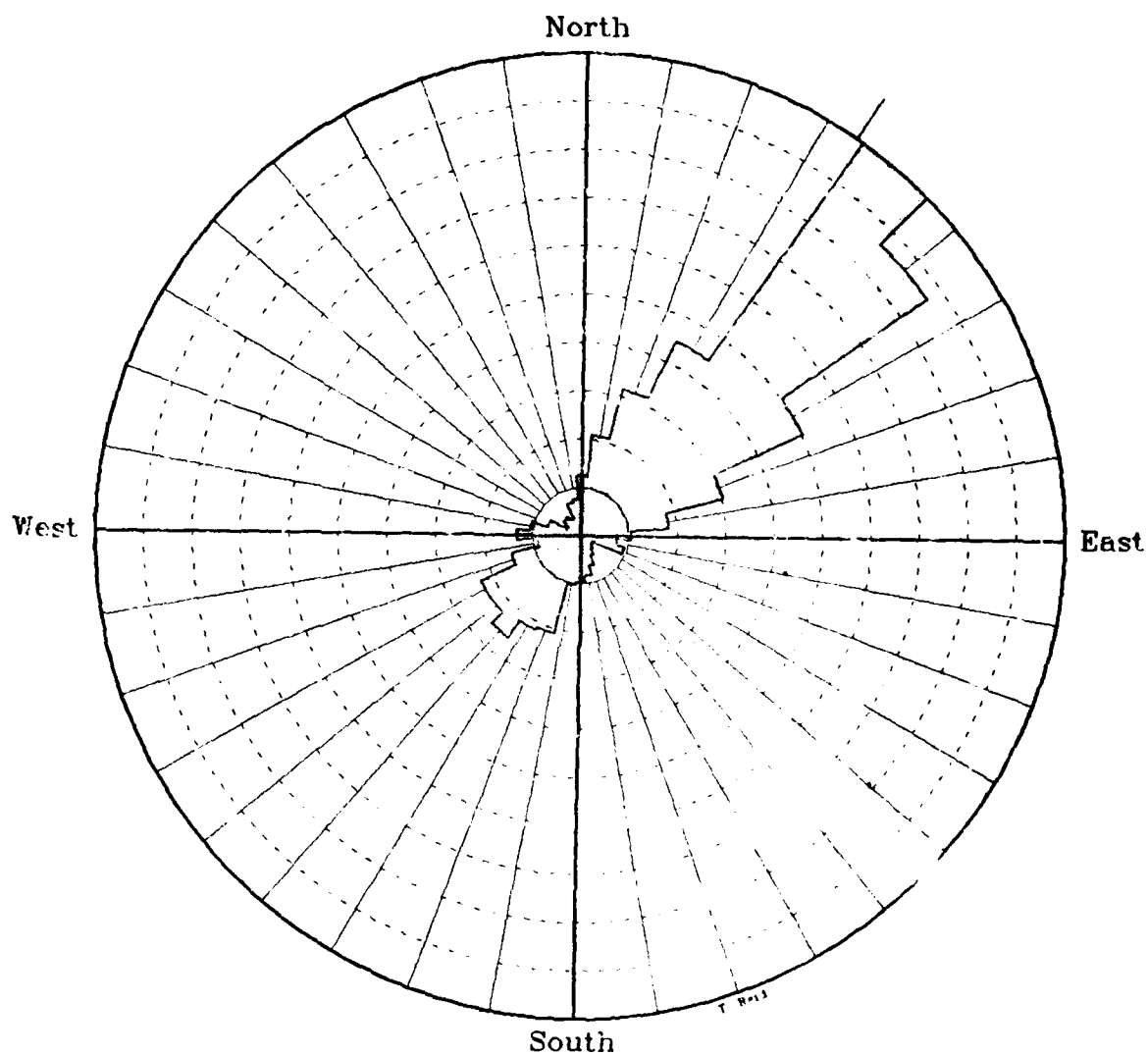


Figure 10. Polar histogram for instrument B-bot showing the normalized magnitude distribution of the 3 HRLP velocity, accumulated vectorially in ten degree sectors. The downstream (+ v) direction of the rotated coordinate system is shown by the radial tick mark.

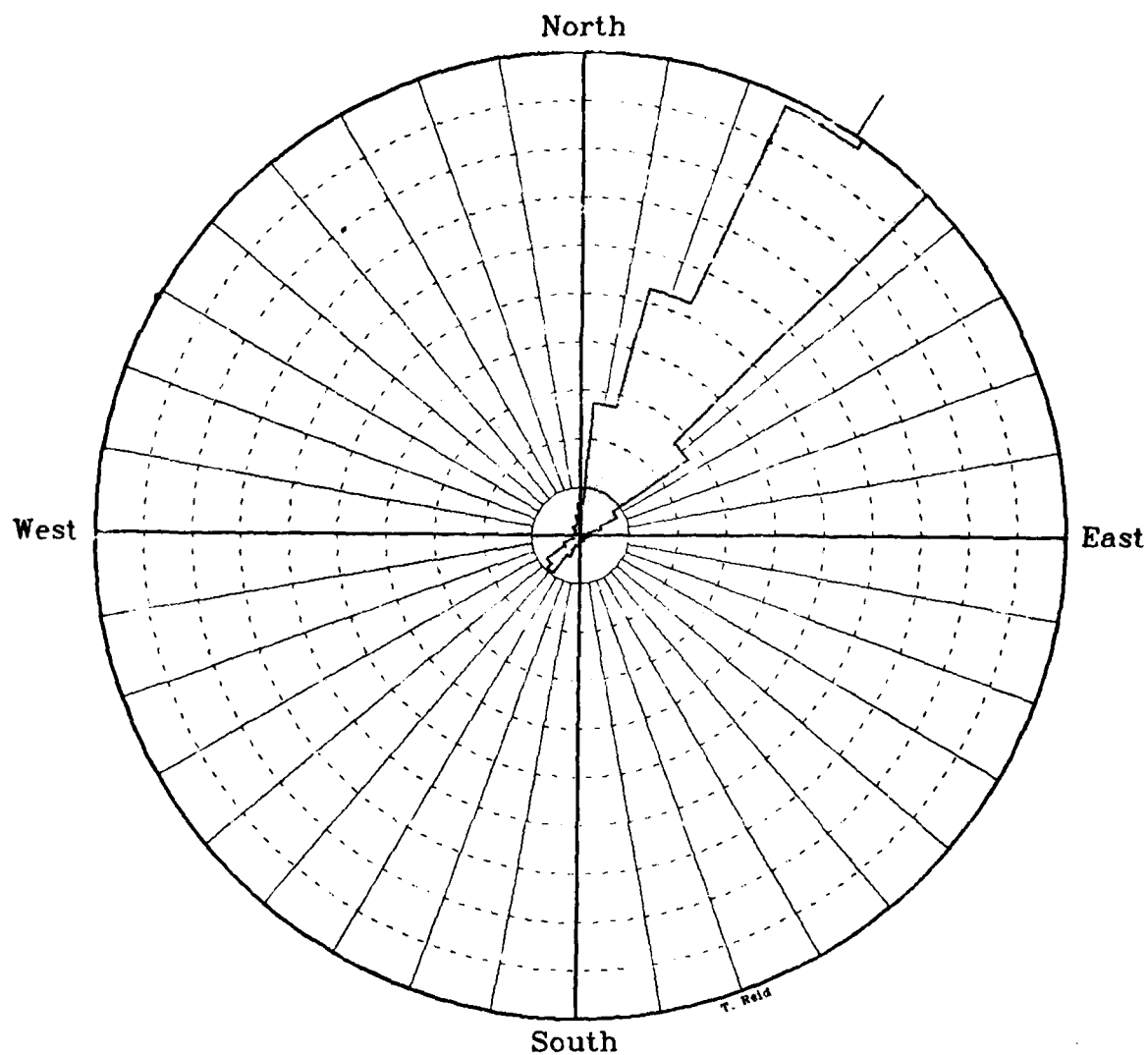
C_T 3 HRLP

Figure 11. Polar histogram for instrument C-top showing the normalized magnitude distribution of the 3 HRLP velocity, accumulated vectorially in ten degree sectors. The downstream (+ v) direction of the rotated coordinate system is shown by the radial tick mark.

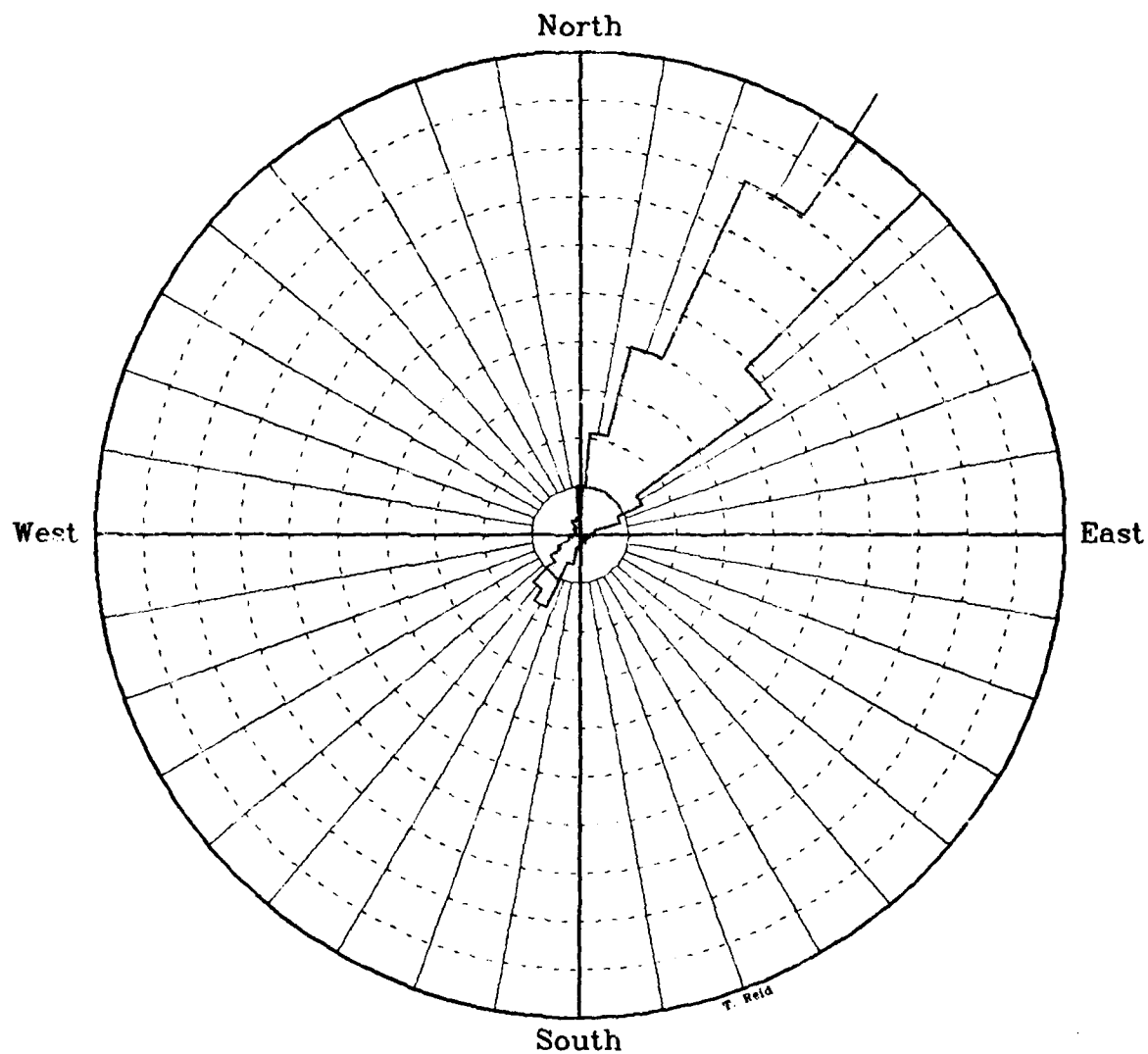
C_M 3 HRLP

Figure 12. Polar histogram for instrument C-mid showing the normalized magnitude distribution of the 3 HRLP velocity, accumulated vectorially in ten degree sectors. The downstream (+ v) direction of the rotated coordinate system is shown by the radial tick mark.

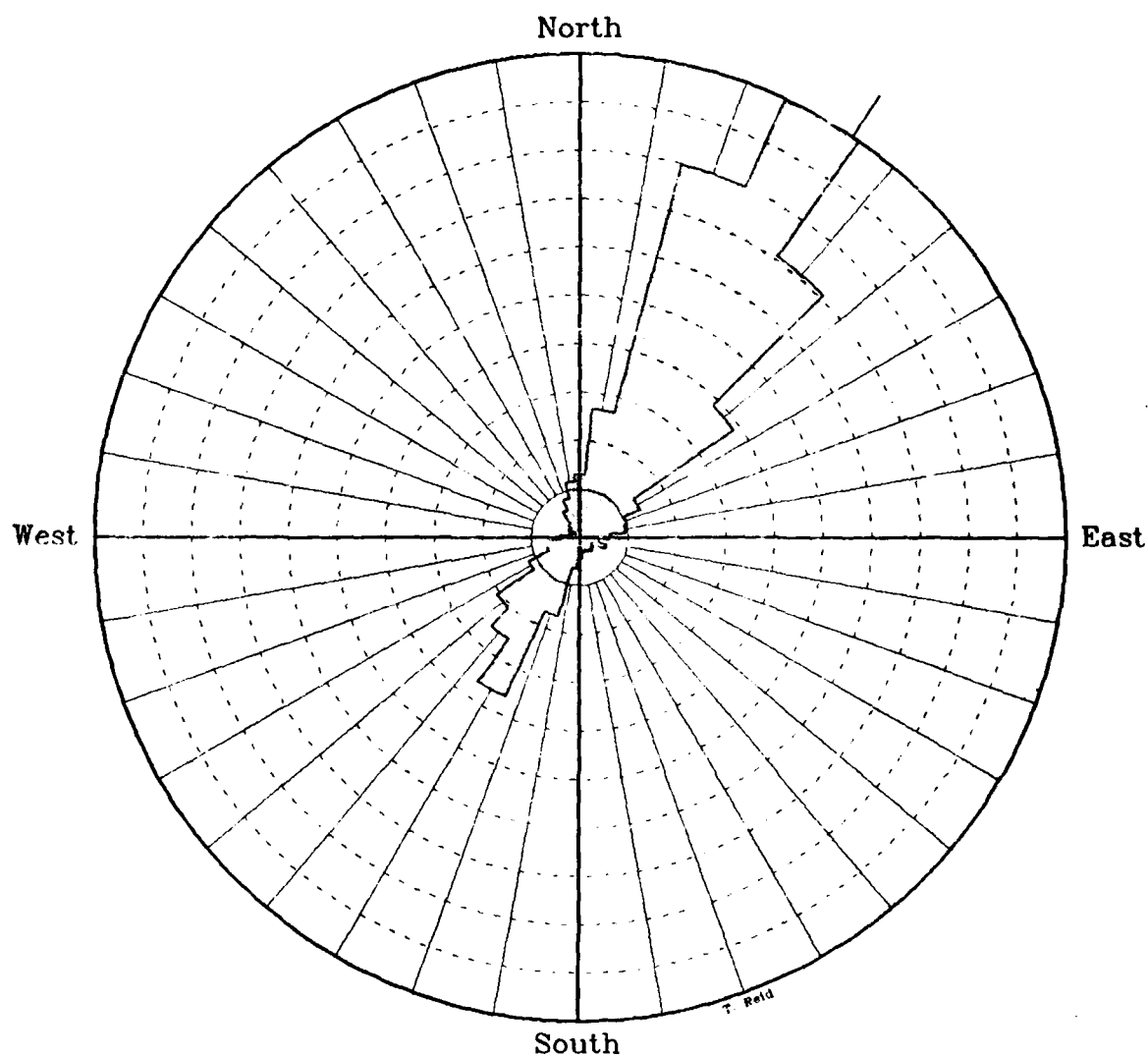
C_B 3 HRLP

Figure 13. Polar histogram for instrument C-bot showing the normalized magnitude distribution of the 3 HRLP velocity, accumulated vectorially in ten degree sectors. The downstream (+ v) direction of the rotated coordinate system is shown by the radial tick mark.

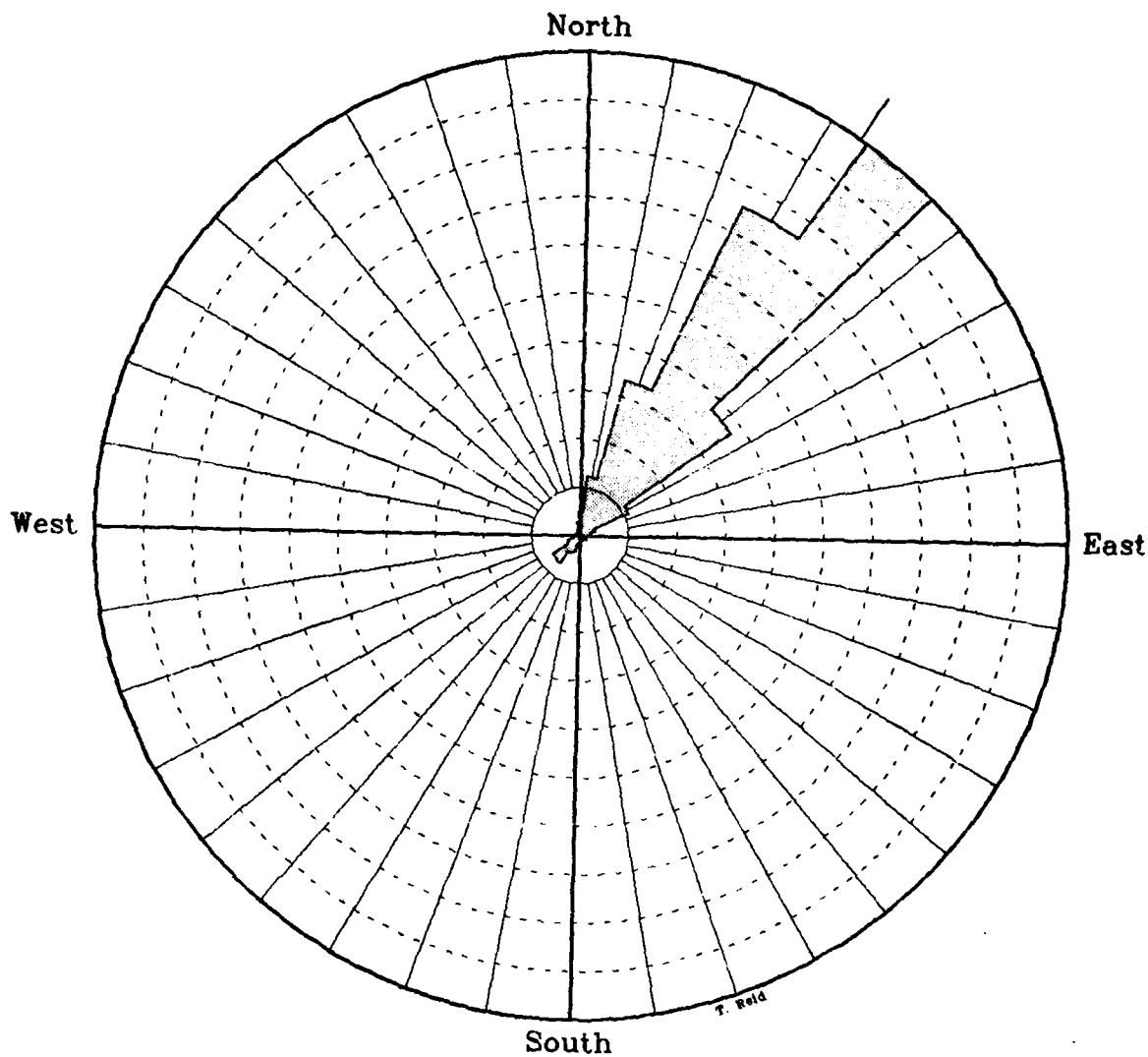
D_T 3 HRLP

Figure 14. Polar histogram for instrument D-top showing the normalized magnitude distribution of the 3 HRLP velocity, accumulated vectorially in ten degree sectors. The downstream (+ v) direction of the rotated coordinate system is shown by the radial tick mark.

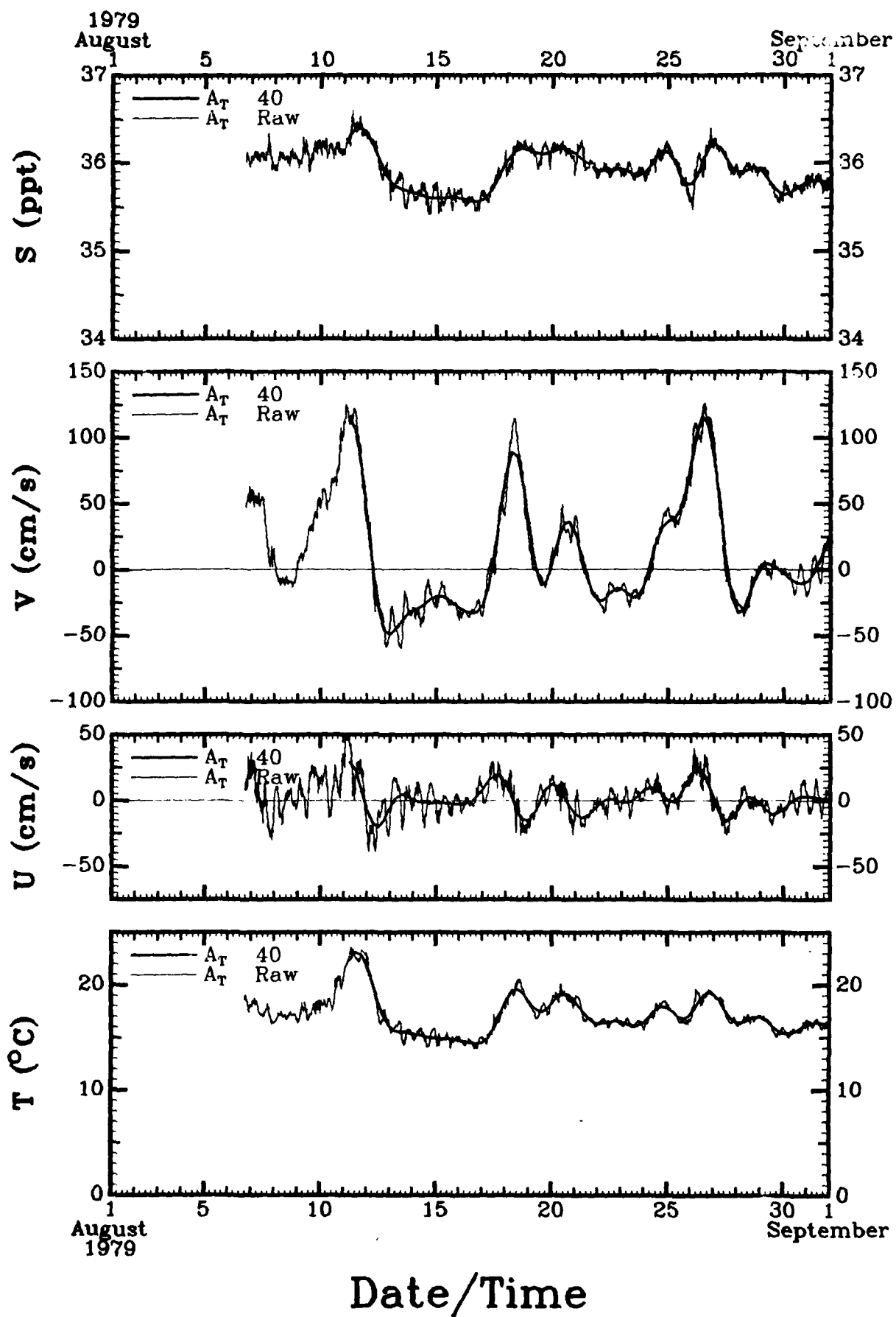
2.7 DATA PRESENTATION FORMATS

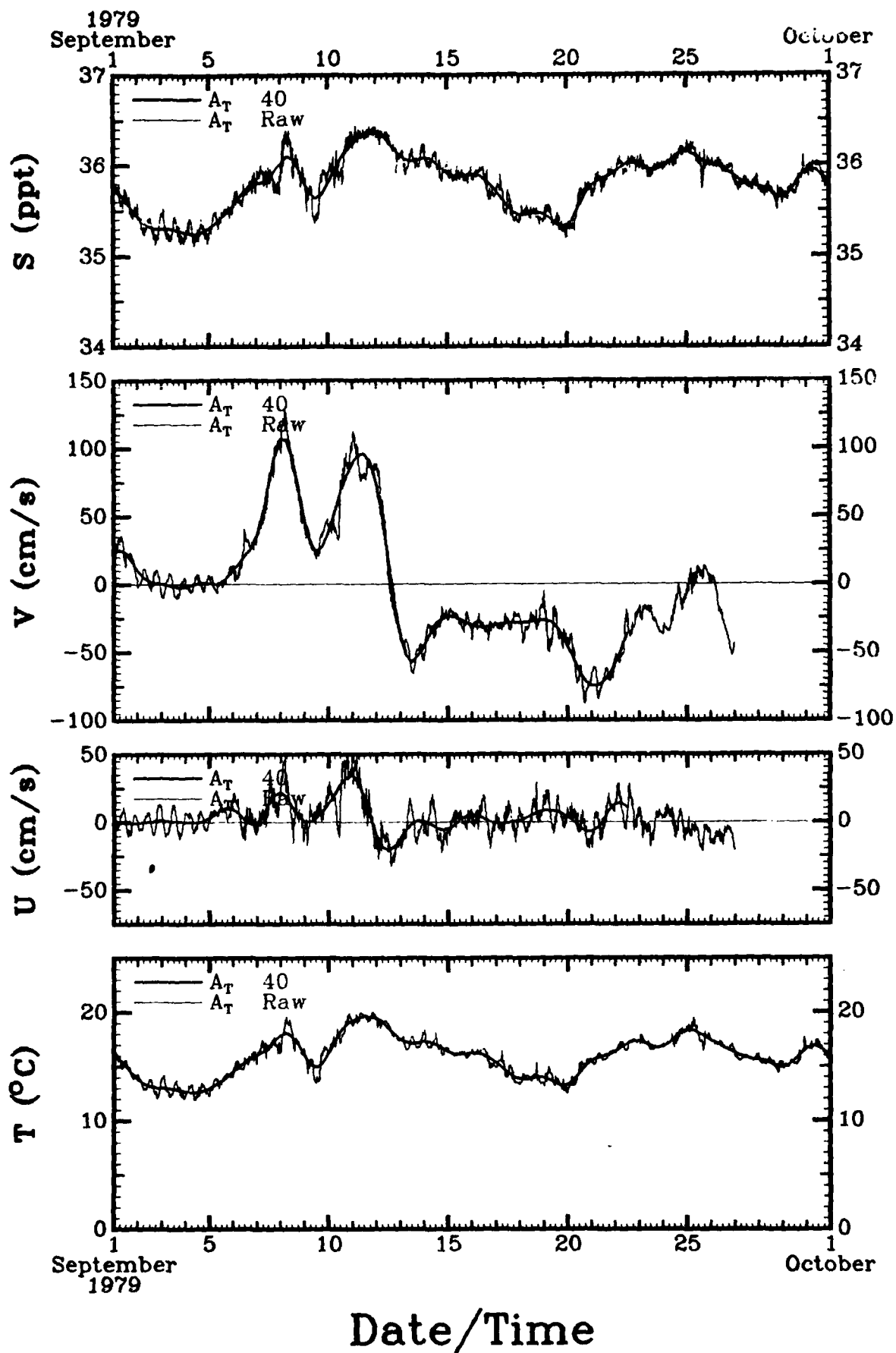
The current meter and atmospheric data sets are presented in the remainder of the report. Sections 3 through 5 show the current meter data in time series format and Section 6 shows the currents in "stick" plot format. Sections 7 and 8 show various combinations of the two data sets in time series format. All times in this report are given in Greenwich Mean Time (GMT). Section 9 shows the current meter data separately and in combination with other data sets in the frequency domain, giving spectrum, cross-spectrum, phase, and coherence information. All spectrum calculations employed the Cooley-Tukey method; that is, Fourier transformation of correlation functions. All frequency domain calculations in this report were carried out with an effective bandwidth of 0.033 cycles per day (CPD), to facilitate intercomparison. Current meter spectrum estimates nominally carry 15 degrees of freedom (DOF), although this number varies somewhat because of early termination of several records. For 15 DOF, the 95% confidence interval on phase estimates is about $\pm(27, 18, 12)$ degrees for coherence squared values of (0.4, 0.6, 0.8).

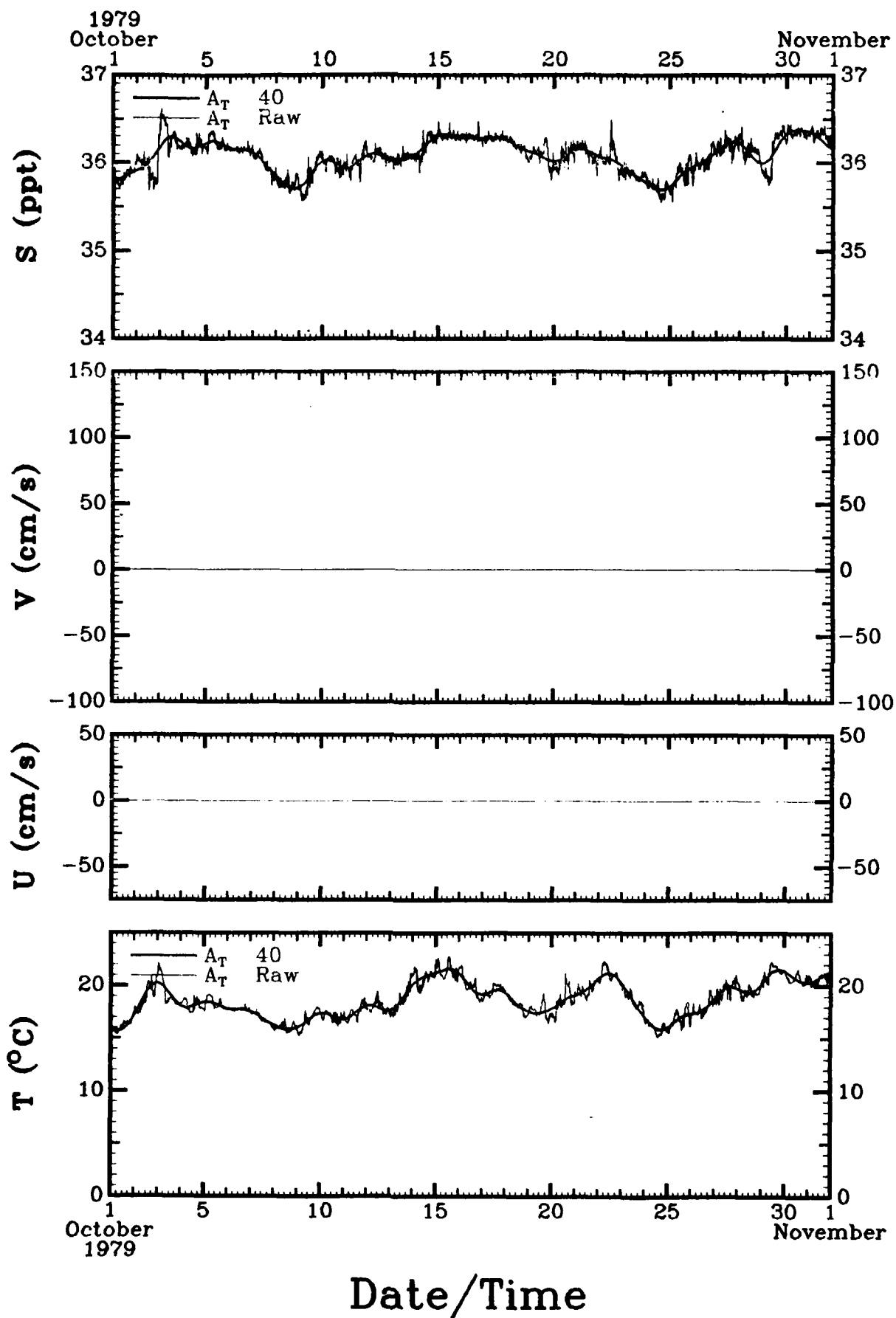
SECTION 3

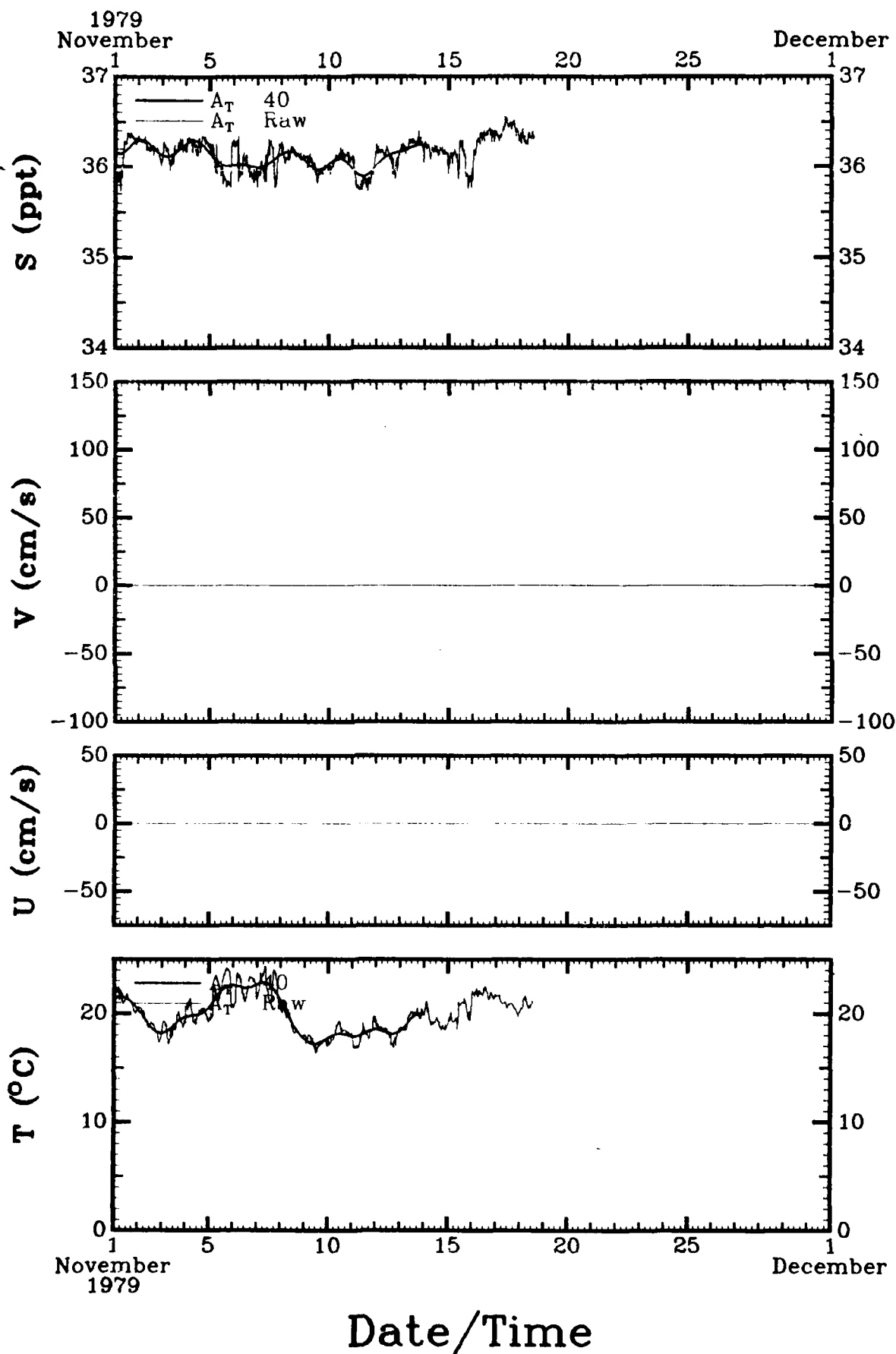
Raw and 40 HRLP Data for Each Instrument

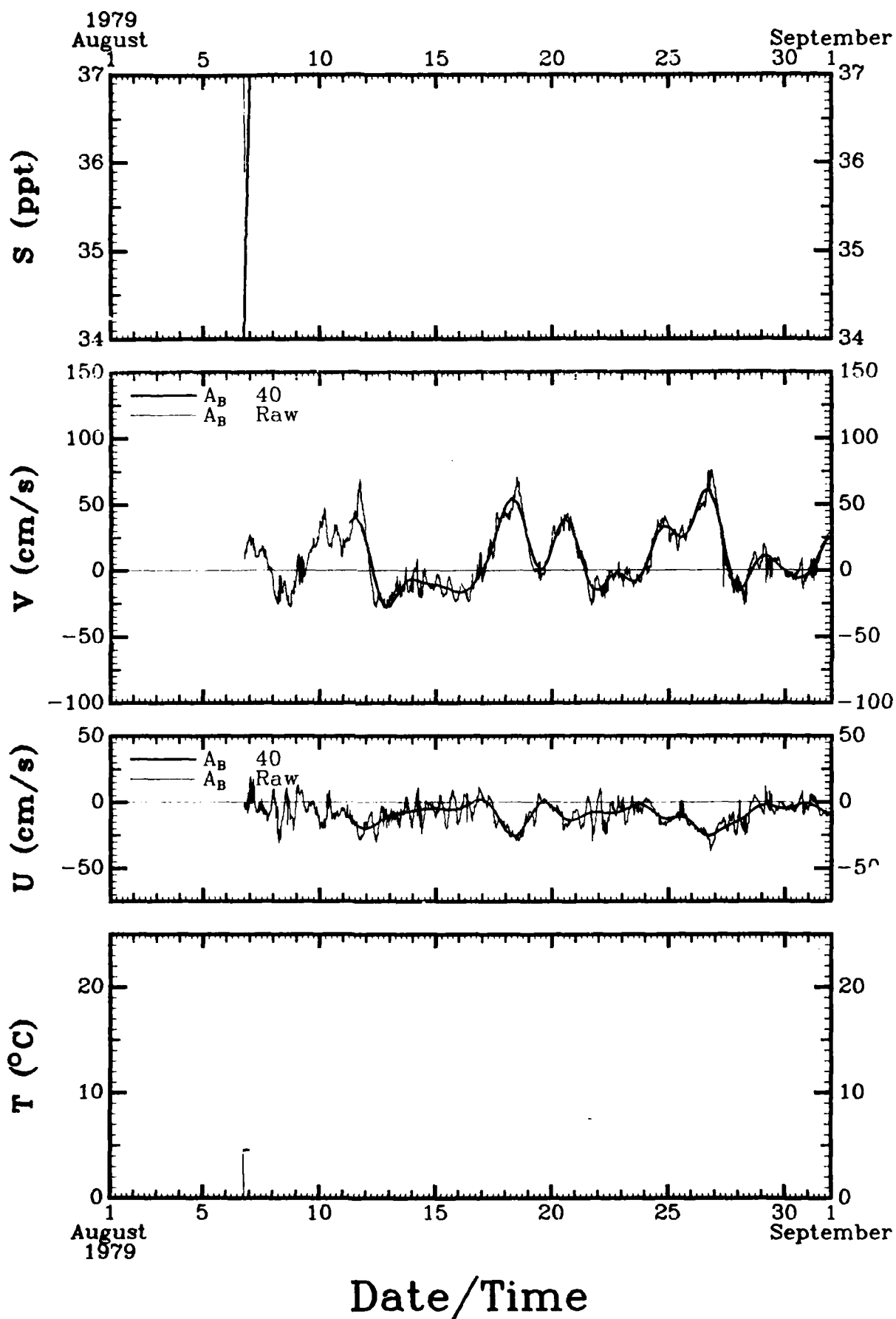
Figures 15 through 22 show the raw and superimposed 40 HRLP current meter data separately by month for each instrument. Common scaling of similar data has been used throughout this section.

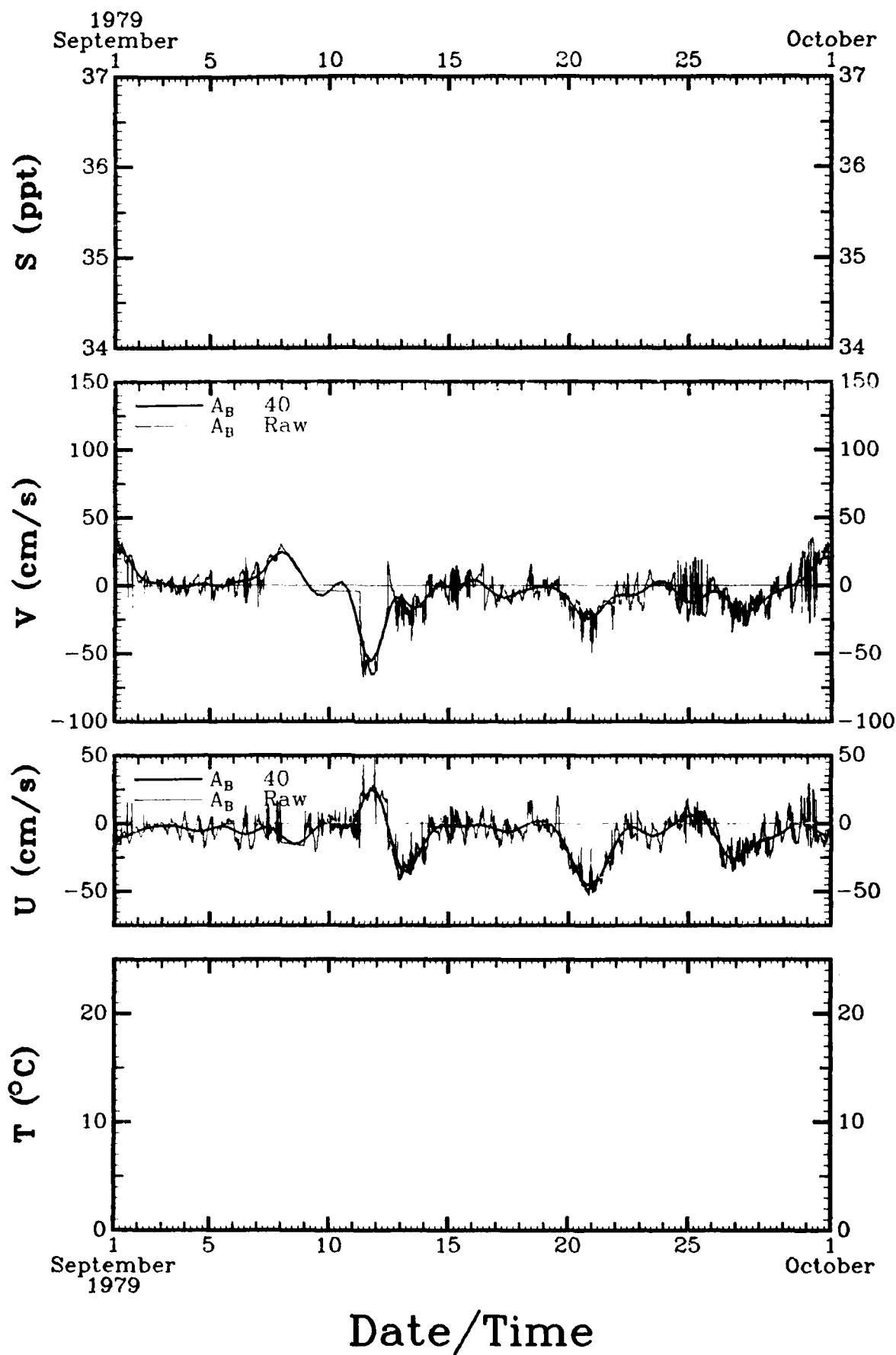


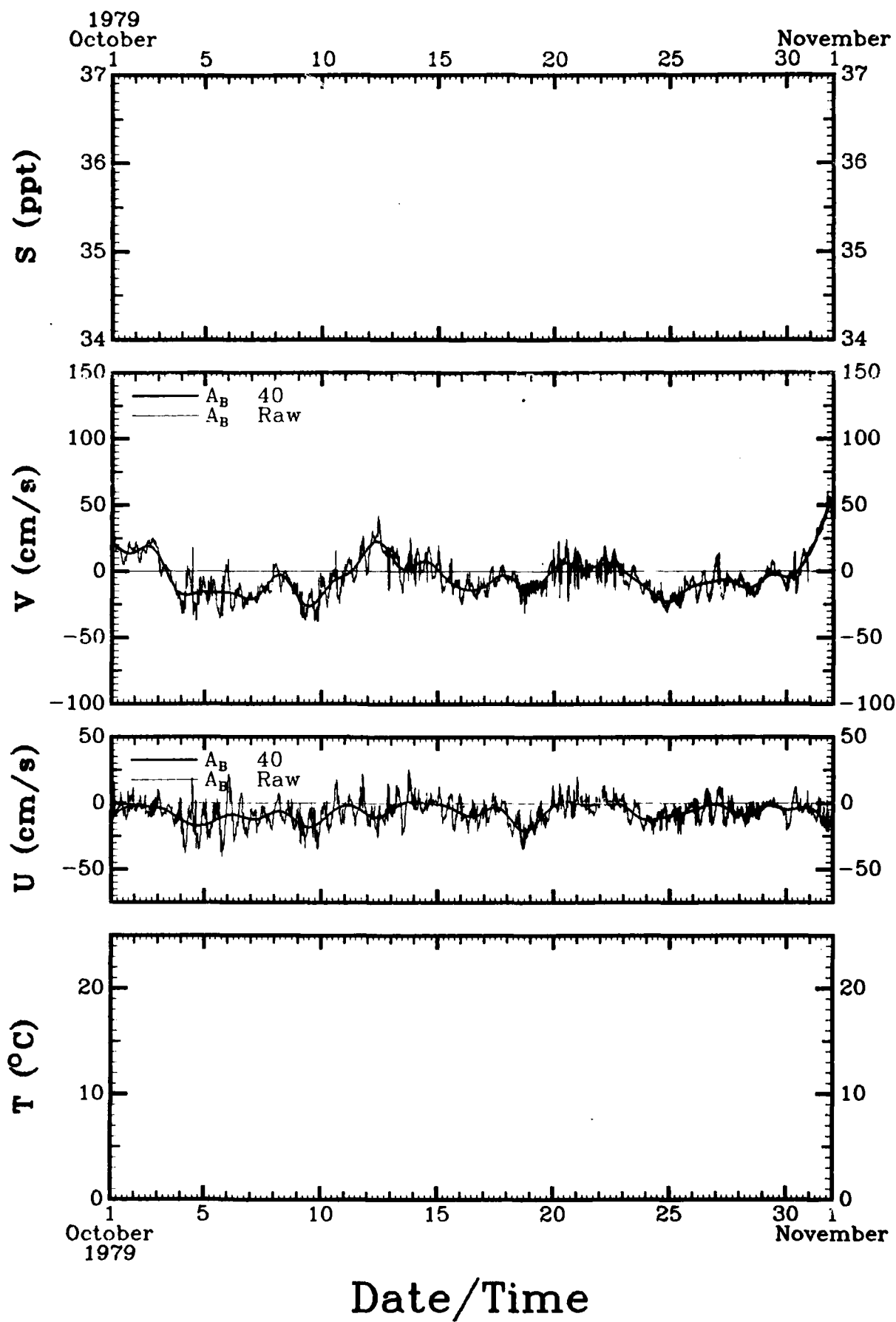


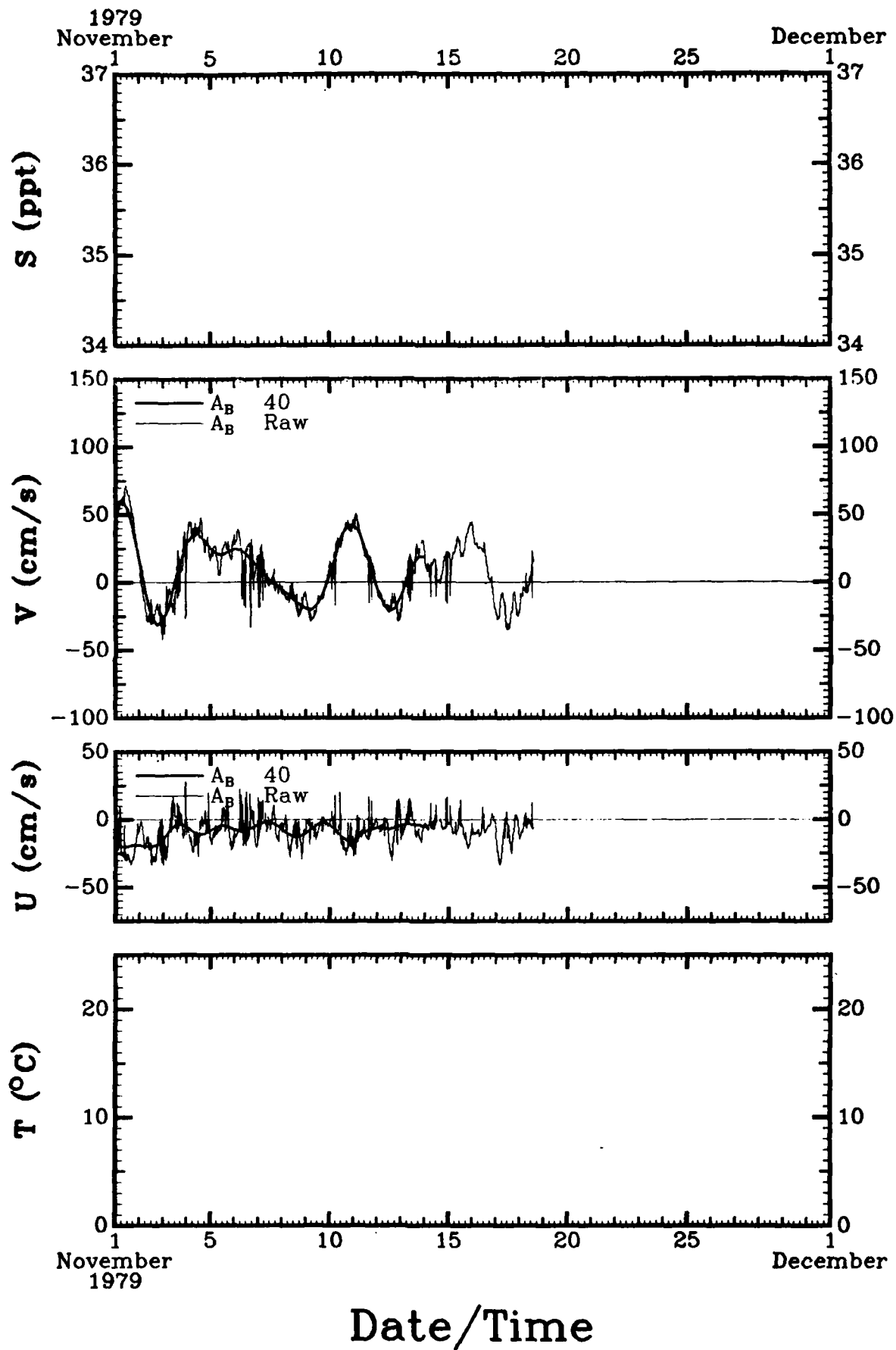


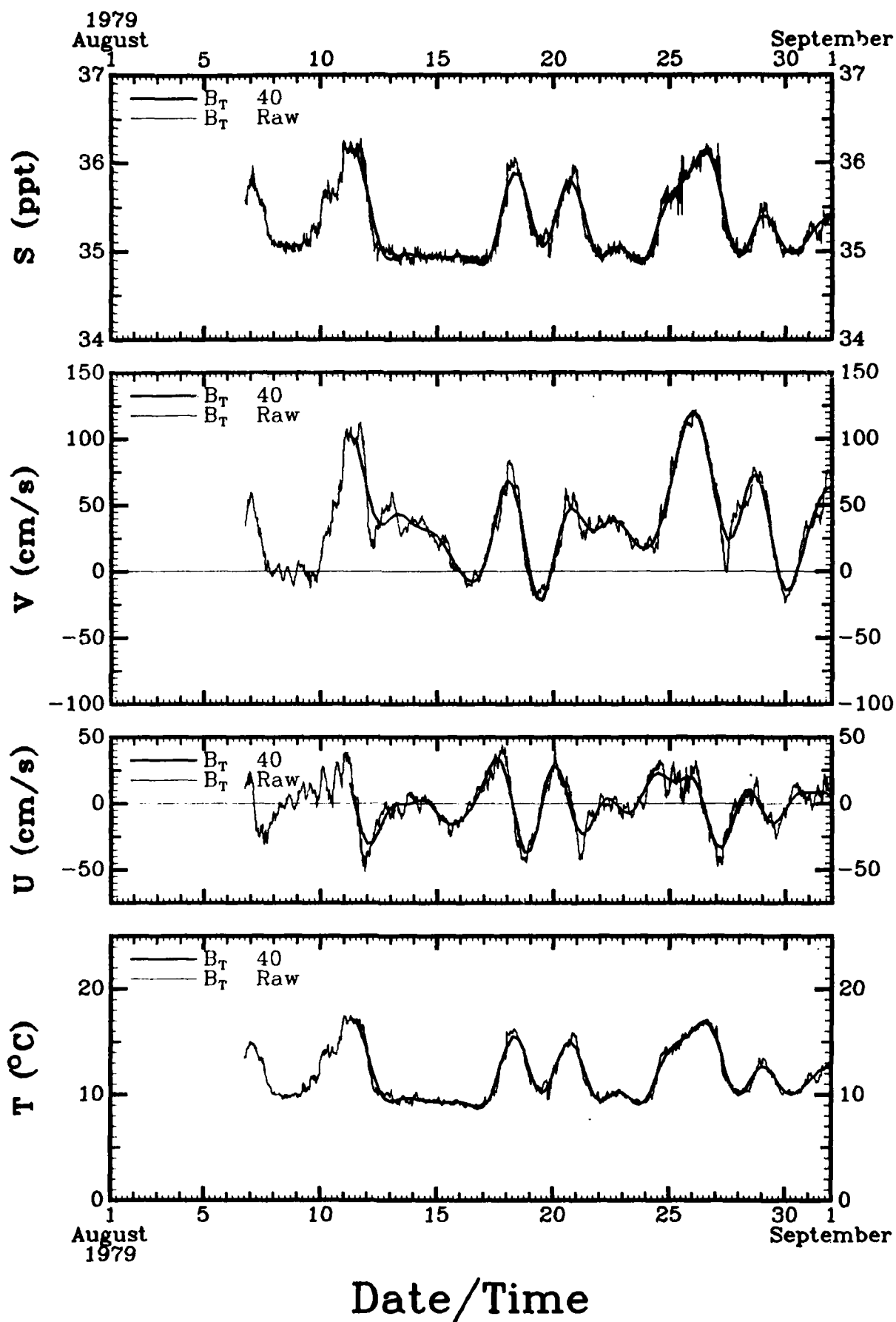


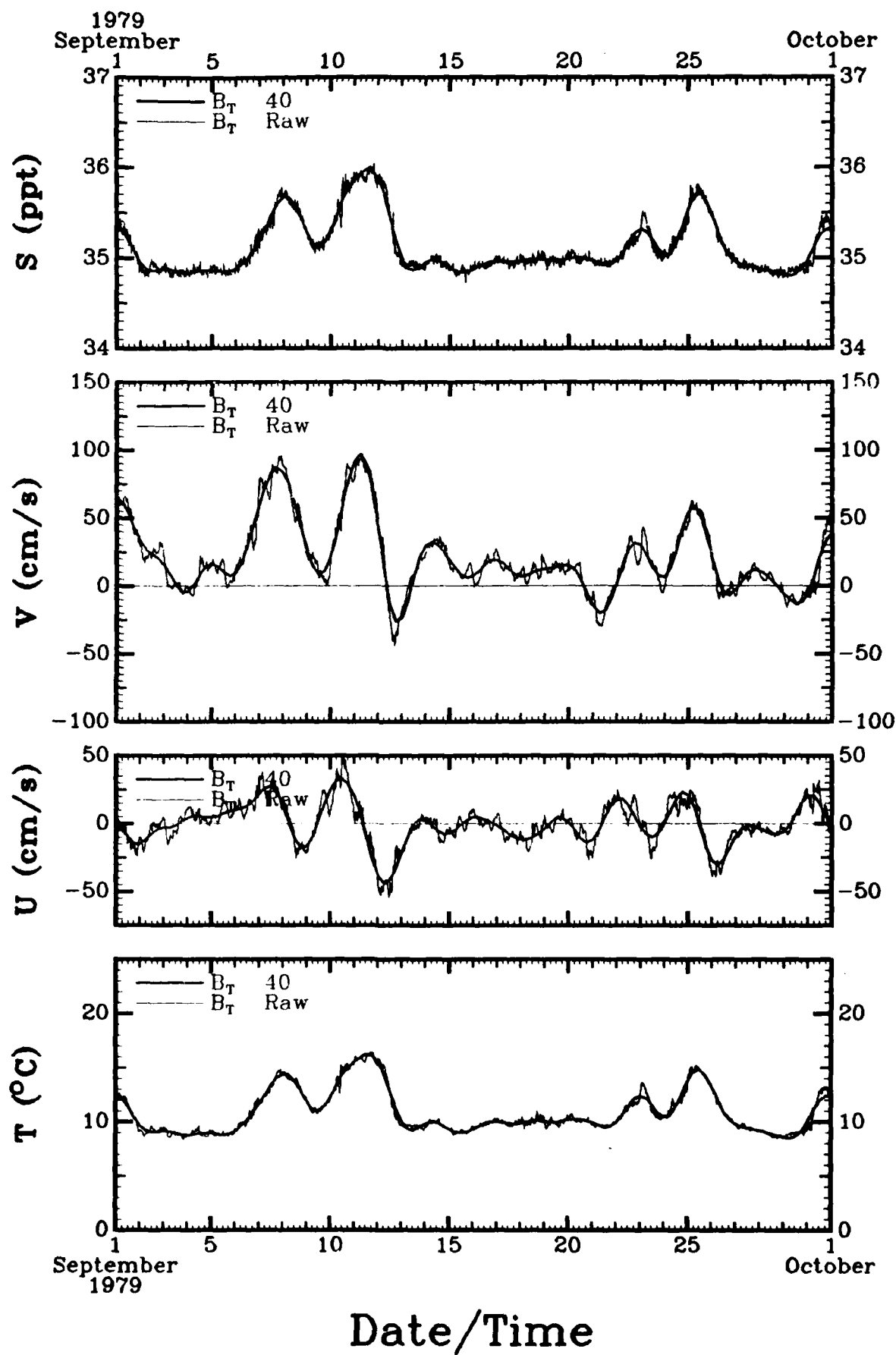


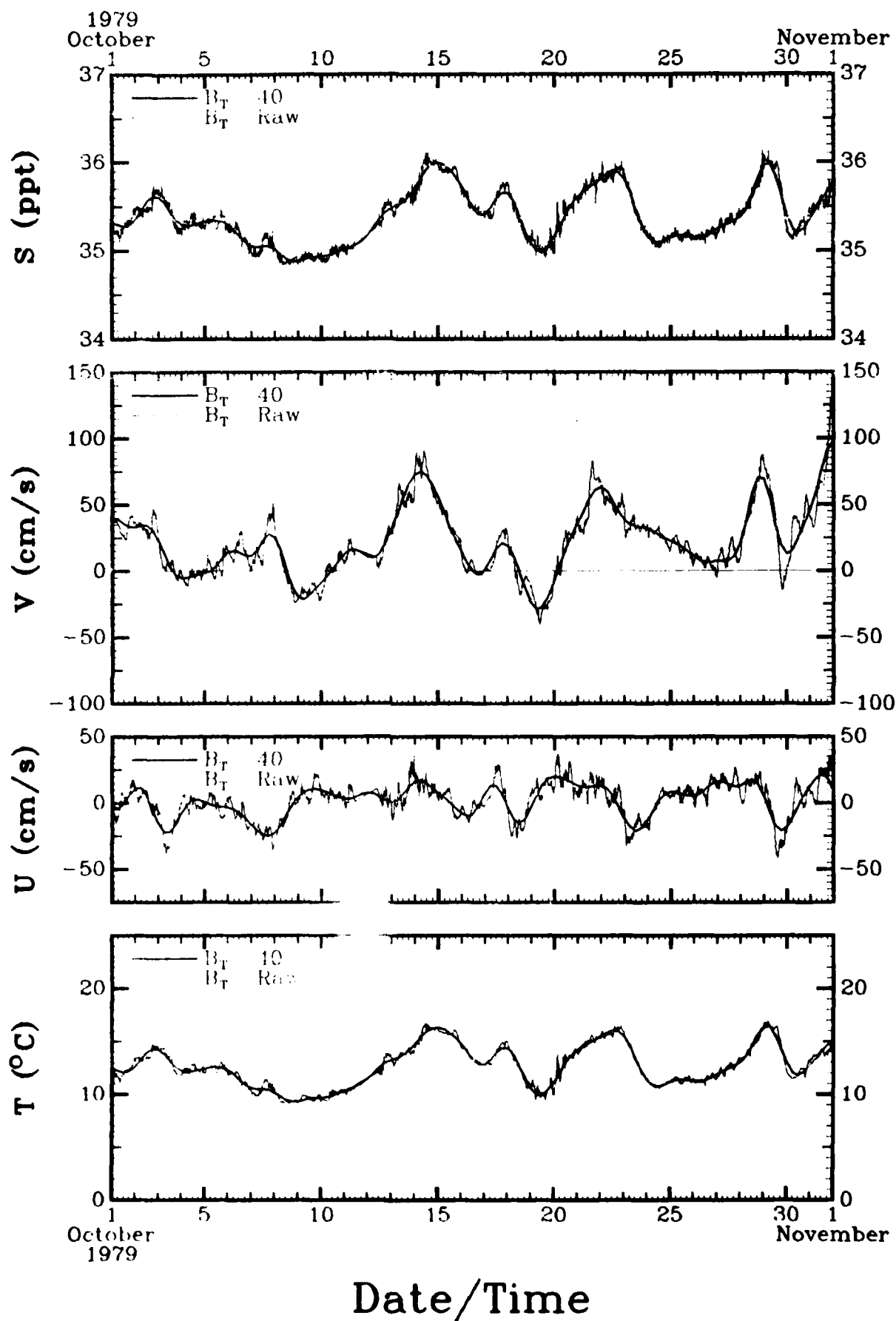


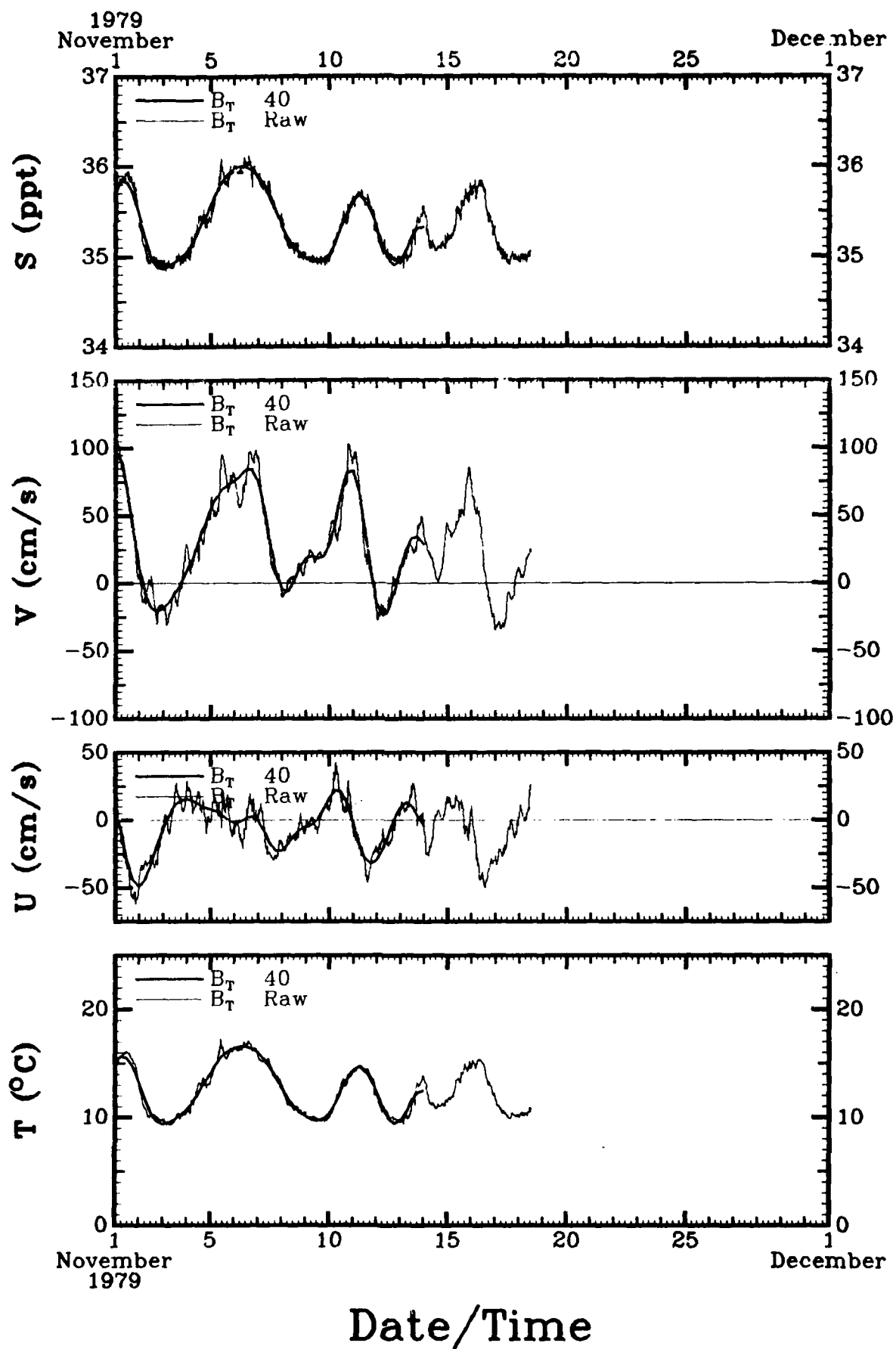


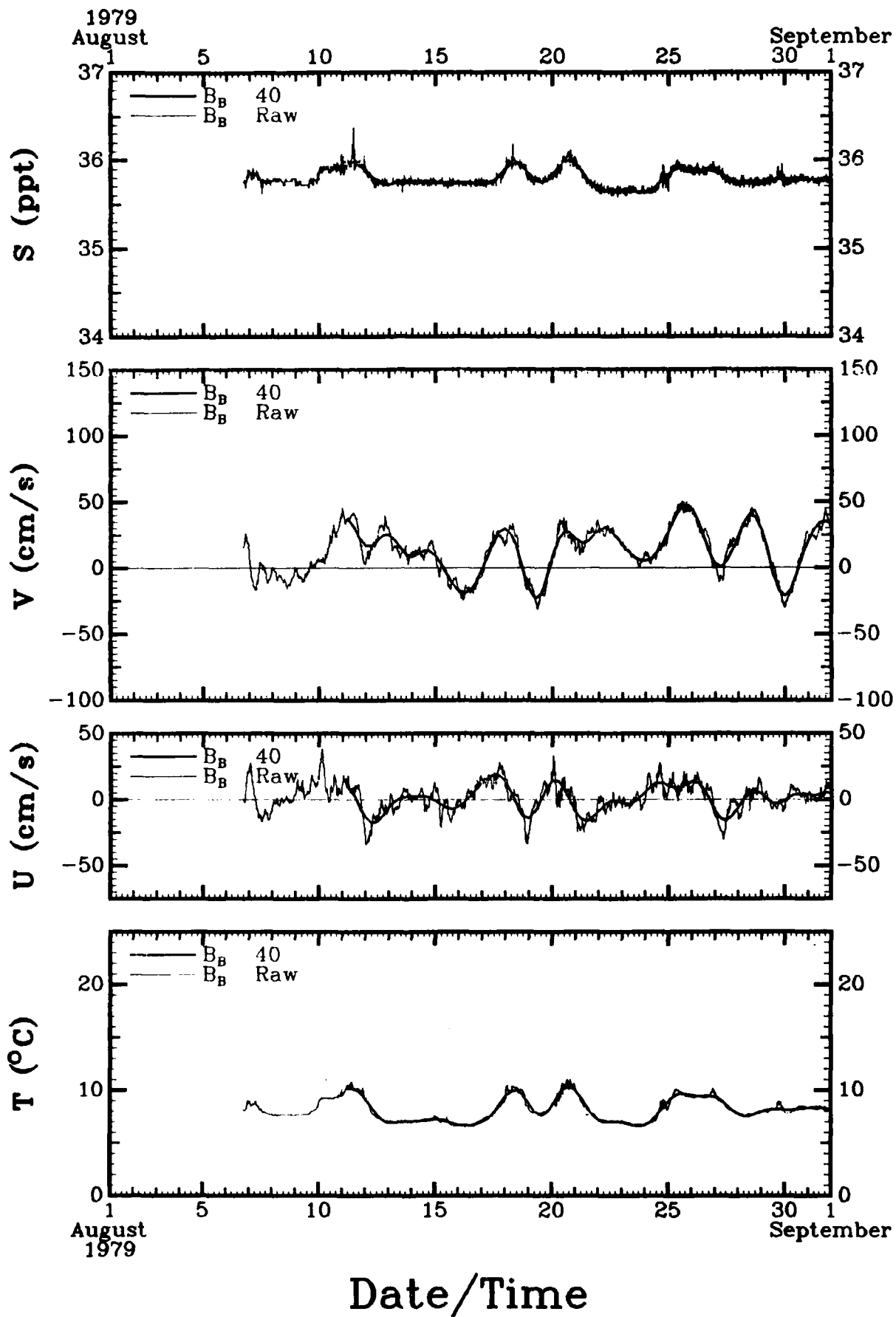


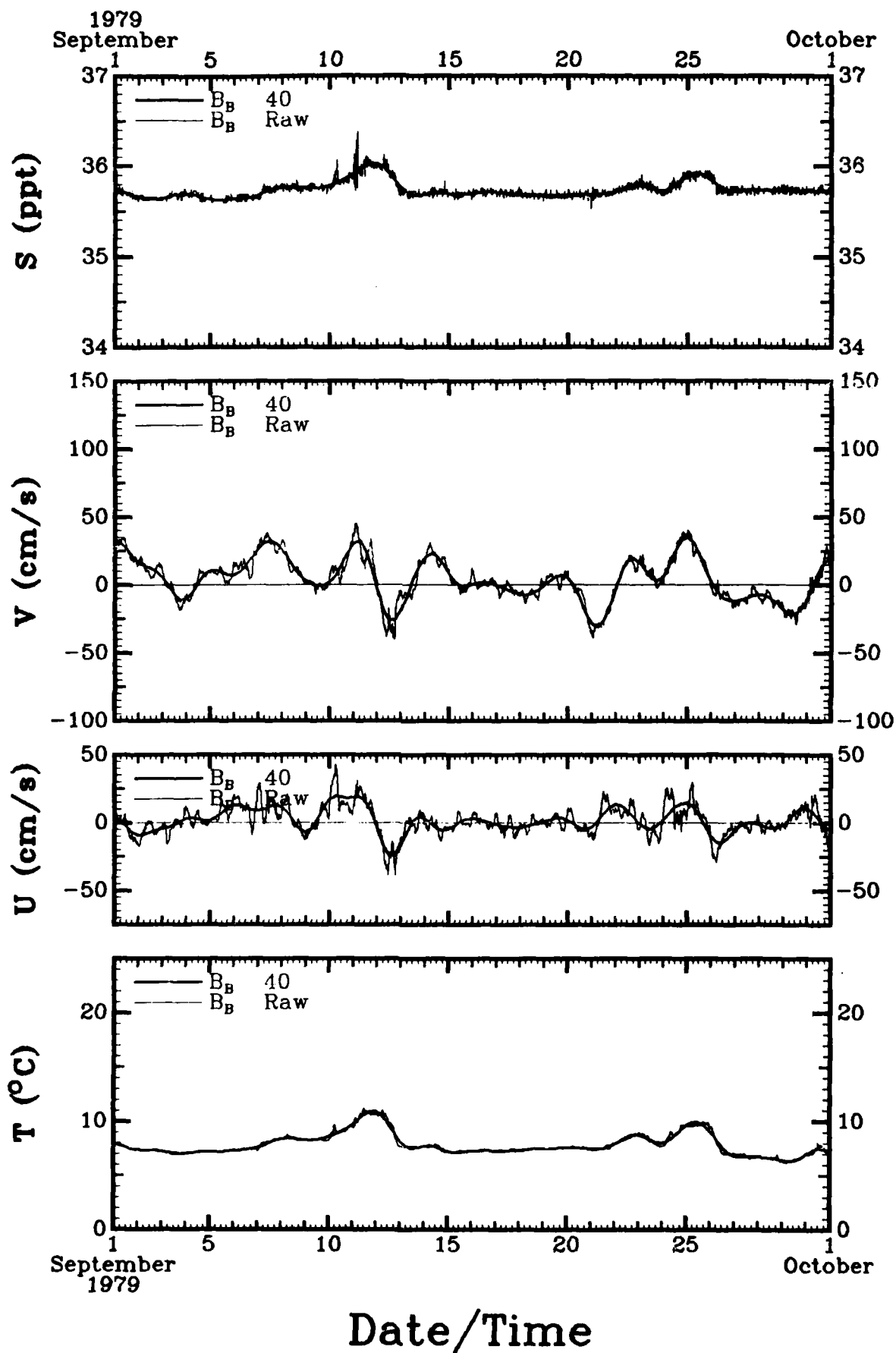


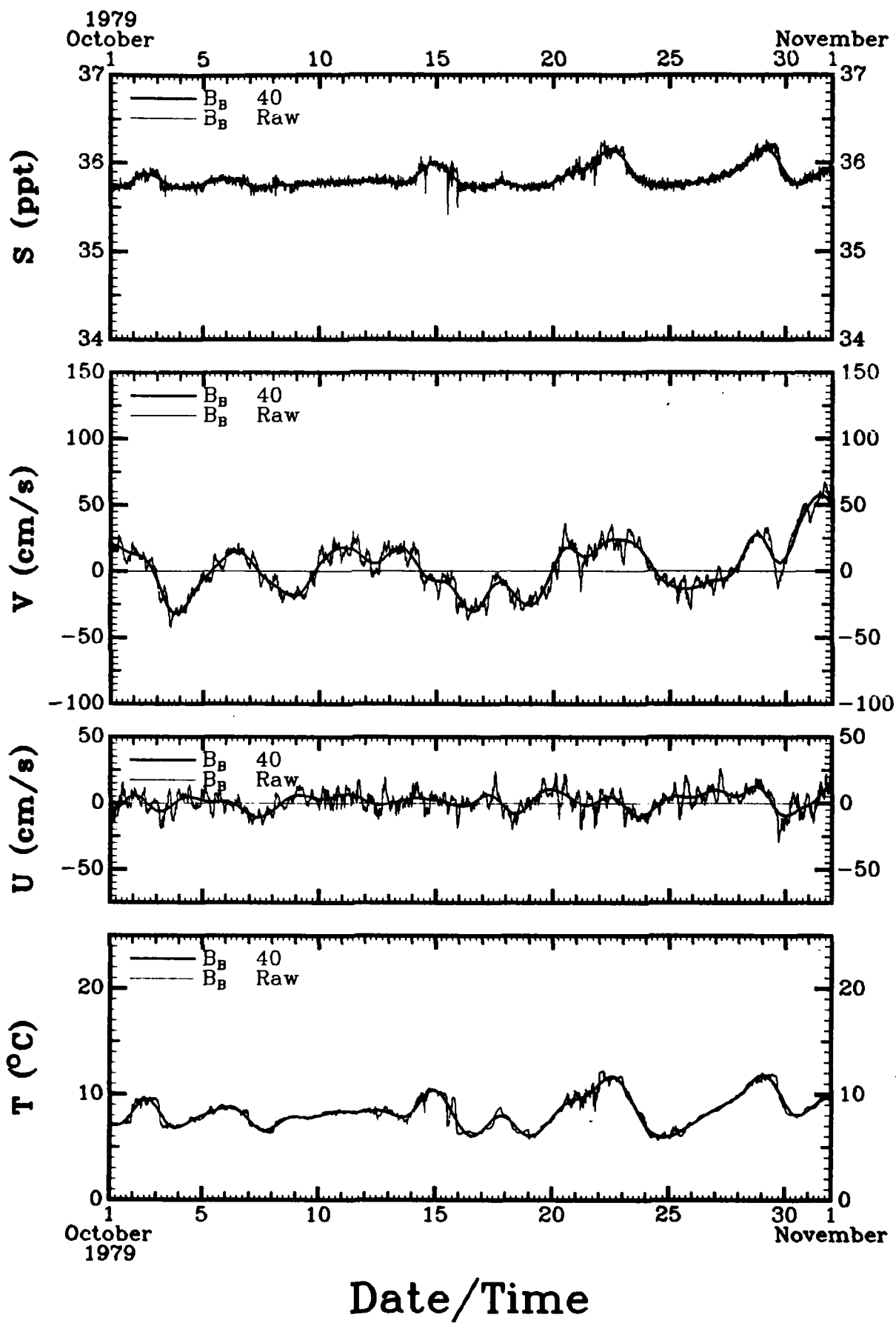


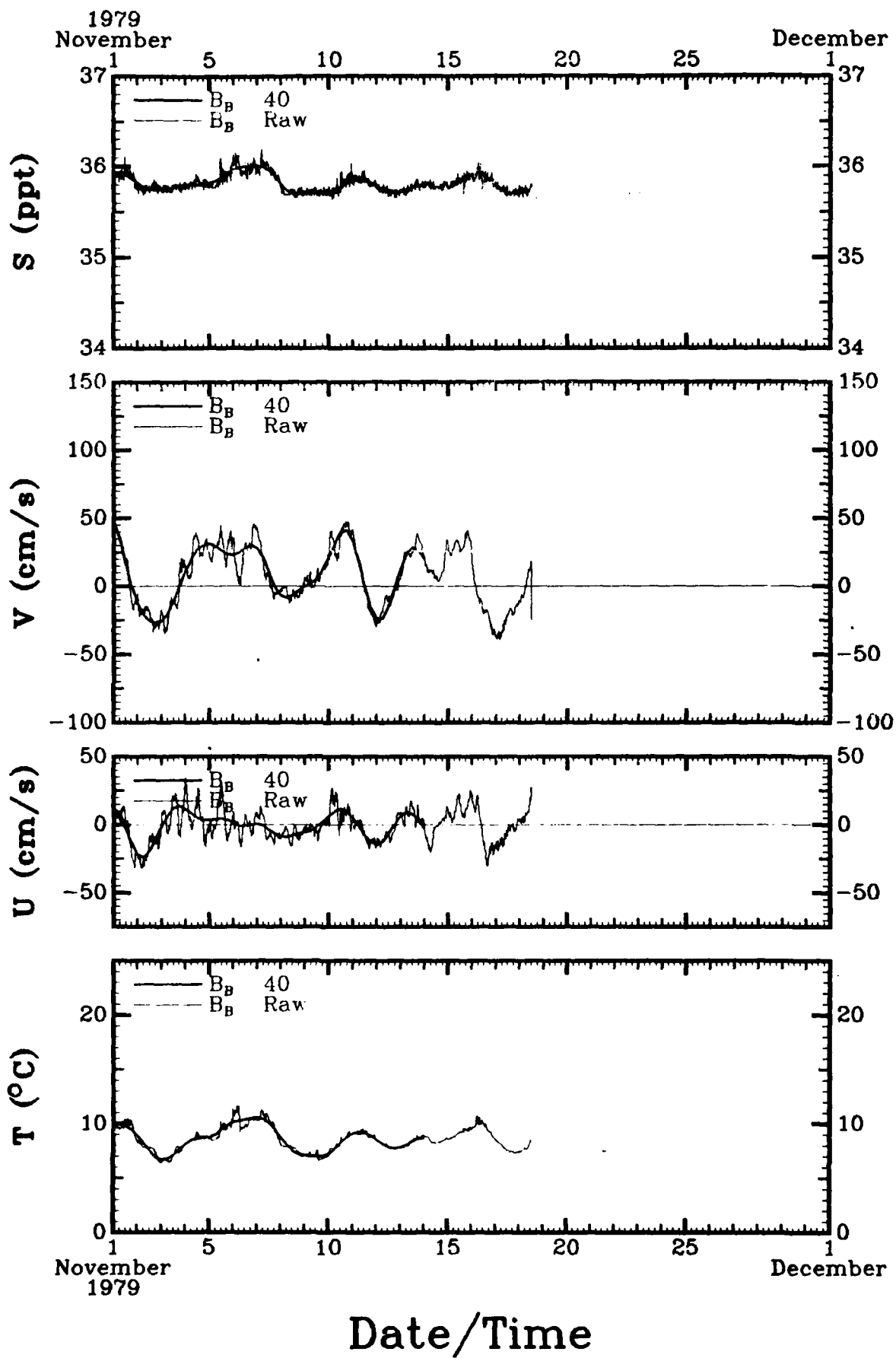


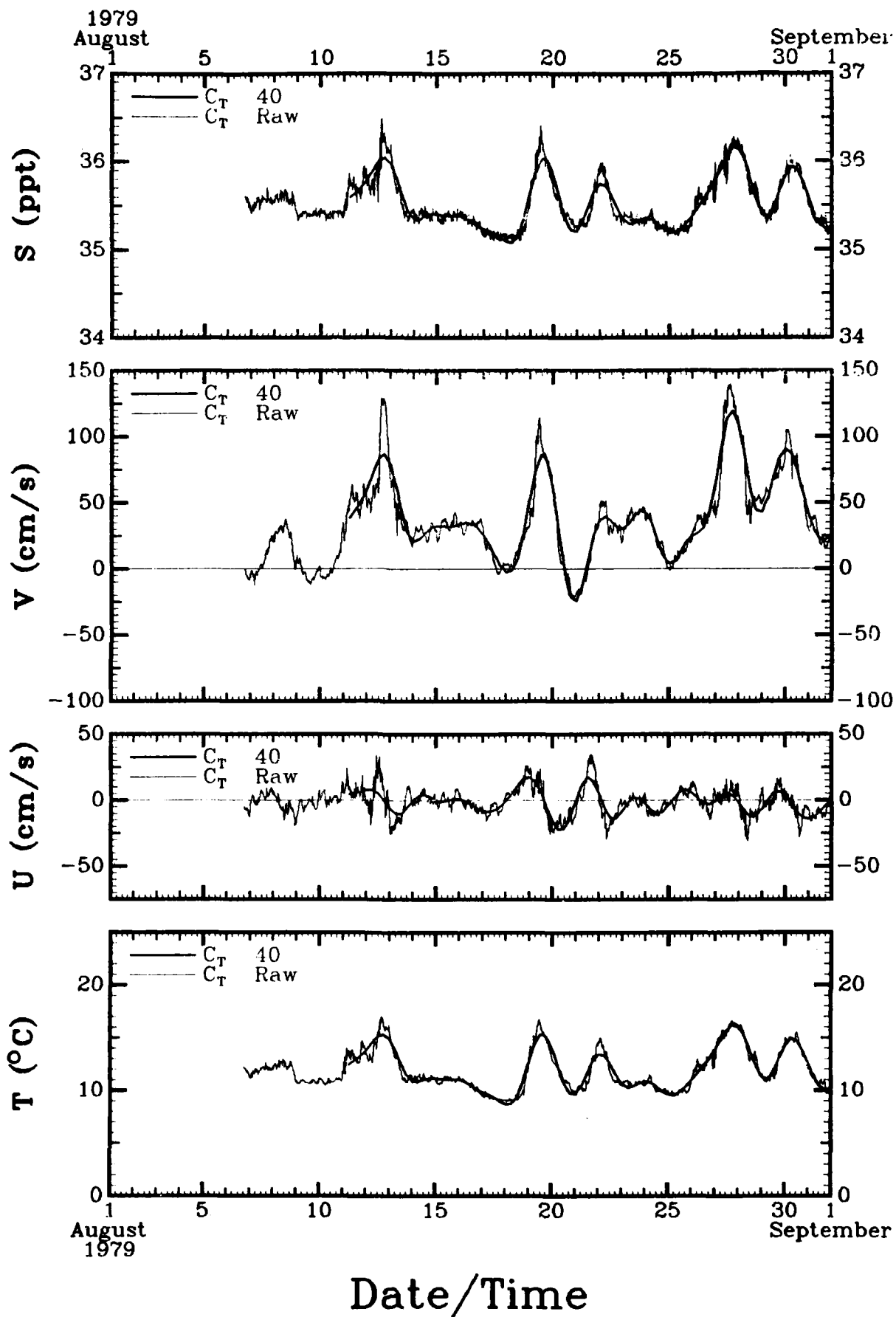


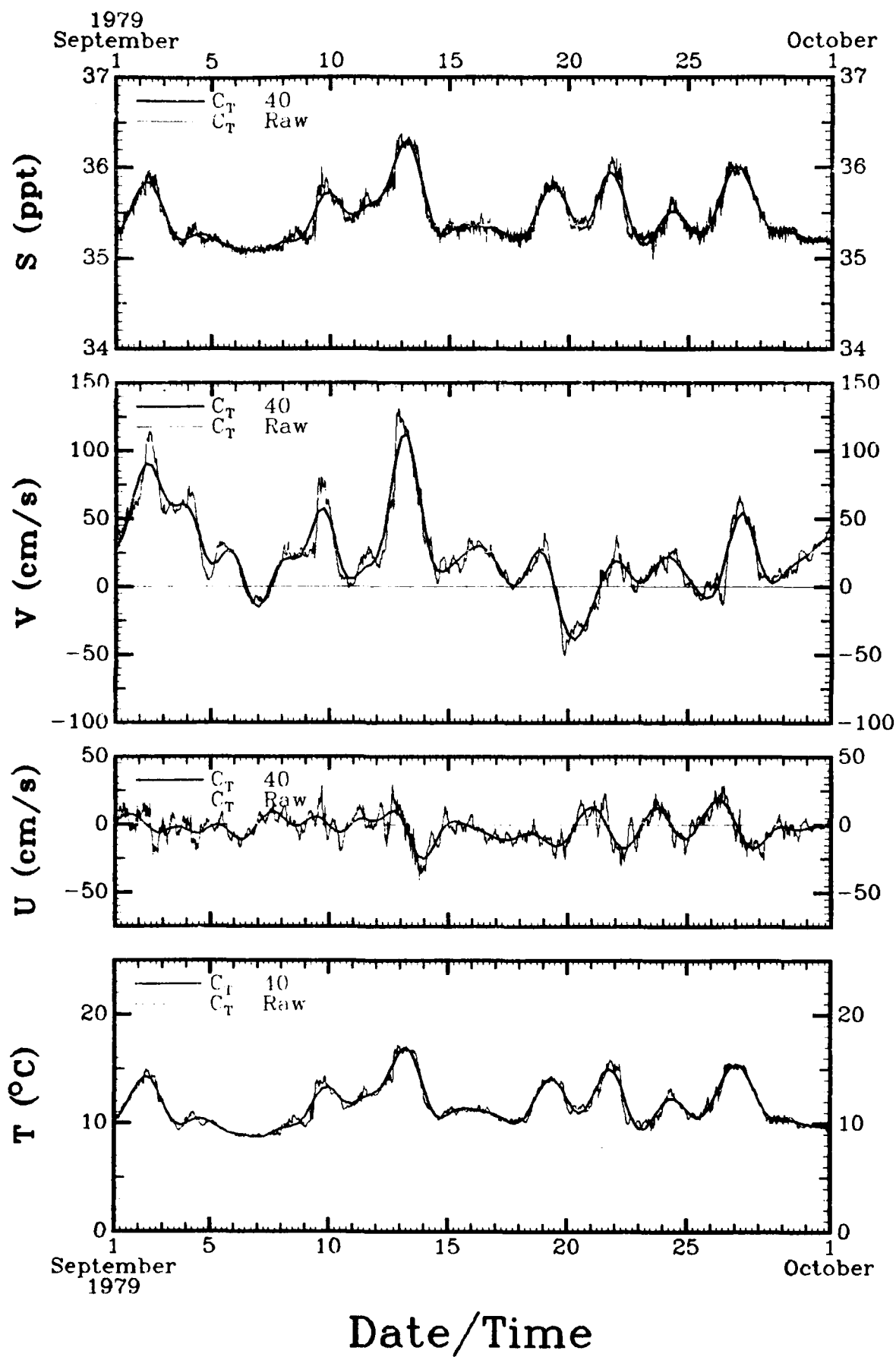


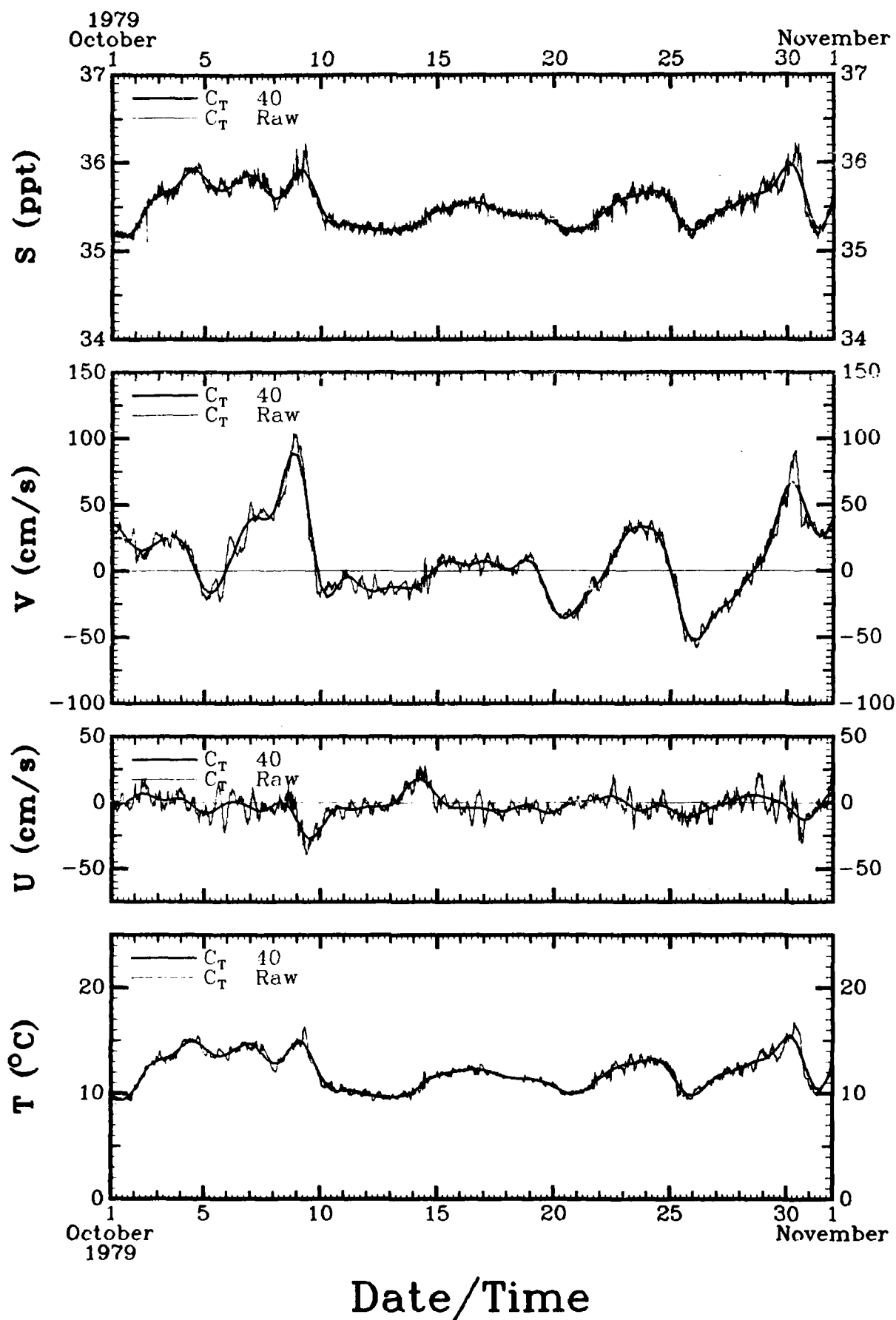


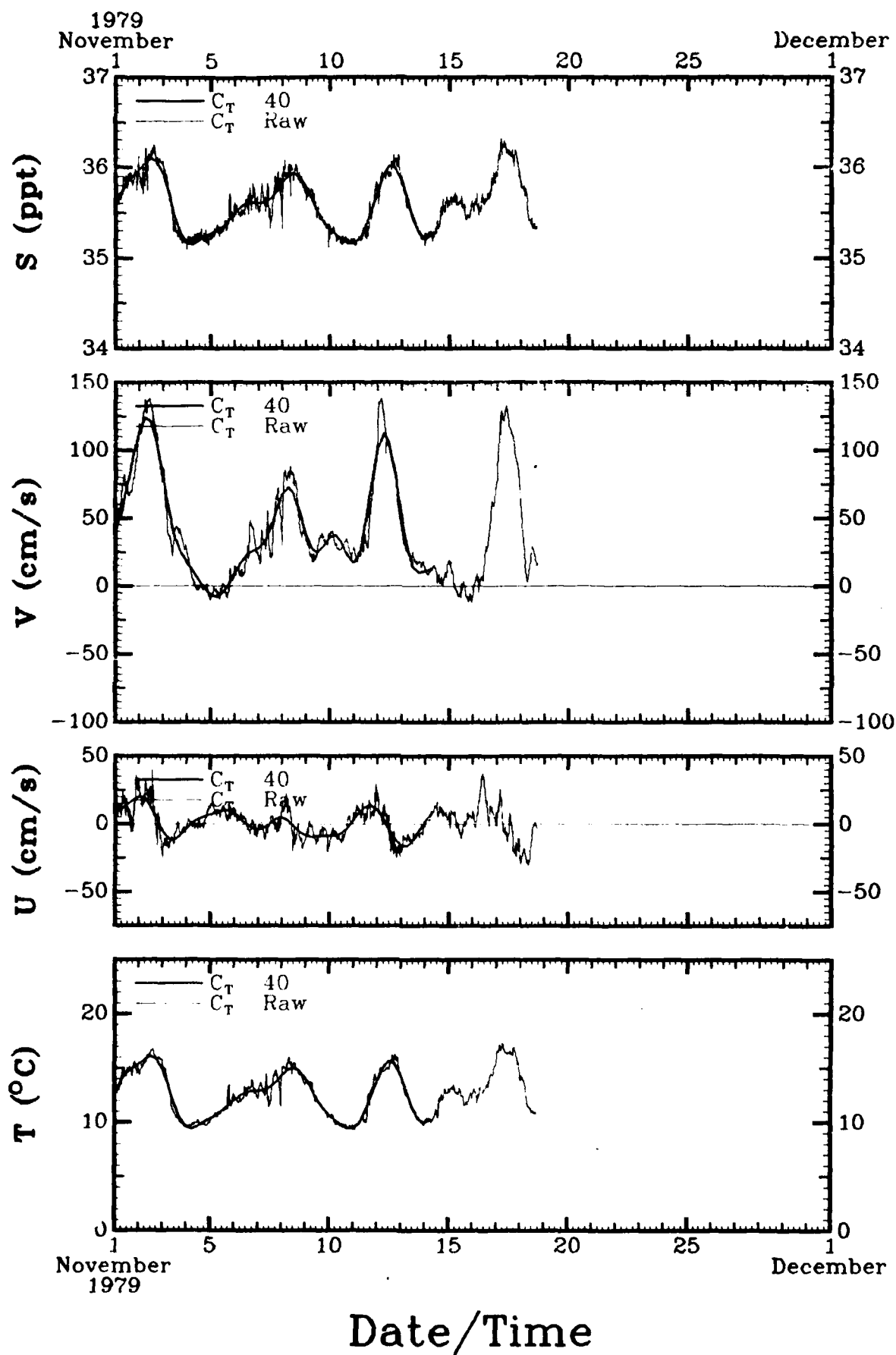


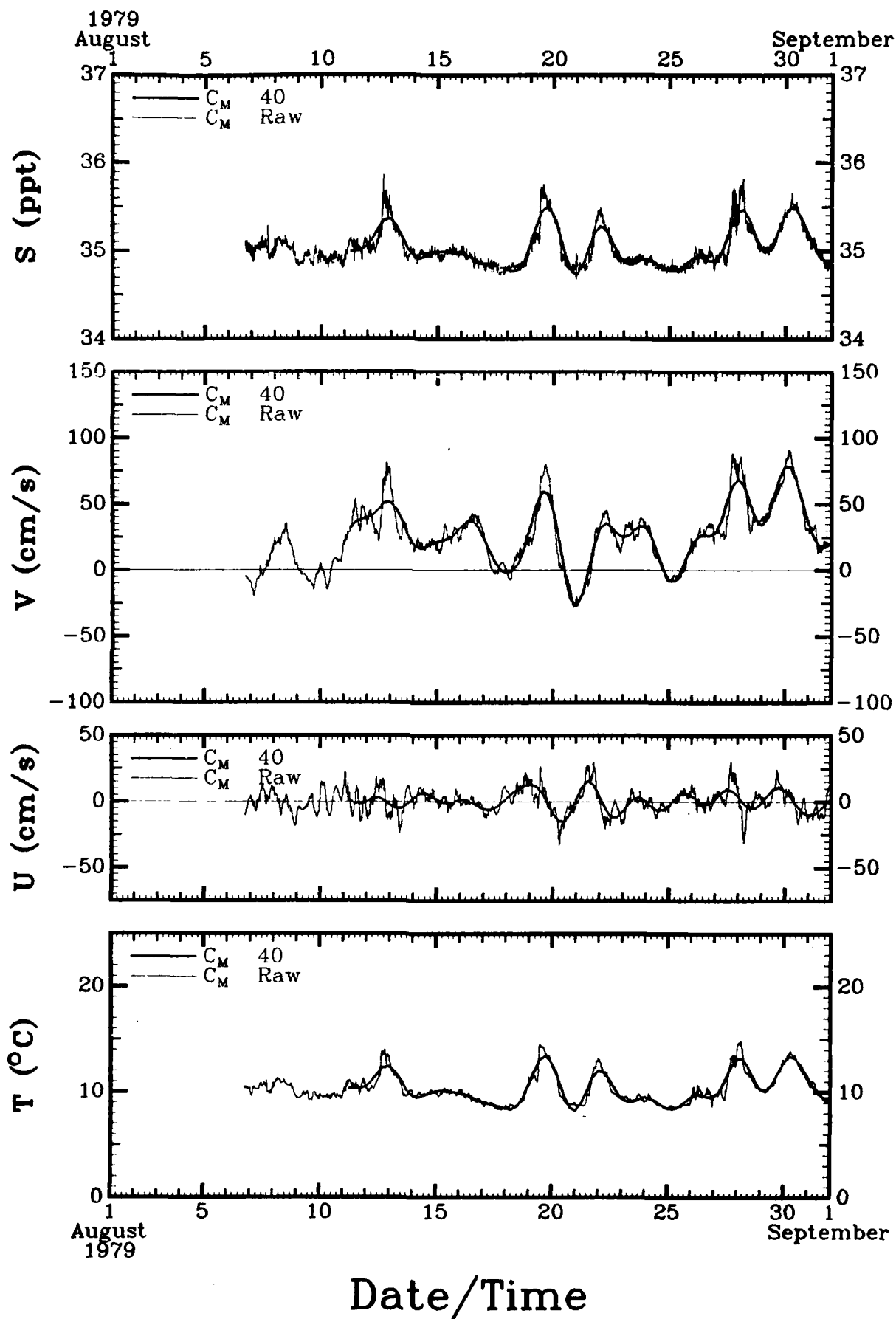


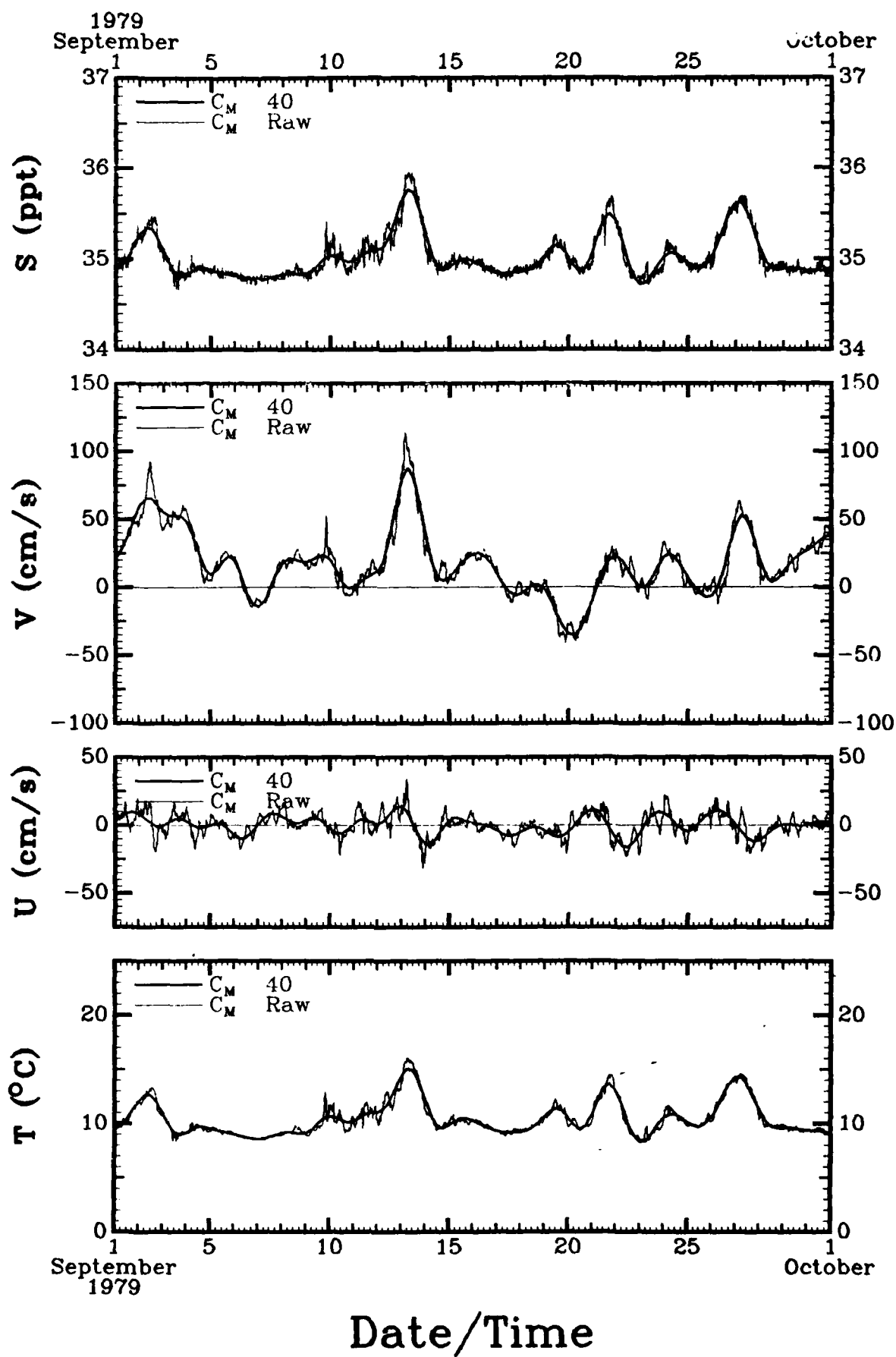


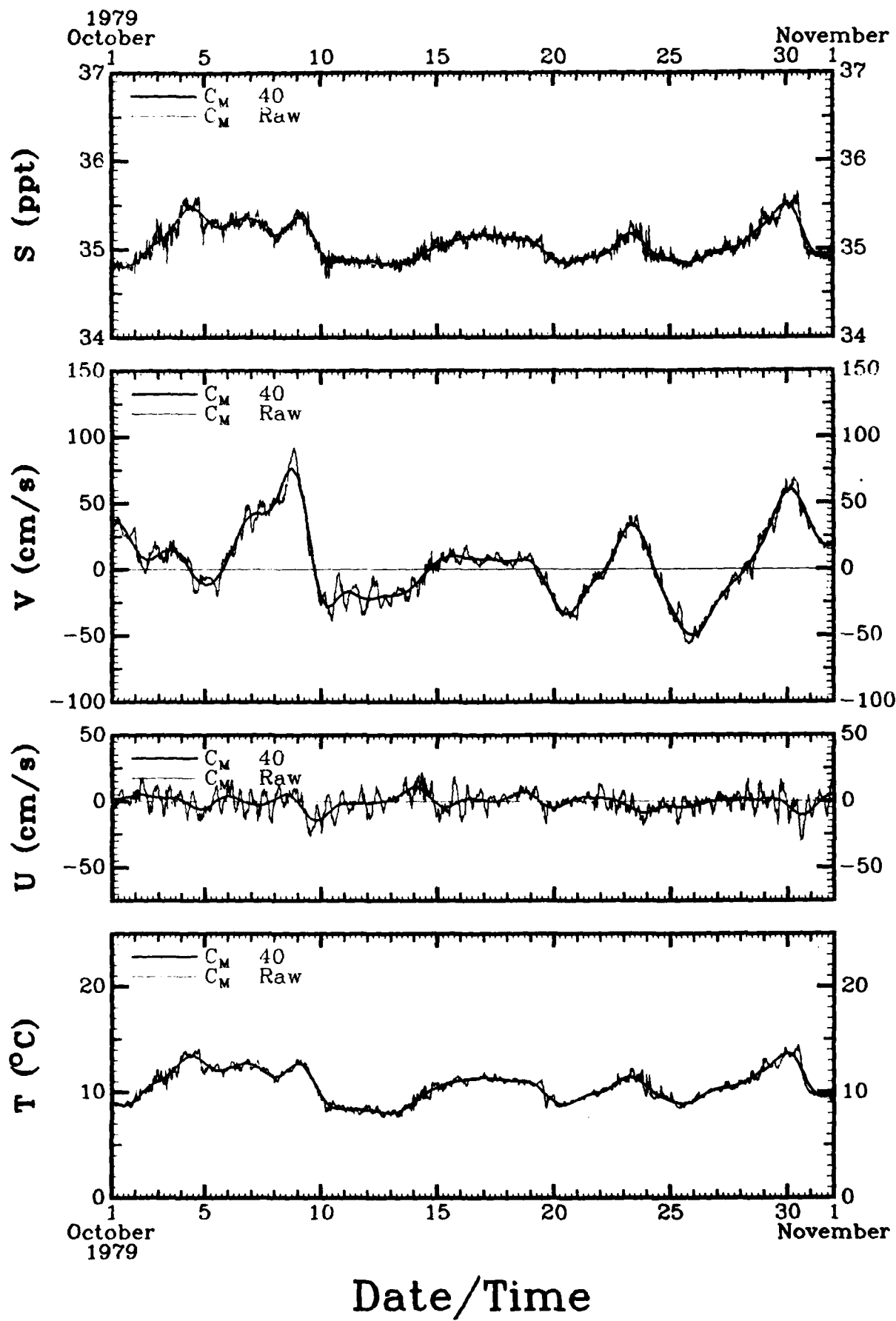


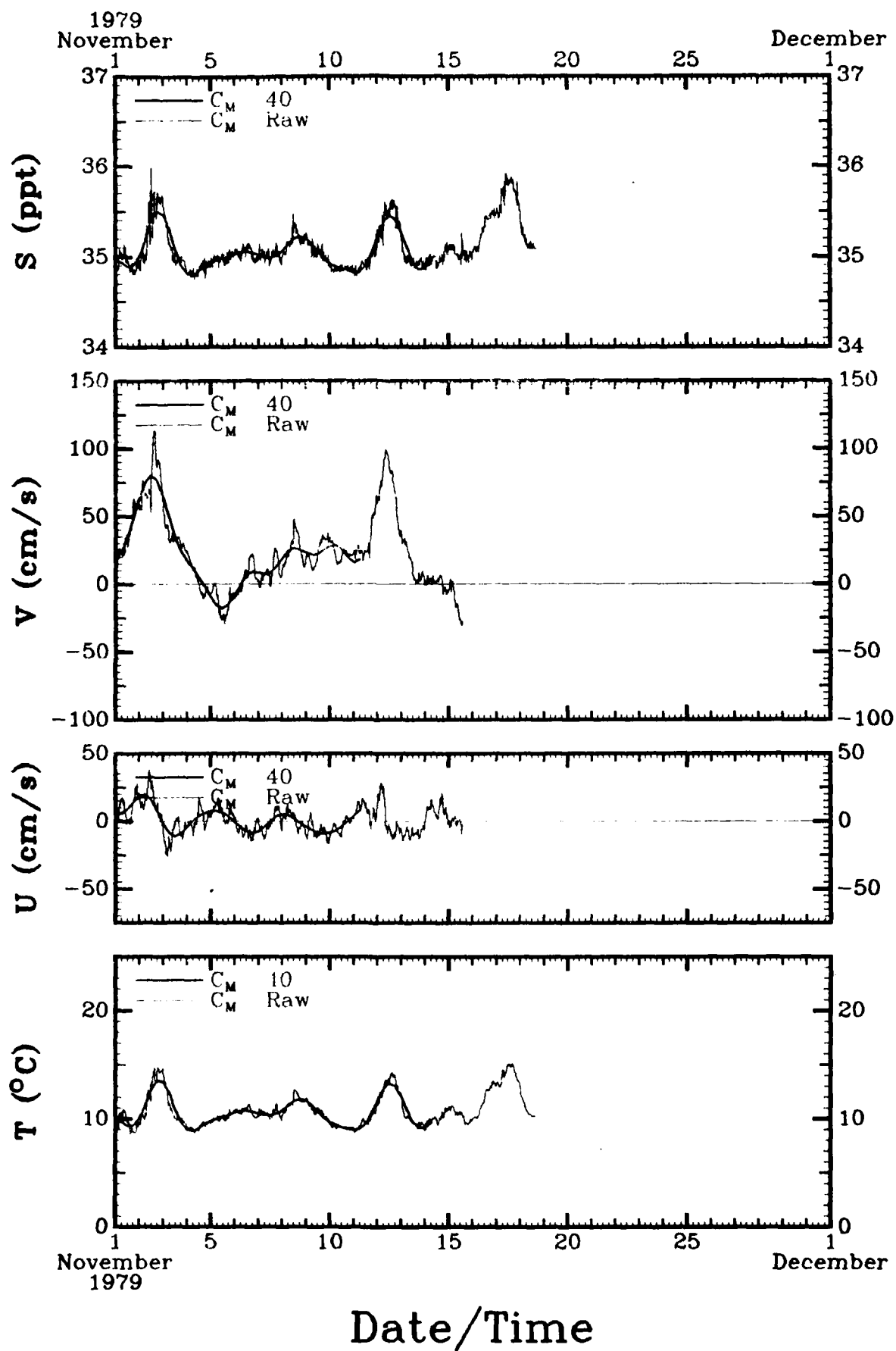


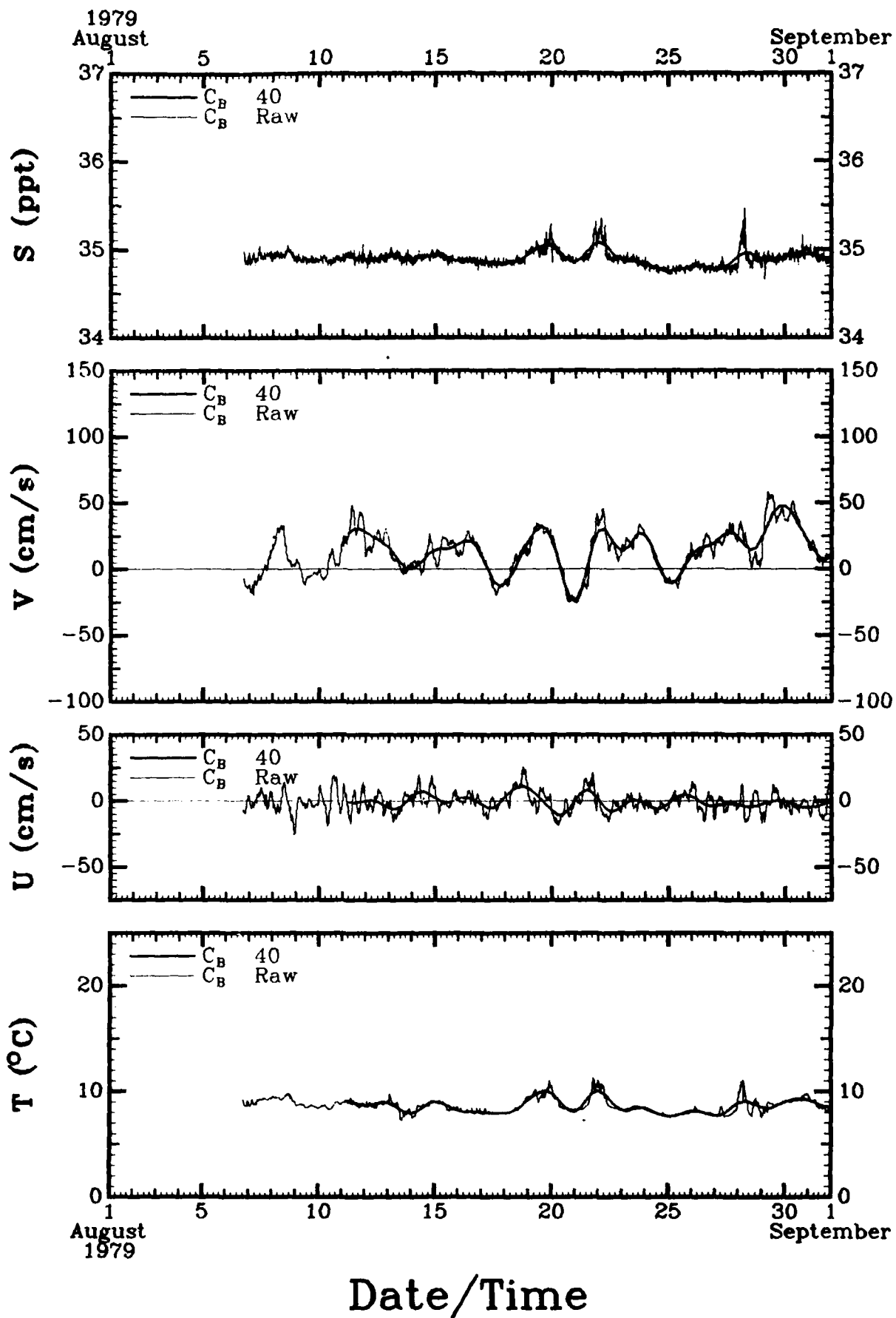


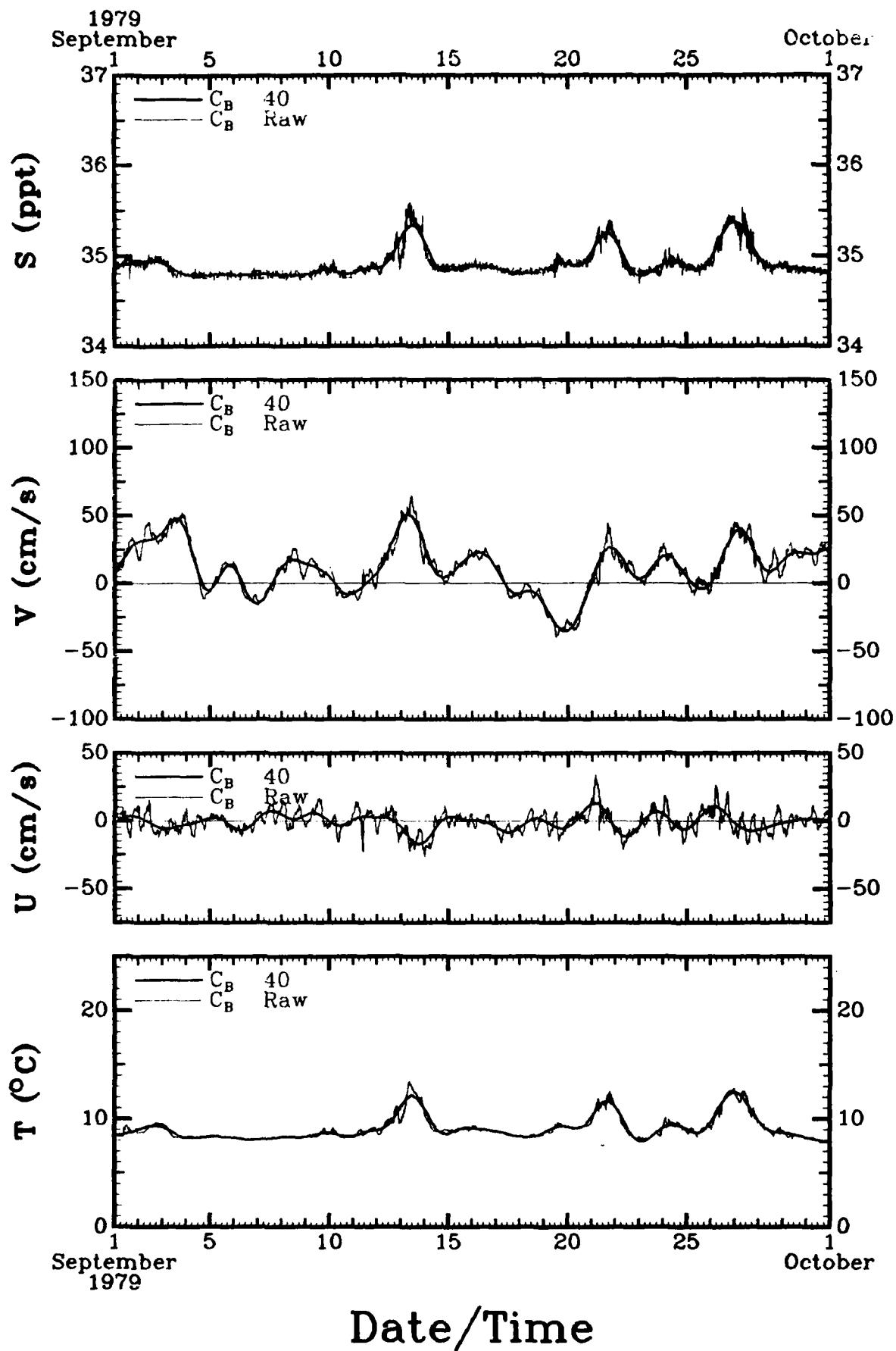


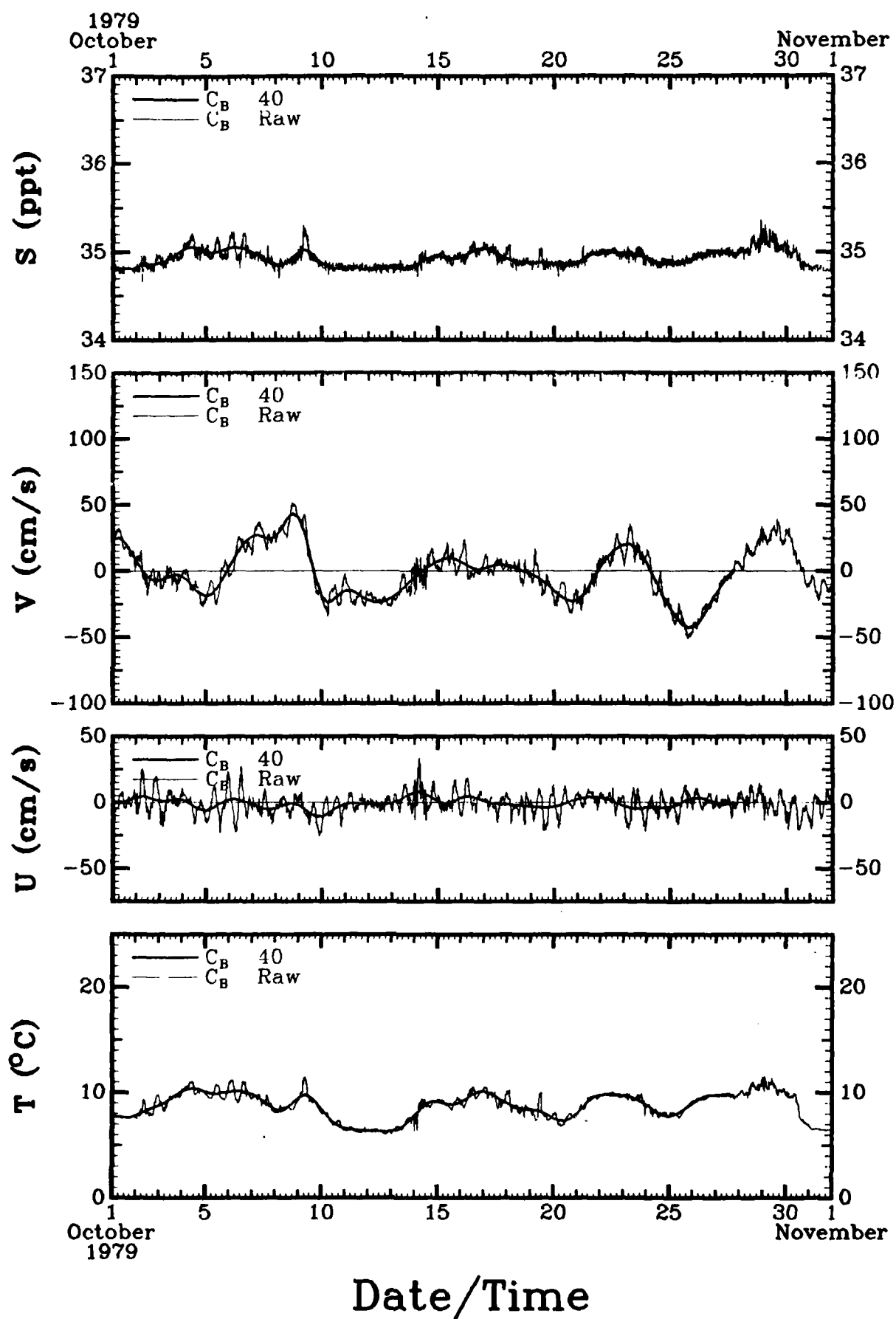


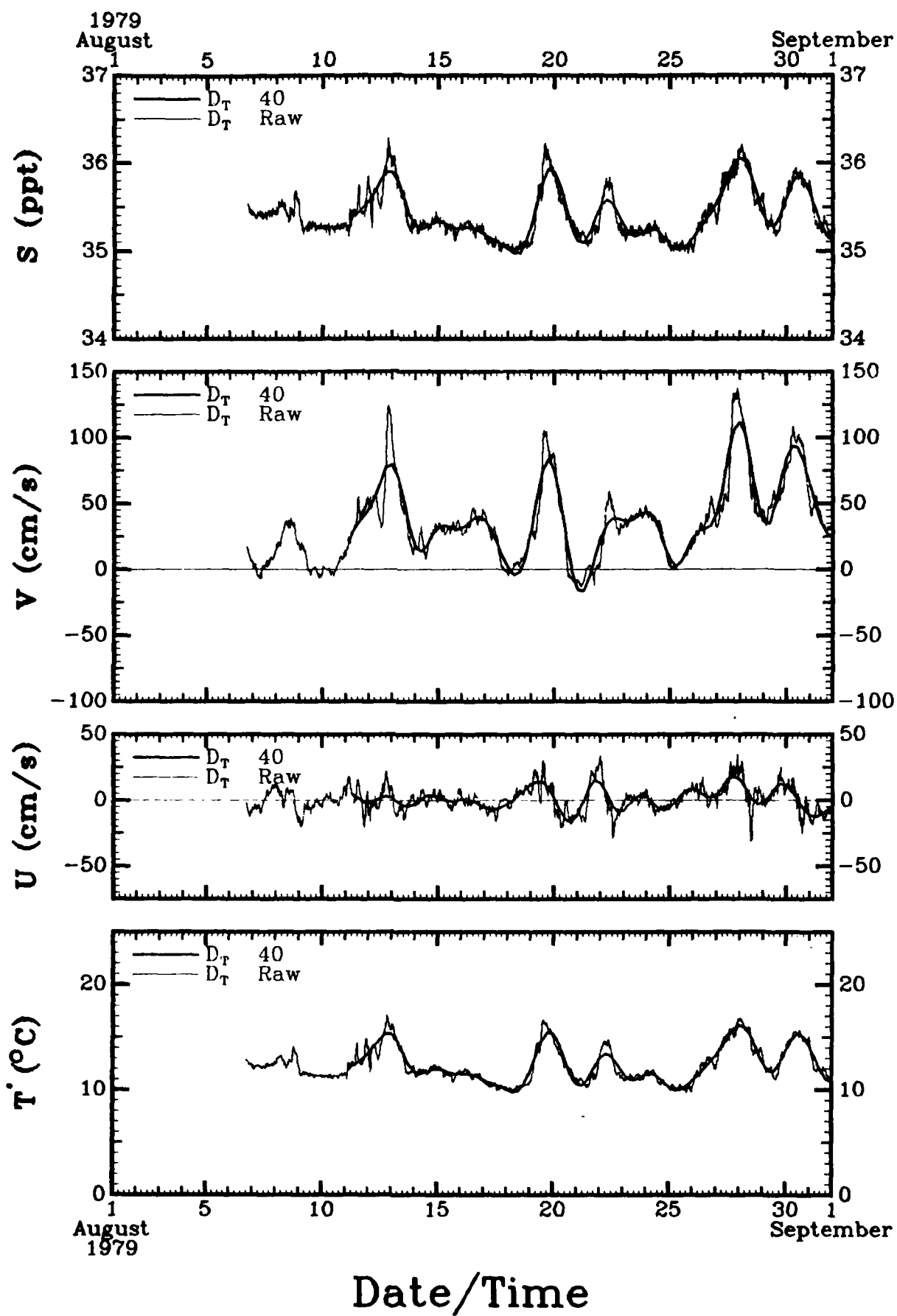


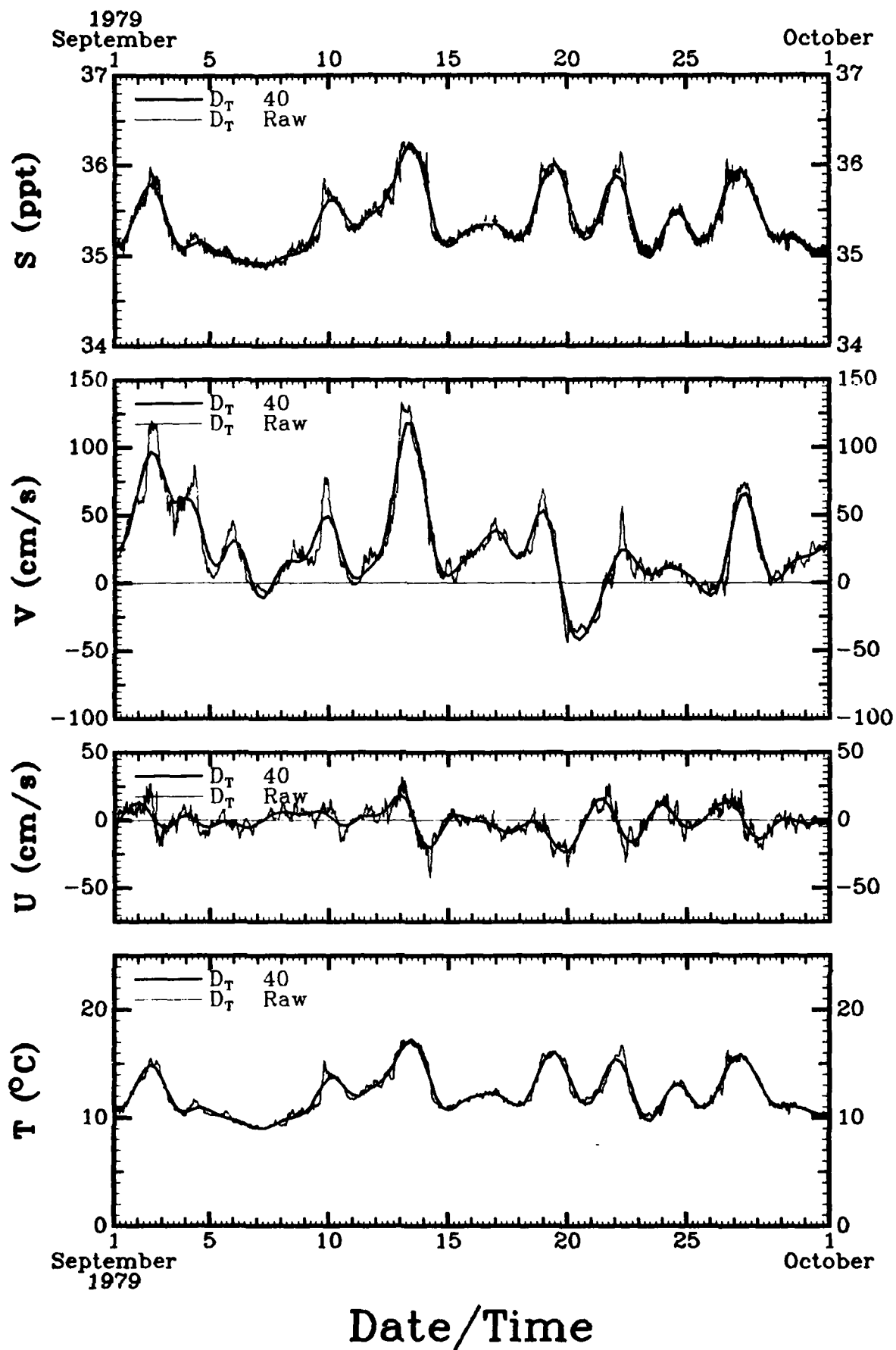


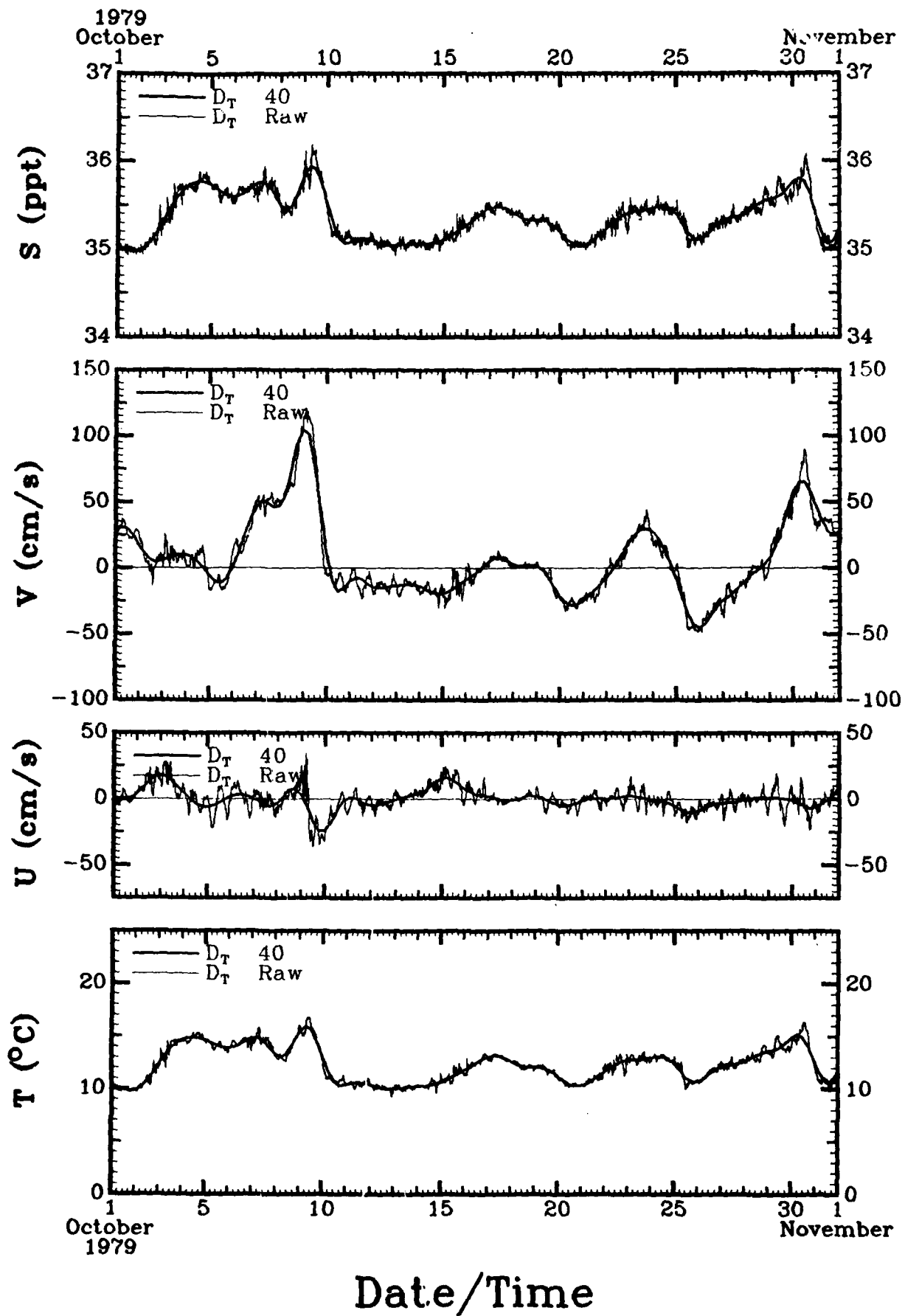


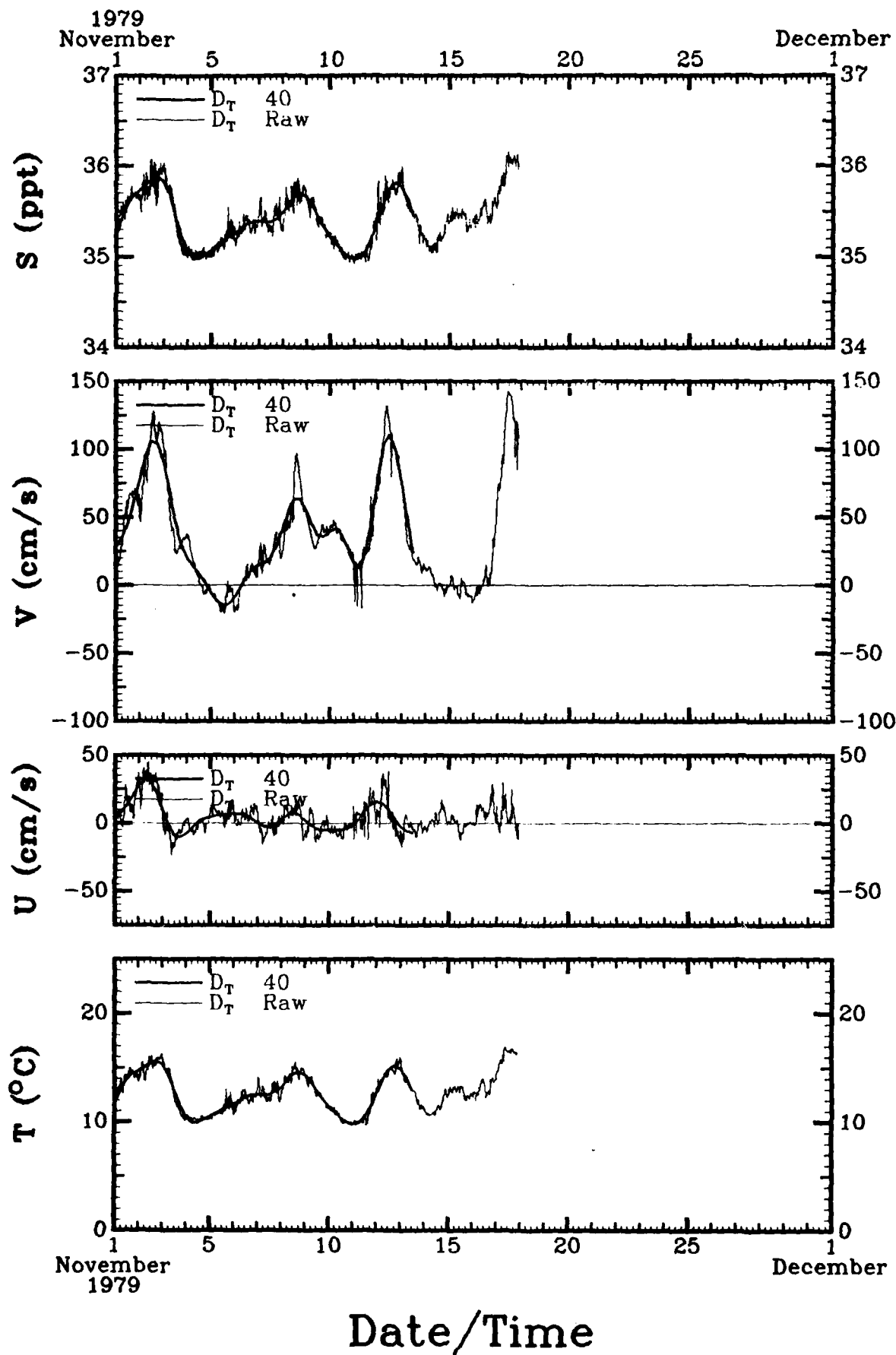








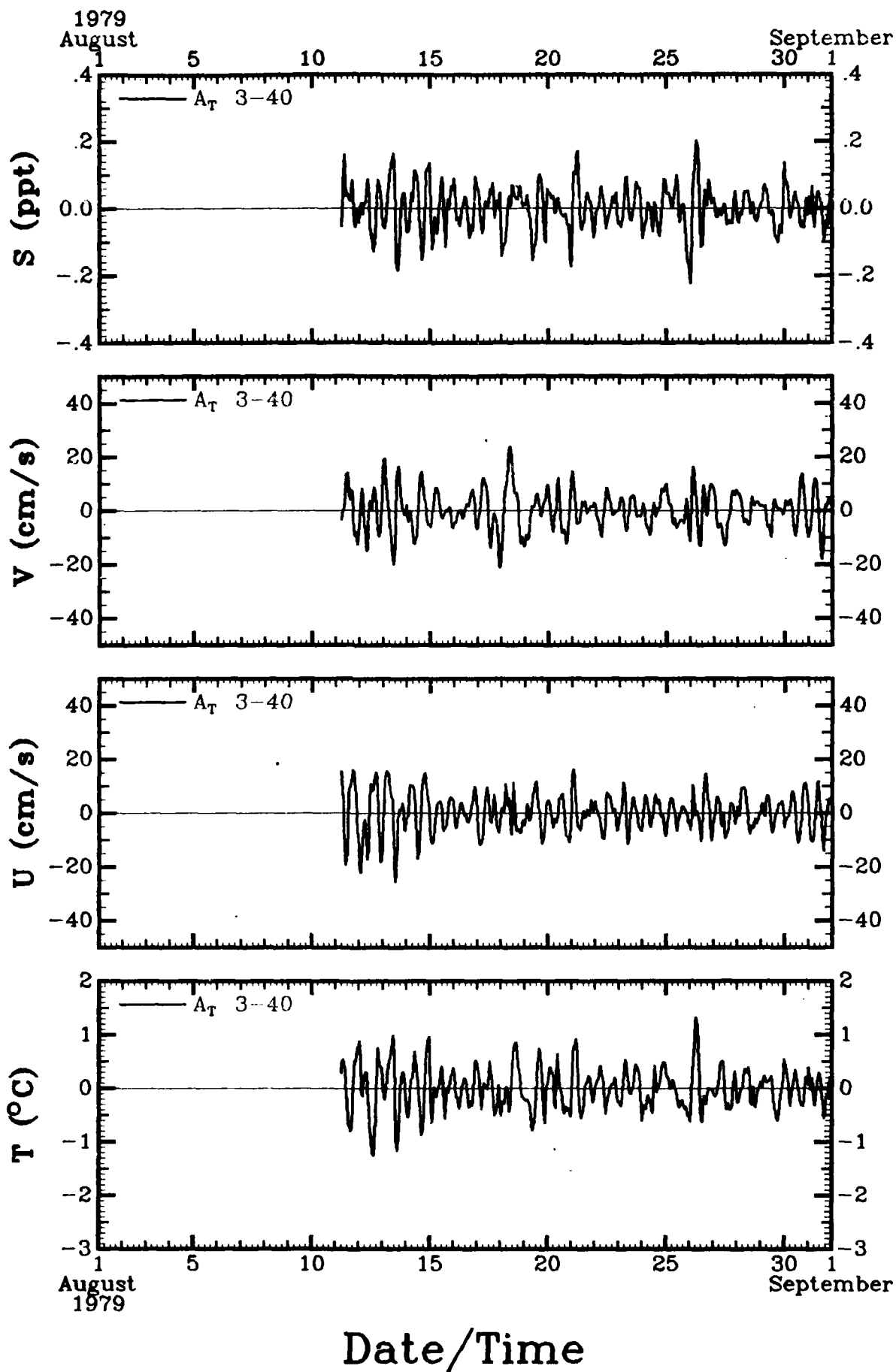


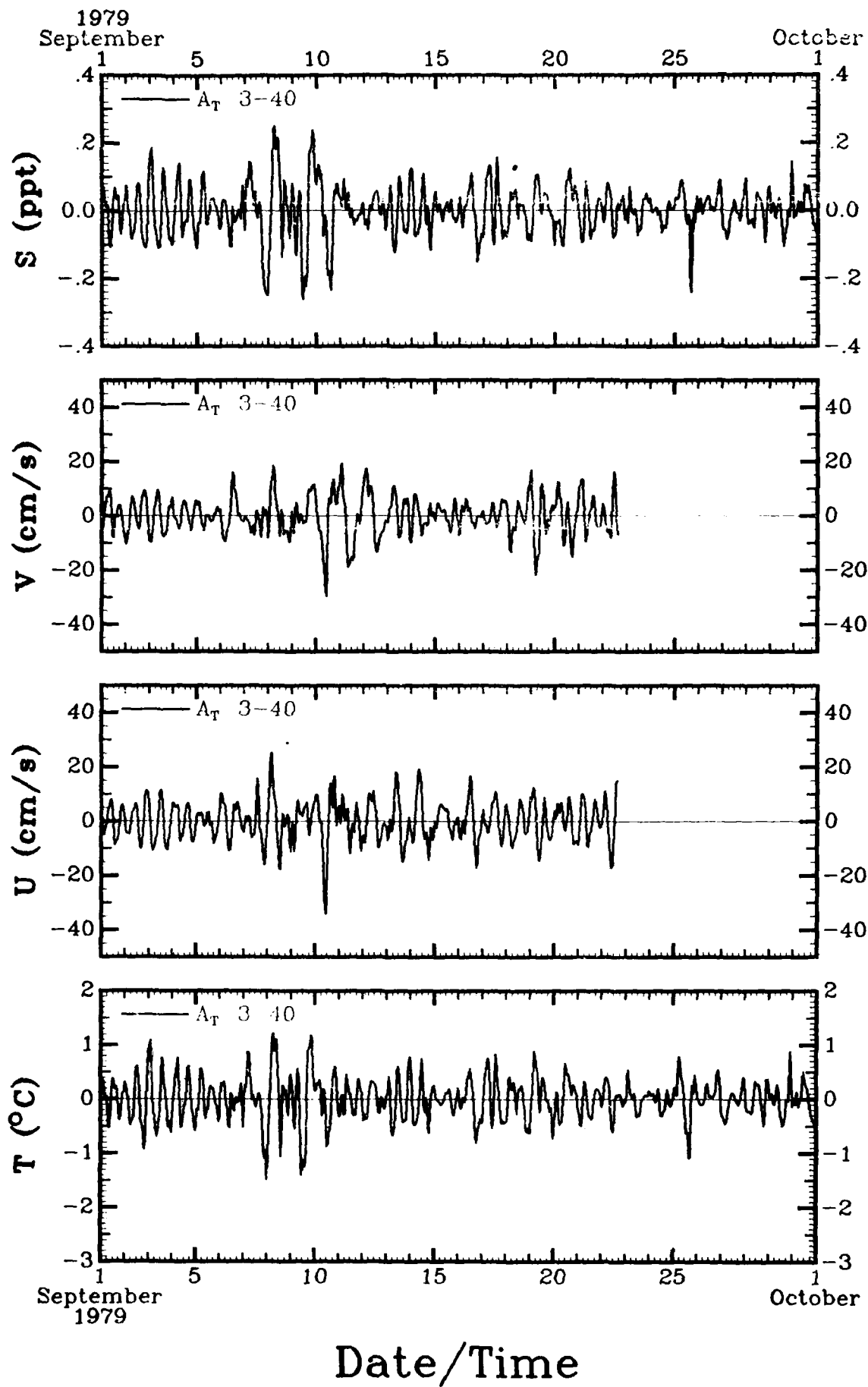


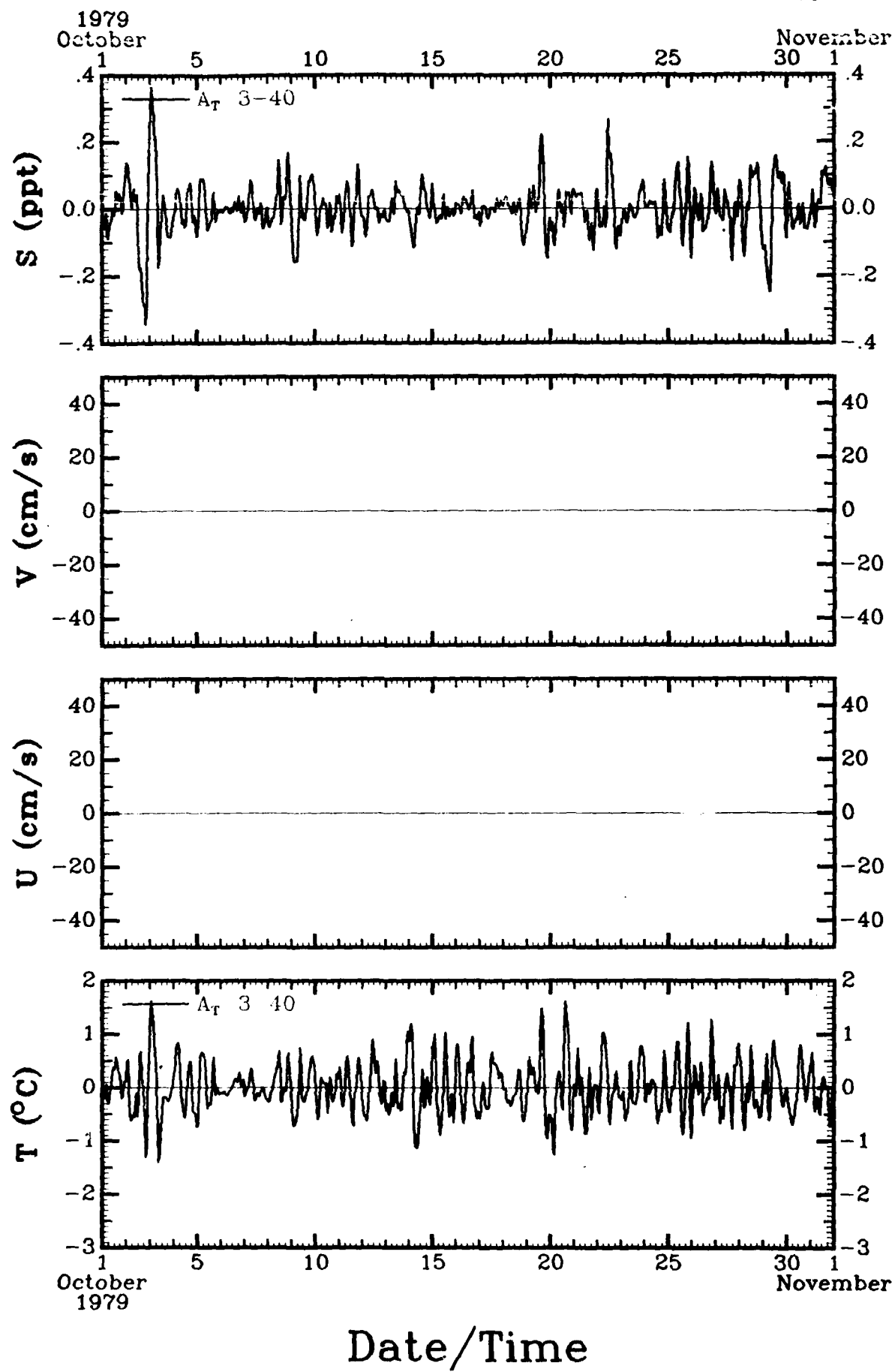
SECTION 4

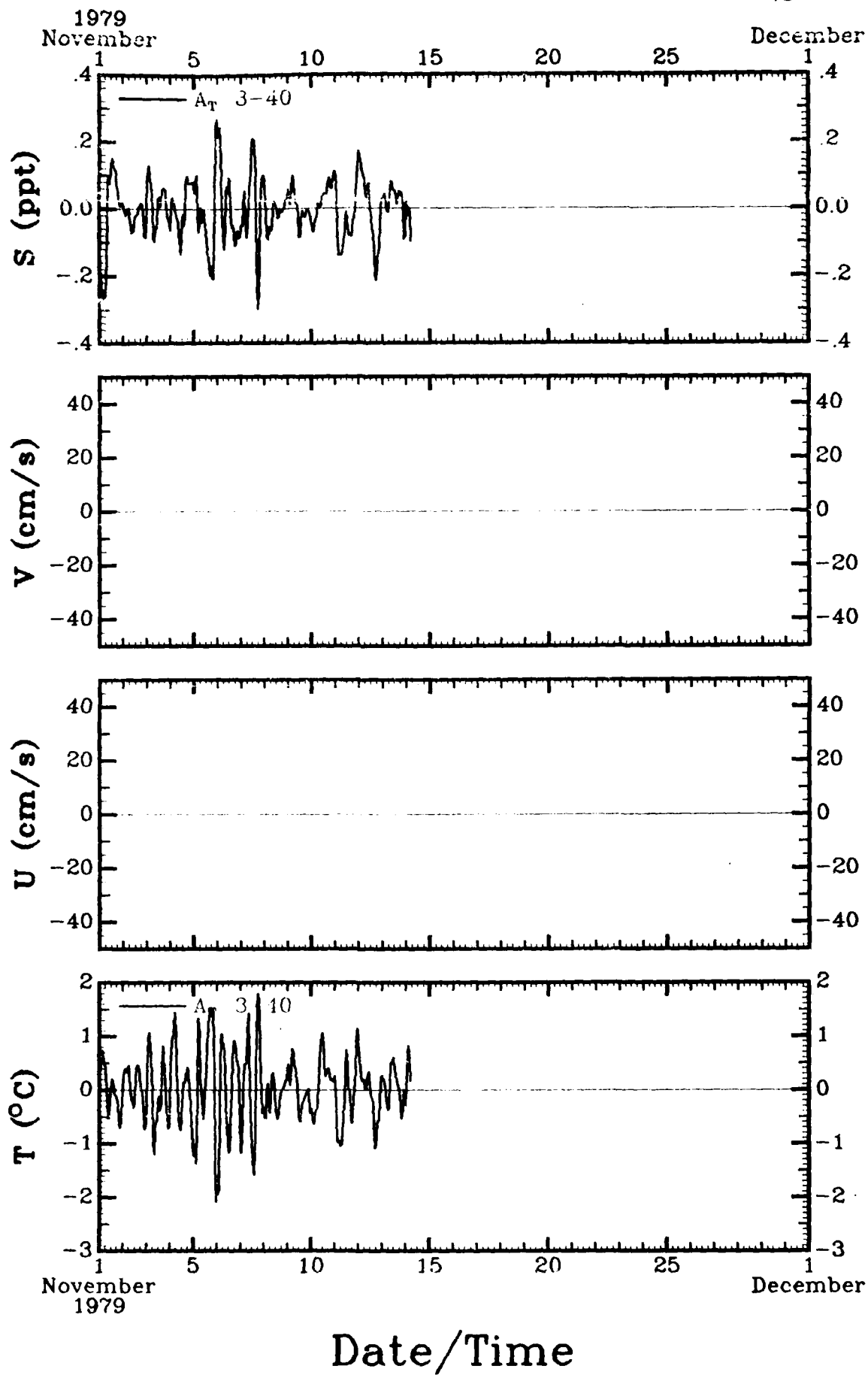
3-40 HRBP Data for Each Instrument

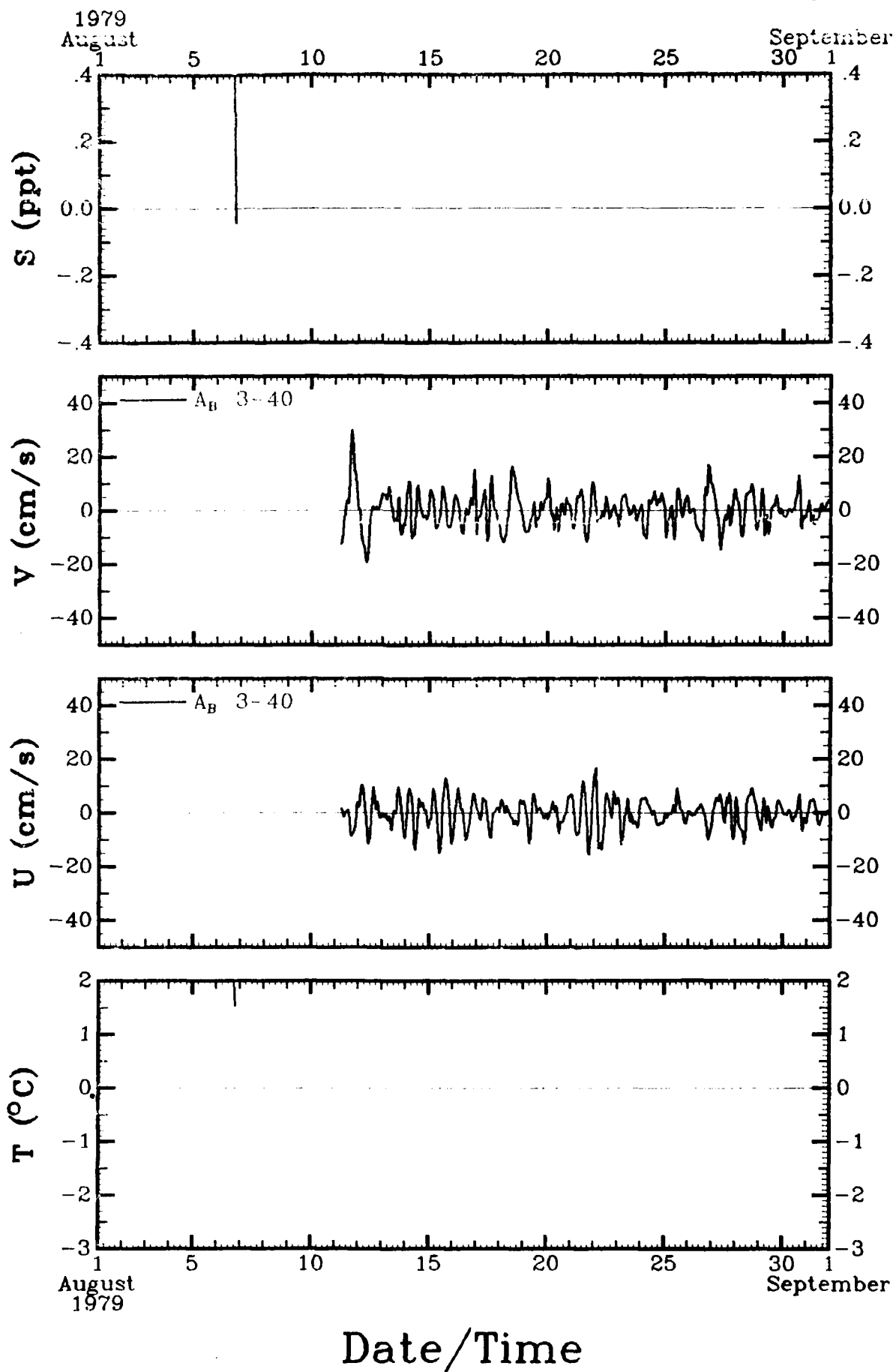
Figures 23 through 30 show the 3-40 HRBP current meter data separately by month for each instrument. The scale factors for similar data are not the same for all instruments in this section. Note that the bandpass operation removes the mean value.

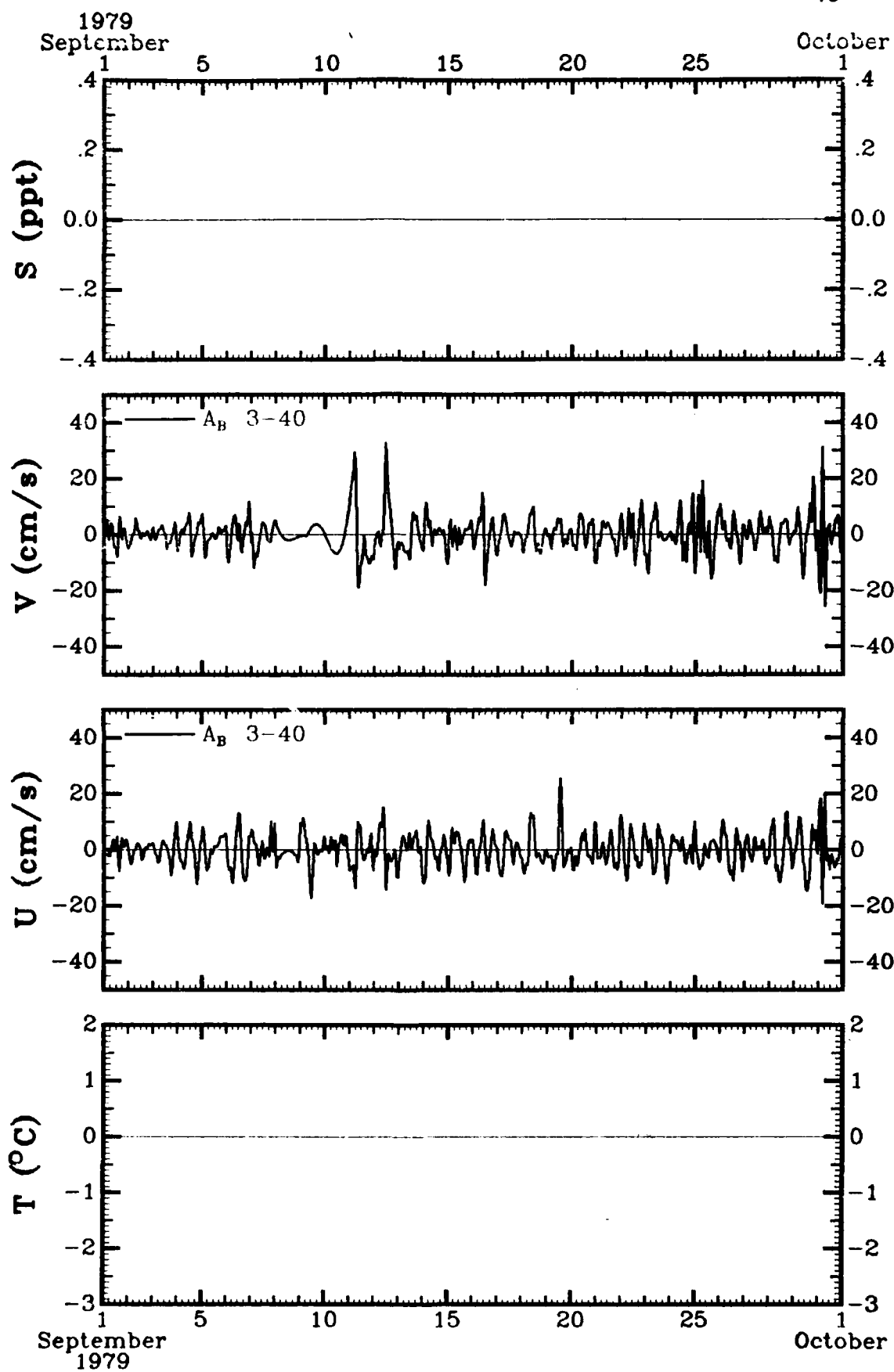


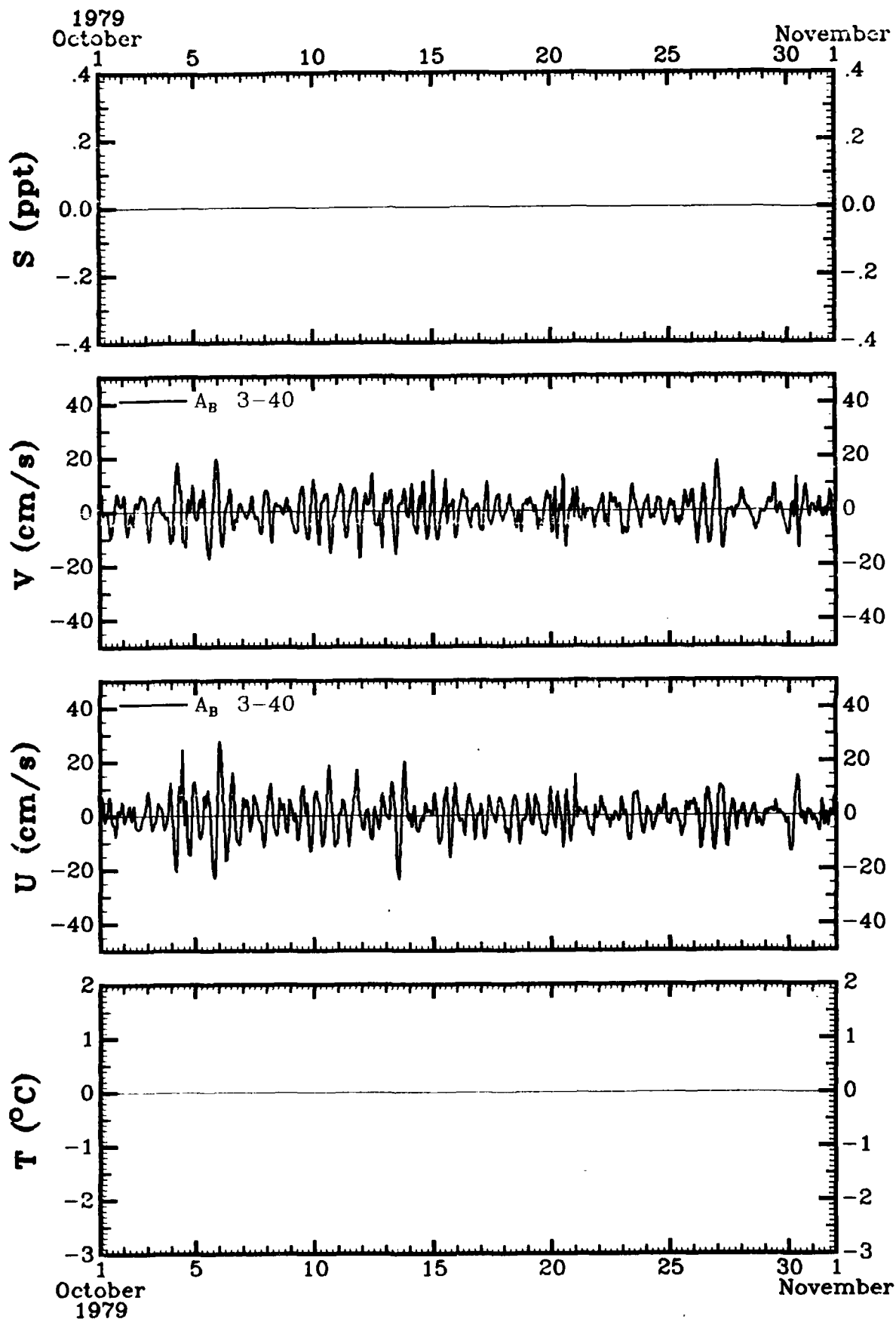


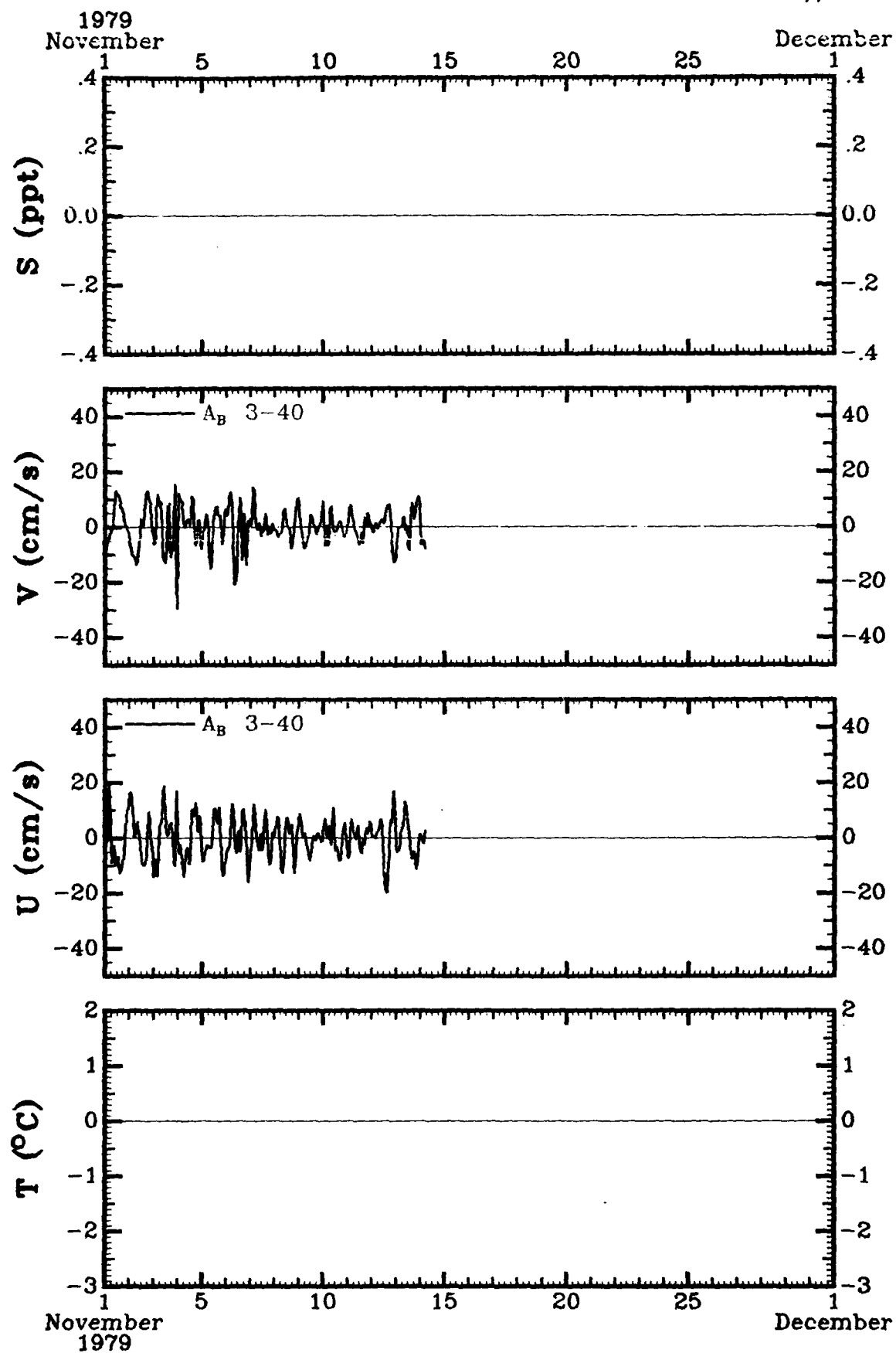


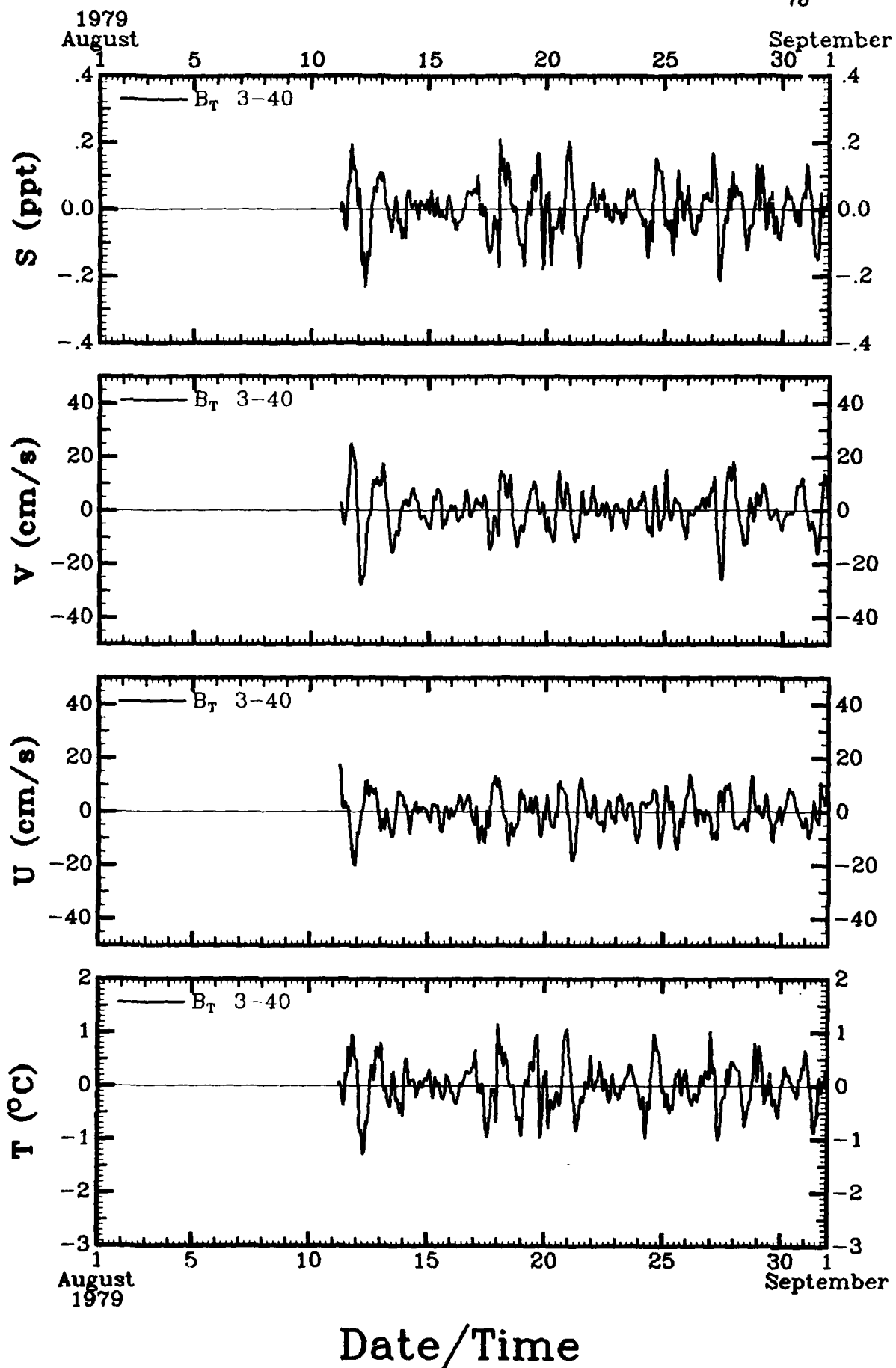


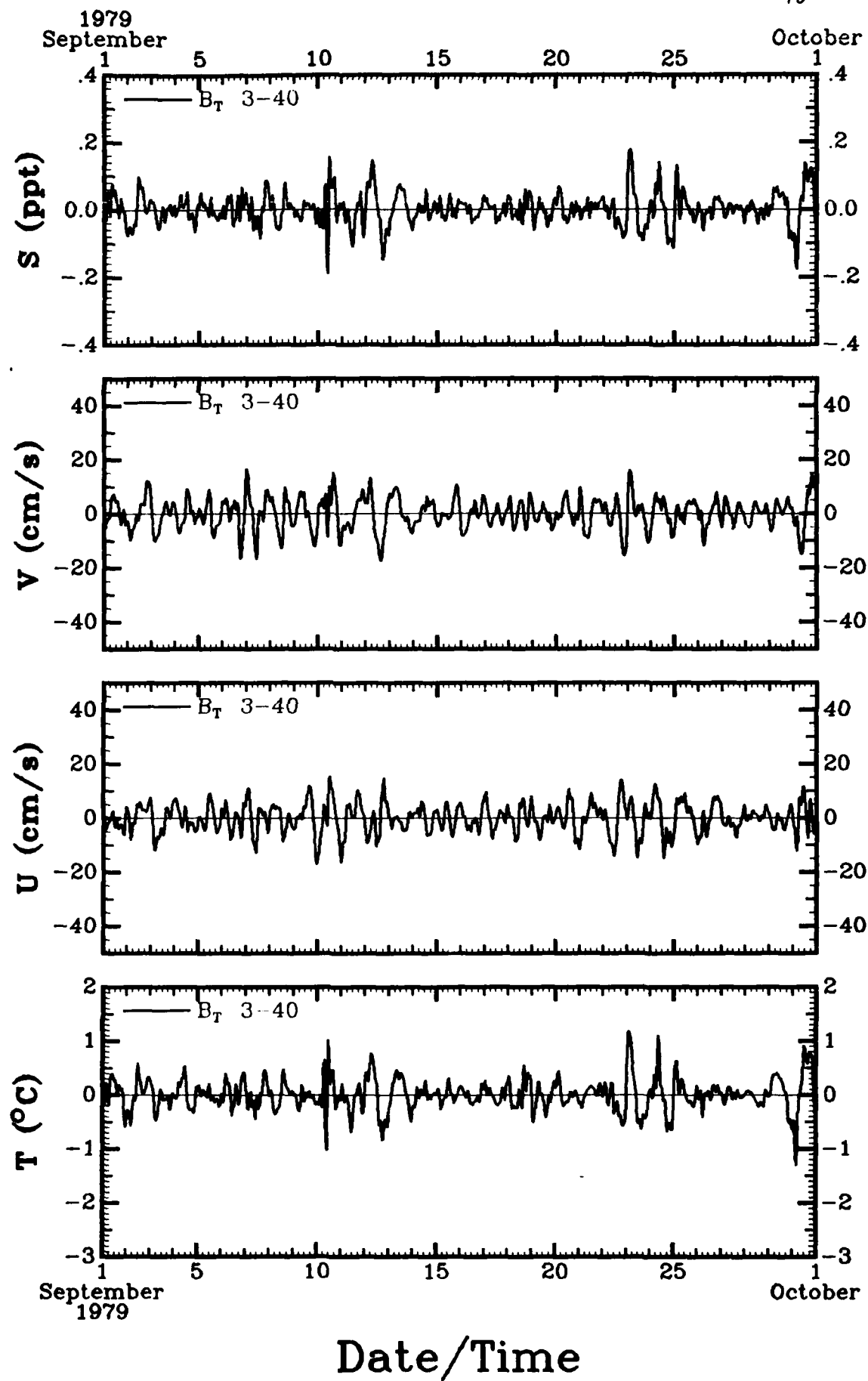


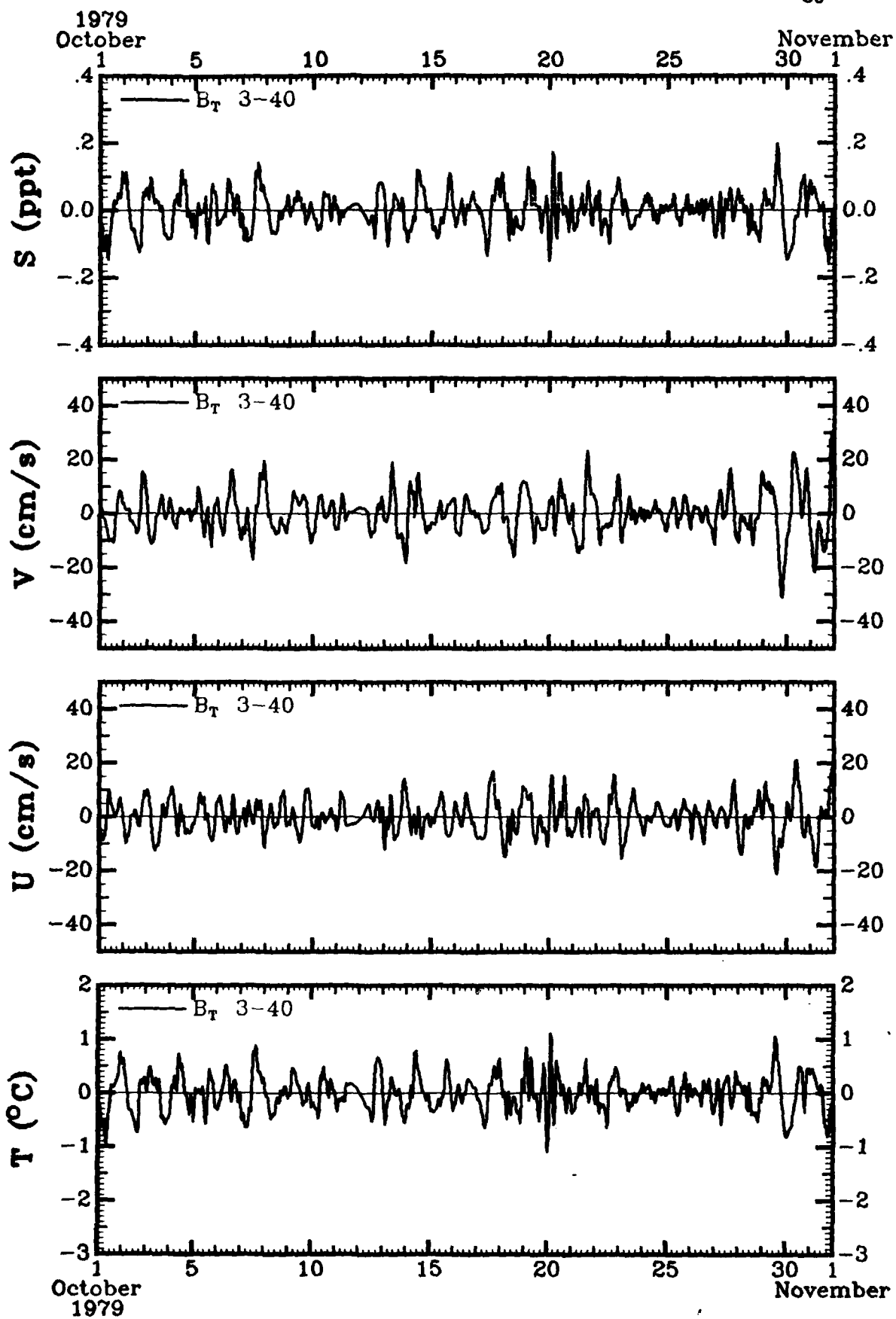




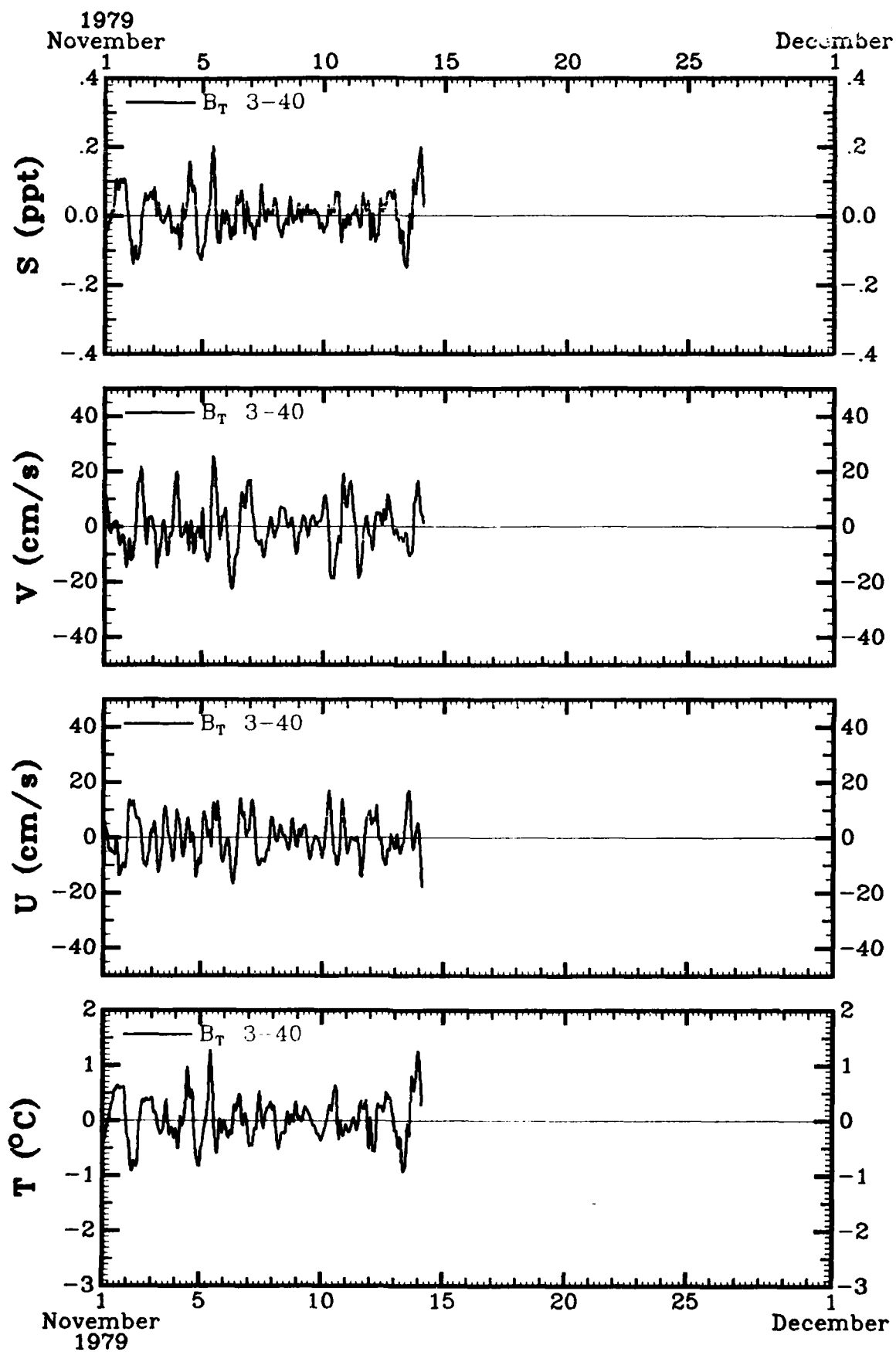




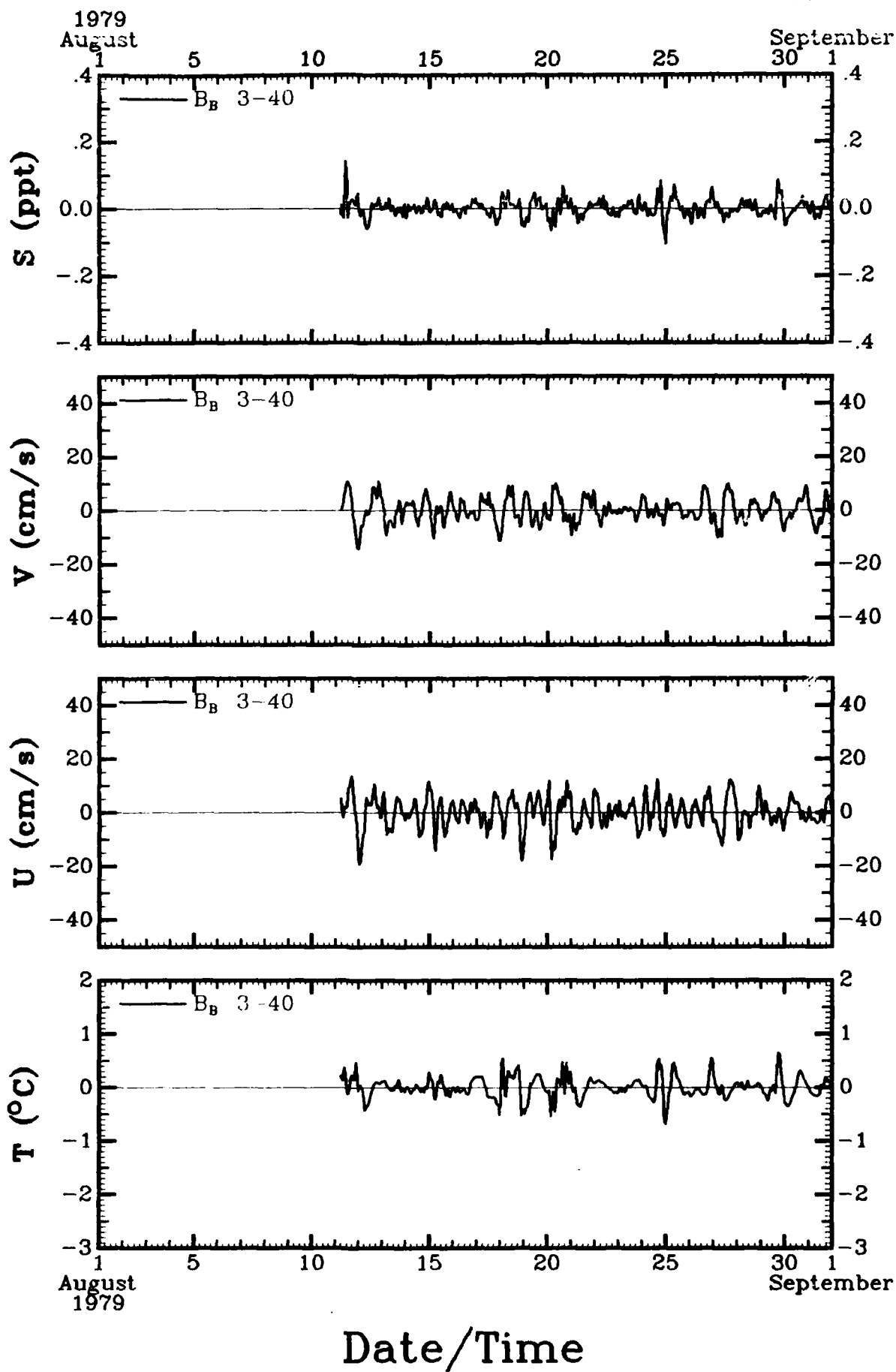


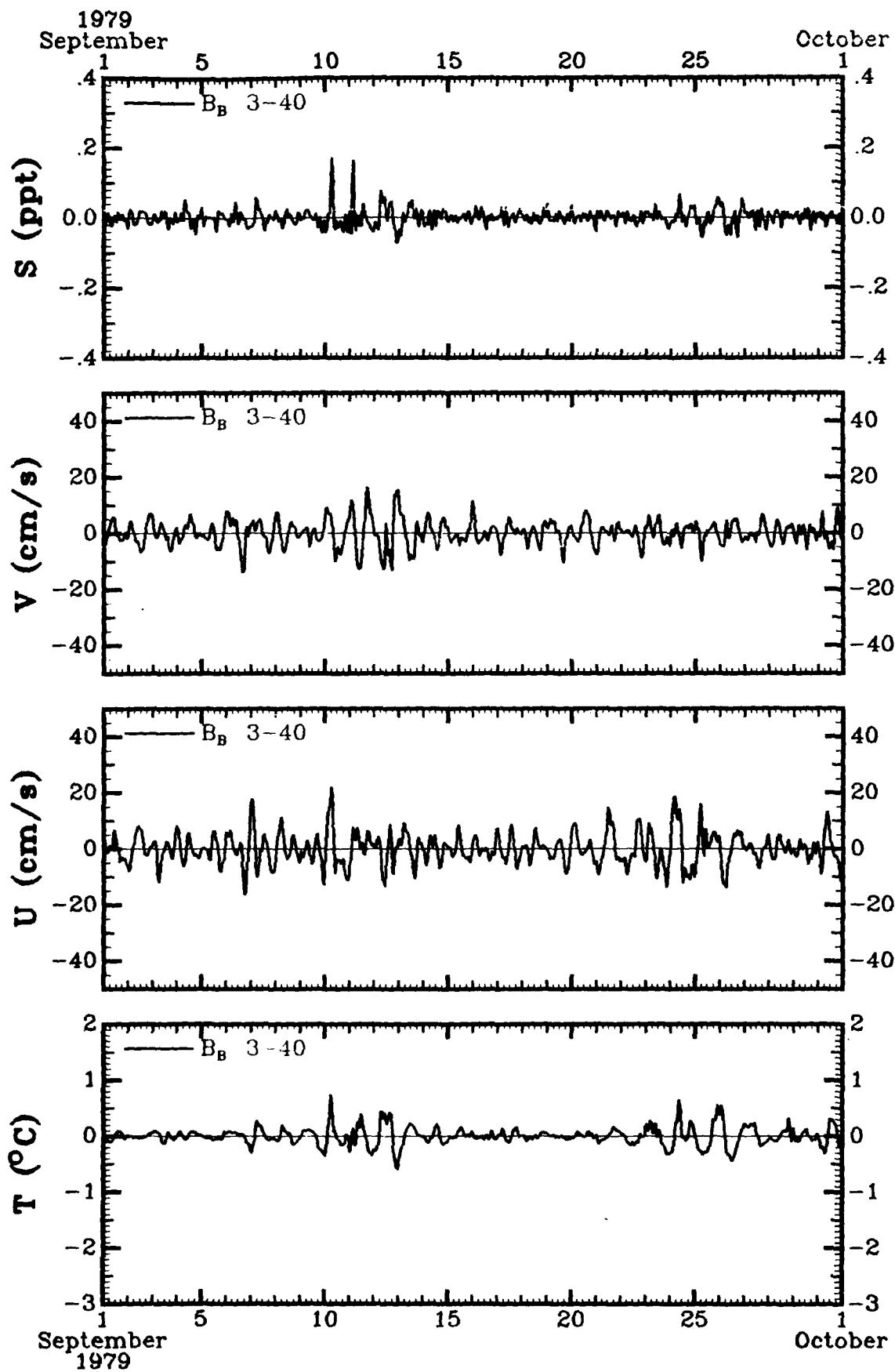


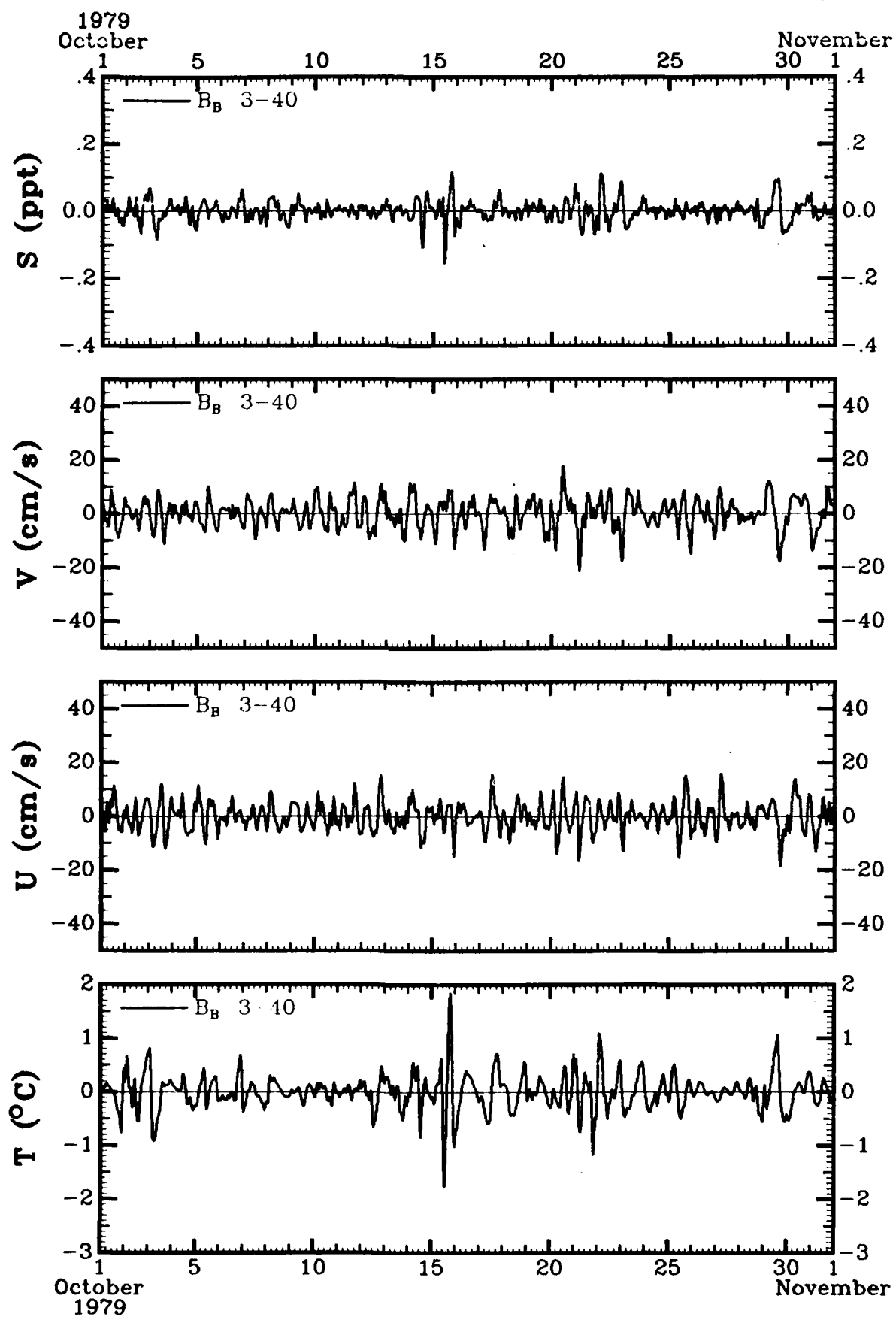
Date/Time



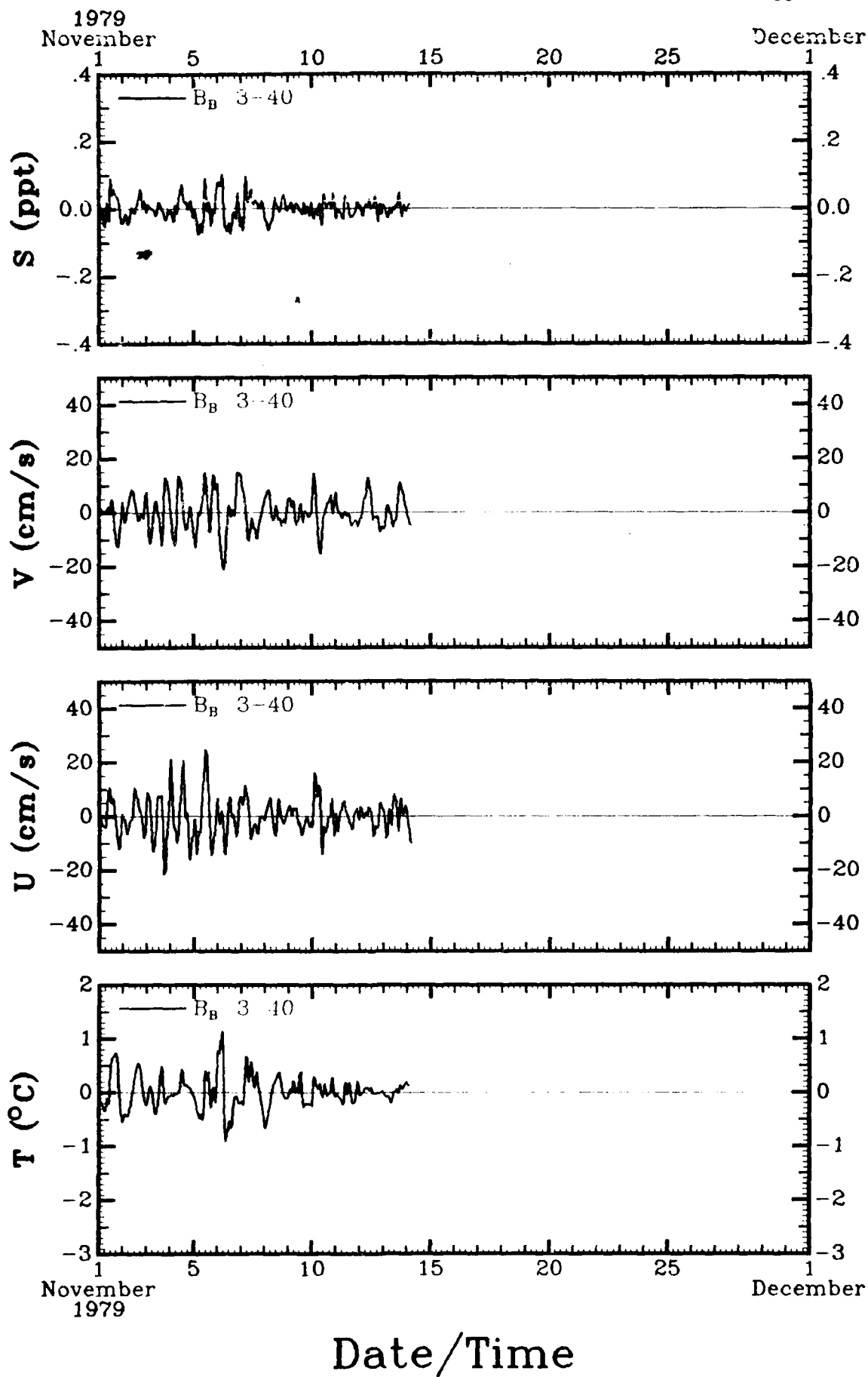
Date/Time







Date/Time



AD-A103 487

NORTH CAROLINA UNIV AT CHAPEL HILL

F/6 8/3

THE GULF STREAM MEANDERS EXPERIMENT. CURRENT METER AND ATMOSPHE--ETC(U)

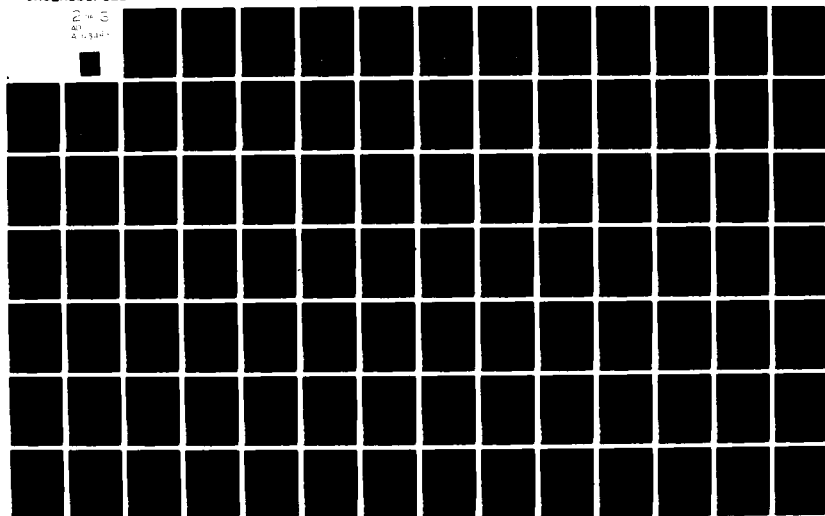
MAY 81 D A BROOKS, J M BANE, R L COHEN

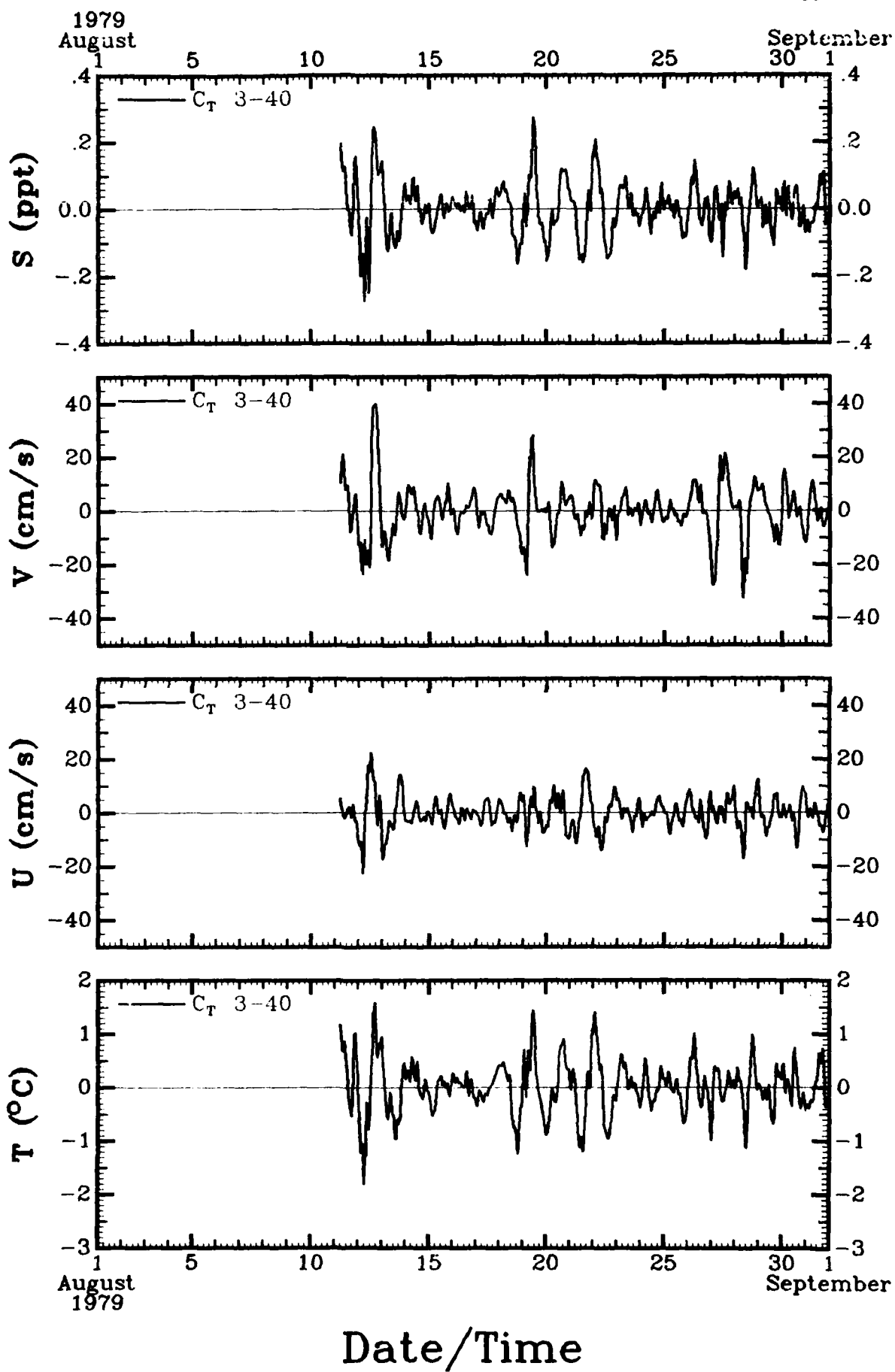
N00014-77-C-0354

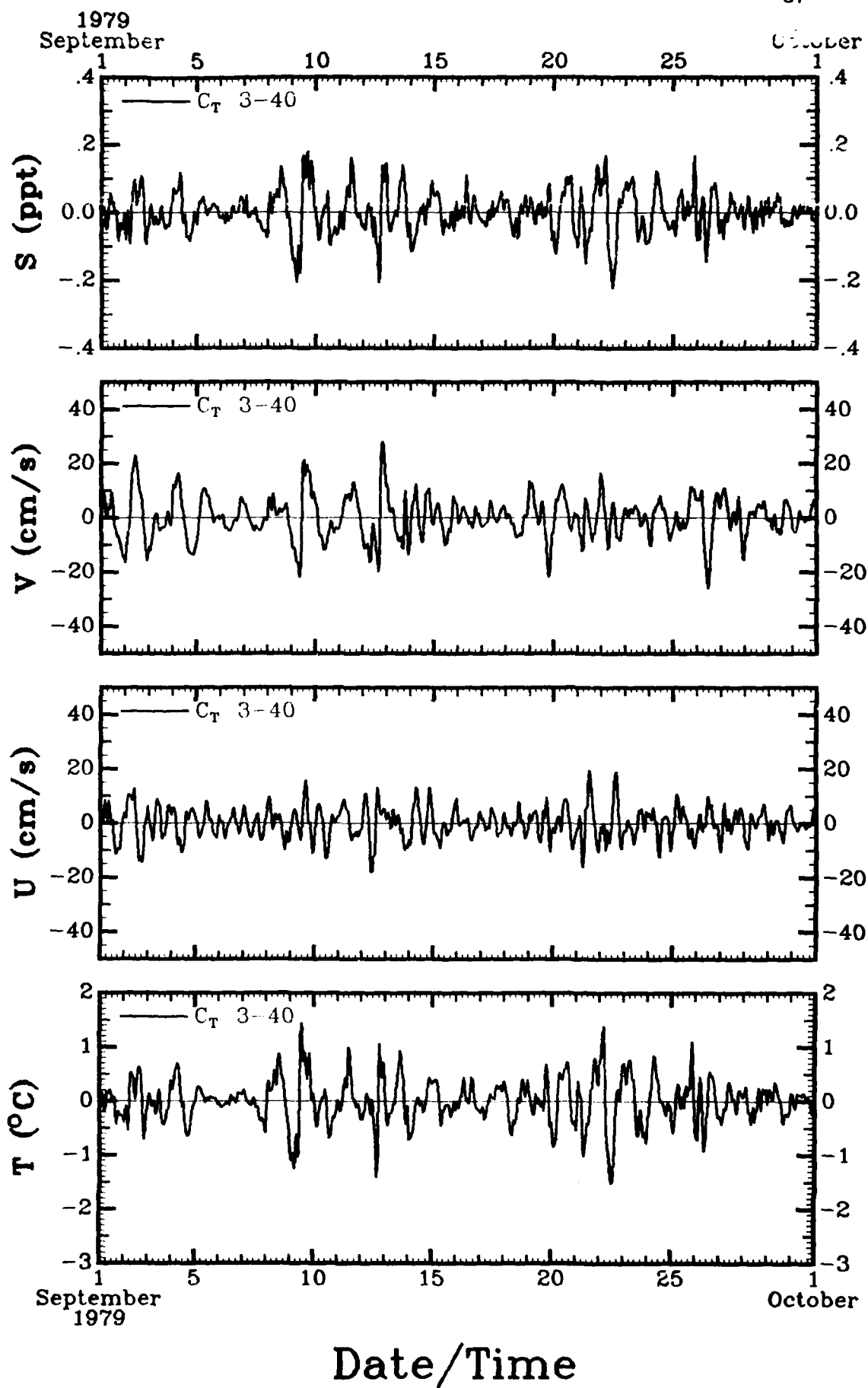
NL

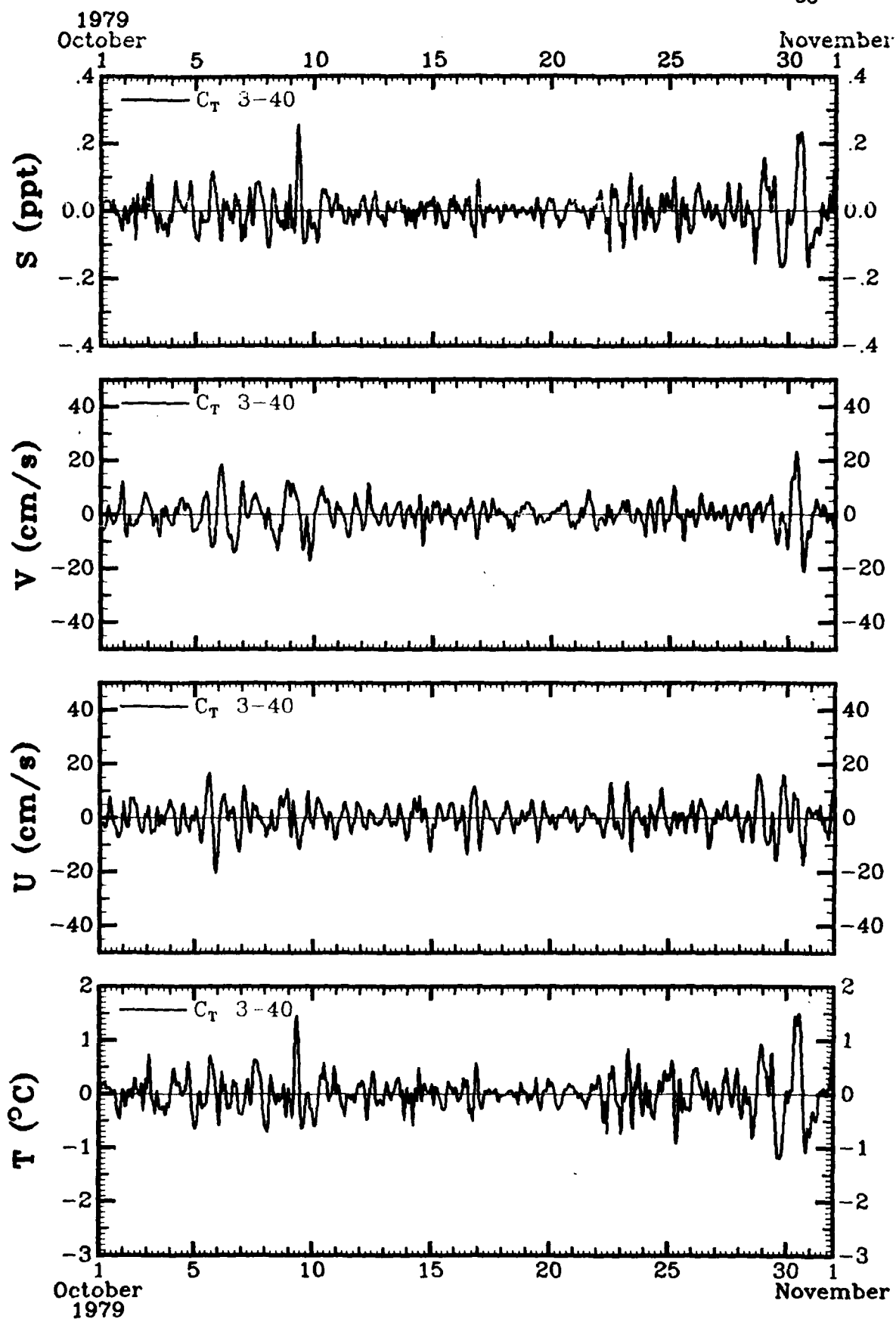
UNCLASSIFIED

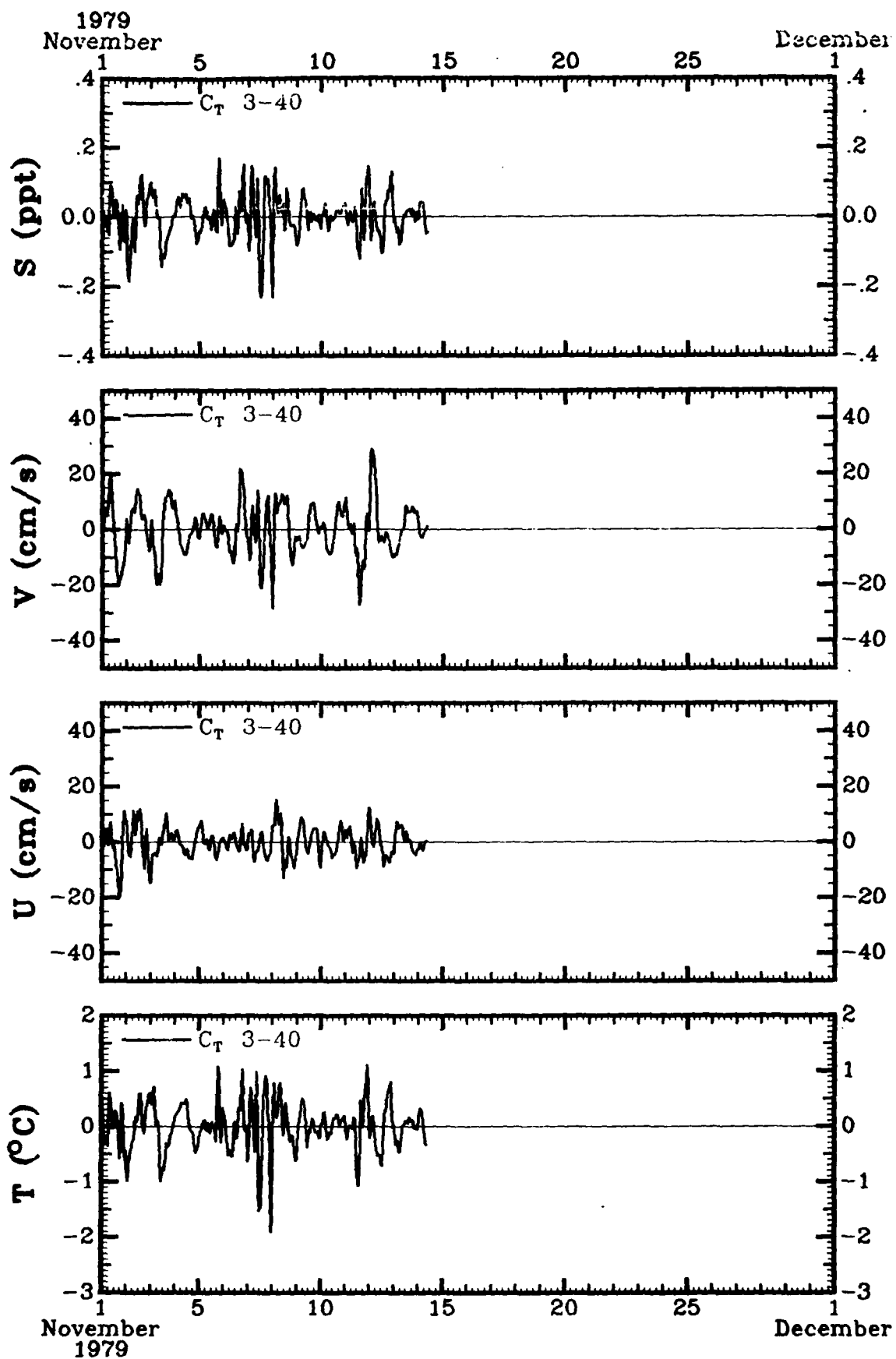
21-5
21-540

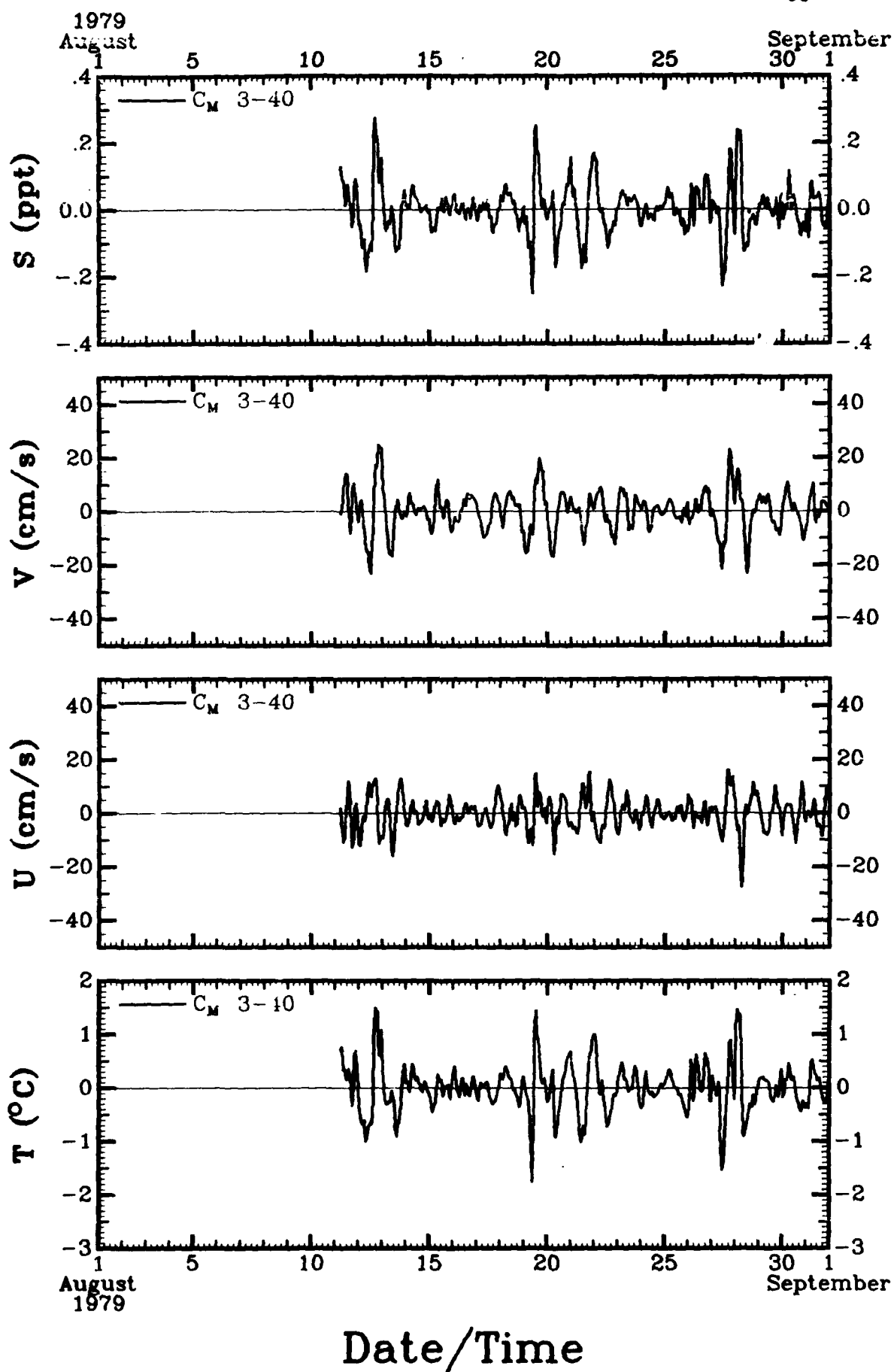


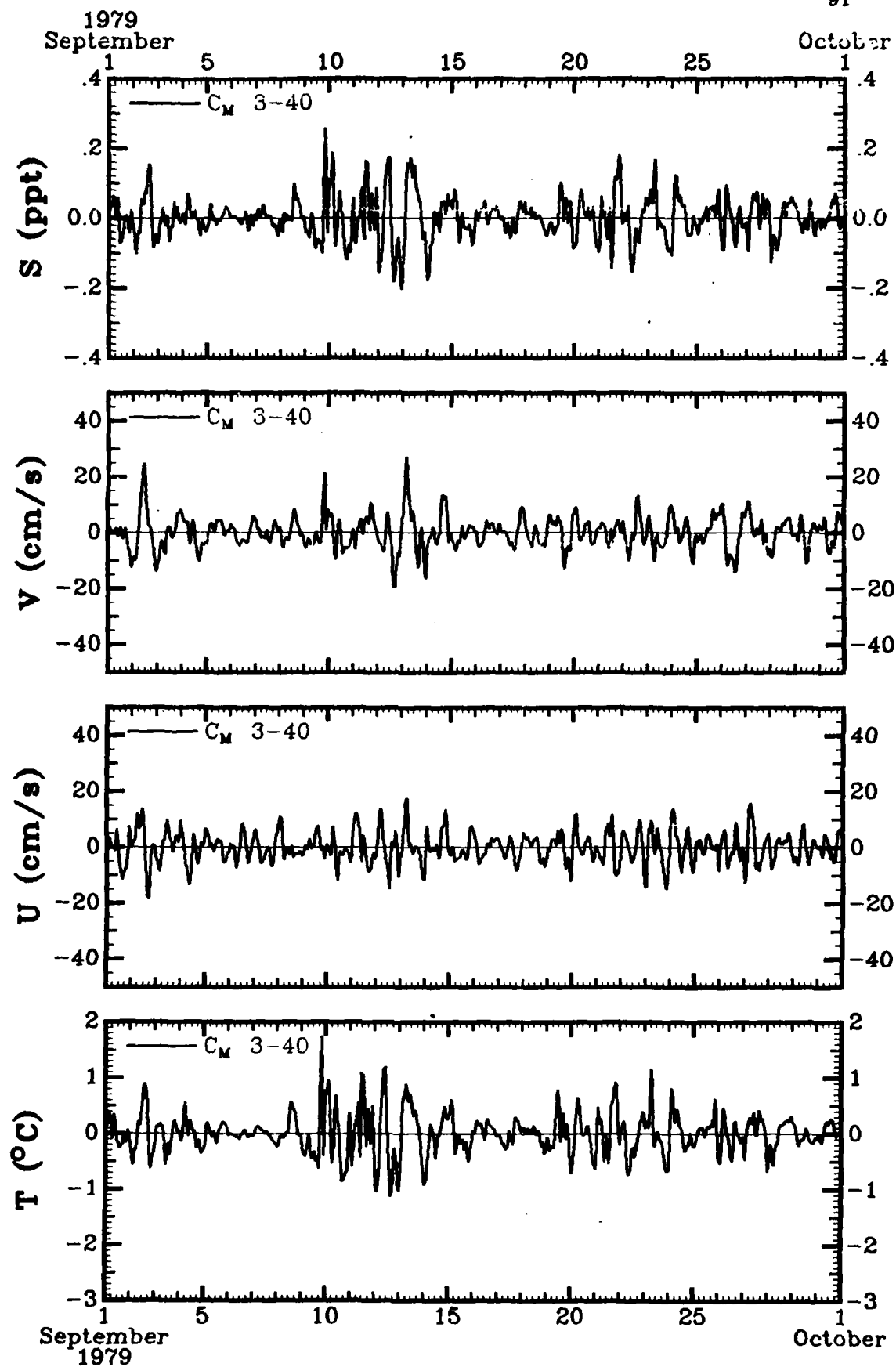




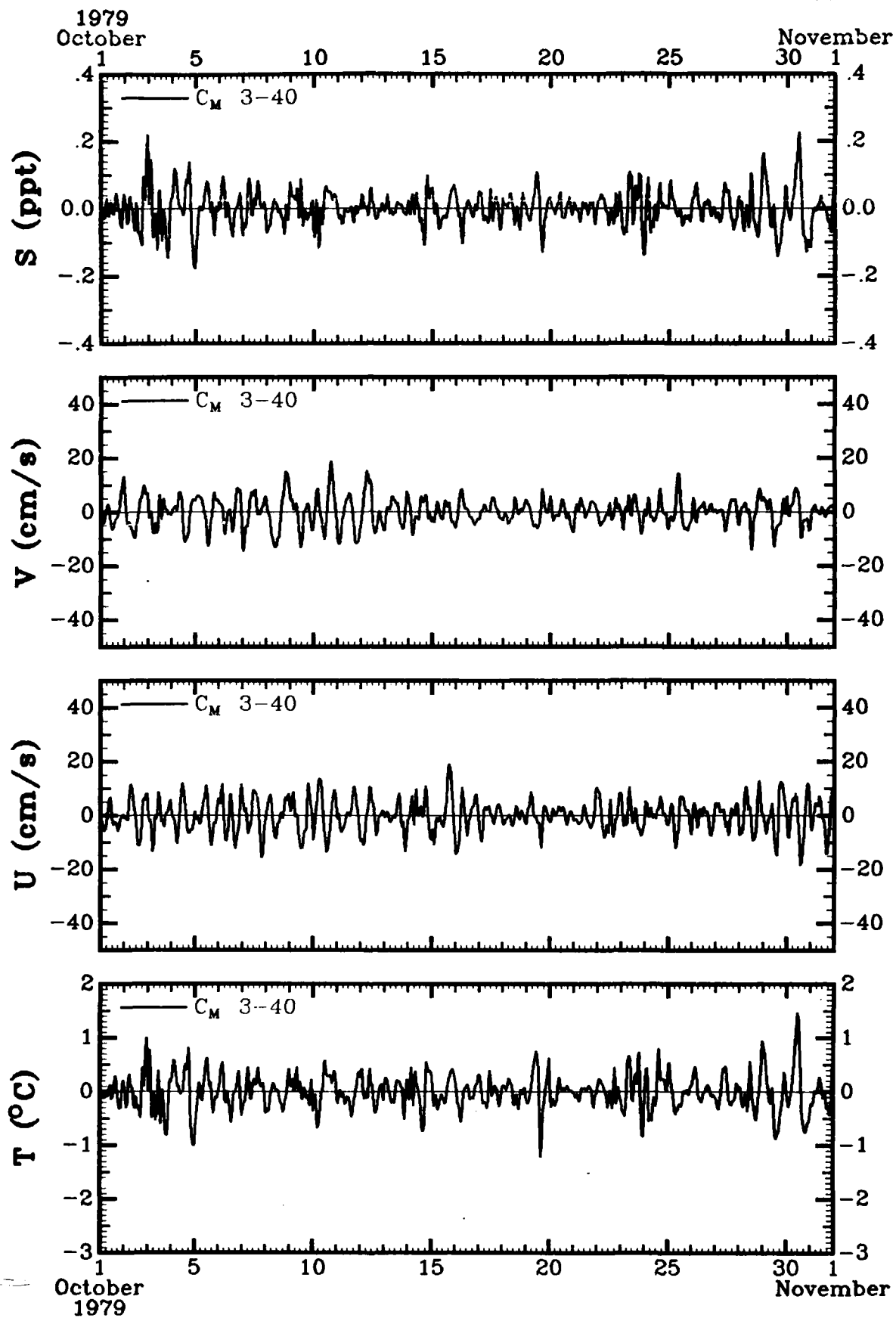




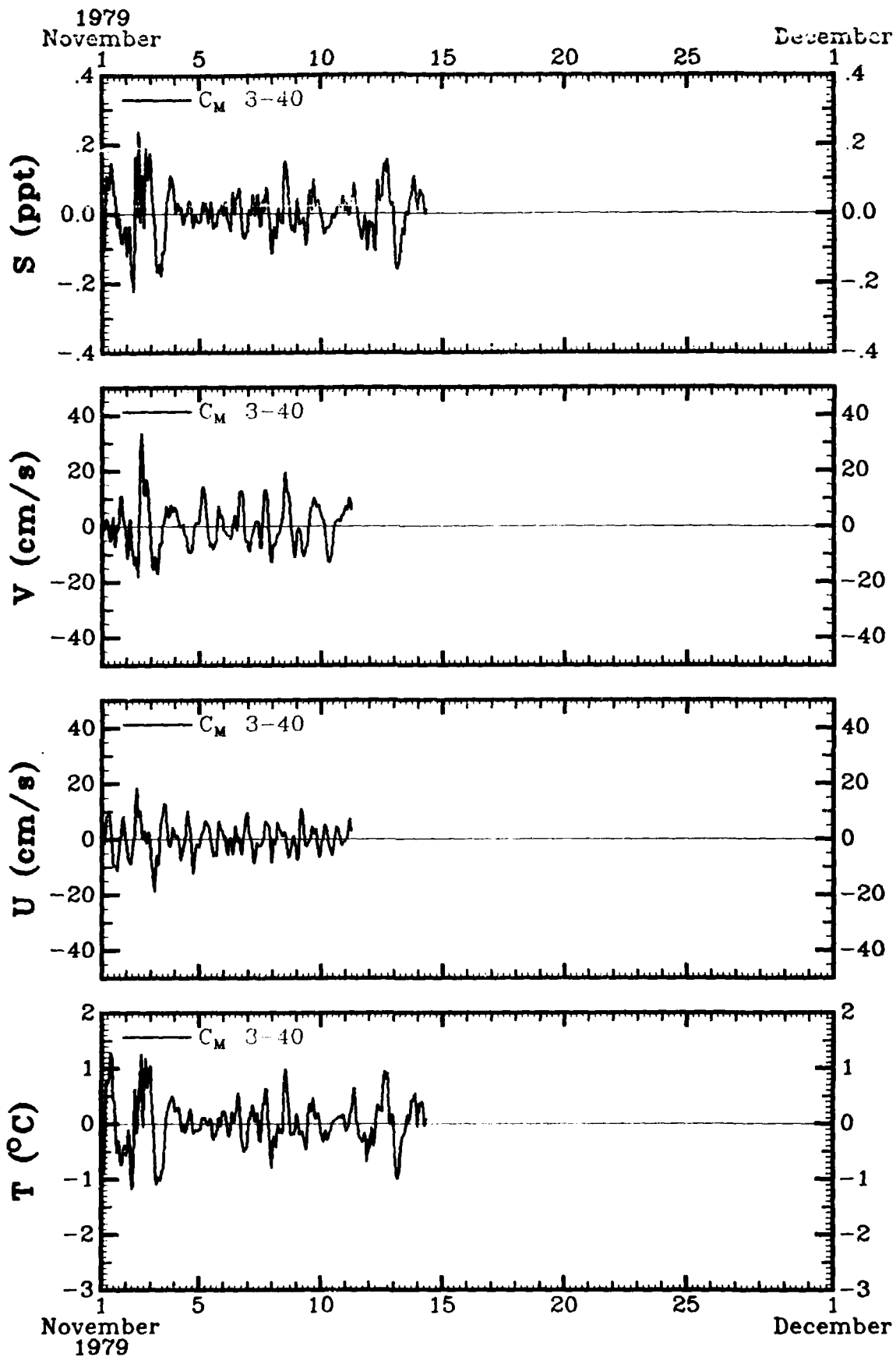




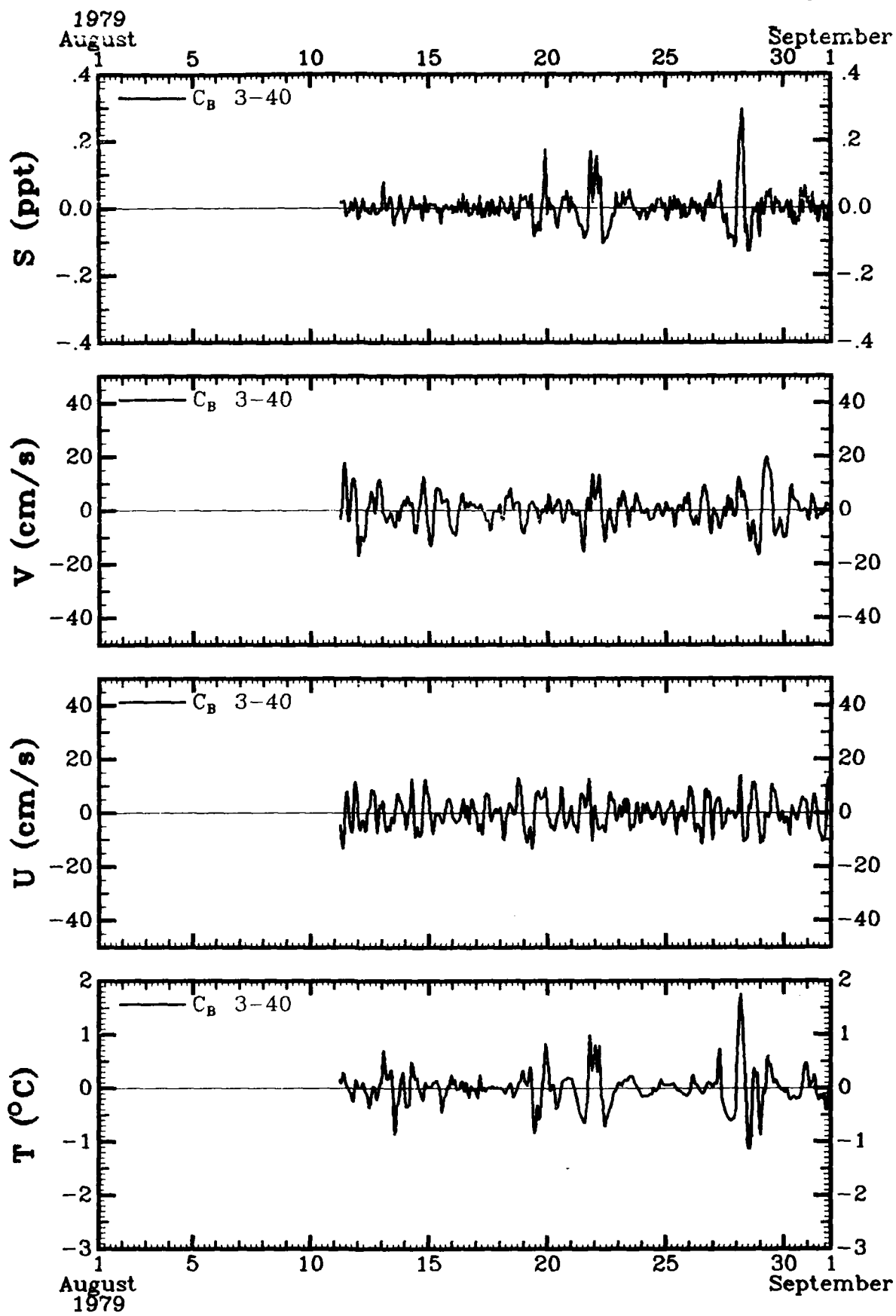
Date/Time



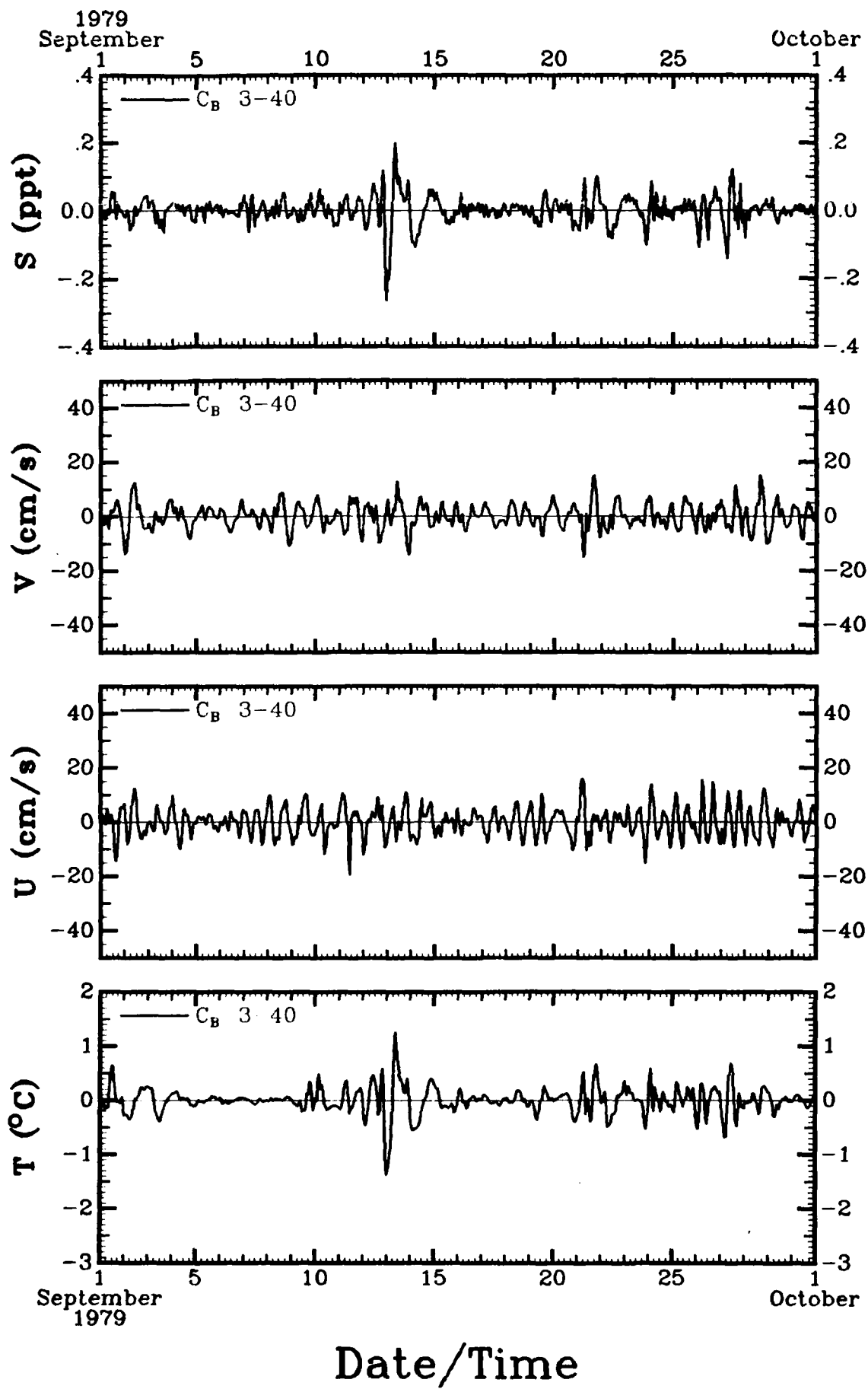
Date/Time

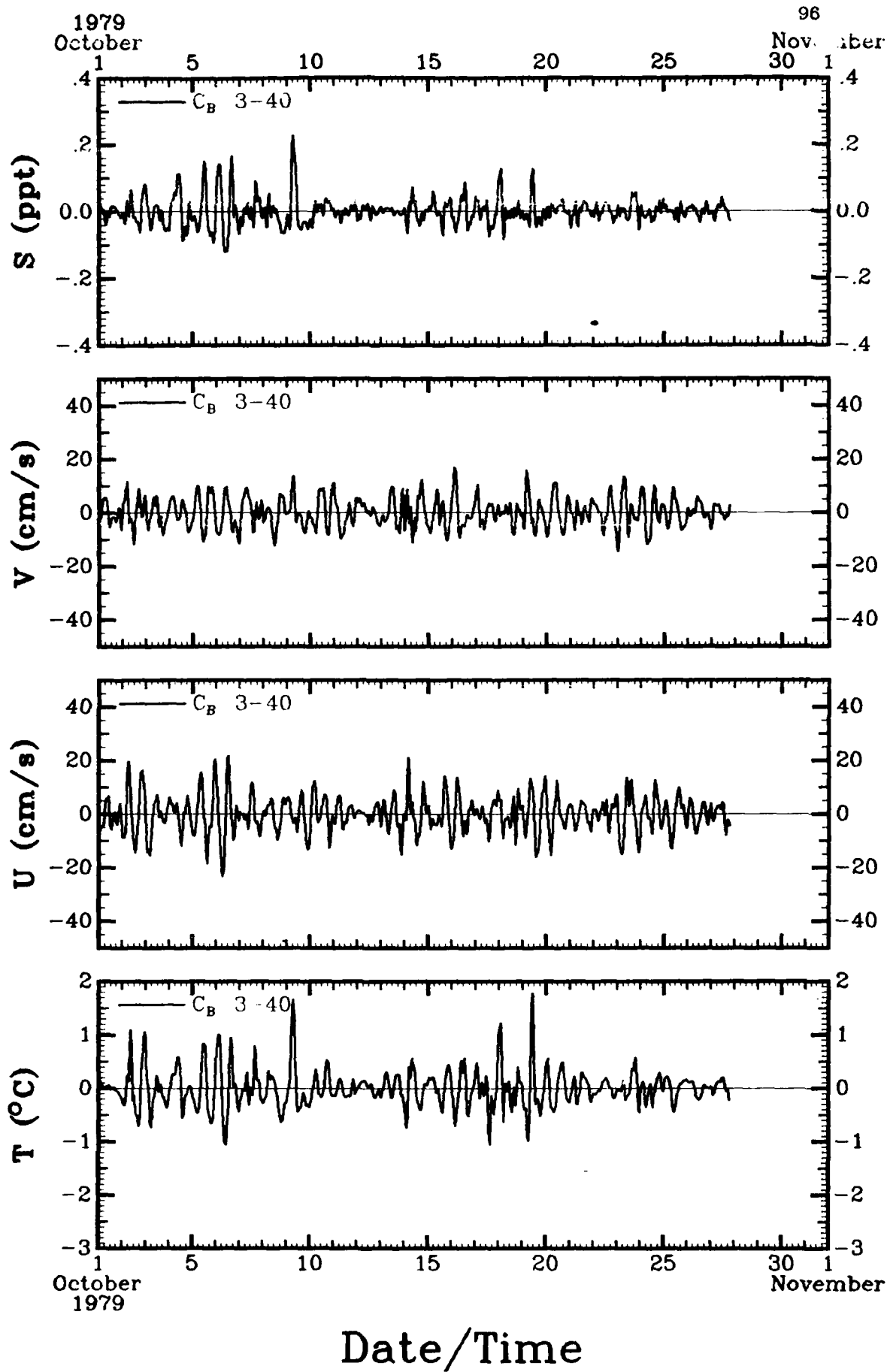


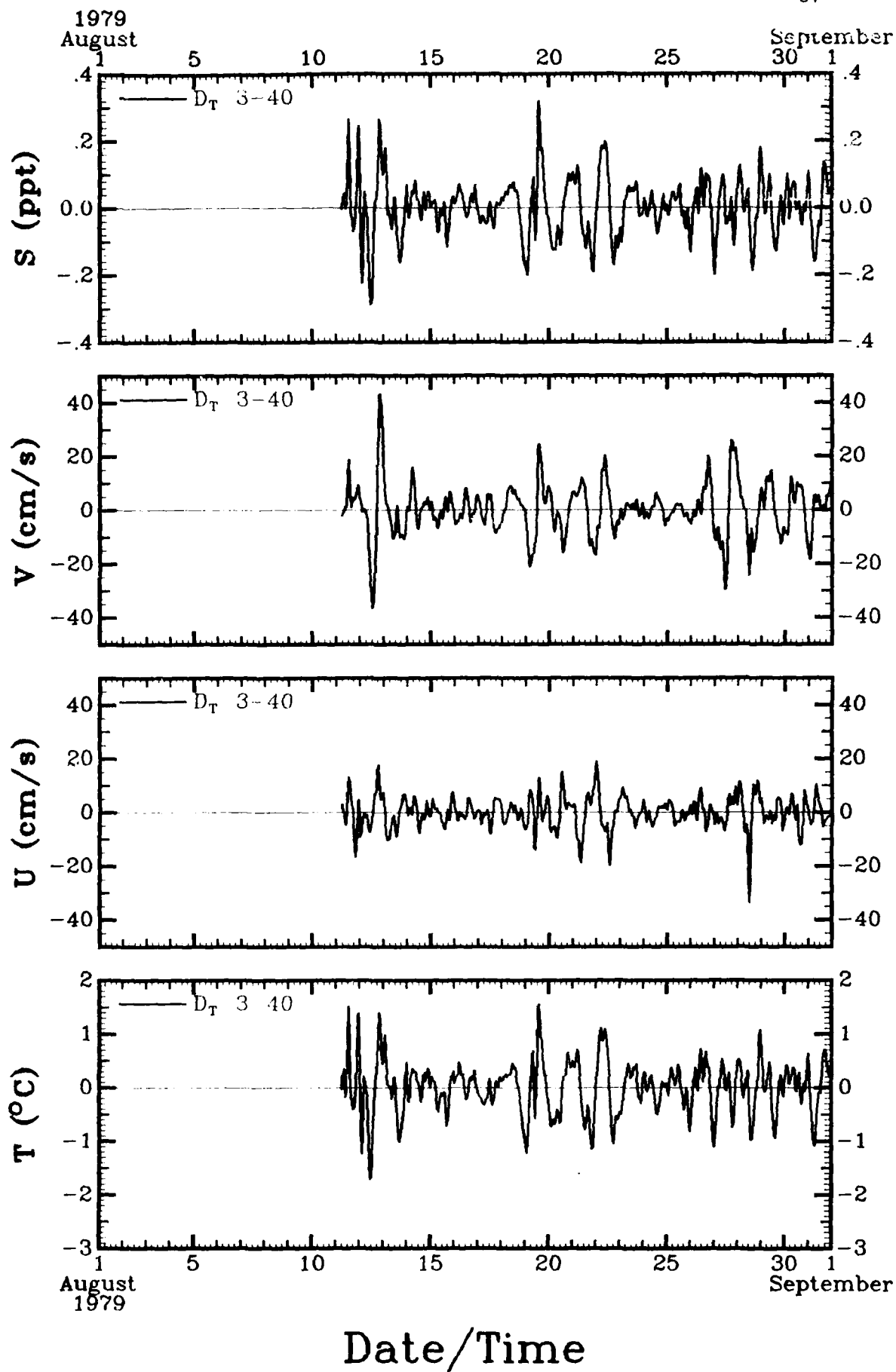
Date/Time

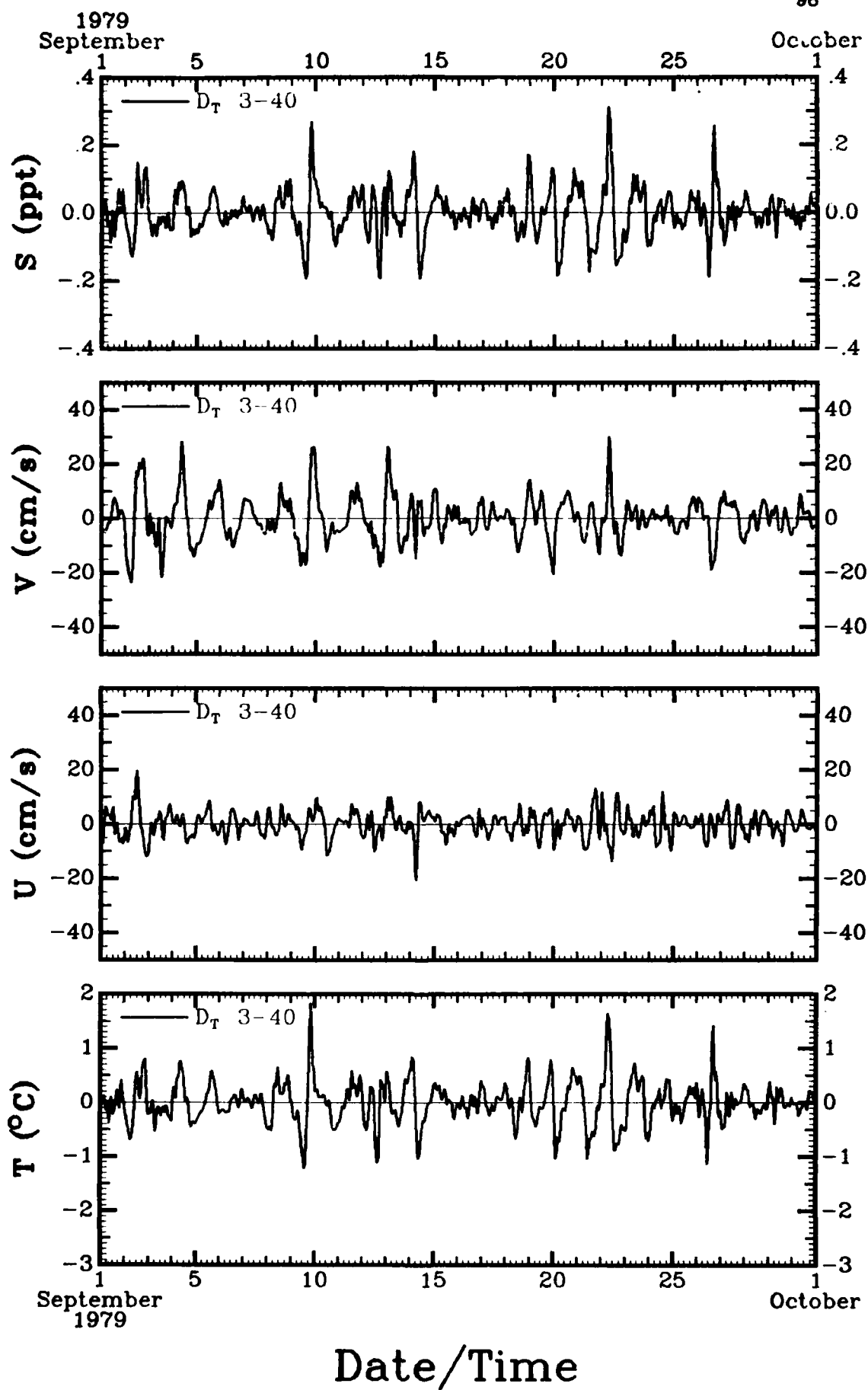


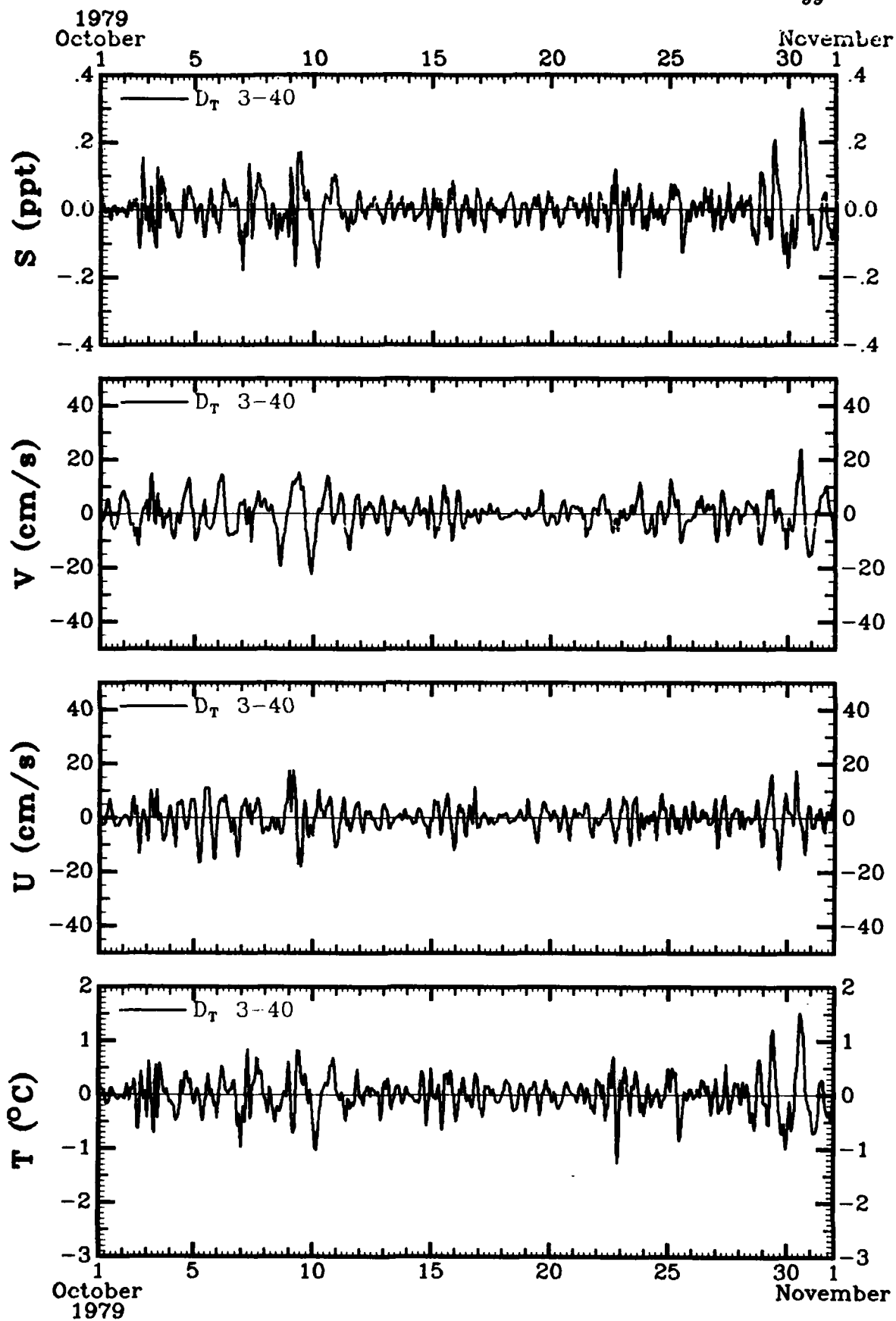
Date/Time



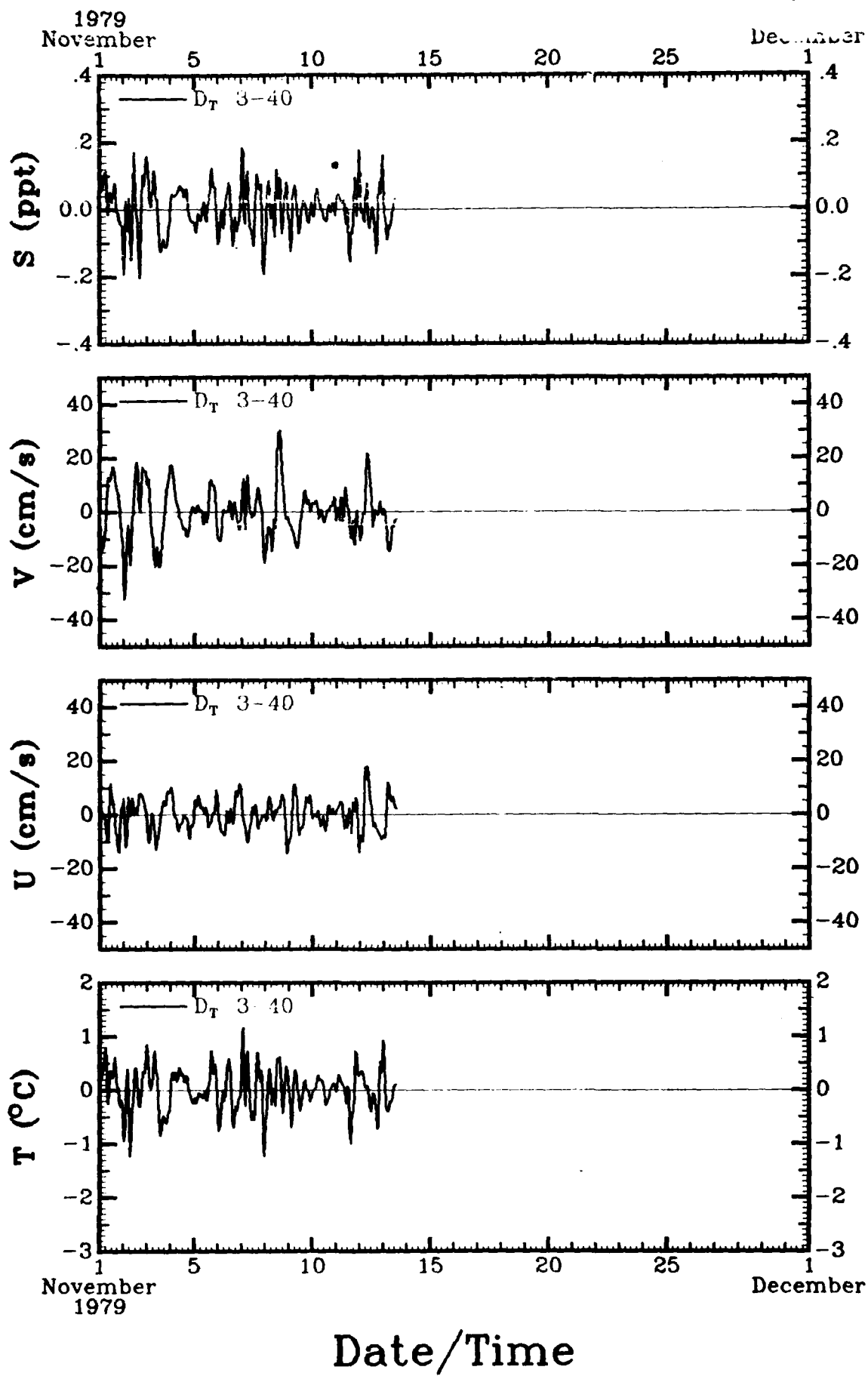








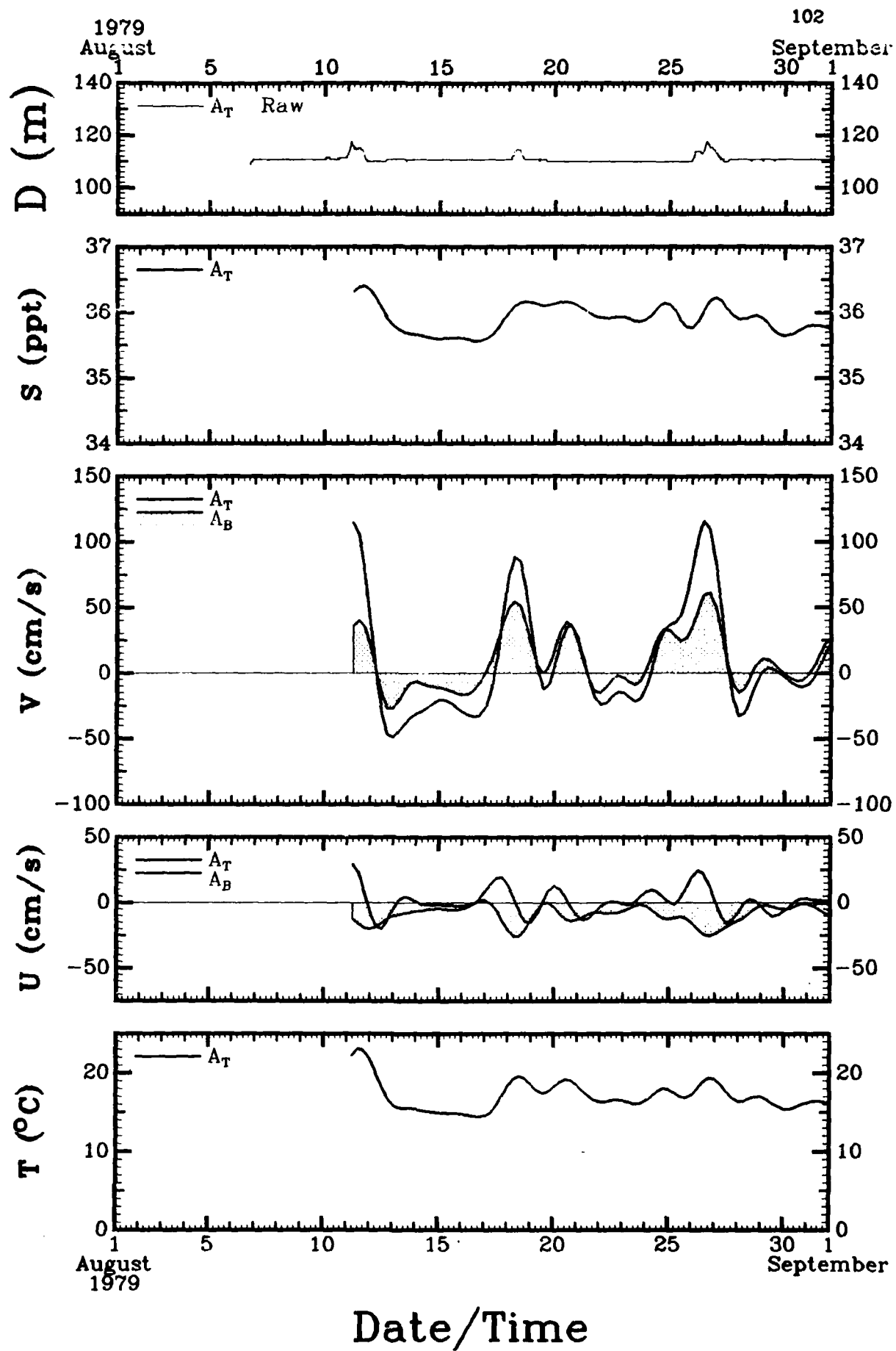
Date/Time

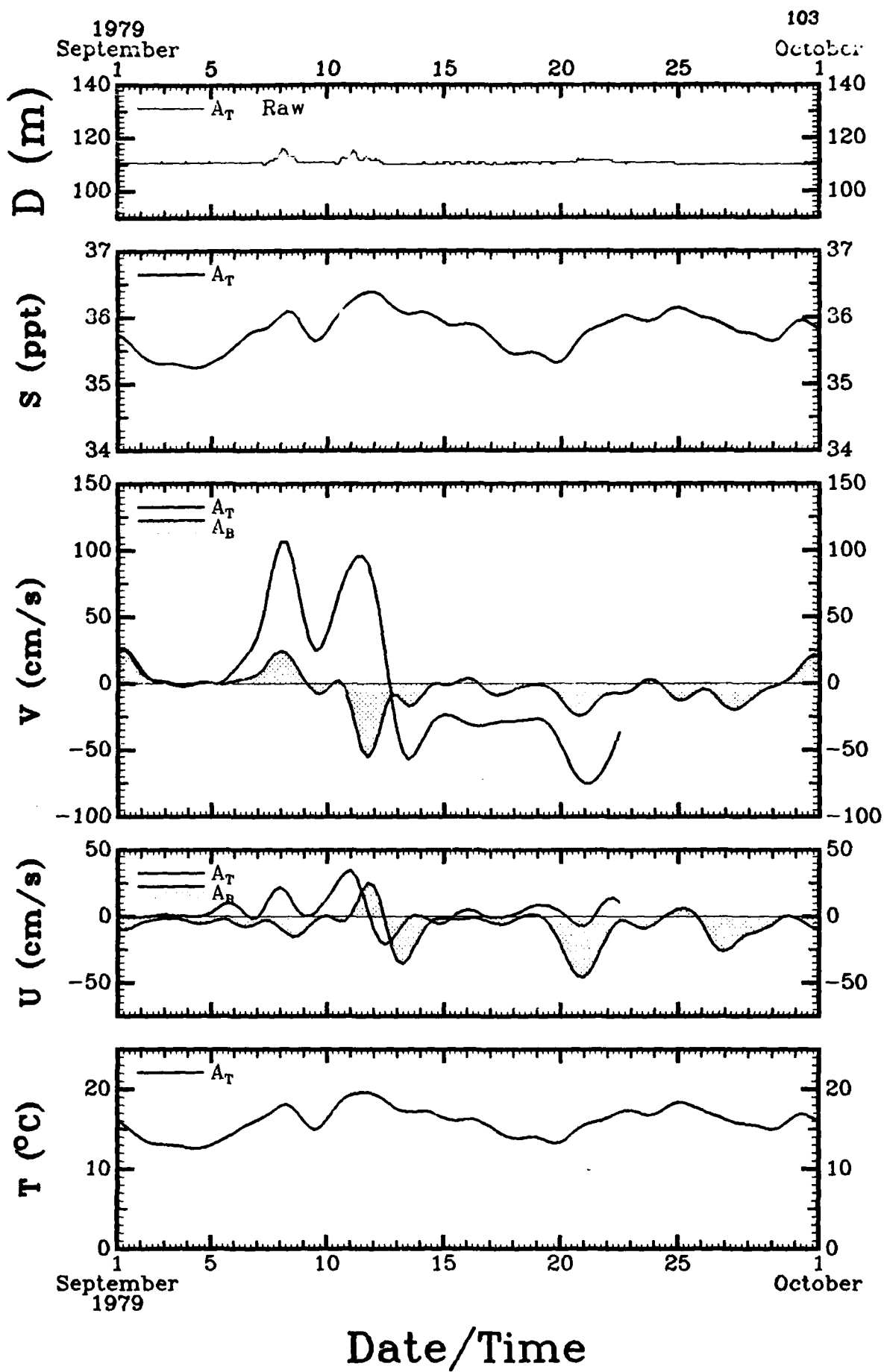


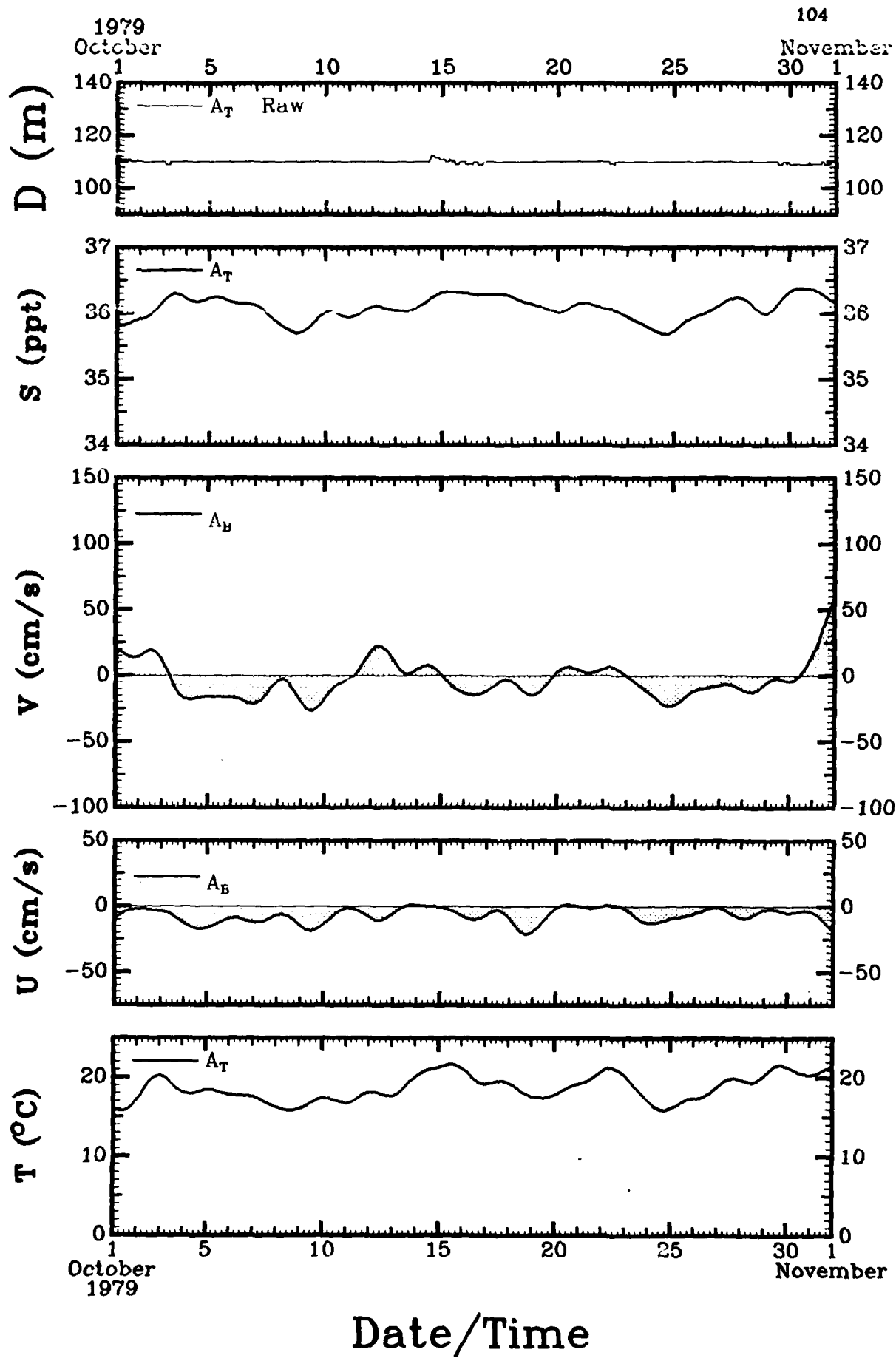
SECTION 5

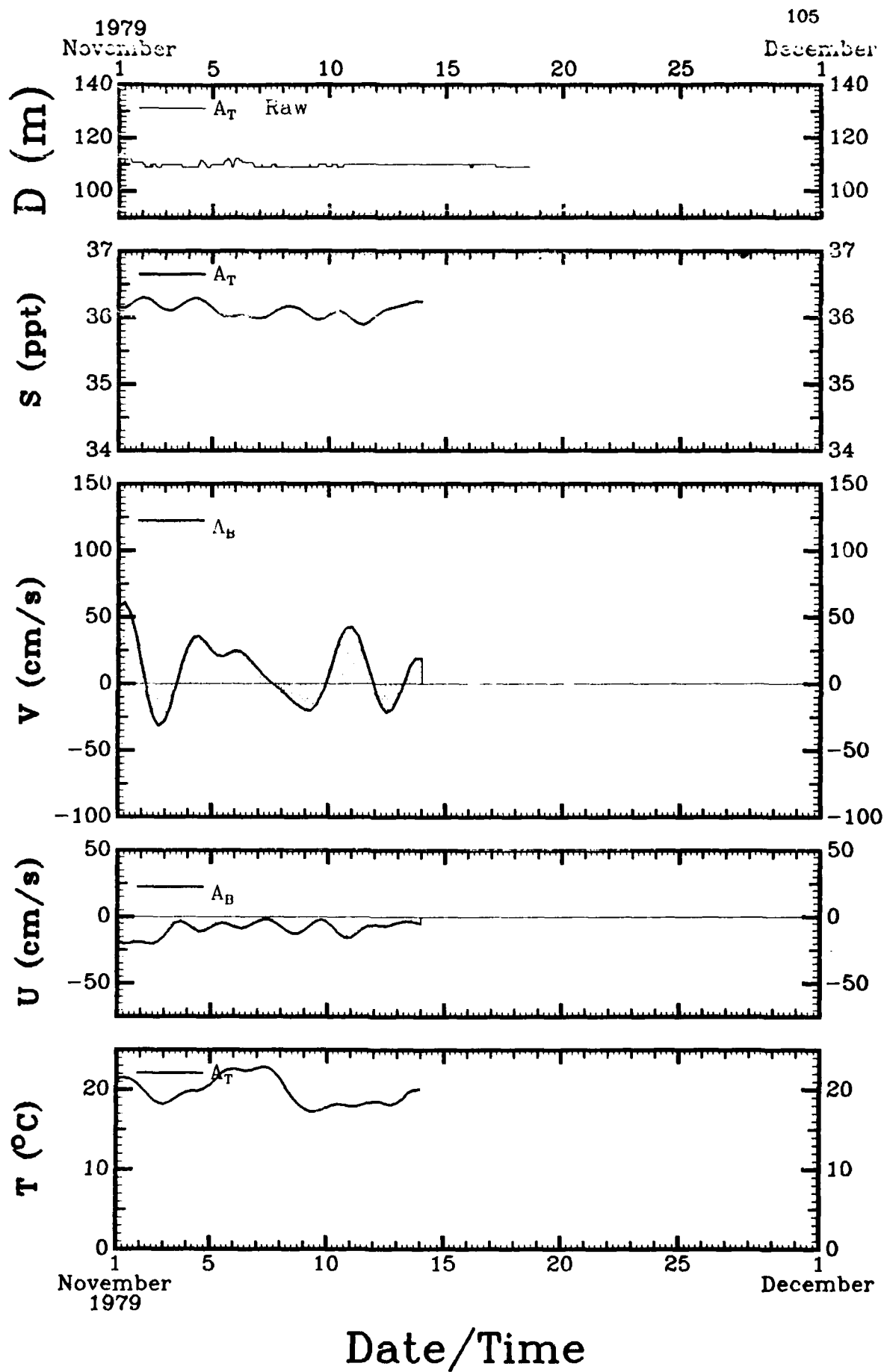
40 HRLP Data for Each Mooring

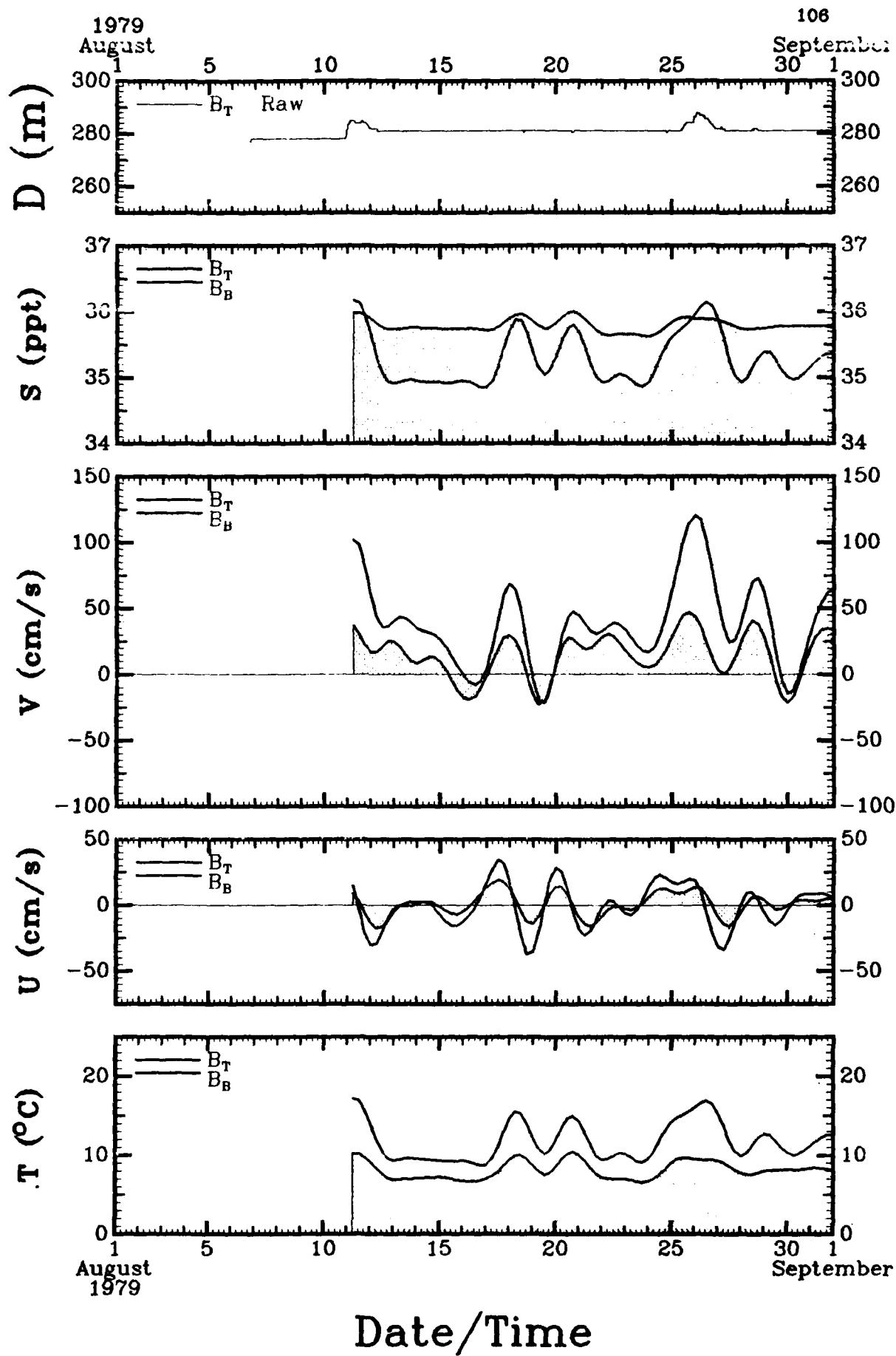
Figures 31 through 34 show the raw pressure data (converted to depth units) and the 40 HRLP current meter data by month for each mooring, superimposing similar data from each instrument on the mooring. Common scaling is used in this section.

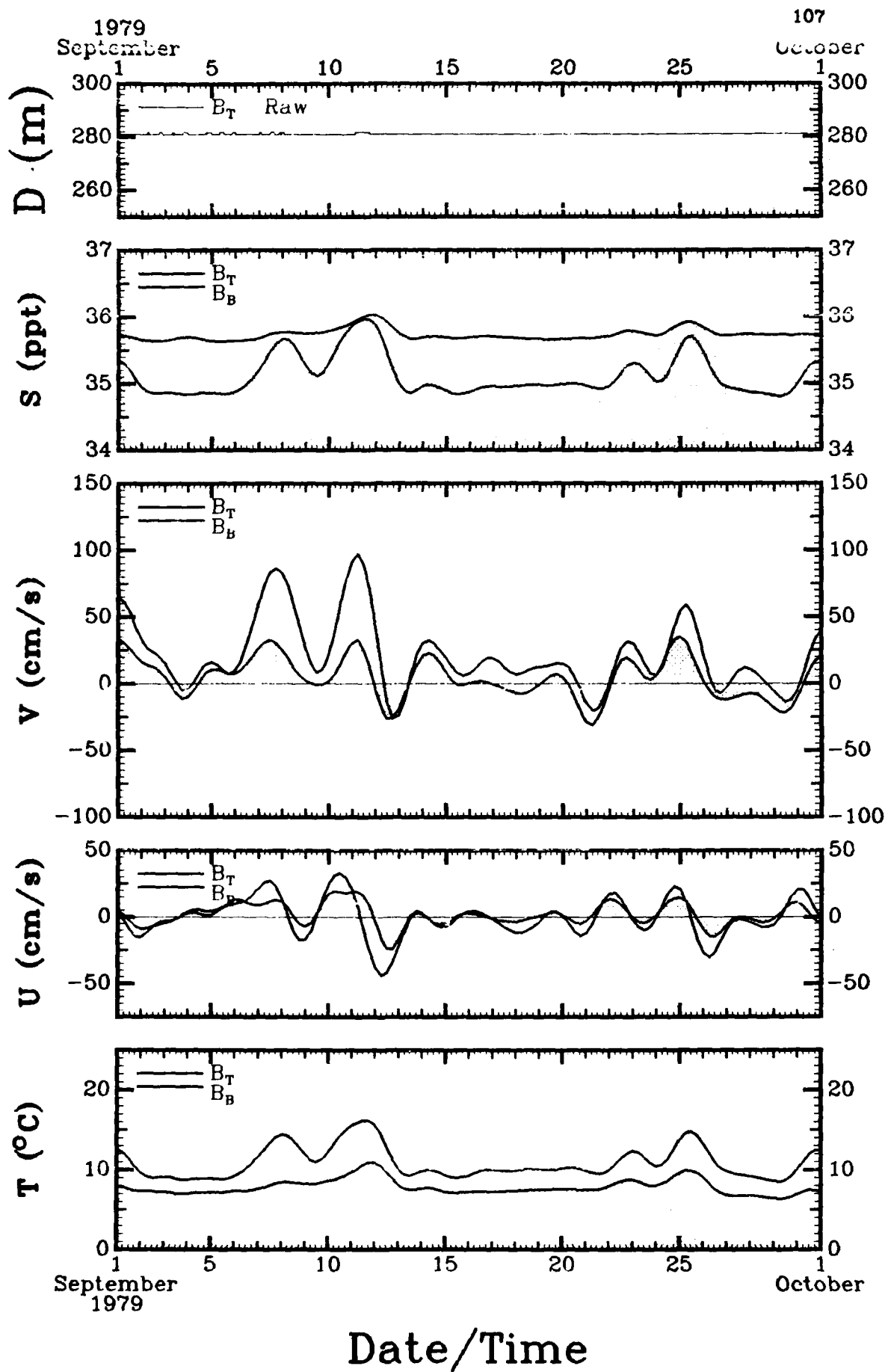


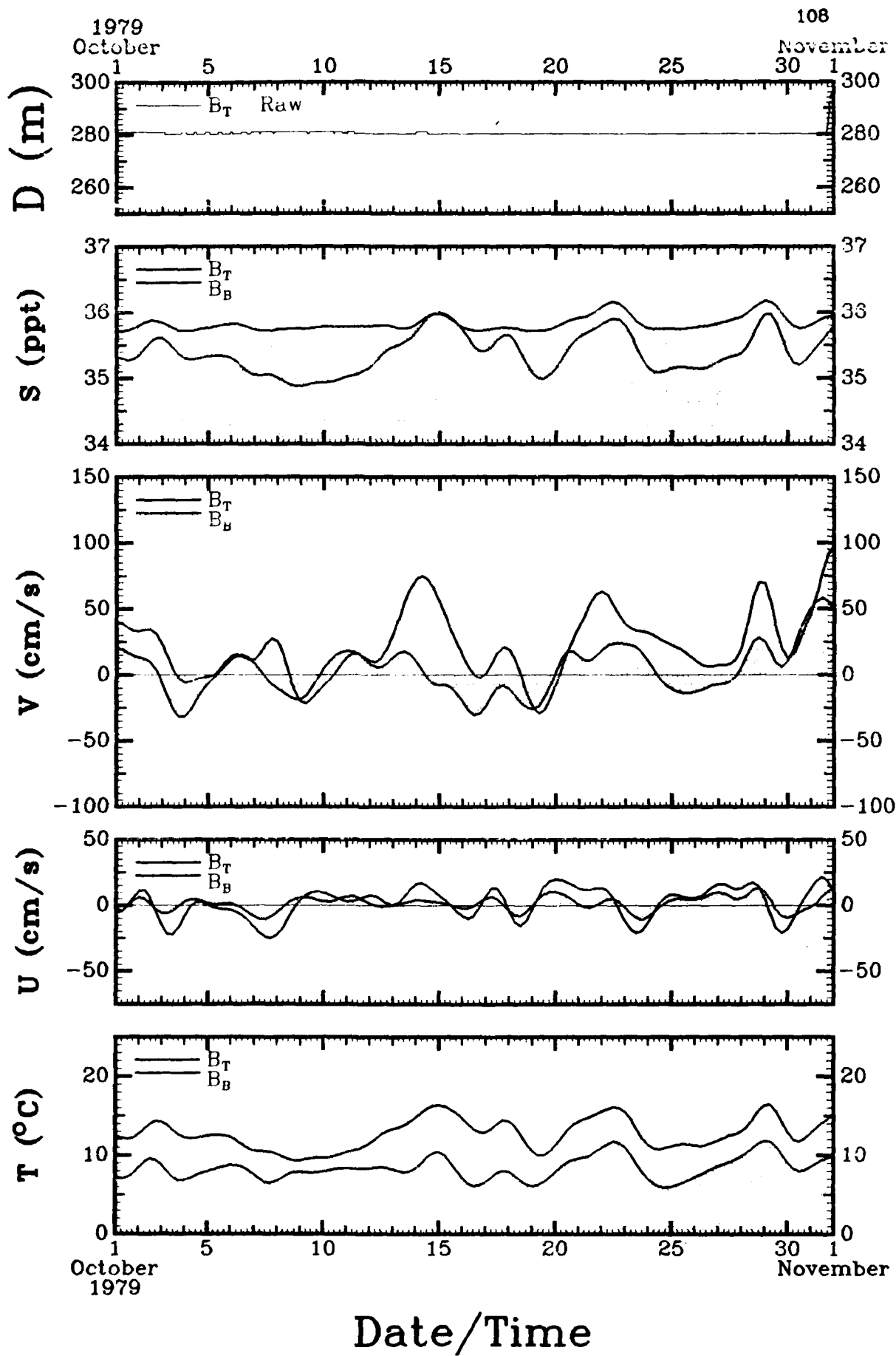


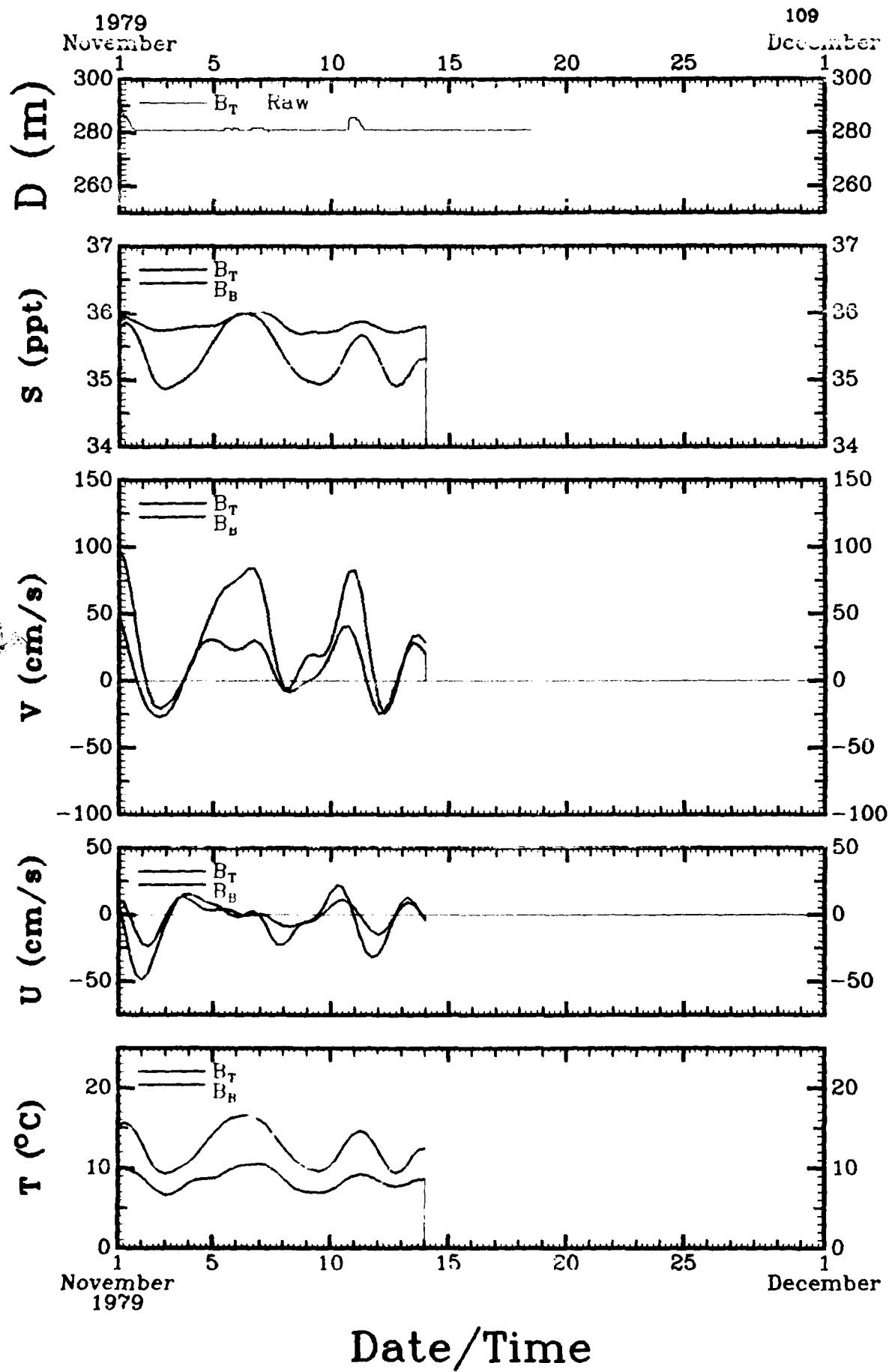


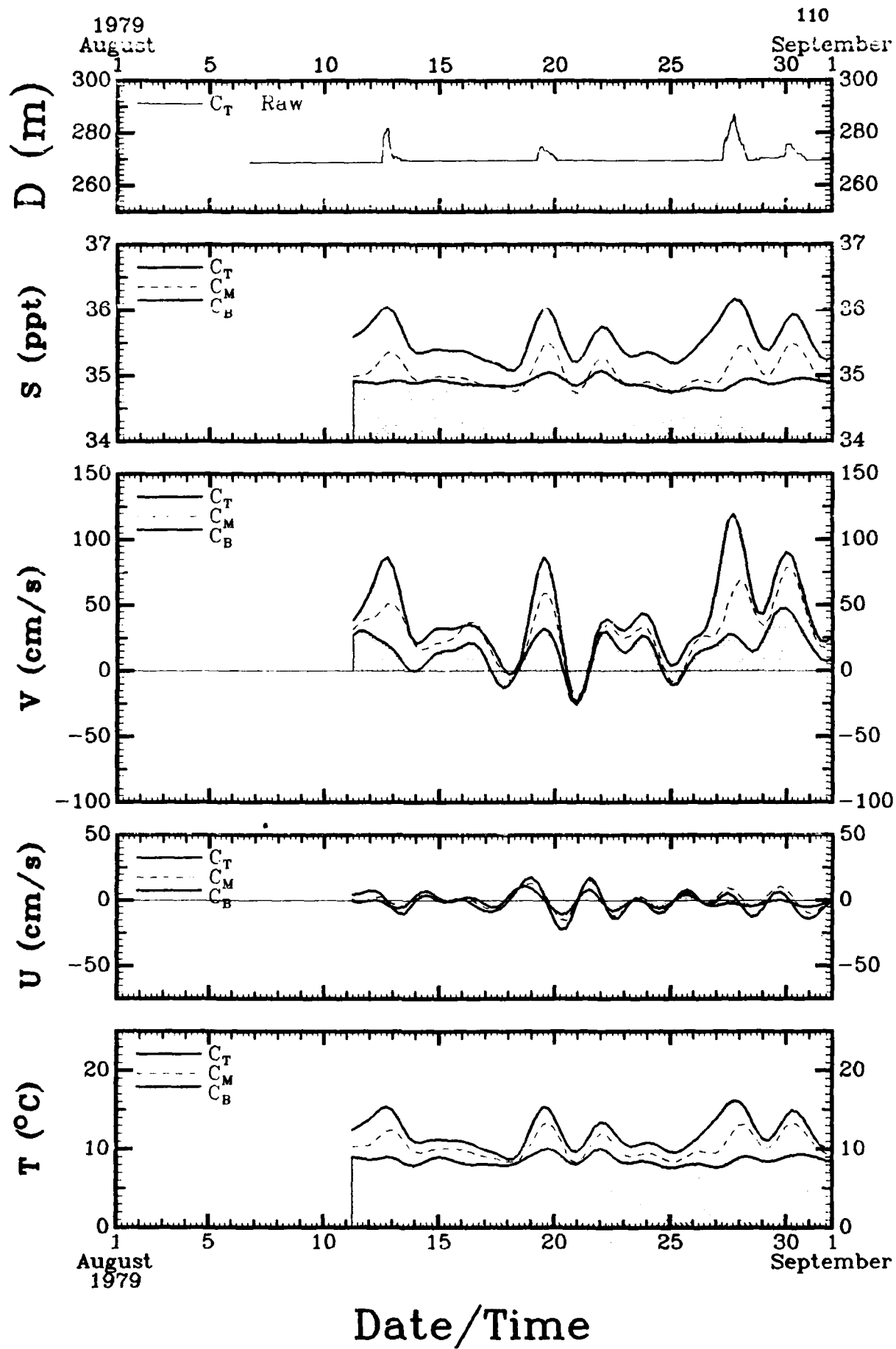


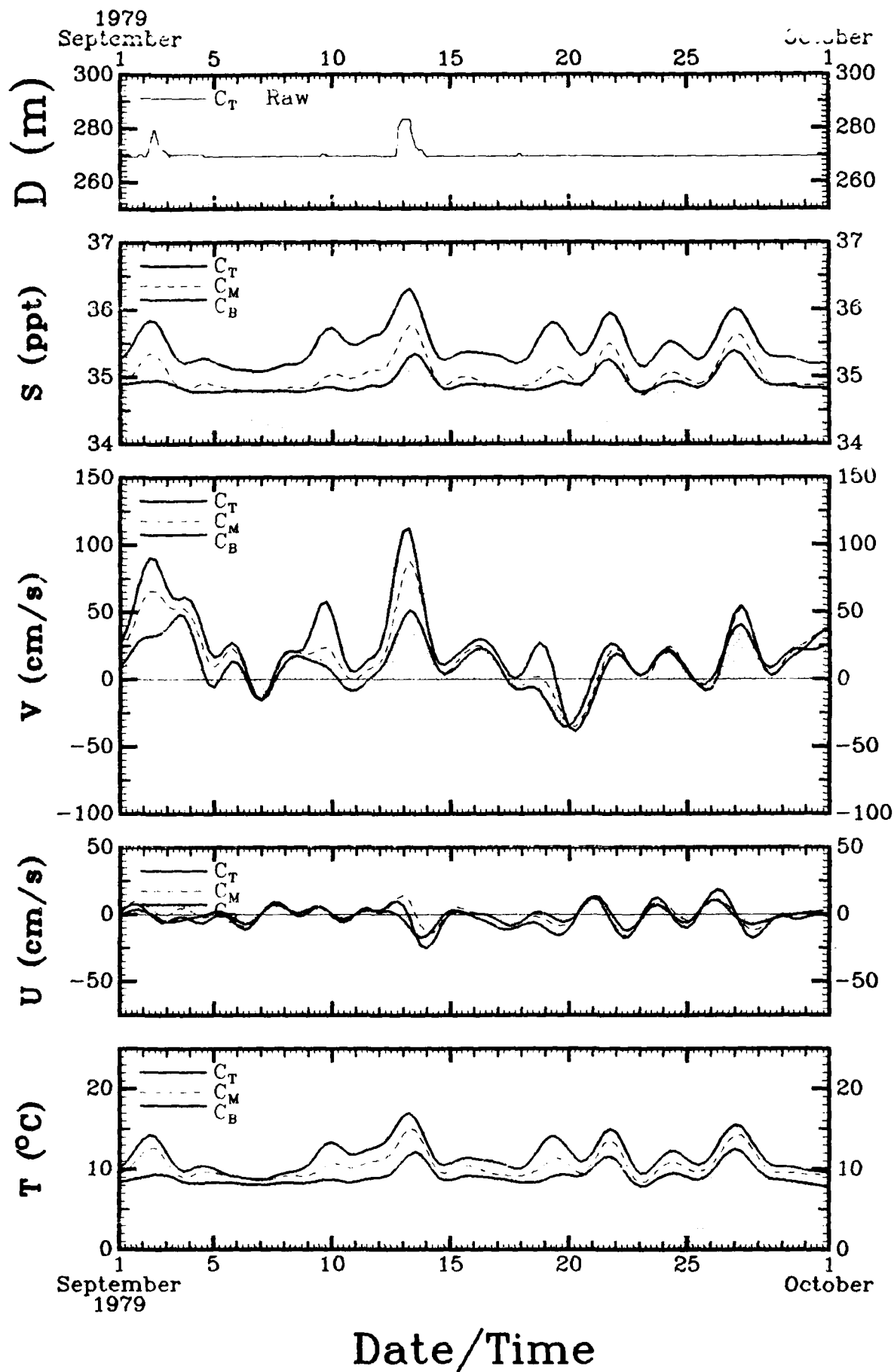


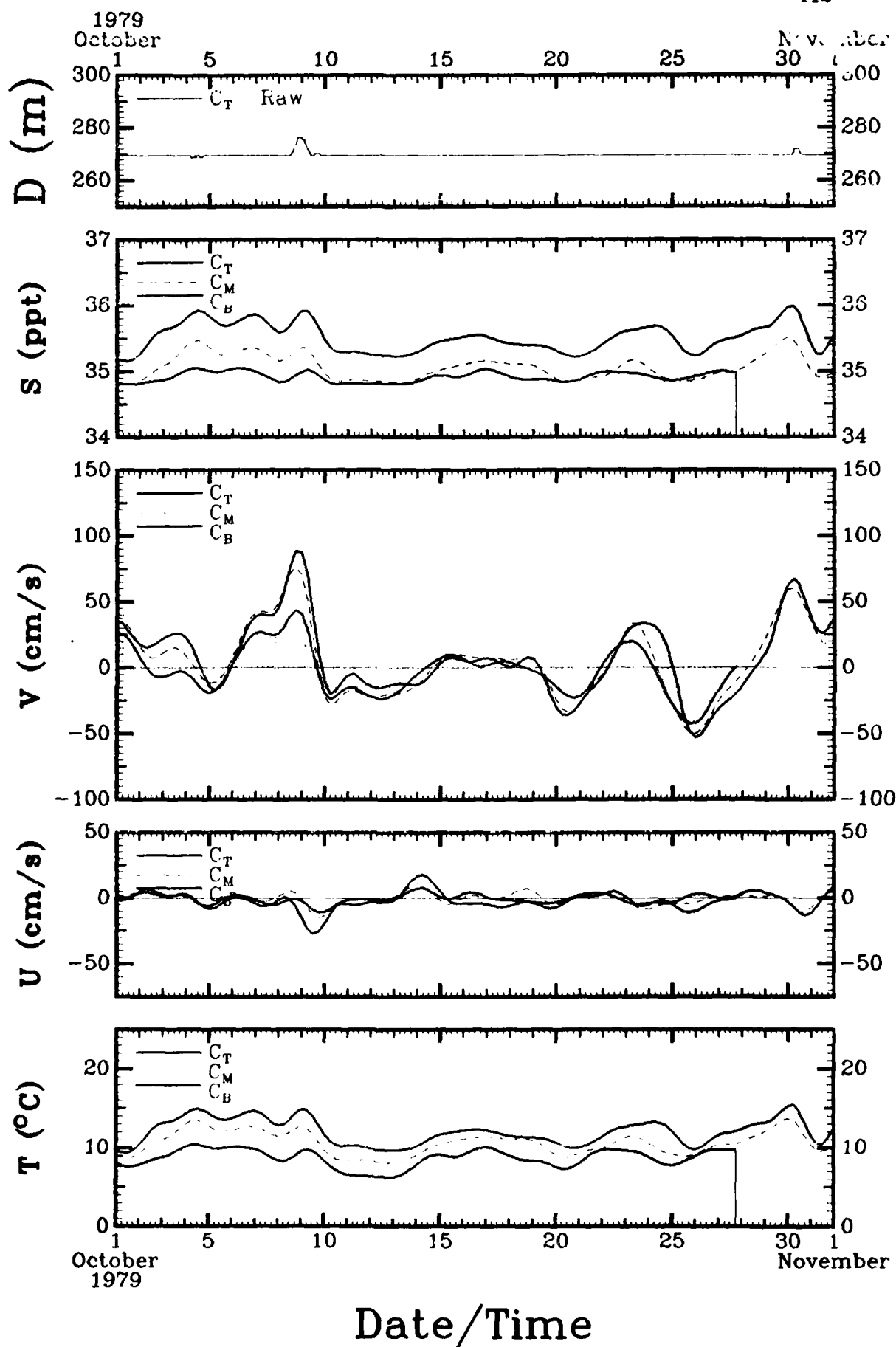


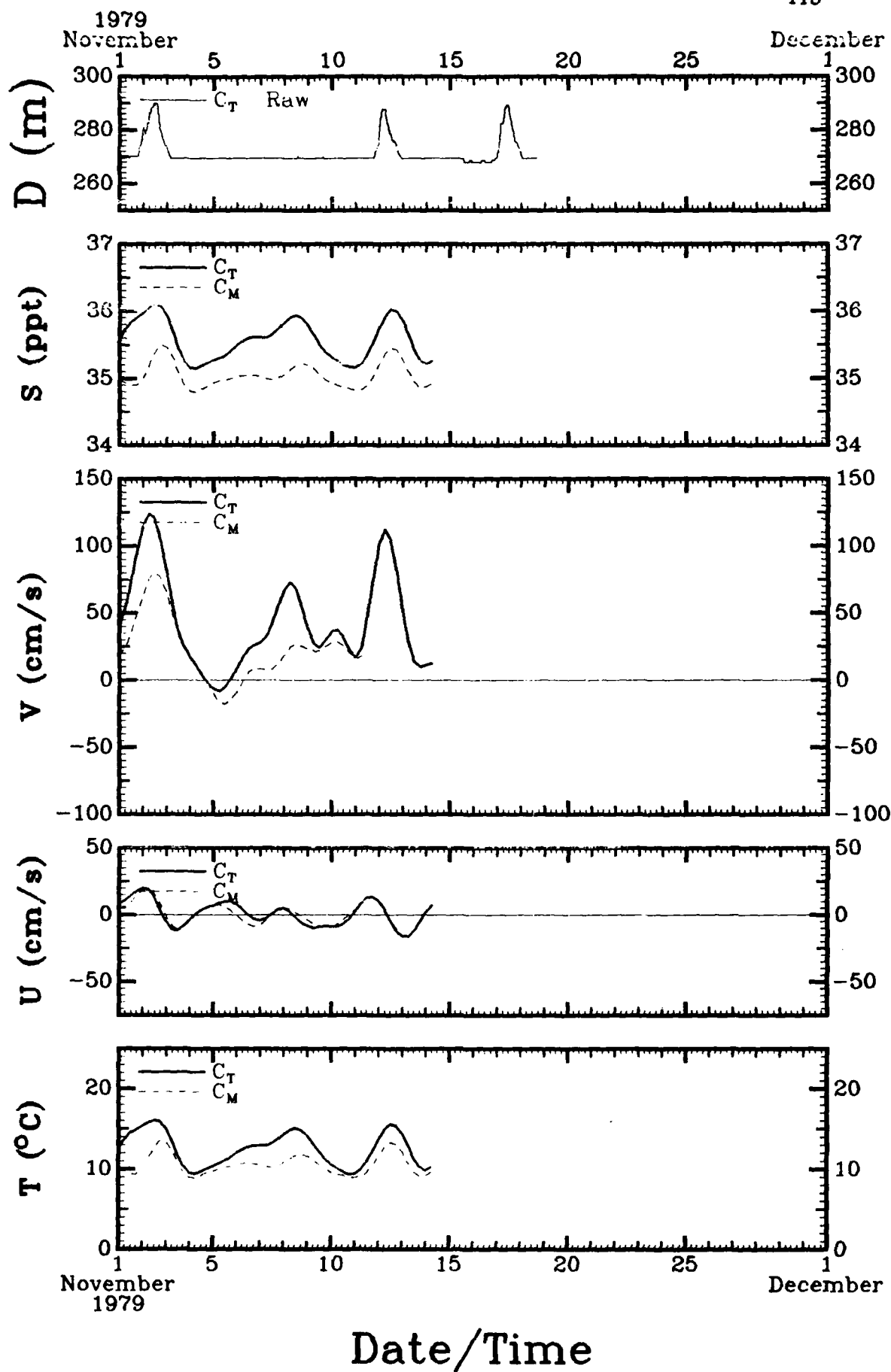


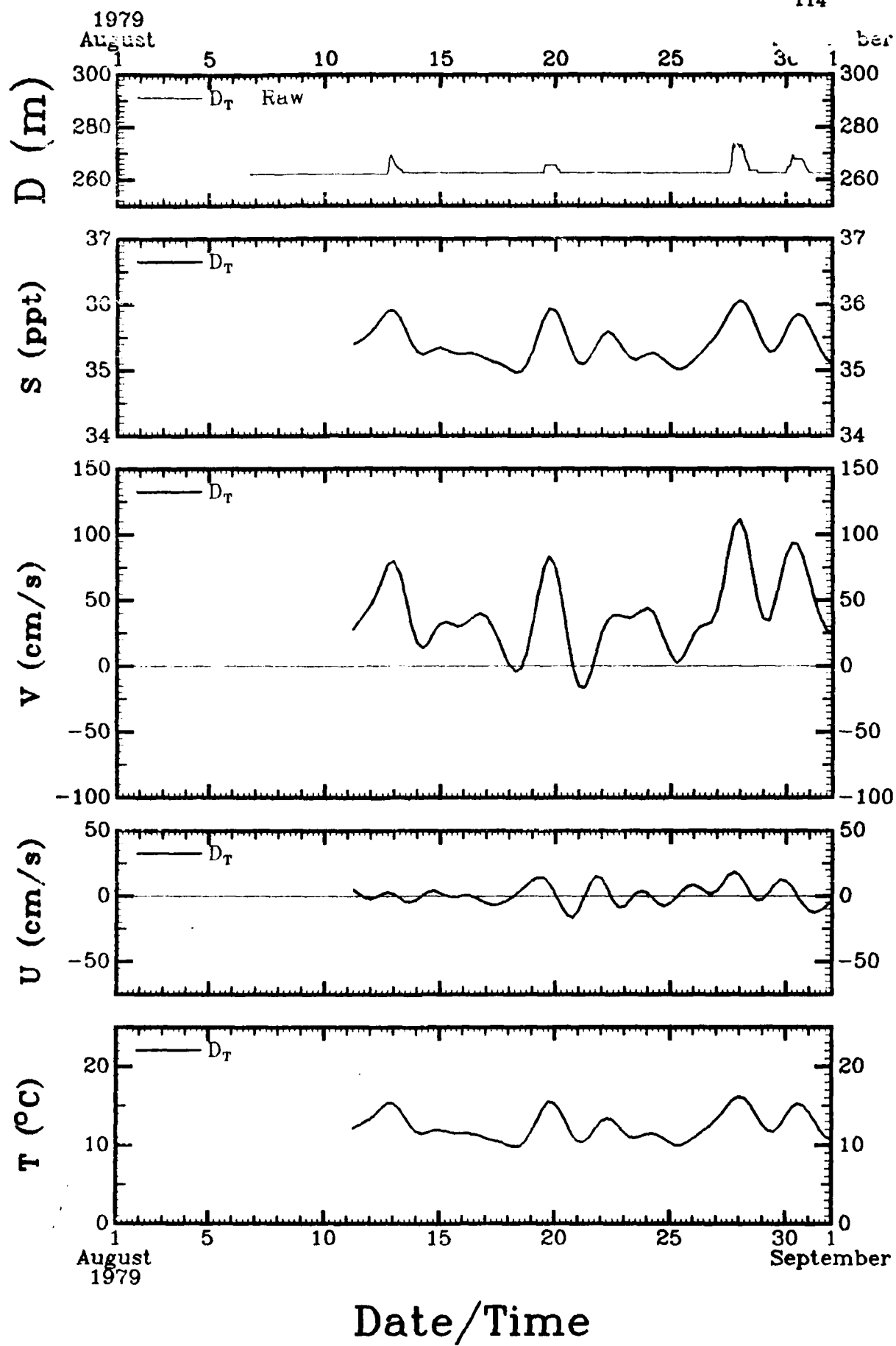


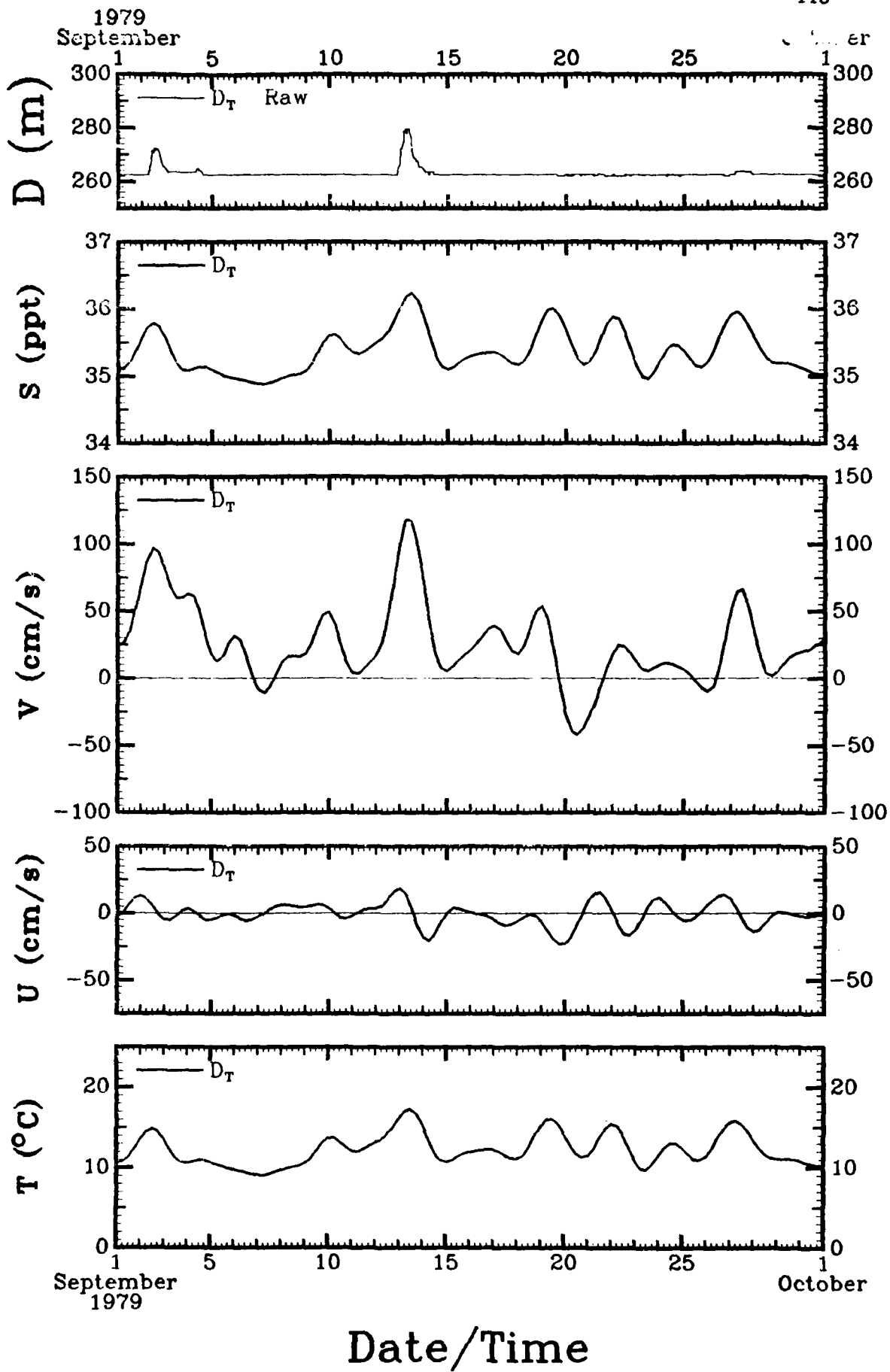


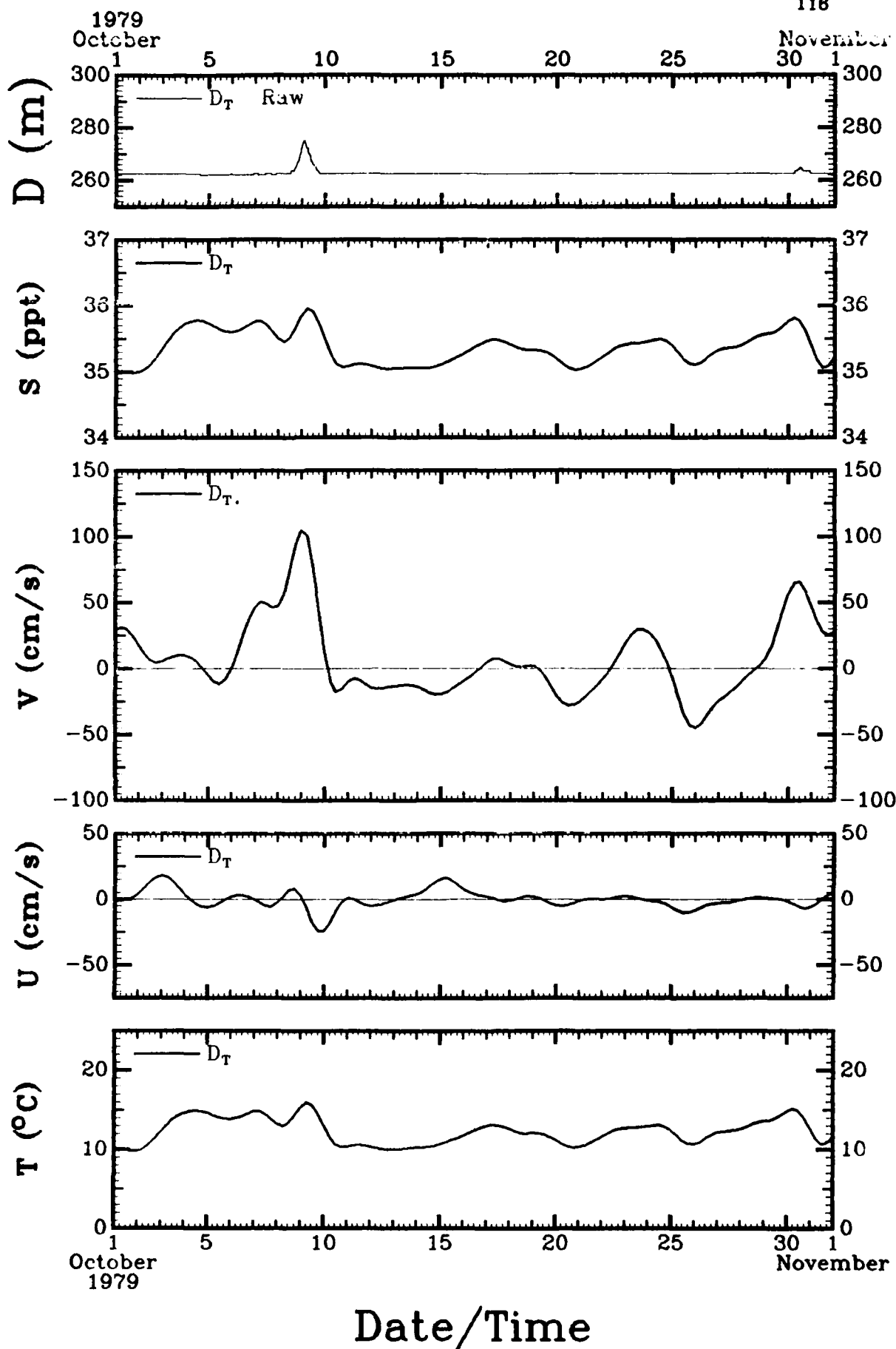


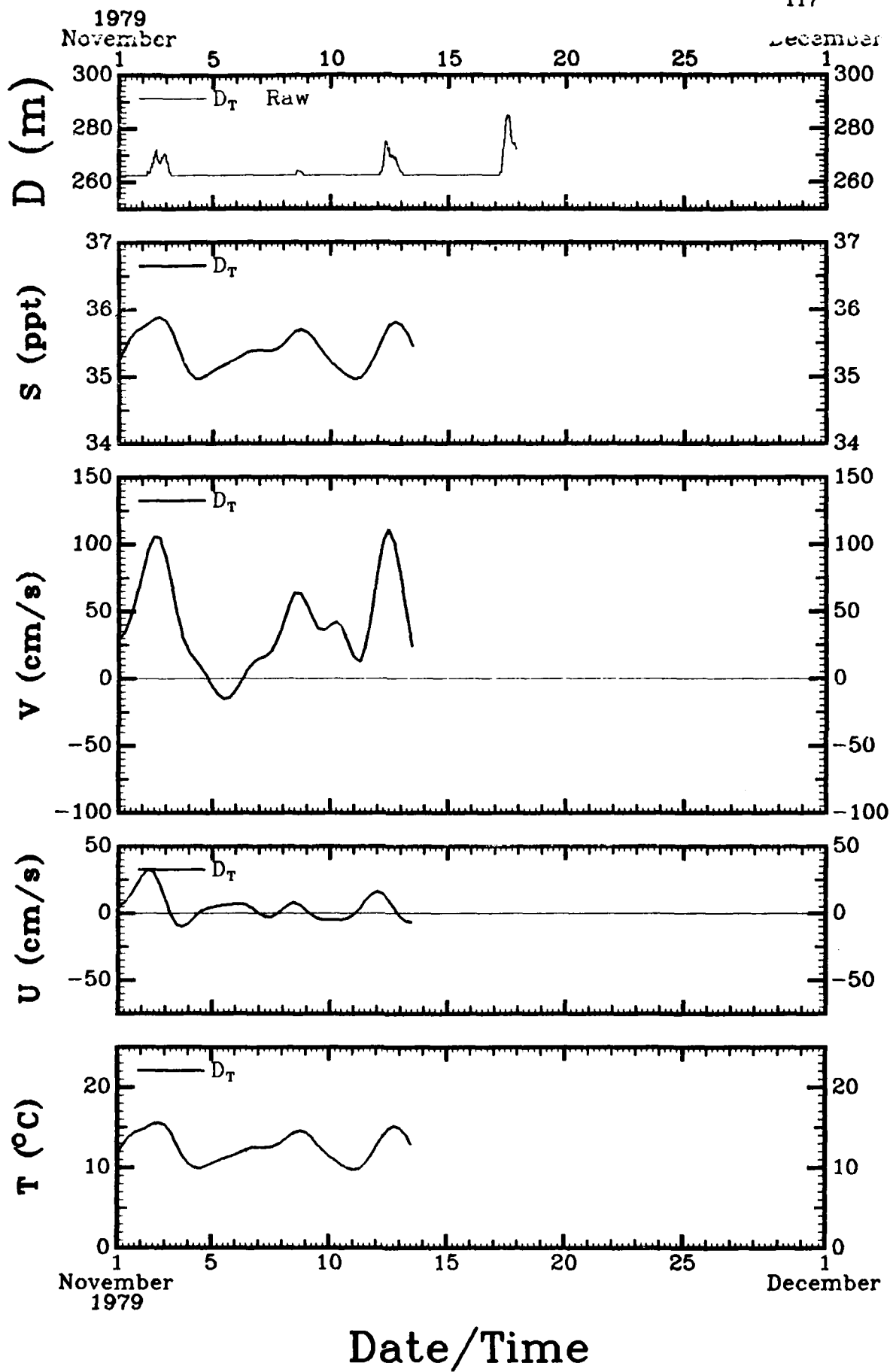








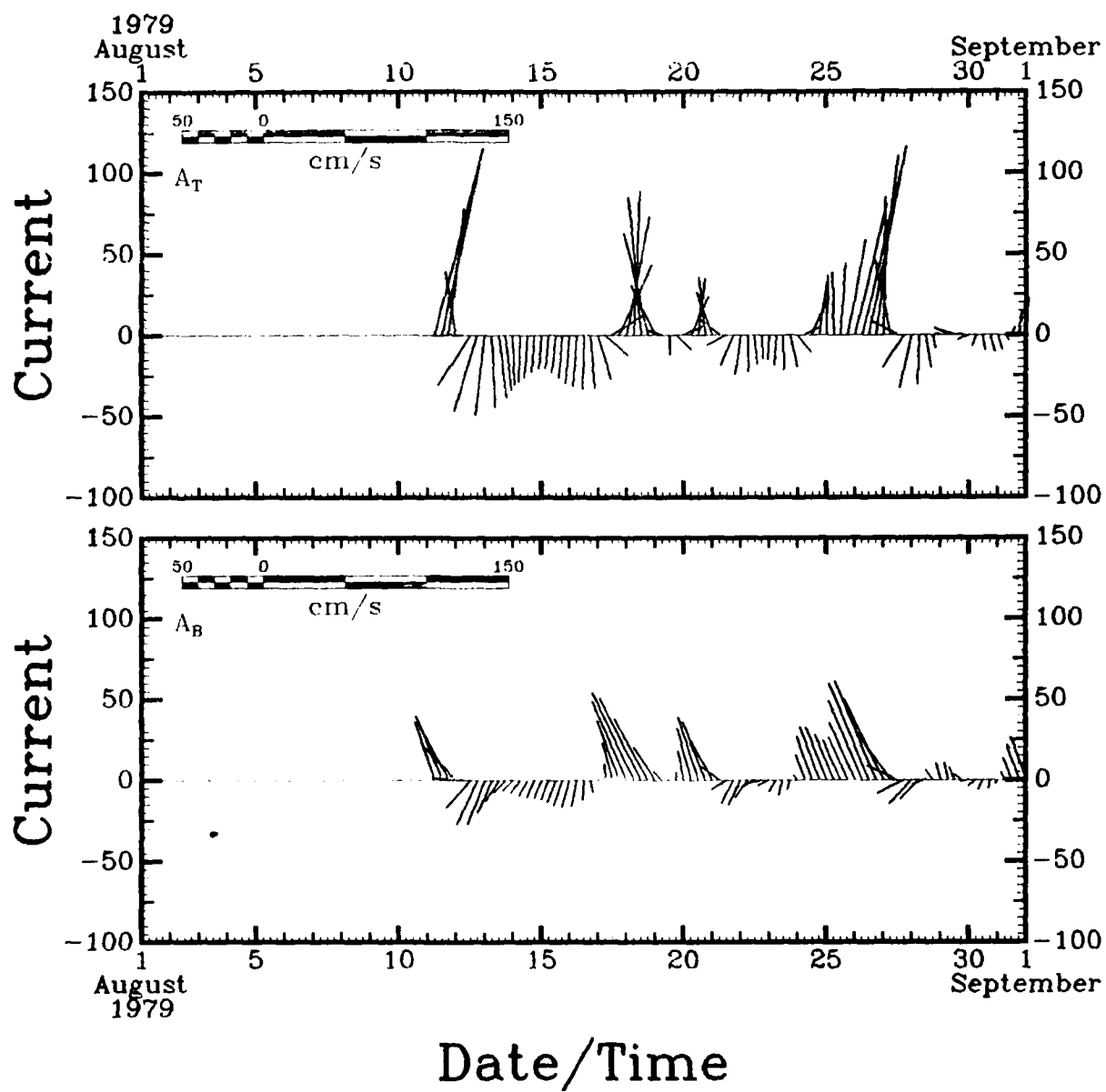


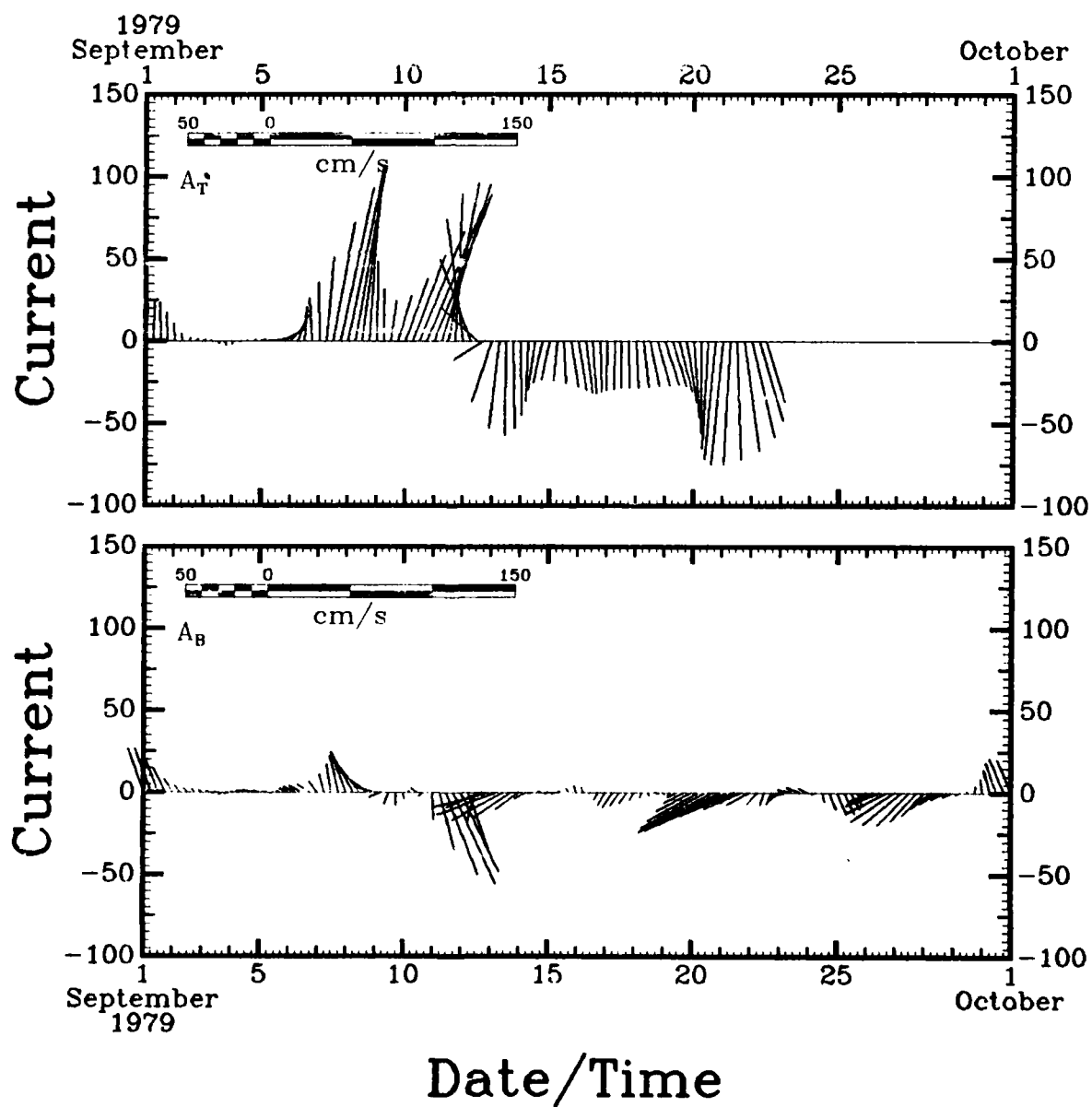


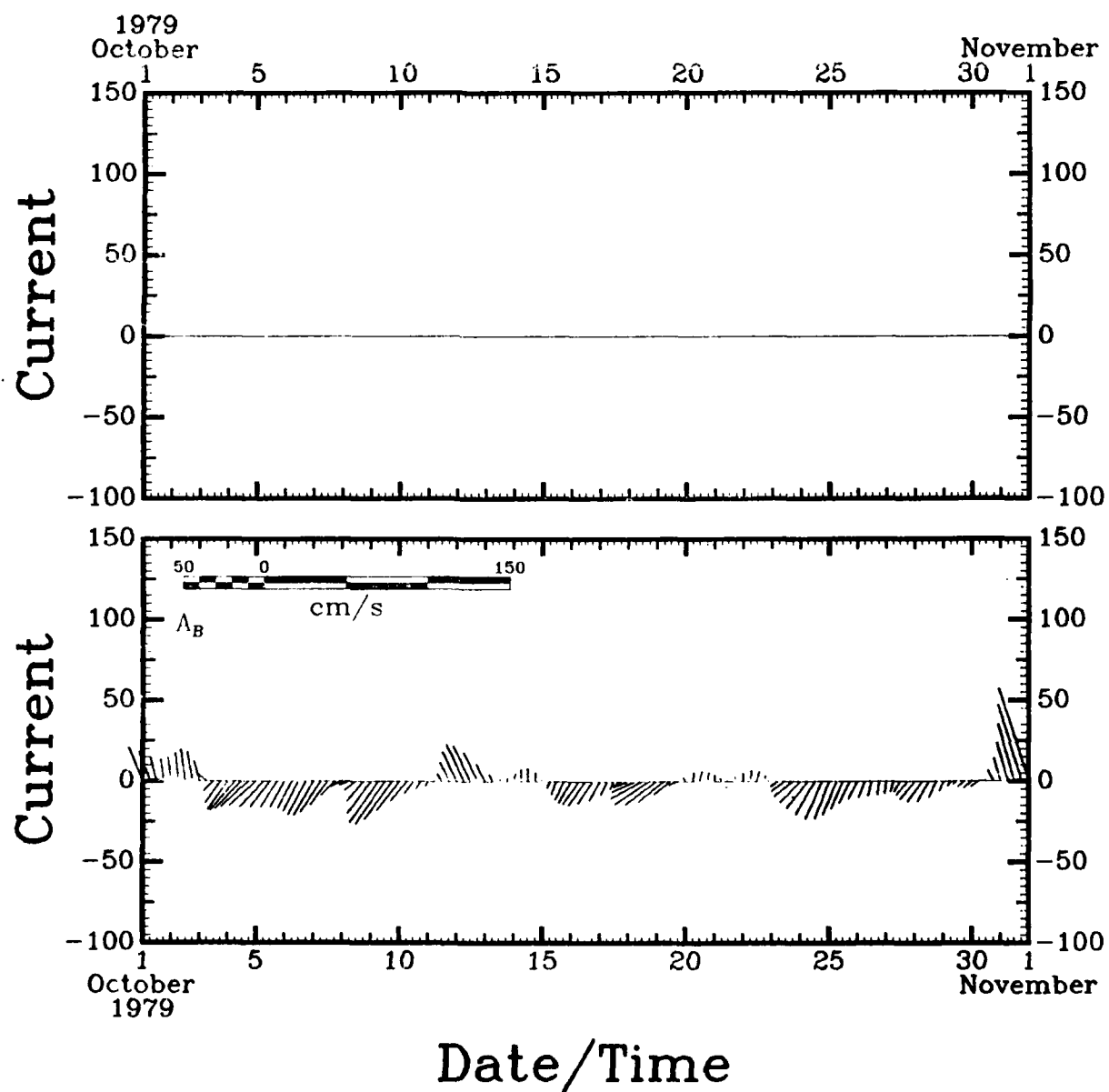
SECTION 6

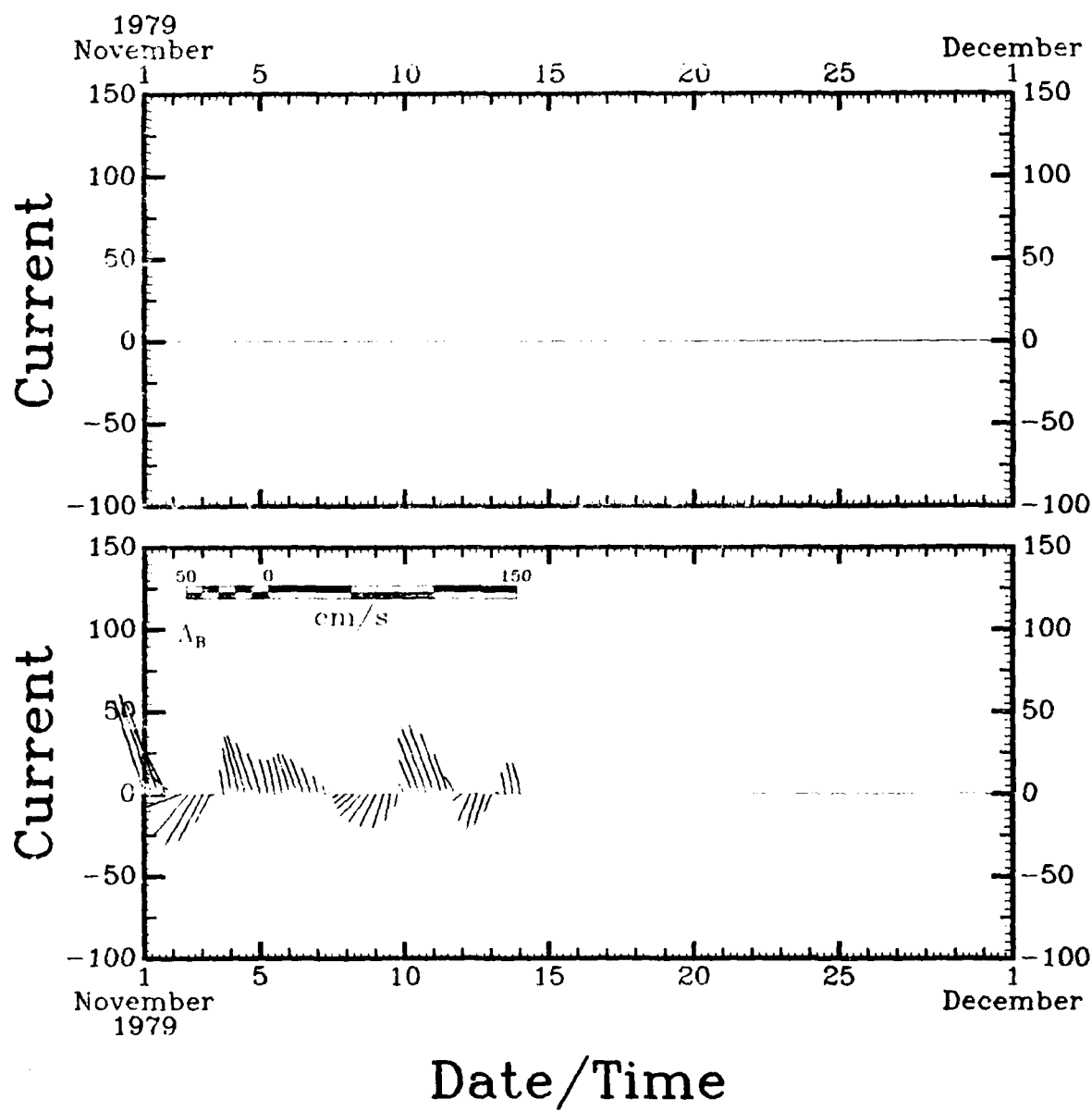
40 HRLP Current Vector "Stick" Plots for Each Mooring

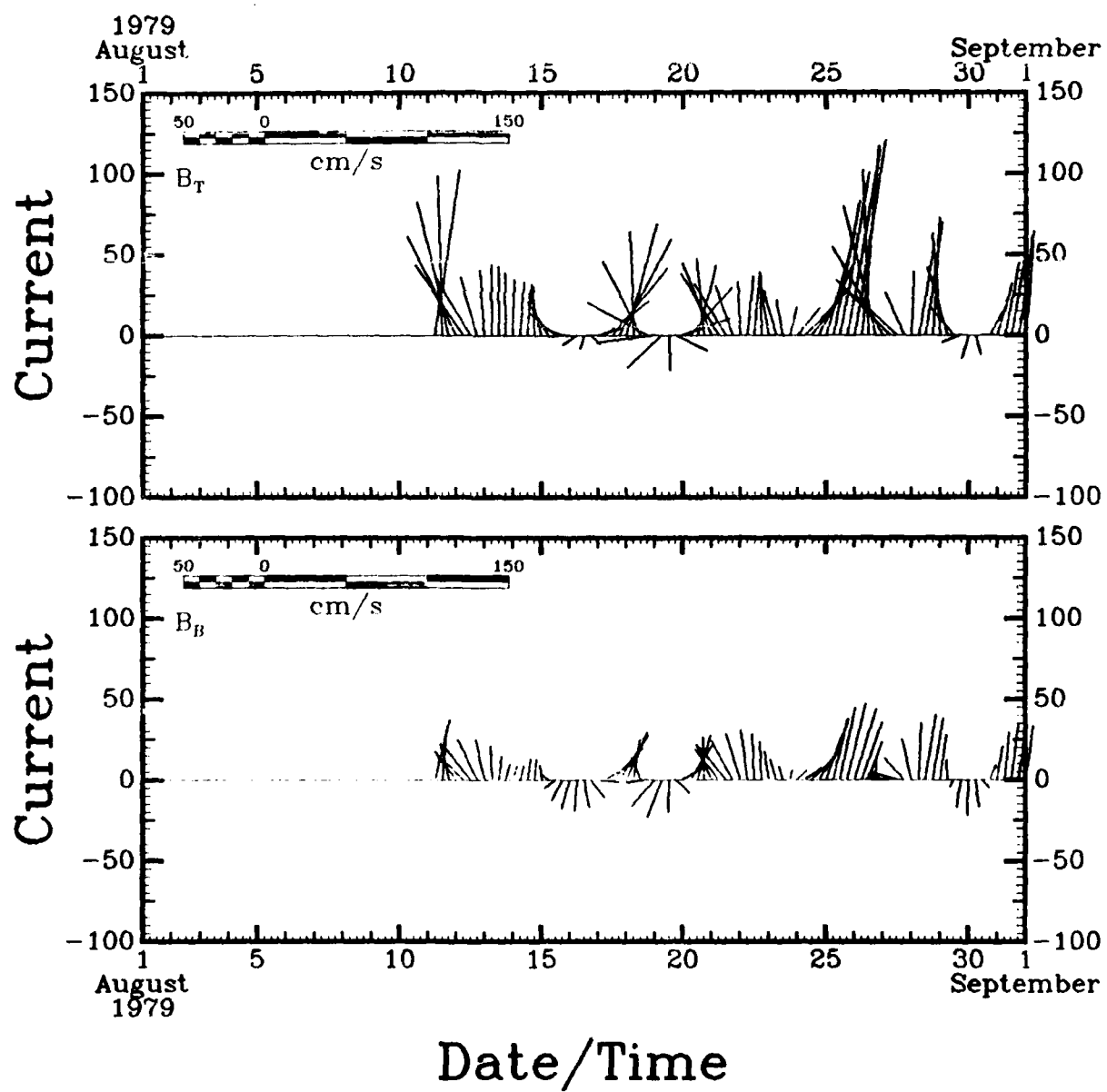
Figures 35 through 38 show the 40 HRLP current vectors in "stick" format by month for each mooring. Vectors pointing toward the top of the page correspond to flow in the downstream (34°T) direction. Common scaling is used in this section.

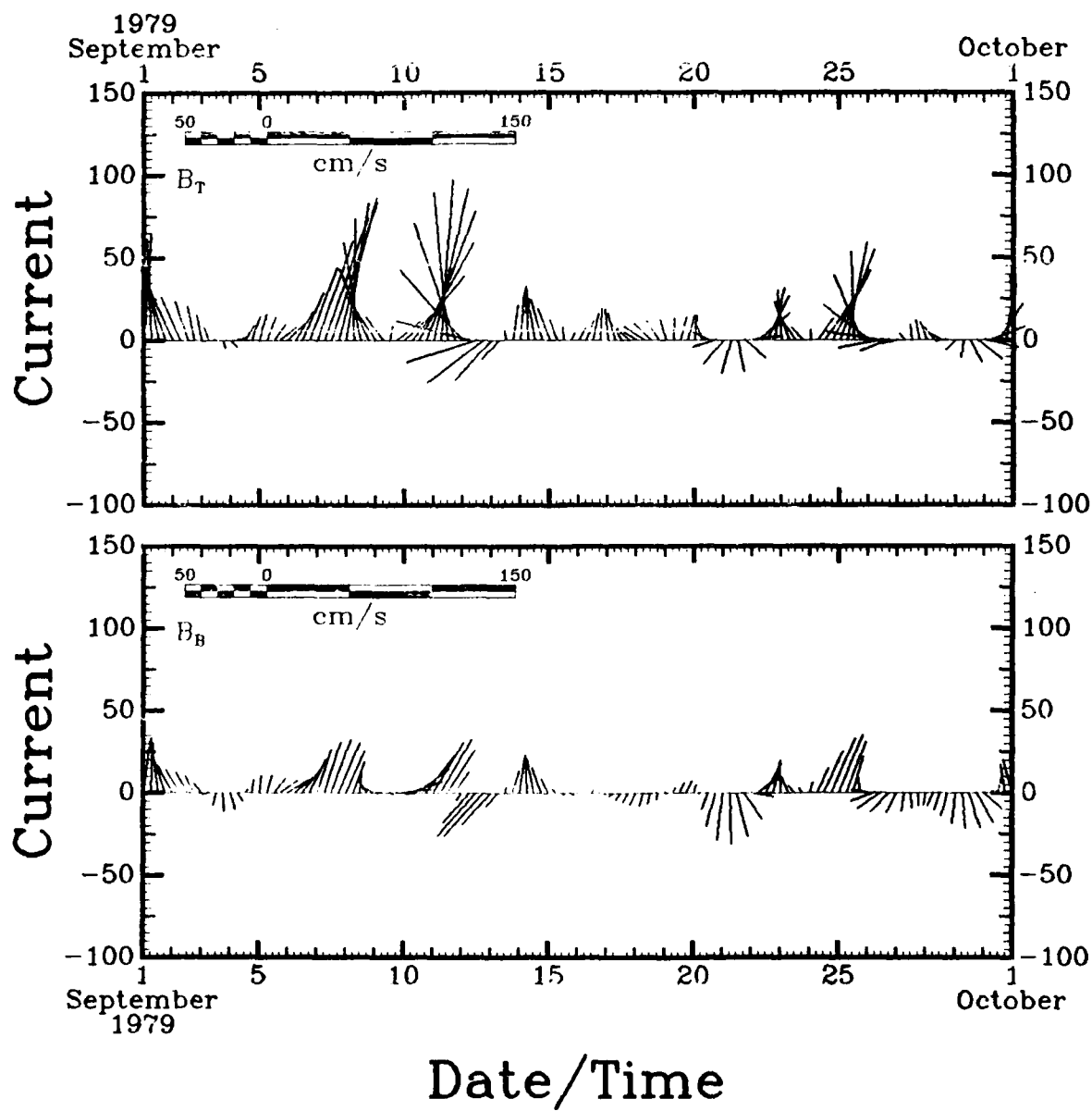


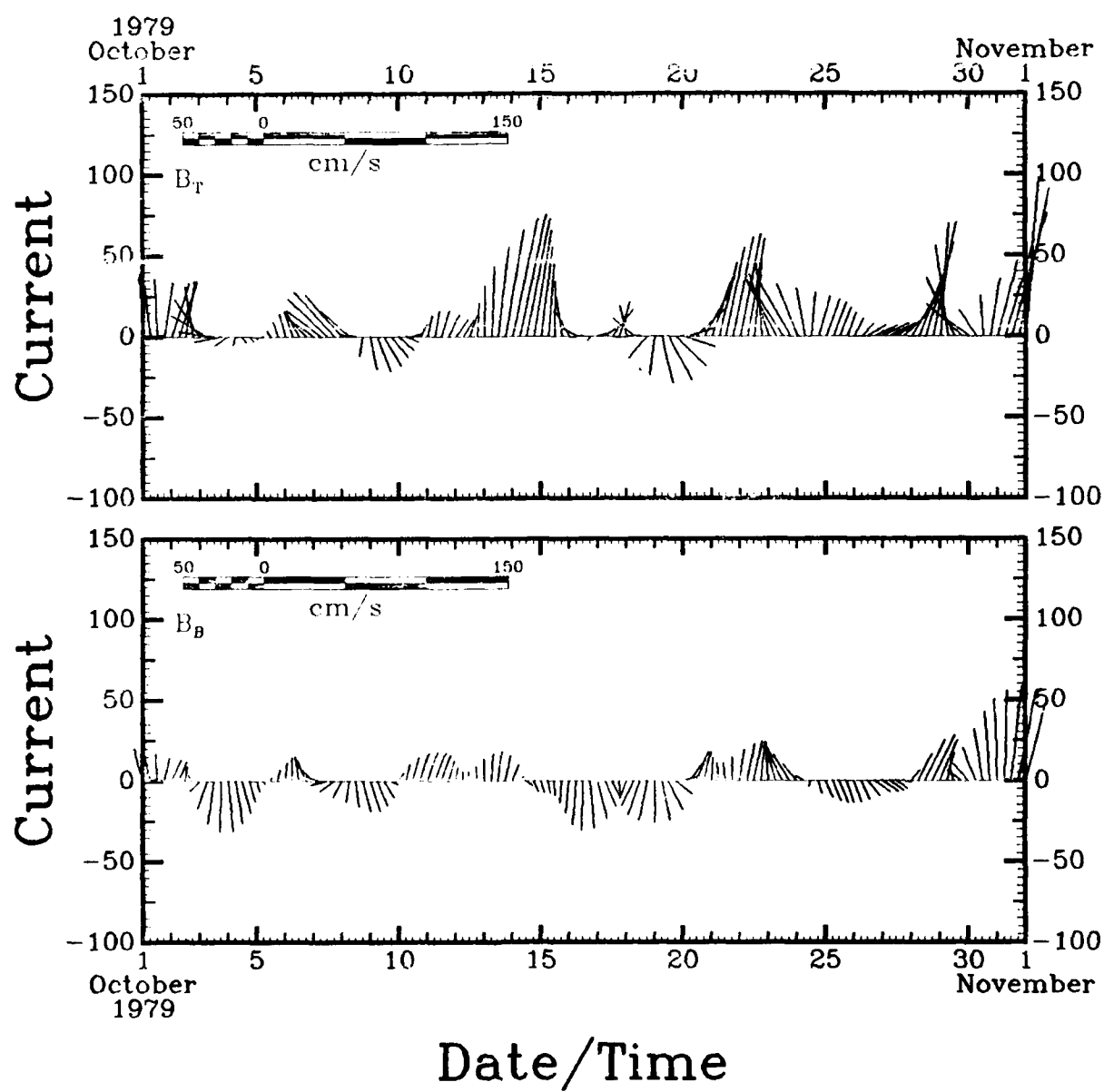


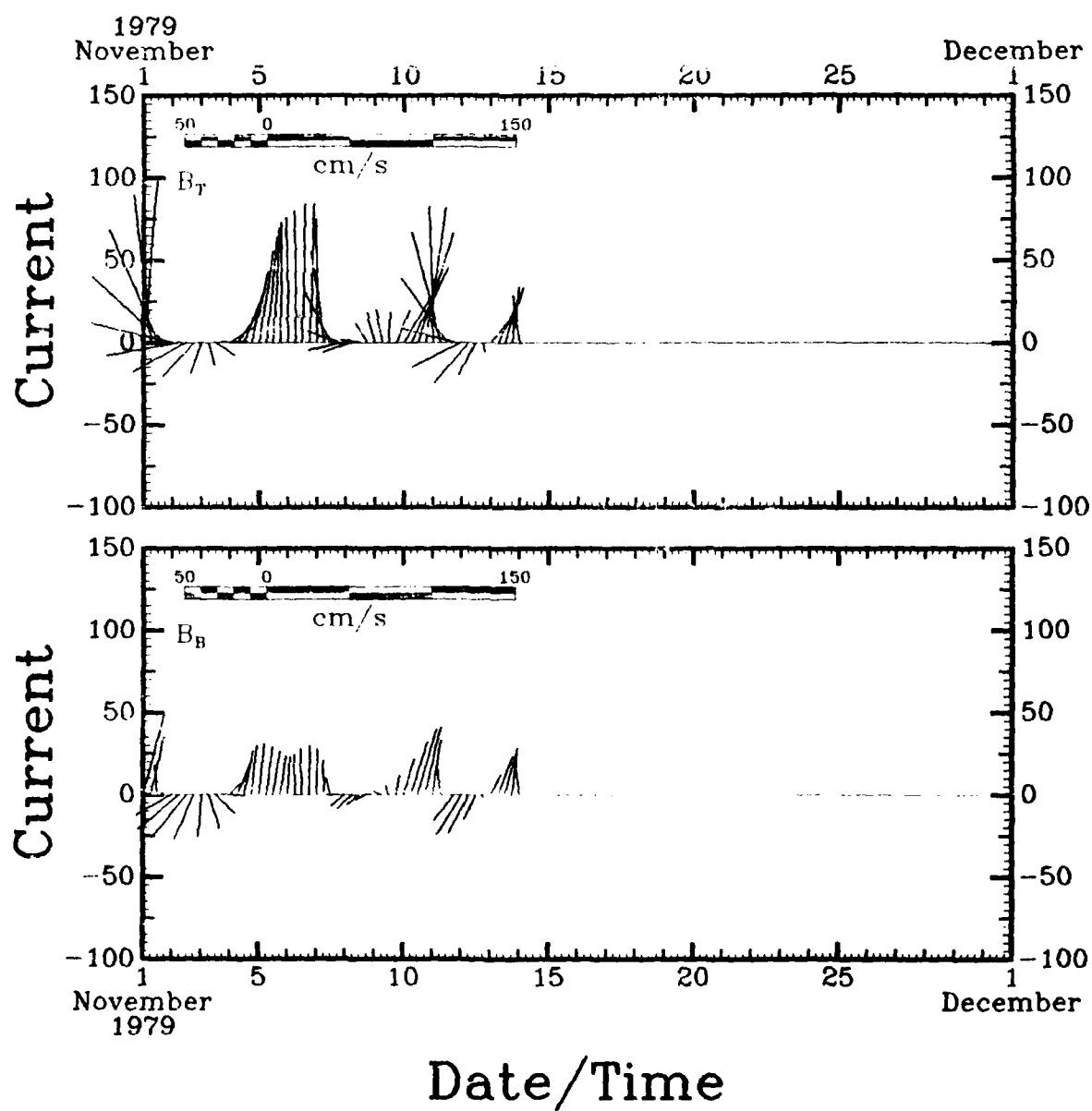


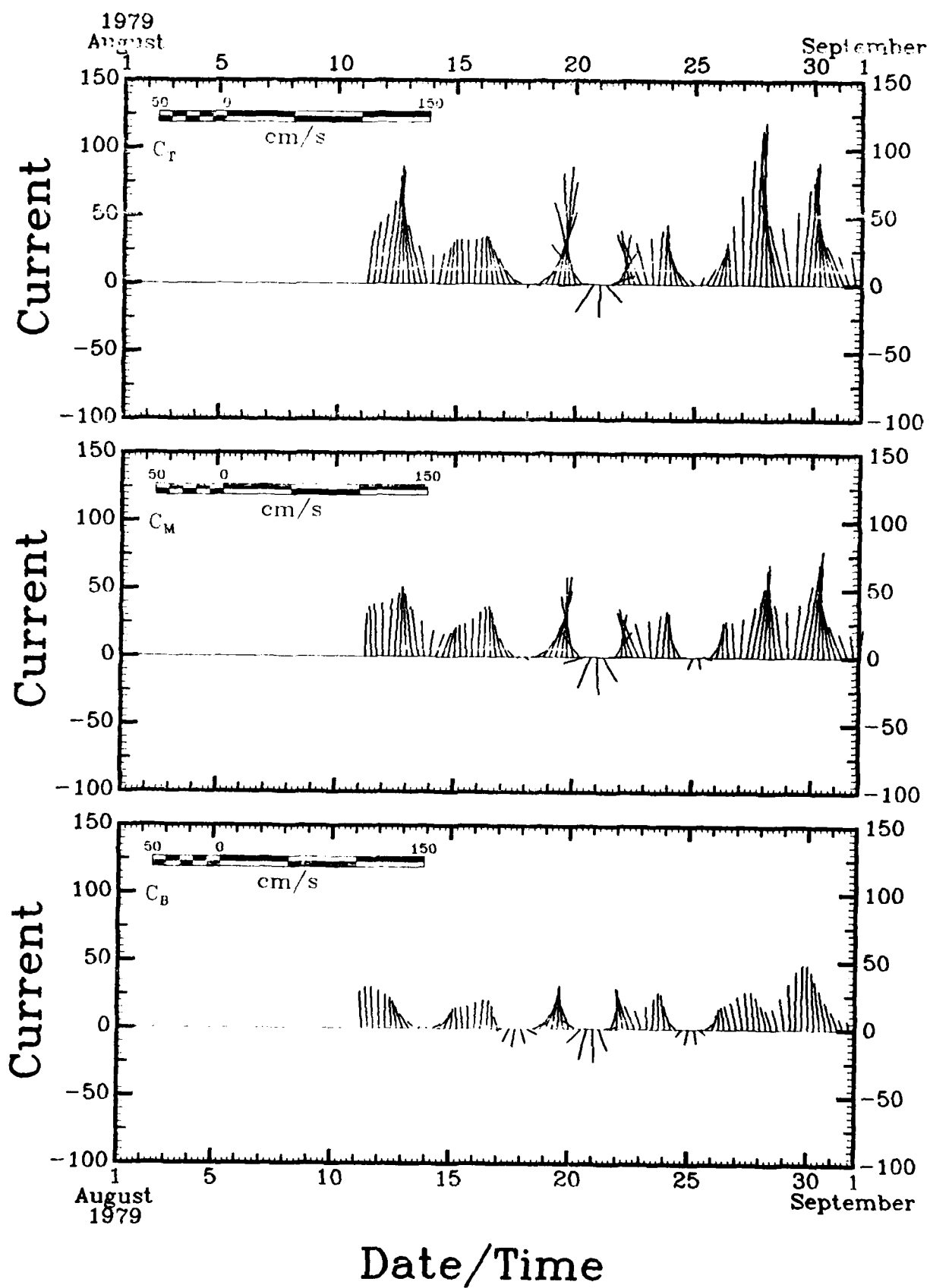


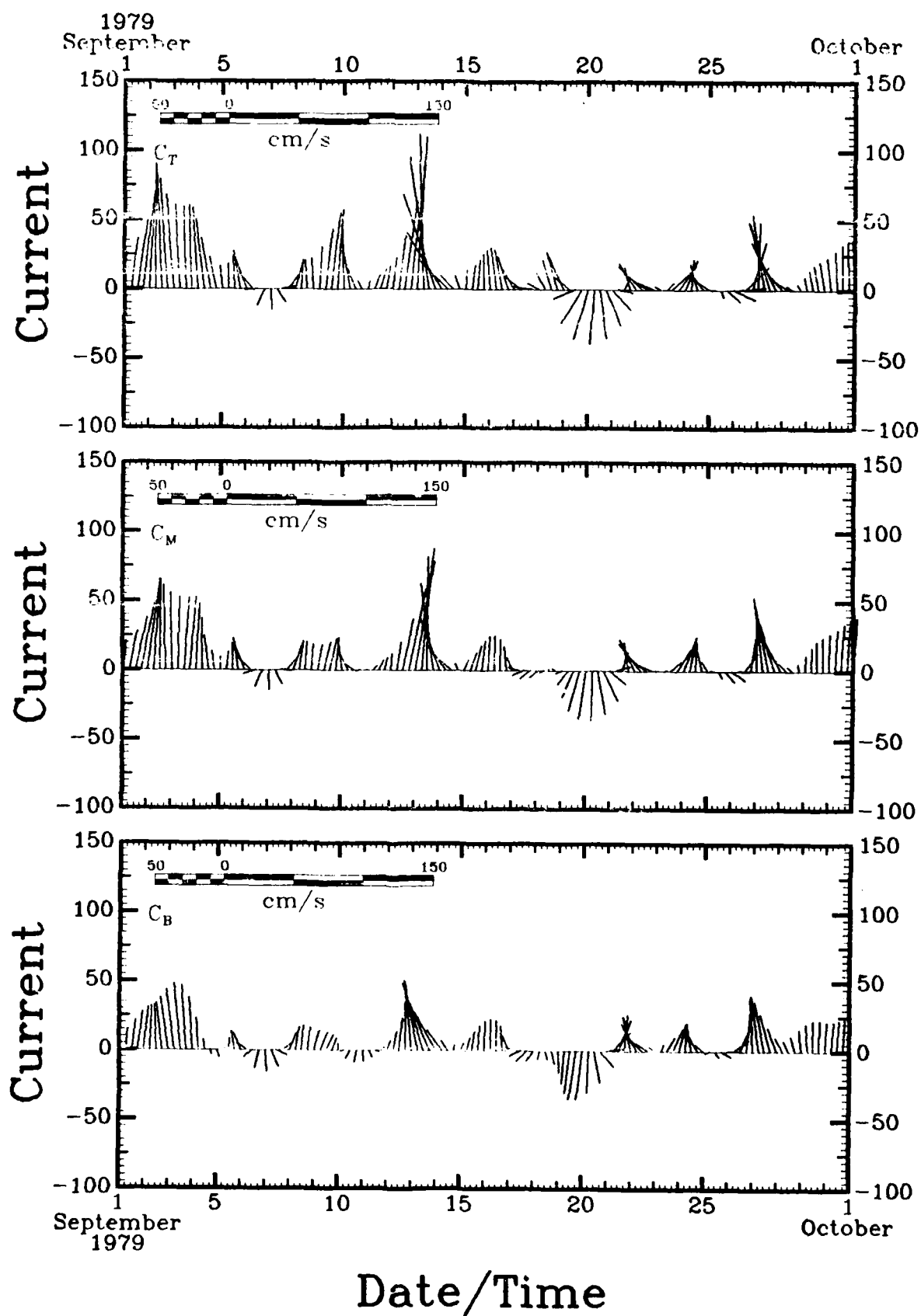


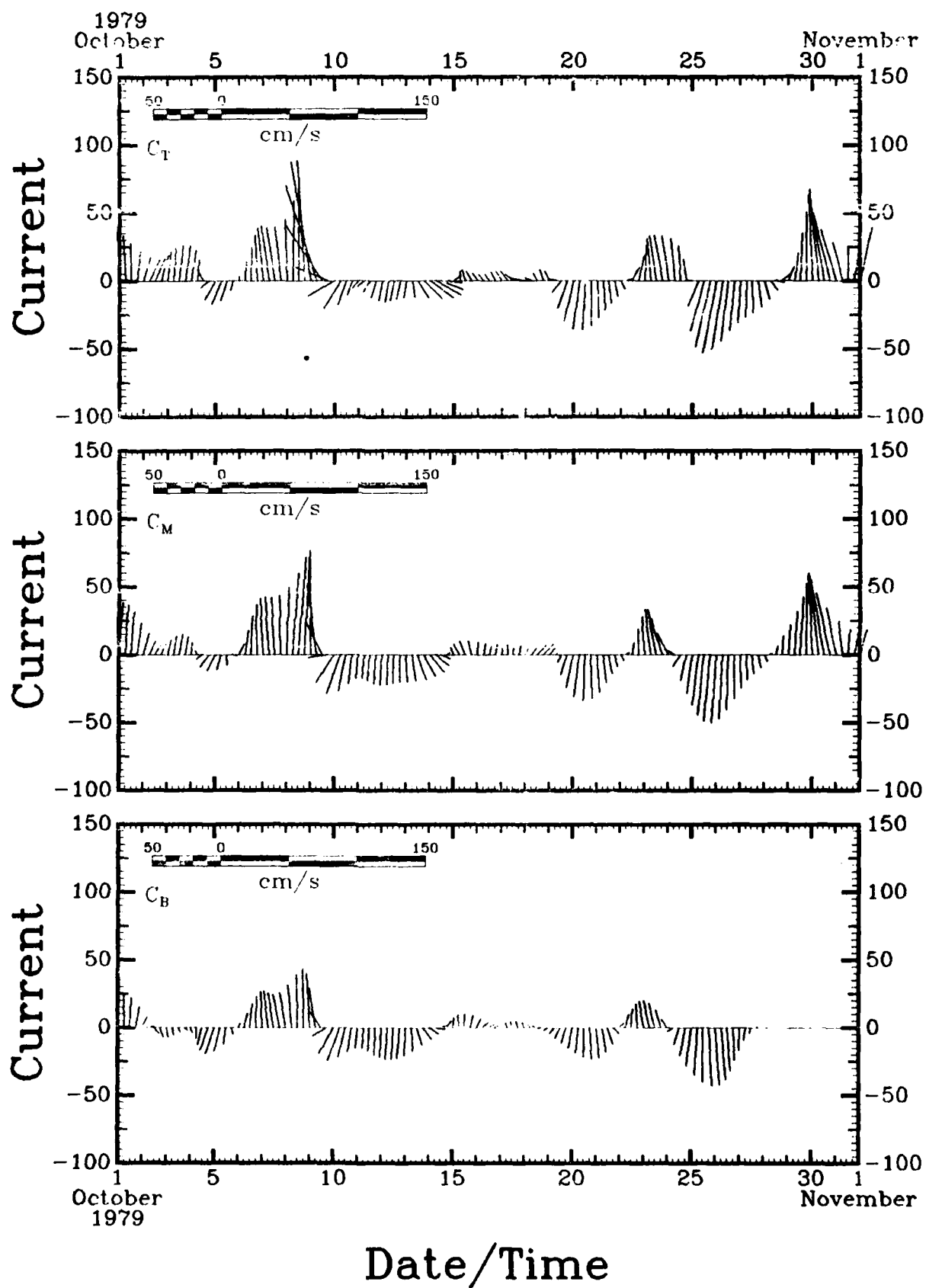


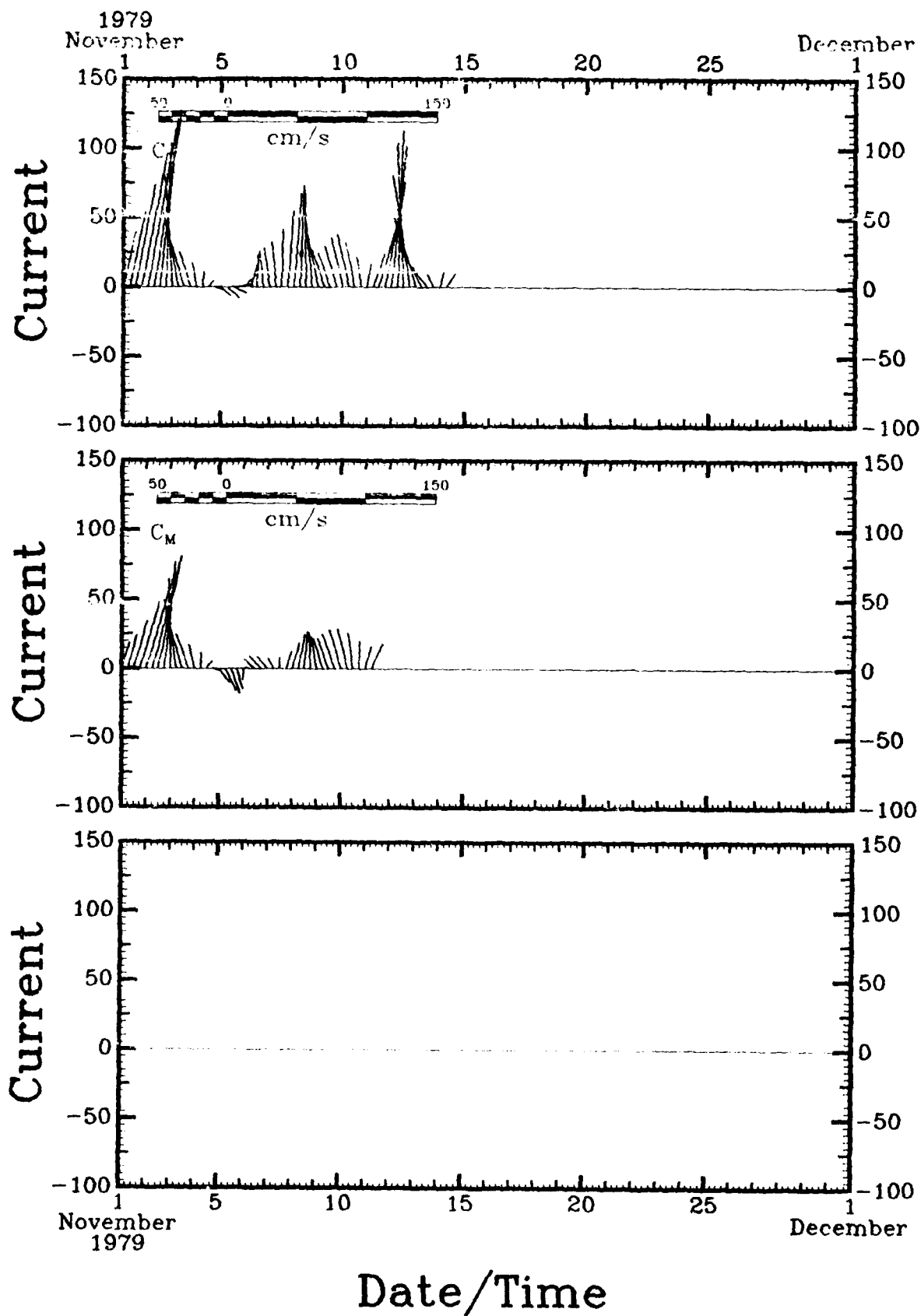


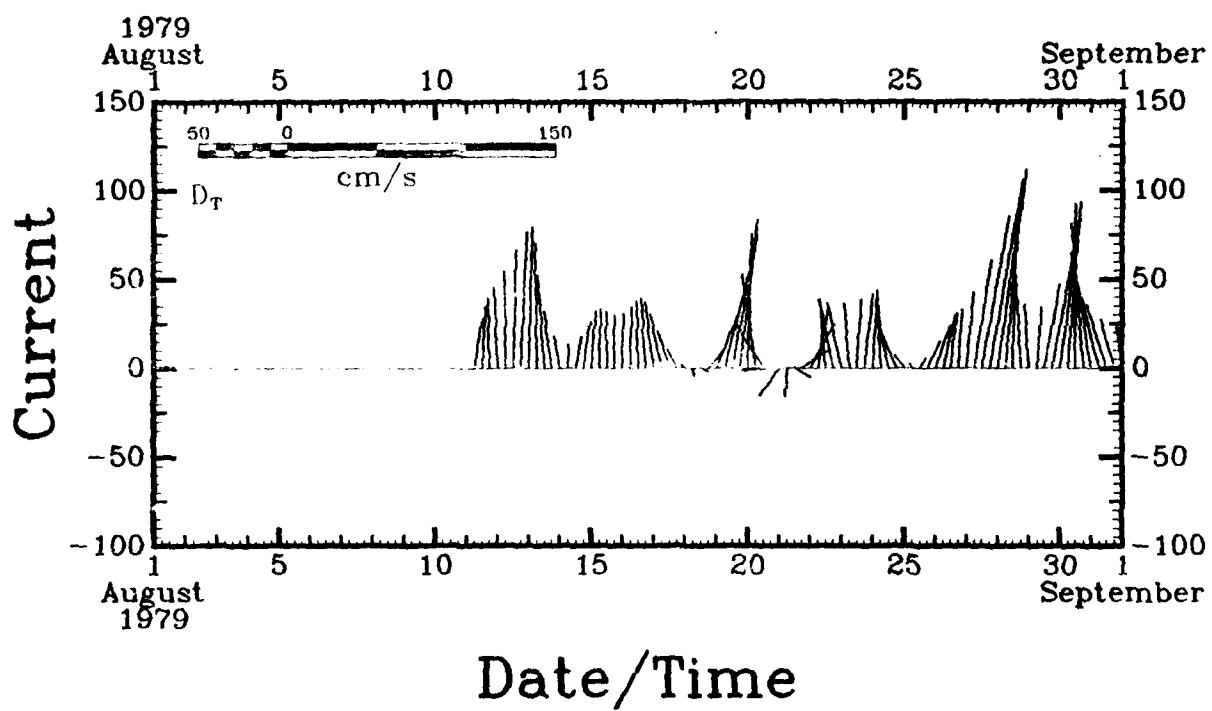


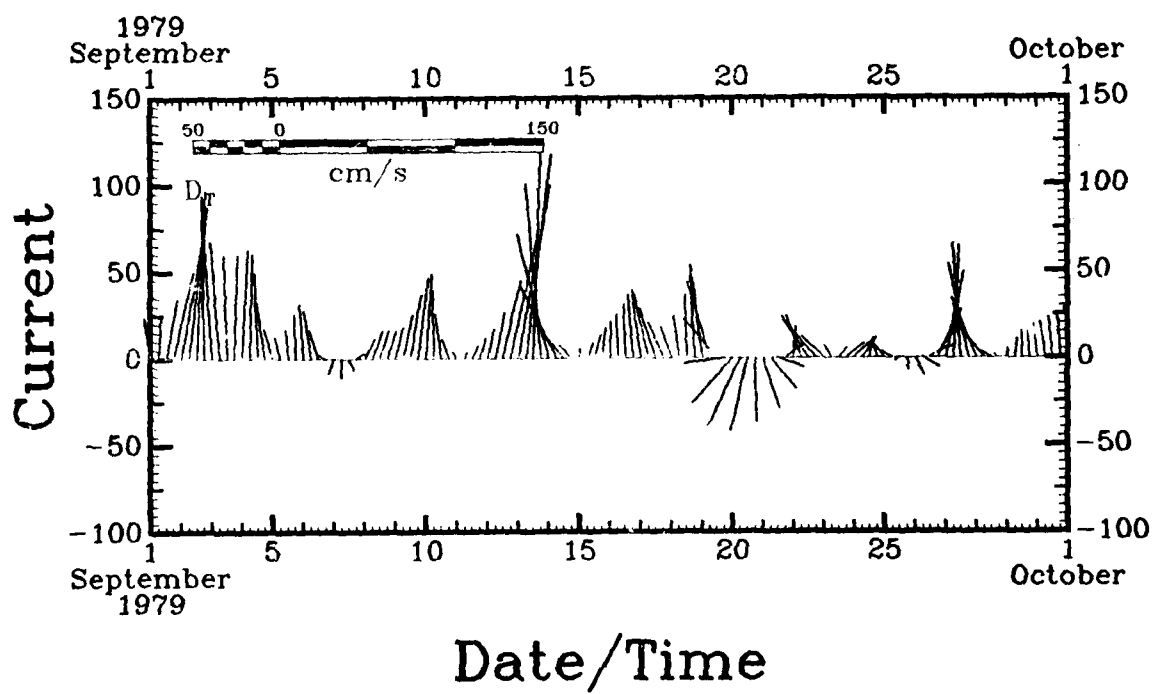


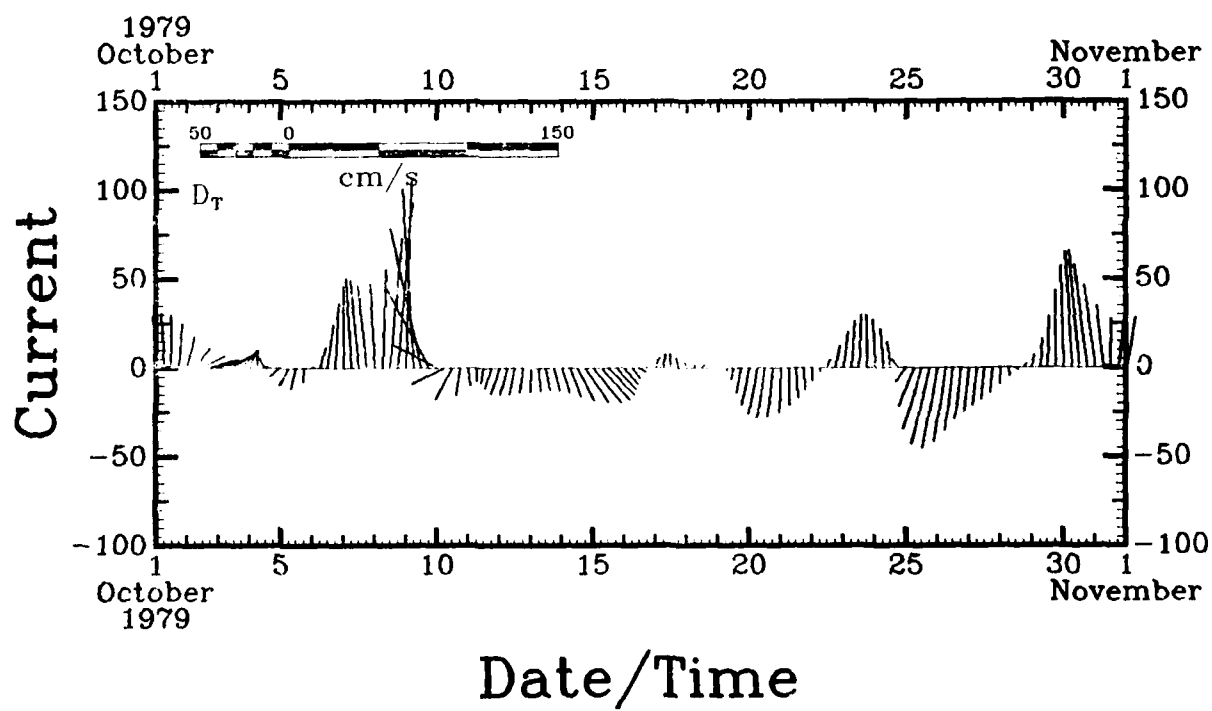


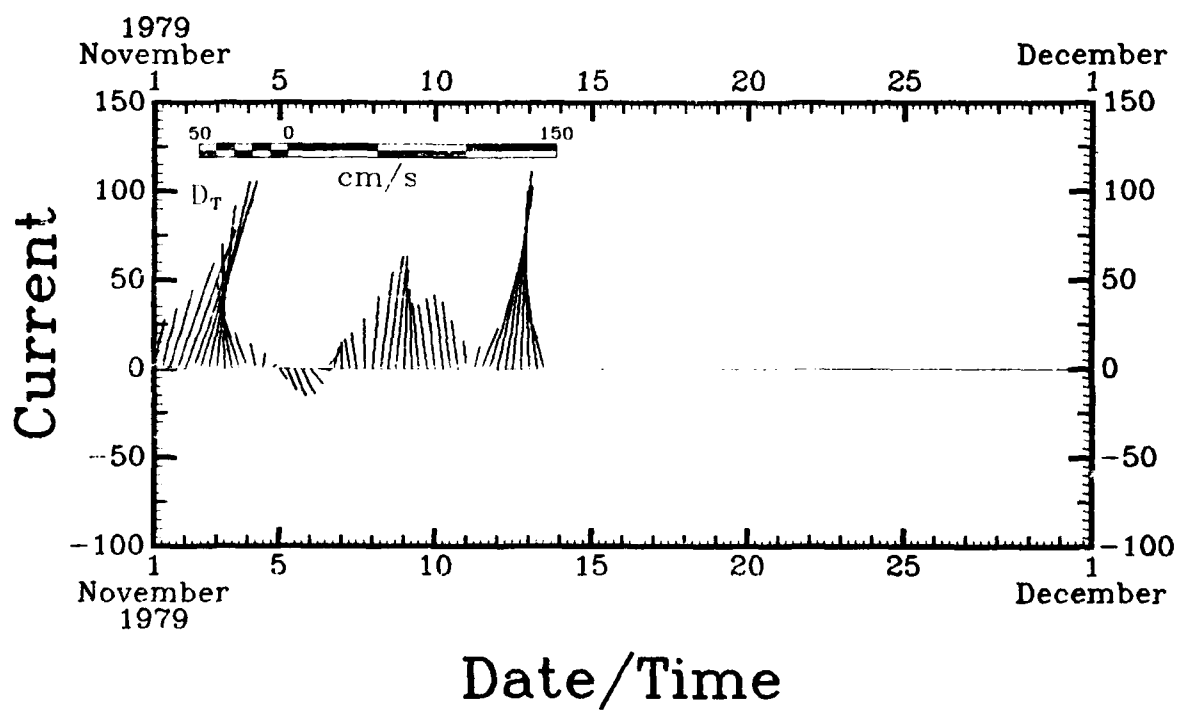








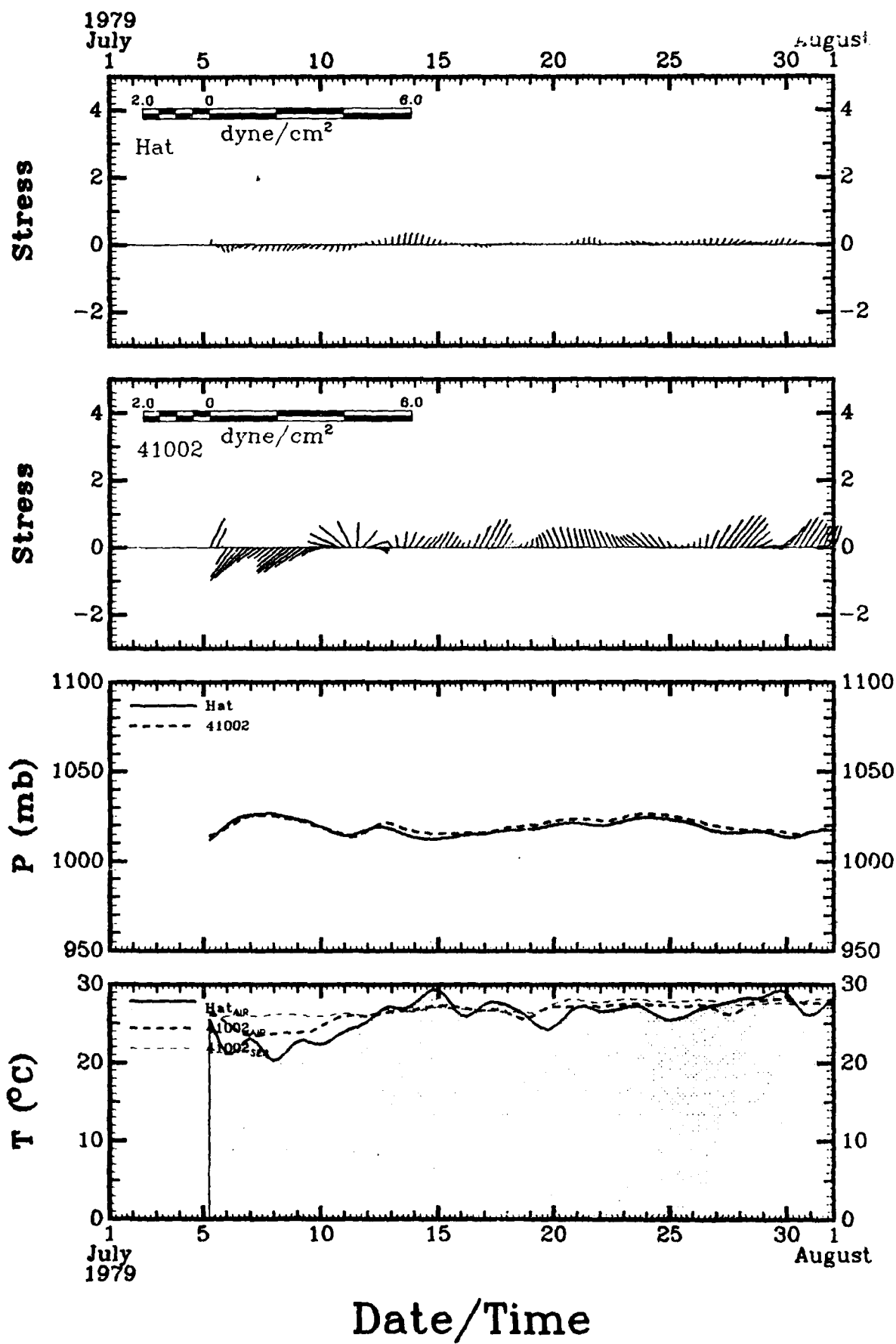


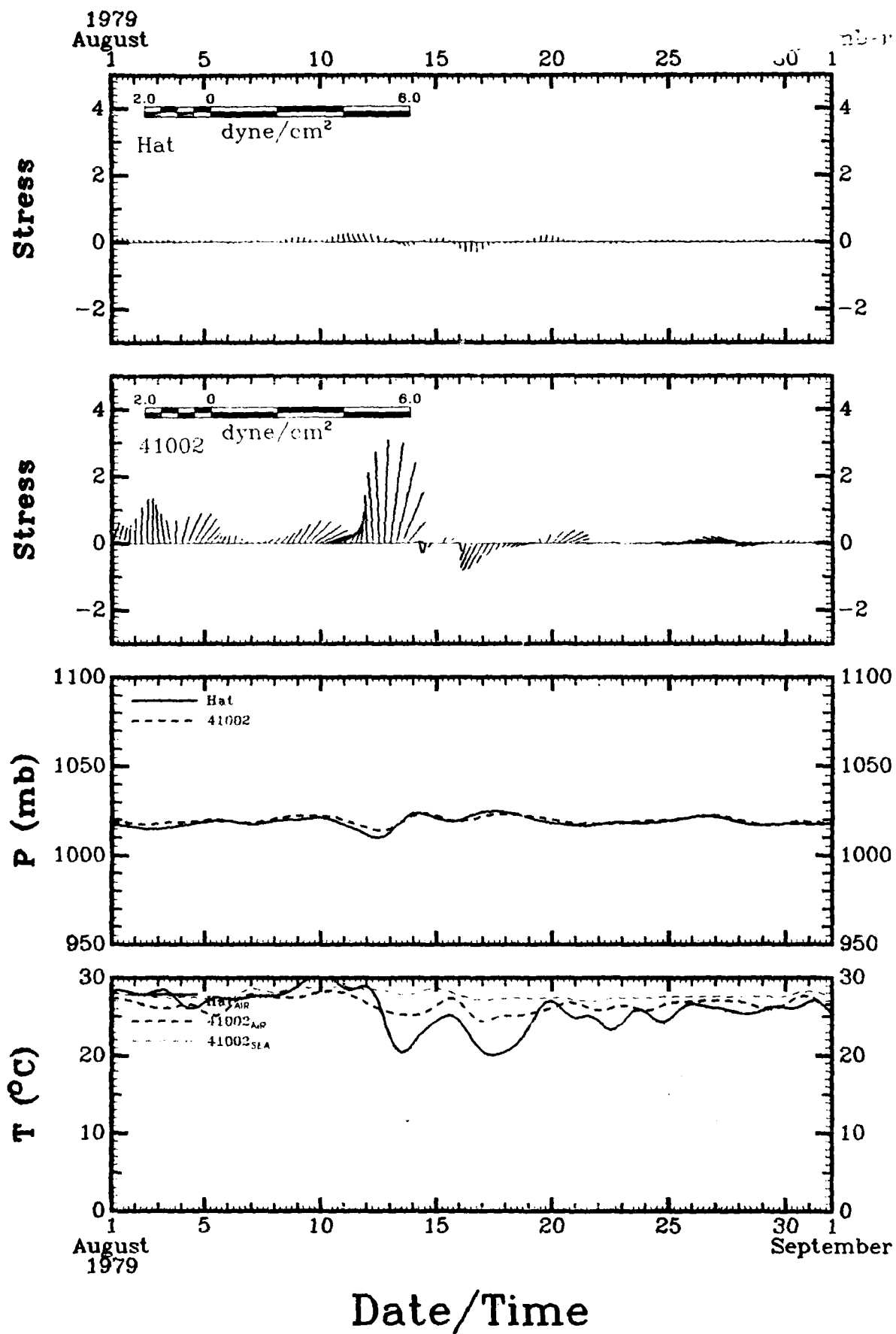


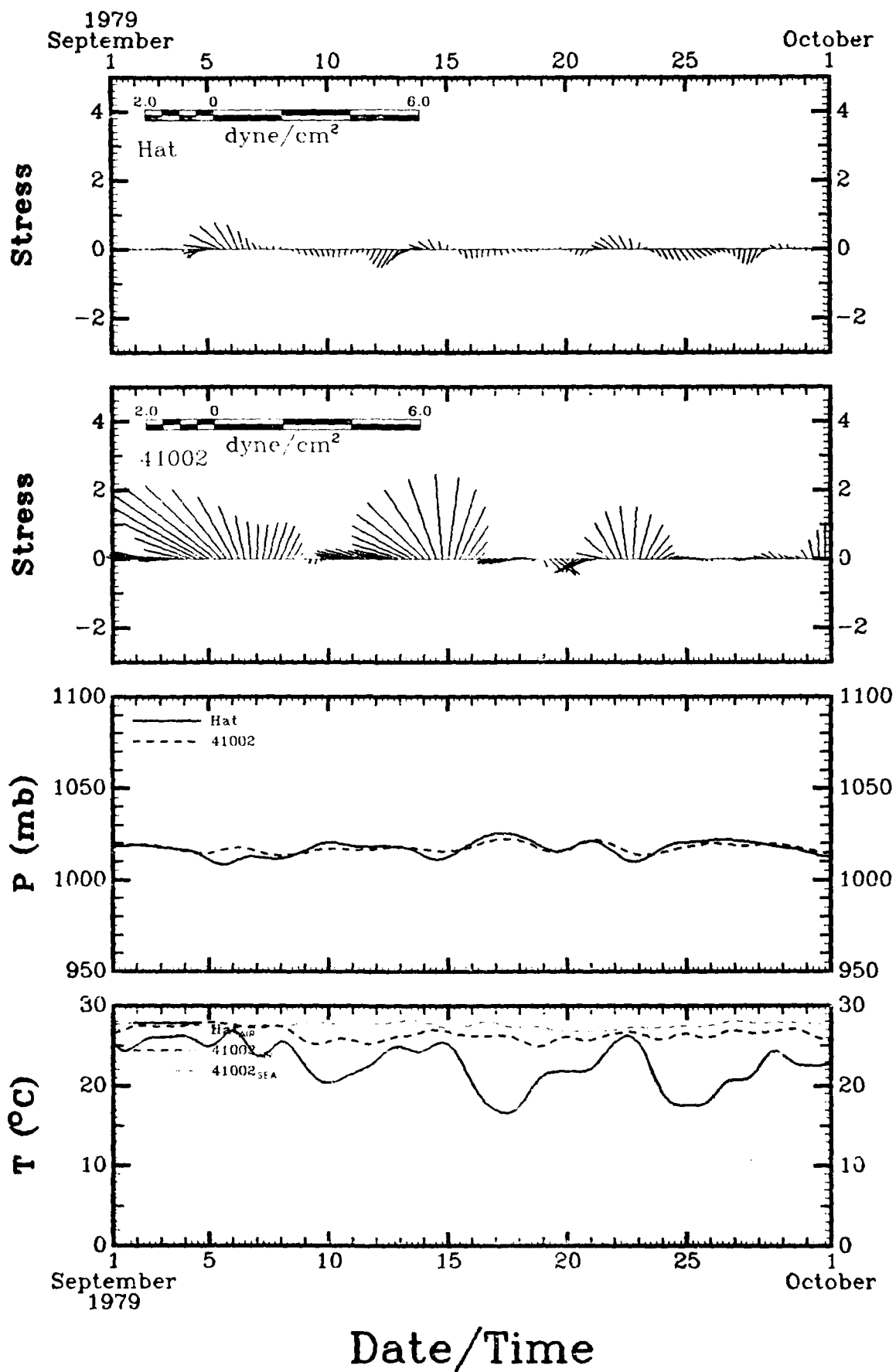
SECTION 7

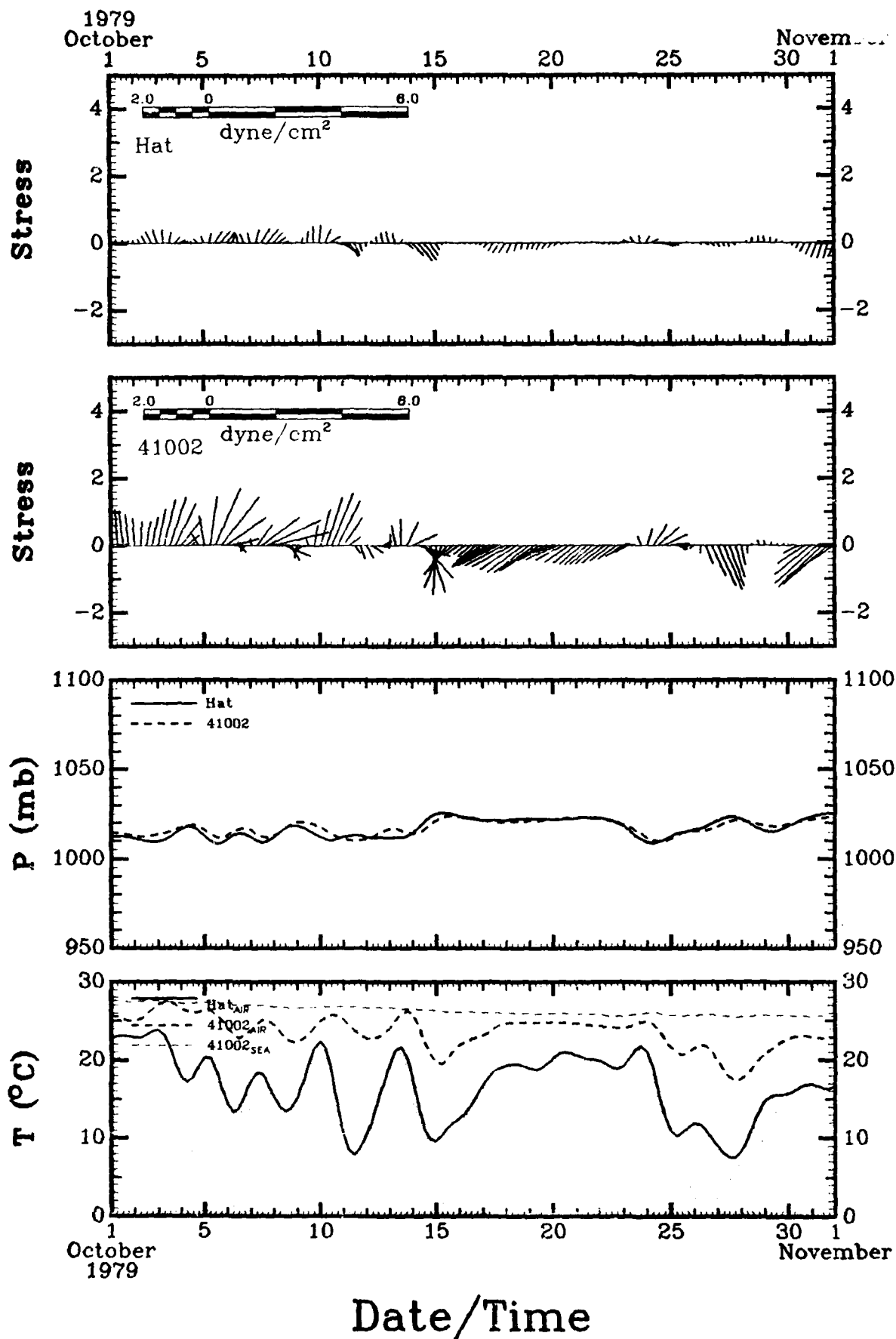
40 HRLP Atmospheric Data from Cape Hatteras and NDBO Buoy 41002

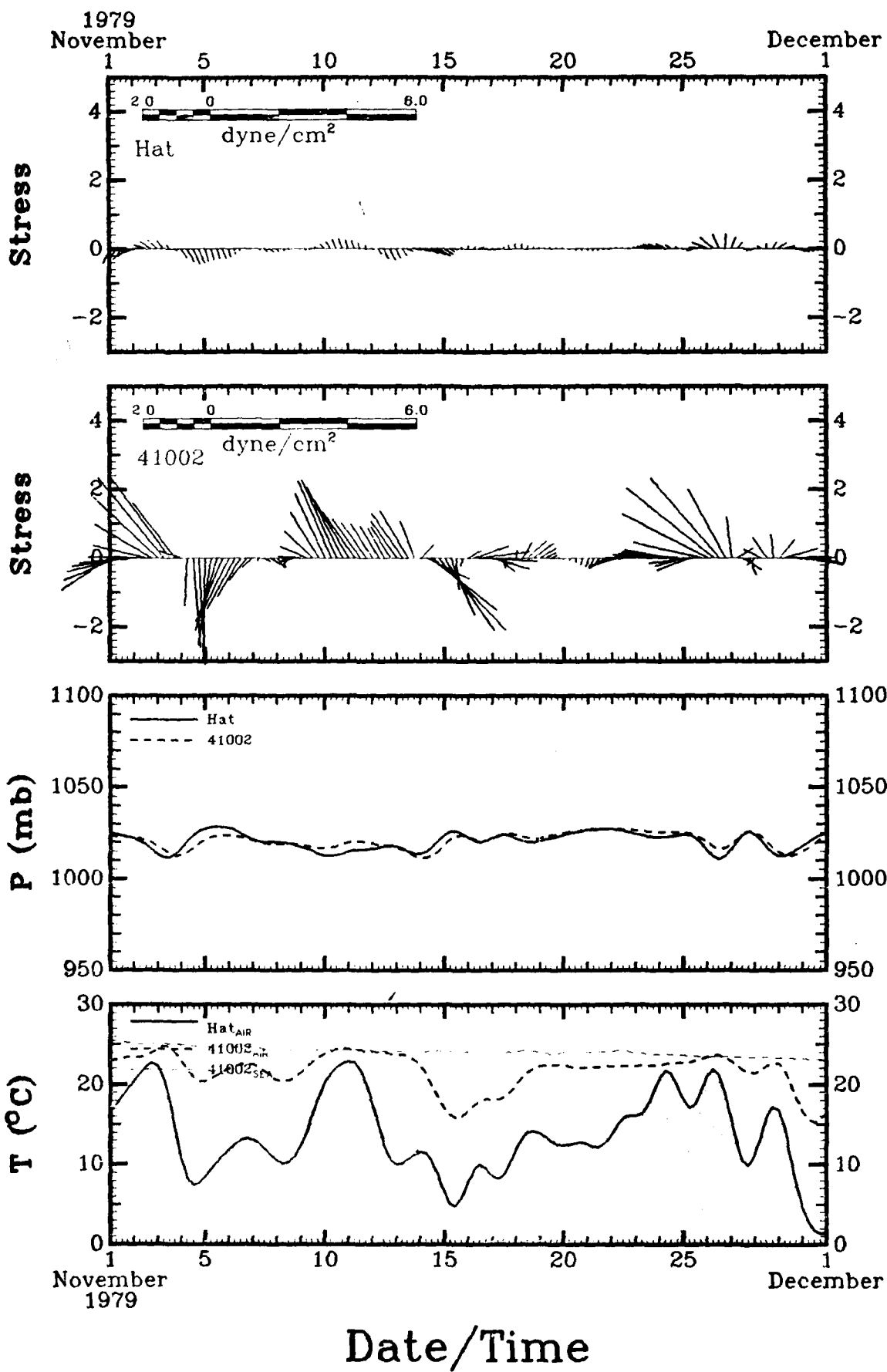
Figure 39 shows by month the 40 HRLP wind stress vector "sticks", the atmospheric pressure, and the air and sea temperatures at Cape Hatteras and the NDBO-2 buoy (see Fig. 1). Vectors pointing toward the top of the page correspond to flow in the downstream (34°T) direction. Common scaling is used in this section.

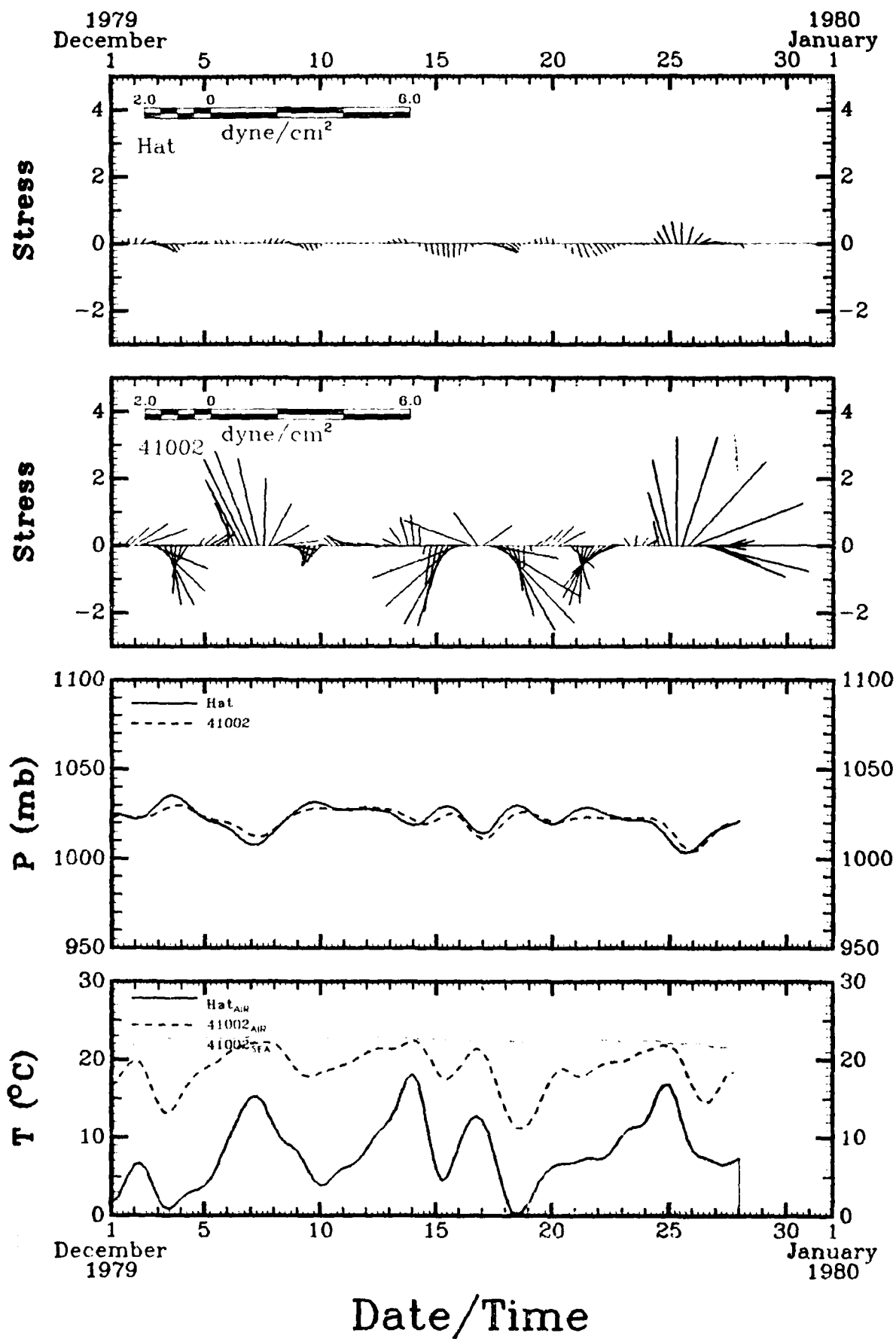








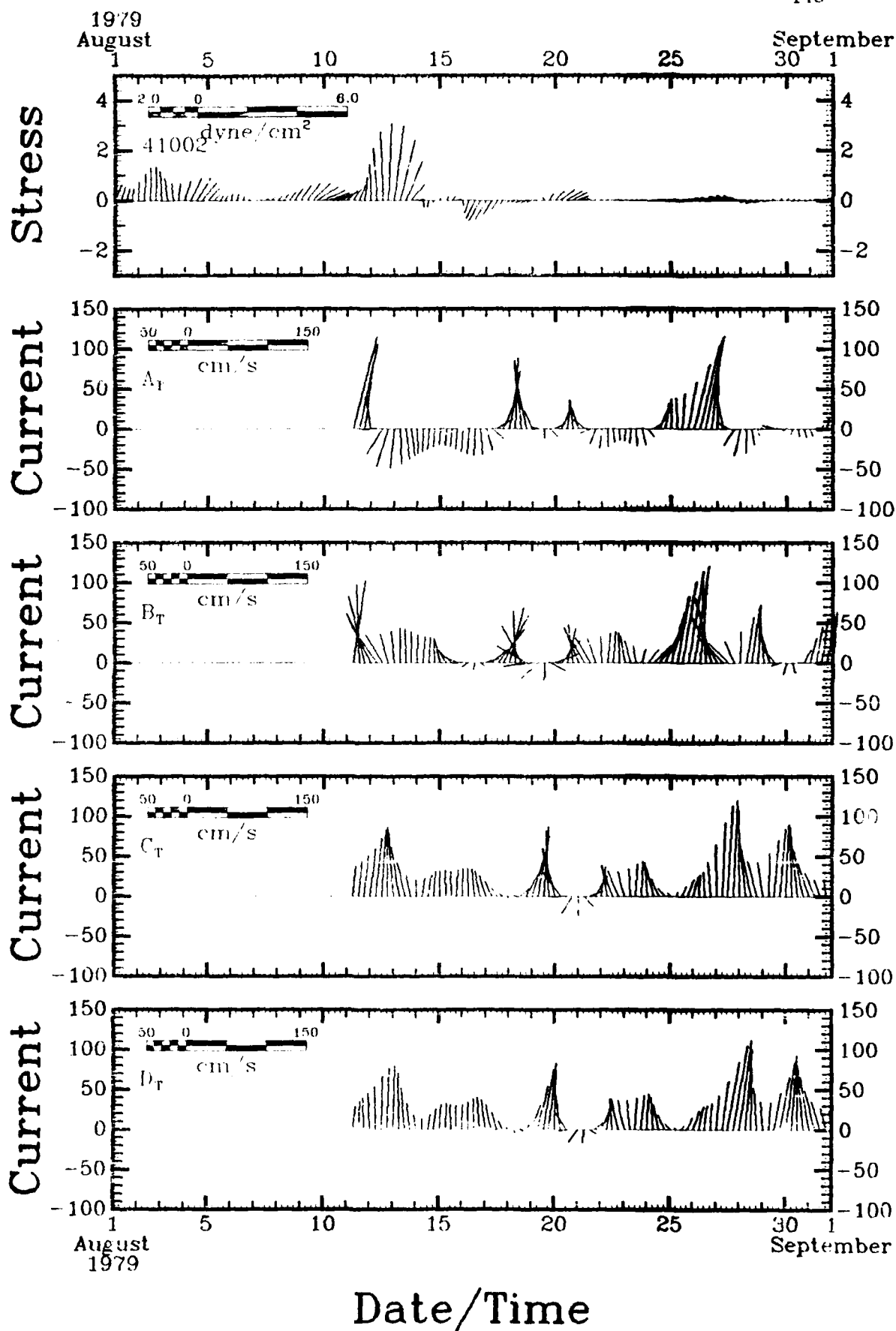


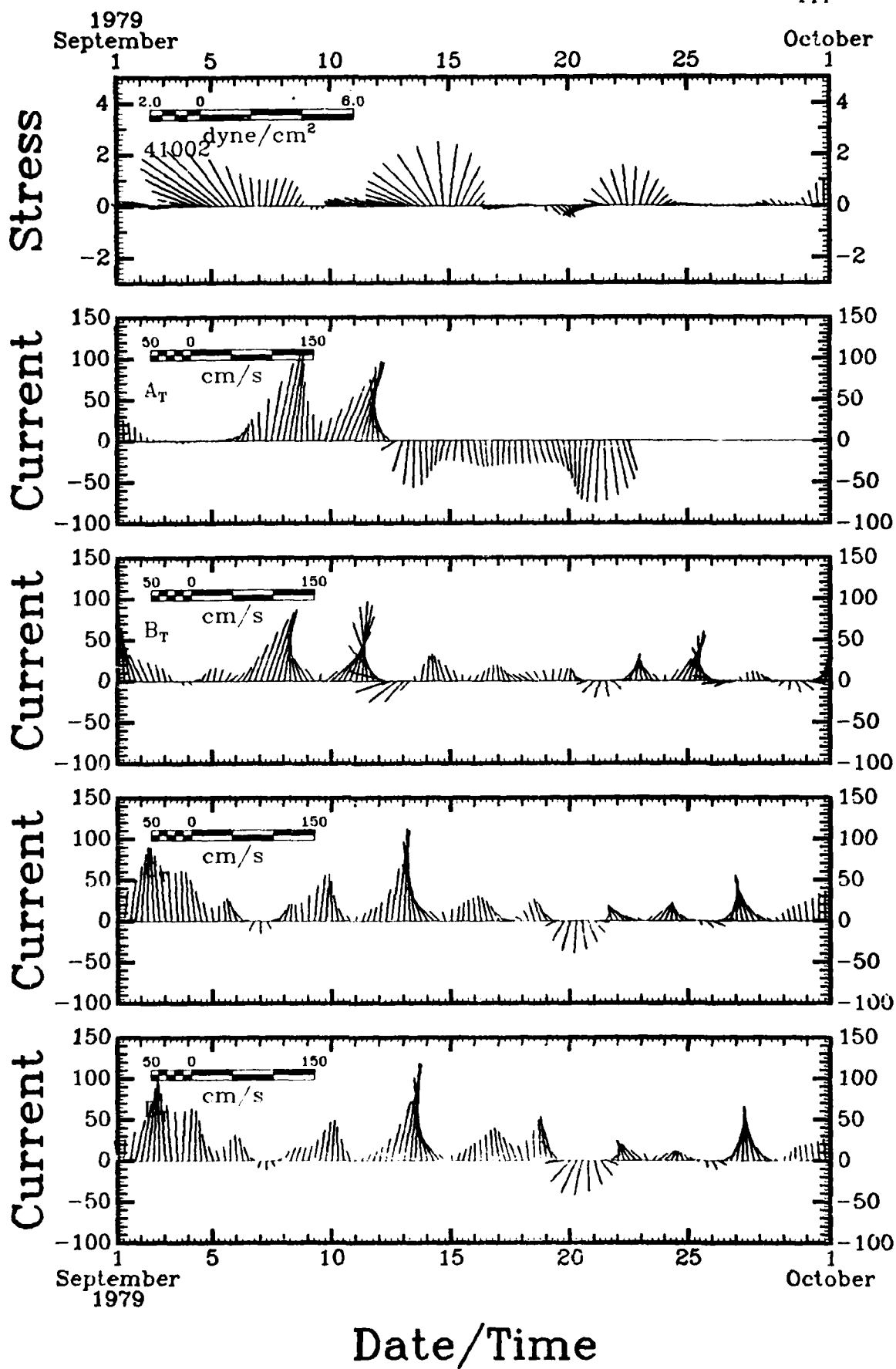


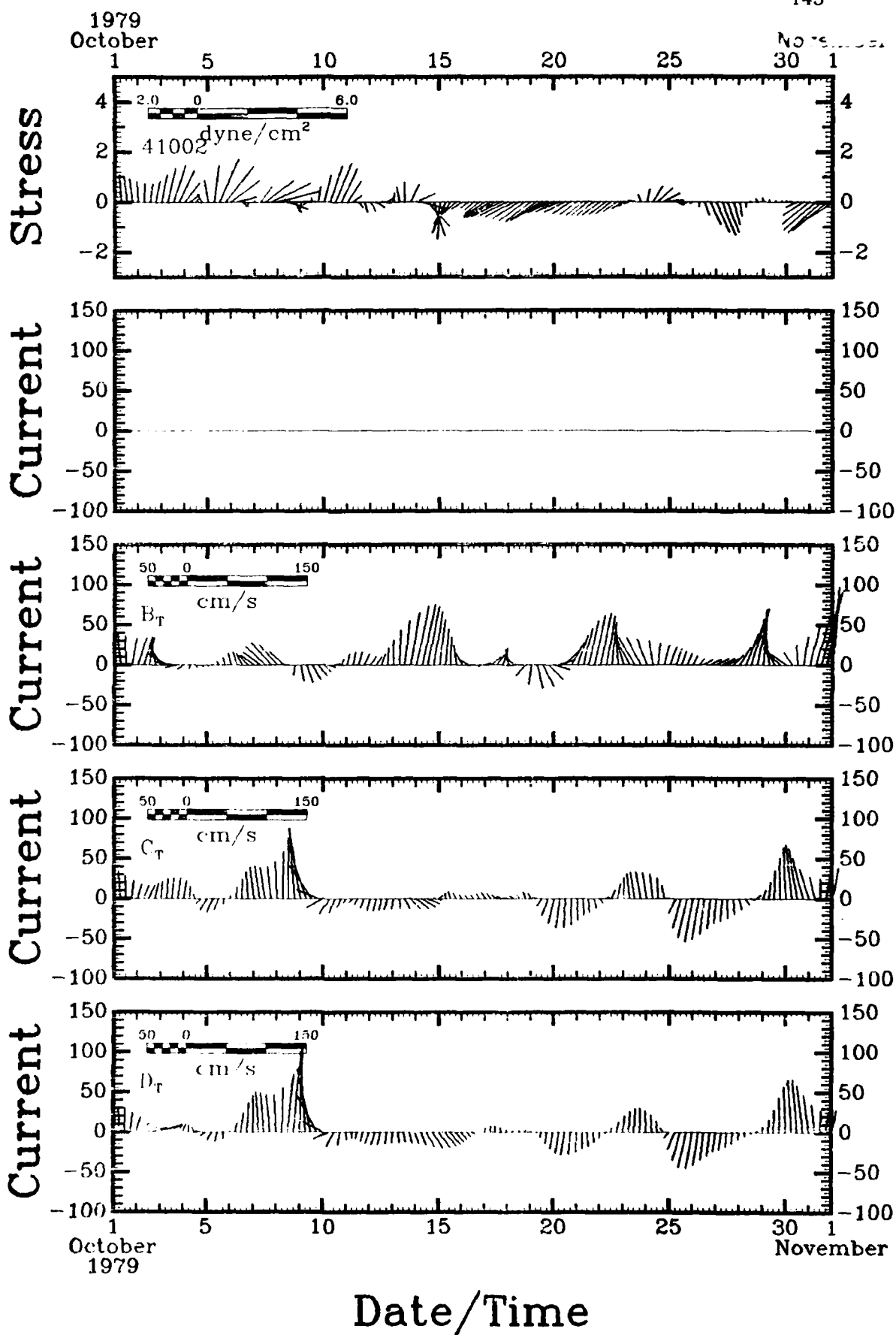
SECTION 8

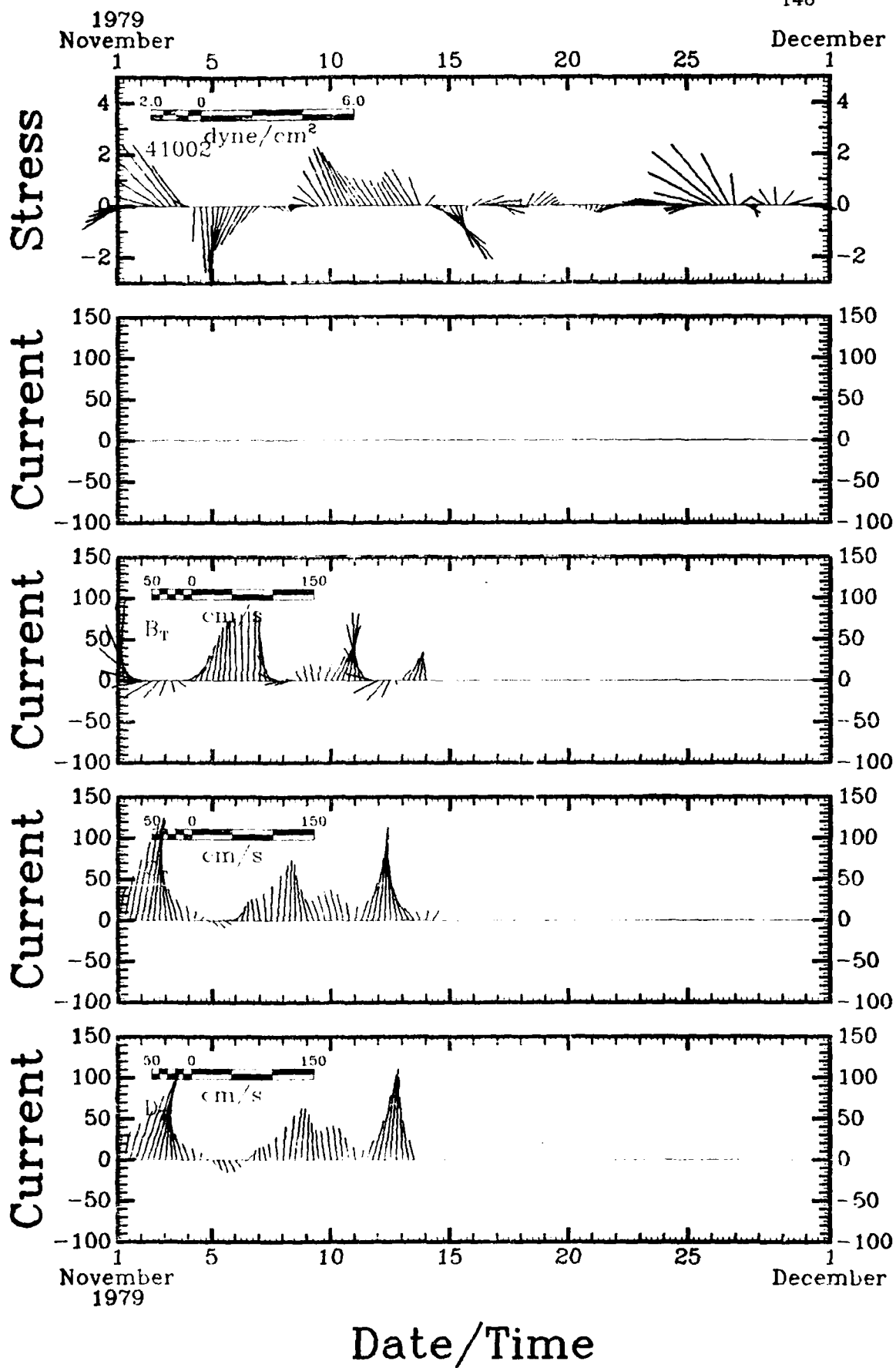
Comparison of 40 HRLP Wind Stress and Current Vector "Sticks"

Figure 40 shows by month the 40 HRLP NDBO-2 wind stress vector "sticks" and the 40 HRLP current vector "sticks" for the topmost instrument on each mooring. Vectors pointing toward the top of the page correspond to flow in the downstream (34°T) direction. Common scaling is used in this section. Very little correlation is evident between the wind stress and currents.





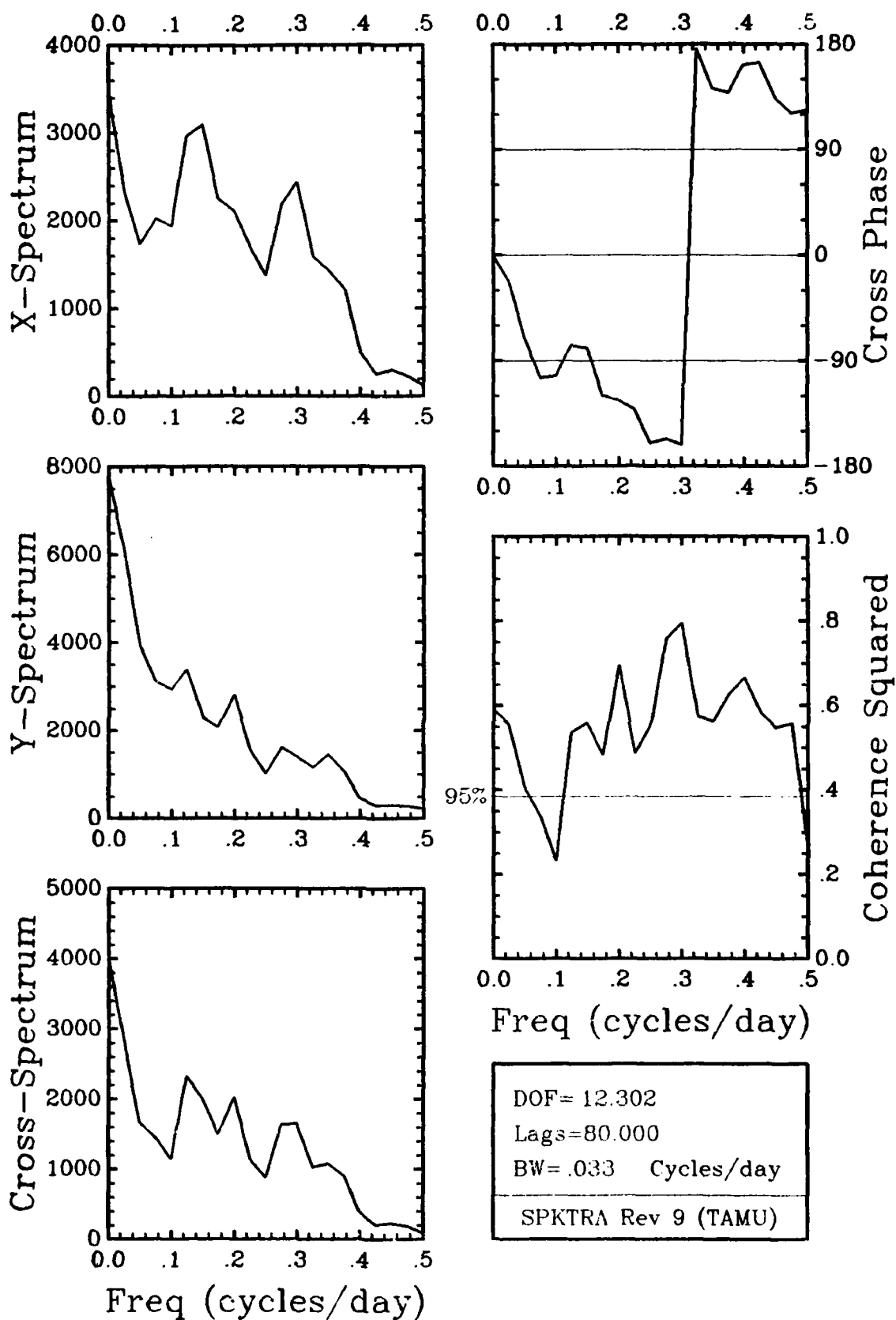




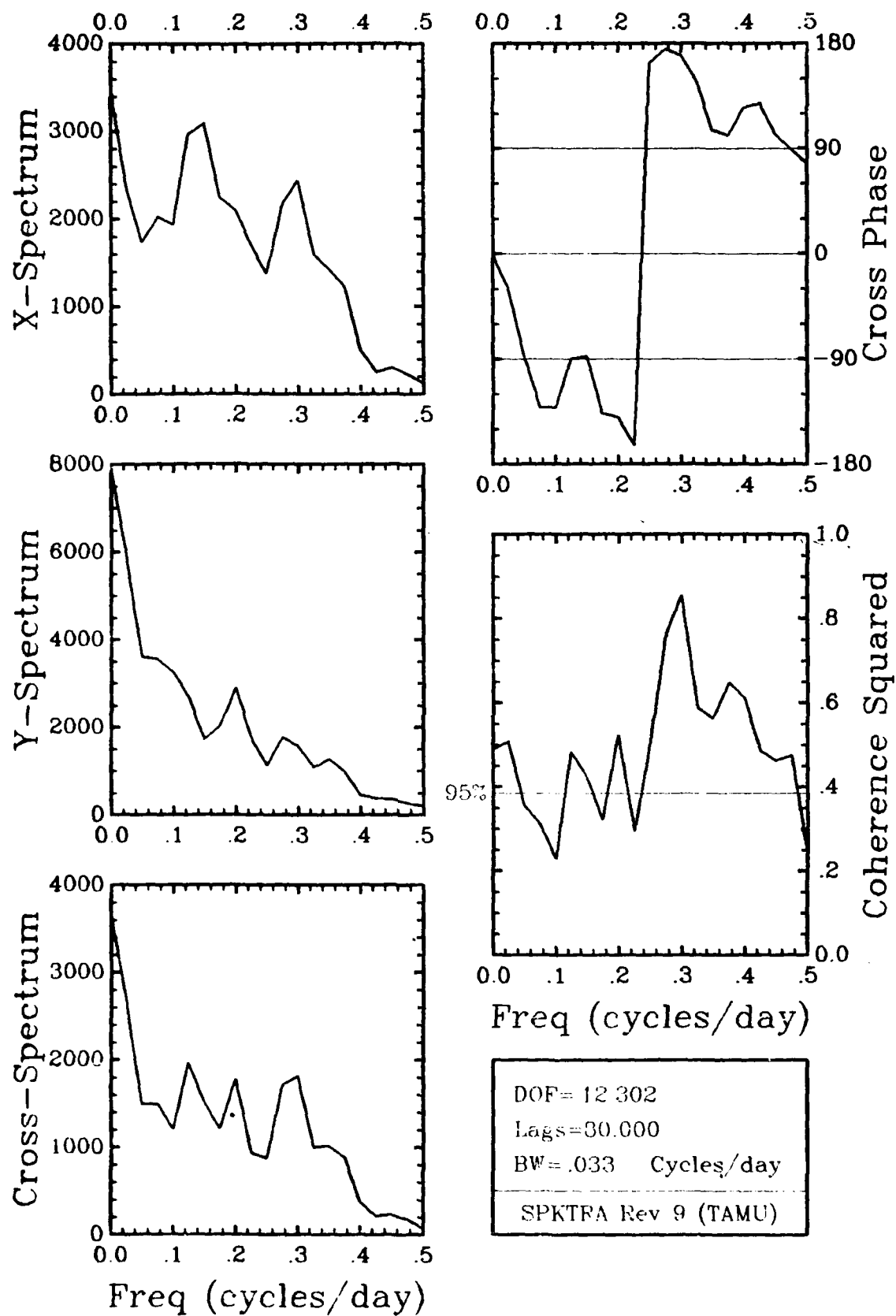
SECTION 9

Spectrum Calculations for Various Combinations of 40 HRLP Data Sets

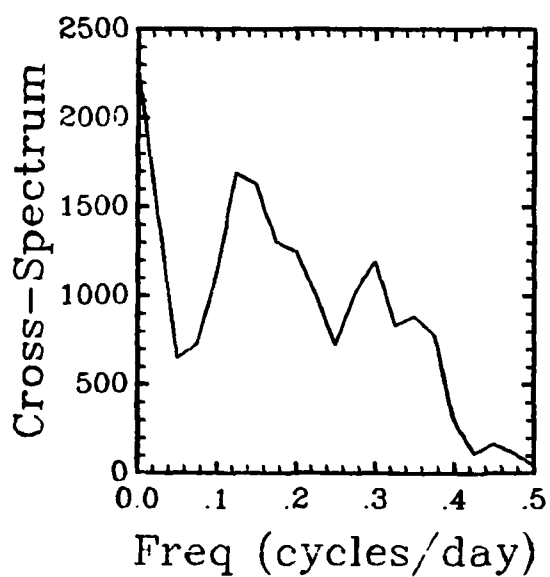
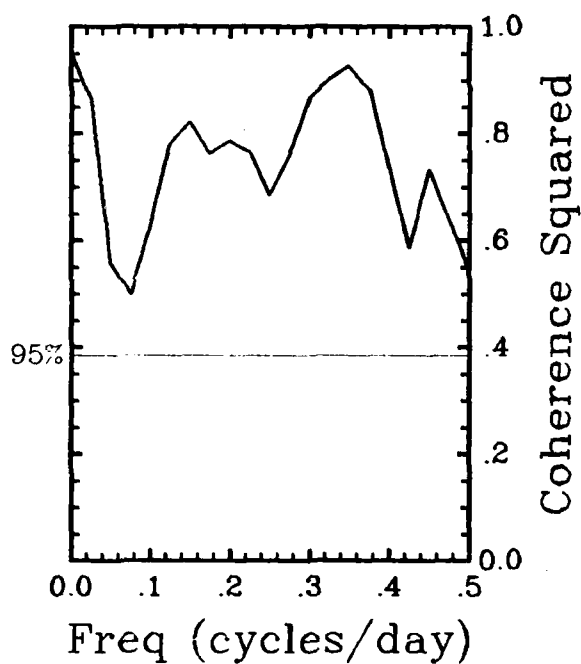
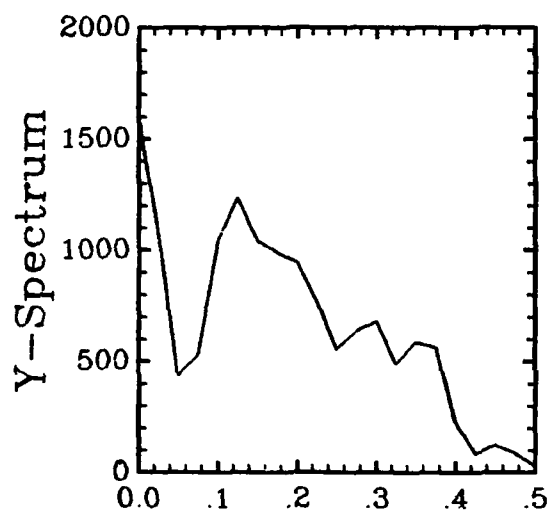
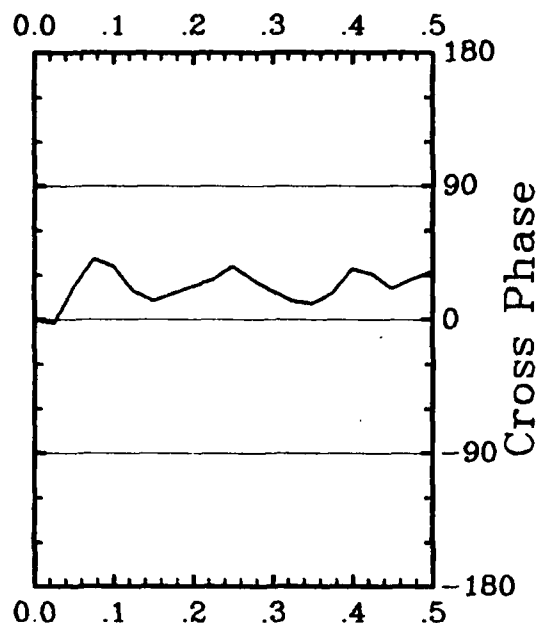
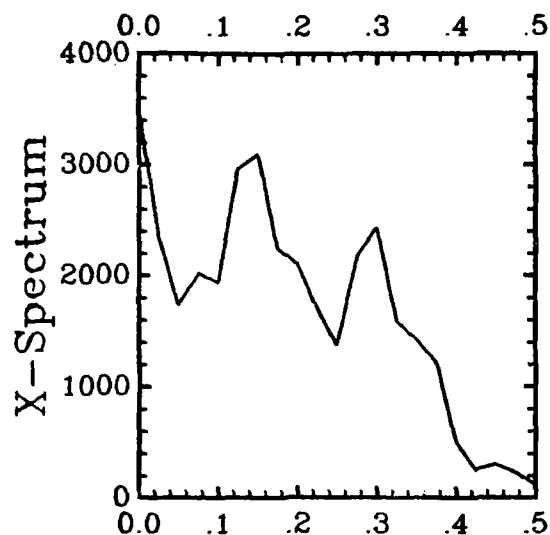
Figures 41 through 73 show spectrum, cross-spectrum, phase, and coherence squared calculations for selected combinations of 40 HRLP current components, Hatteras and NDBO wind stress components. The naming convention gives the "X" time series first and the "Y" time series second. Currents are identified by mooring letter, and instrument position on the mooring is given by subscript letter. The phase convention is such that negative phase values mean the "Y" series lags the "X" series. The spectrum ordinate units in all cases are variance units per cycle per day (CPD), where the variance units are those appropriate for the time series in question. Root-mean-square estimates of a variable in a particular frequency band can be obtained by multiplying the spectrum estimate in that band by the effective bandwidth (0.033 CPD in all cases) and taking the square root of the product. The 95% significance level for coherence squared, the level below which would fall 95% of the coherence estimates between truly uncorrelated variates, is shown by a horizontal line on the coherence graphs. Spectrum estimates nominally possess 15 degrees of freedom (DOF), although some variation in this number, accepted in favor of maintaining the bandwidth invariant, results from differing record lengths. For 15 DOF, the 95% confidence interval on the phase estimate in a particular frequency band is approximately $\pm (27, 18, 12)$ degrees for a coherence squared value of (0.4, 0.6, 0.8) in that band.



$B_T \text{ V} / C_T \text{ V Summer 40 HR LP}$



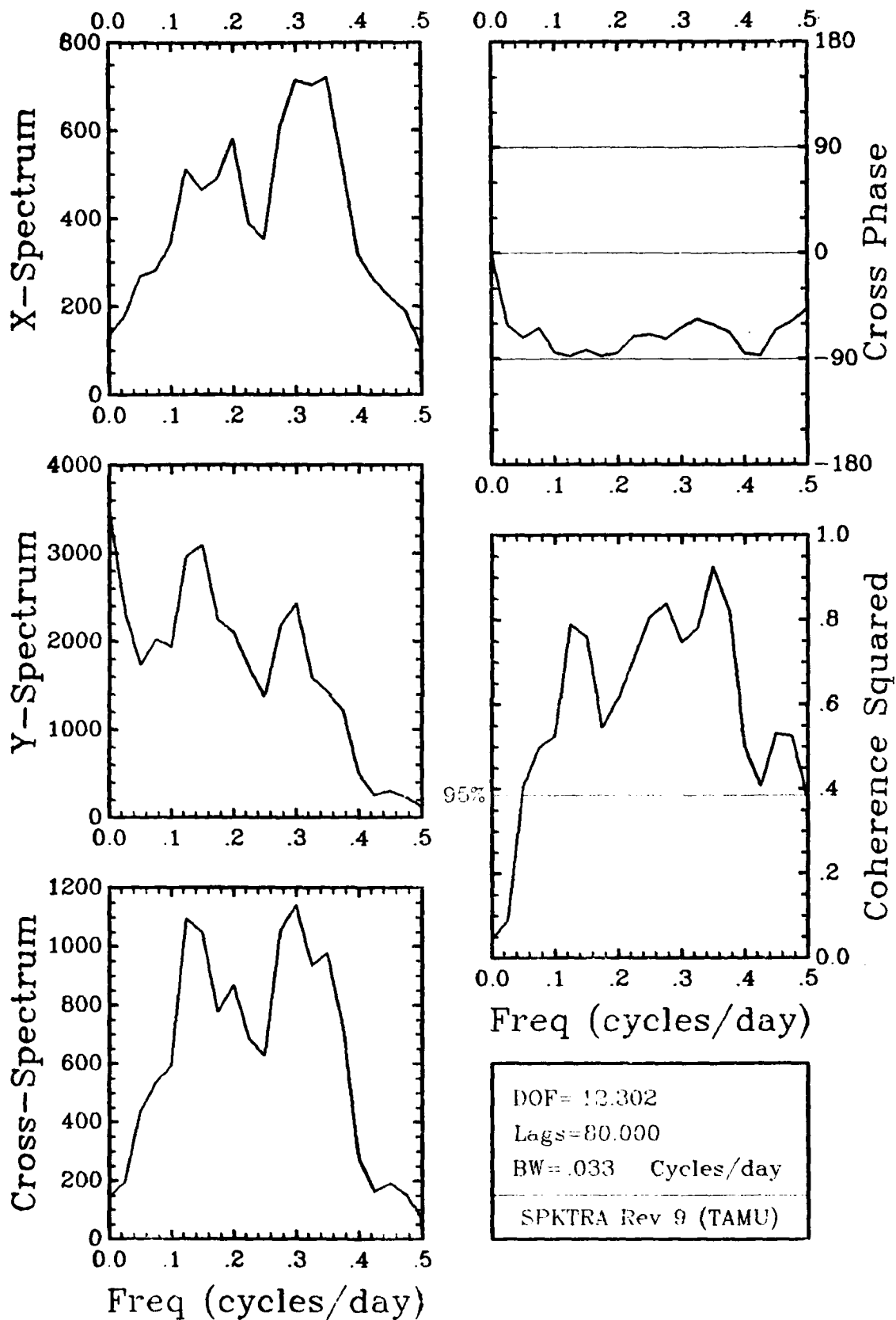
$B_T \ V / D_T \ V$ Summer 40 HR LP



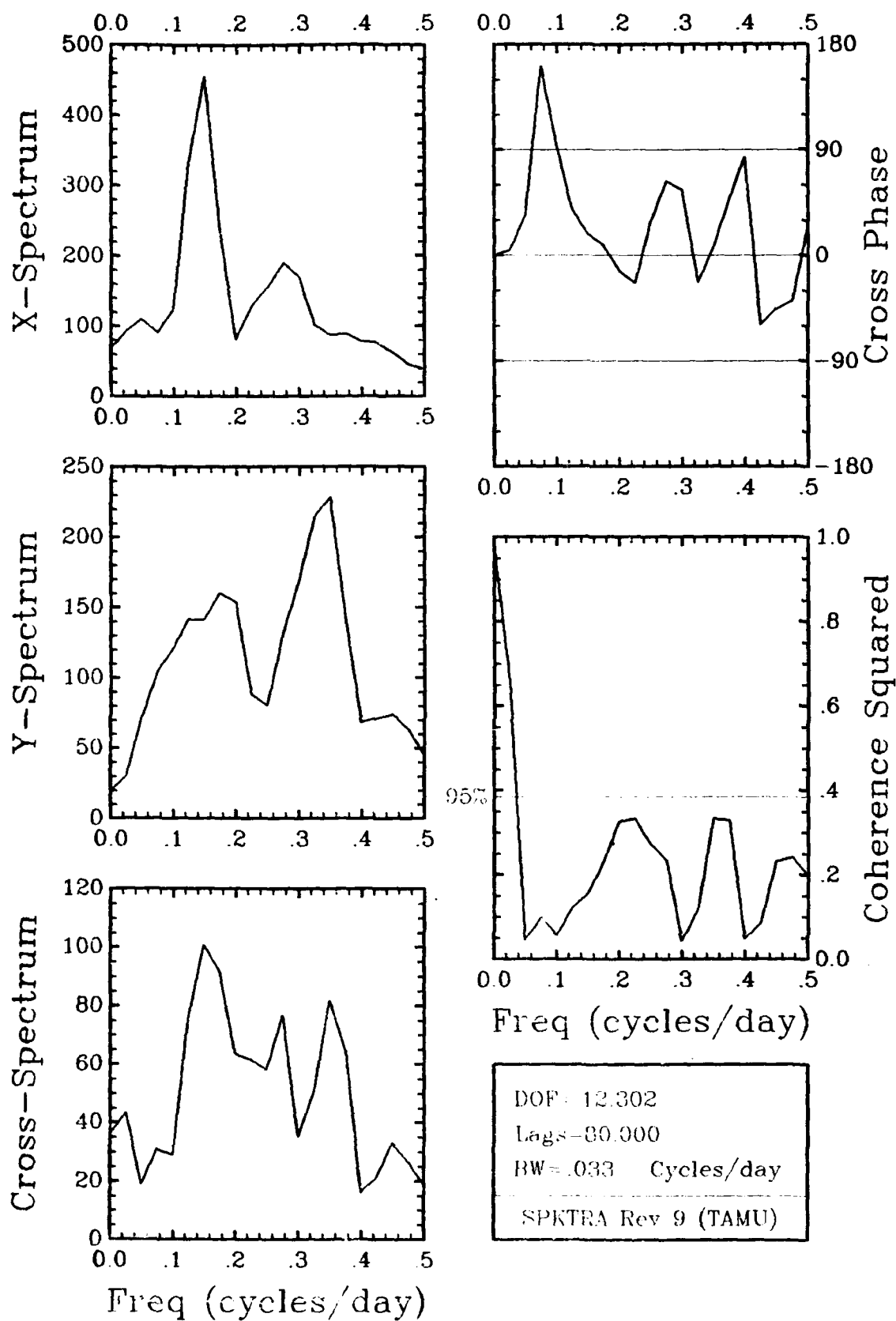
DOF= 12.302
Lags=80.000
BW=.033 Cycles/day

SPKTRA Rev 9 (TAMU)

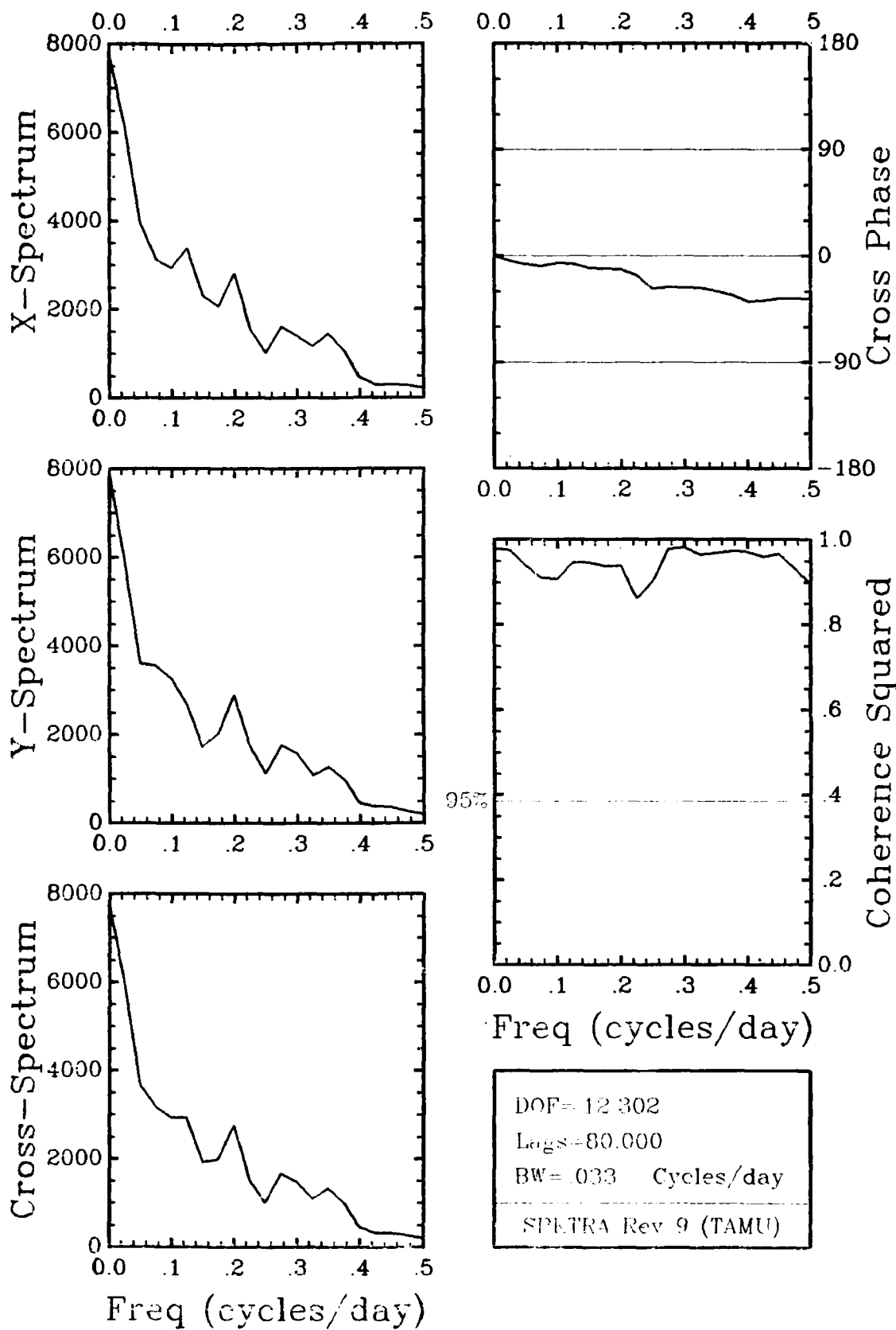
B_T V / B_B V Summer 40 HR LP

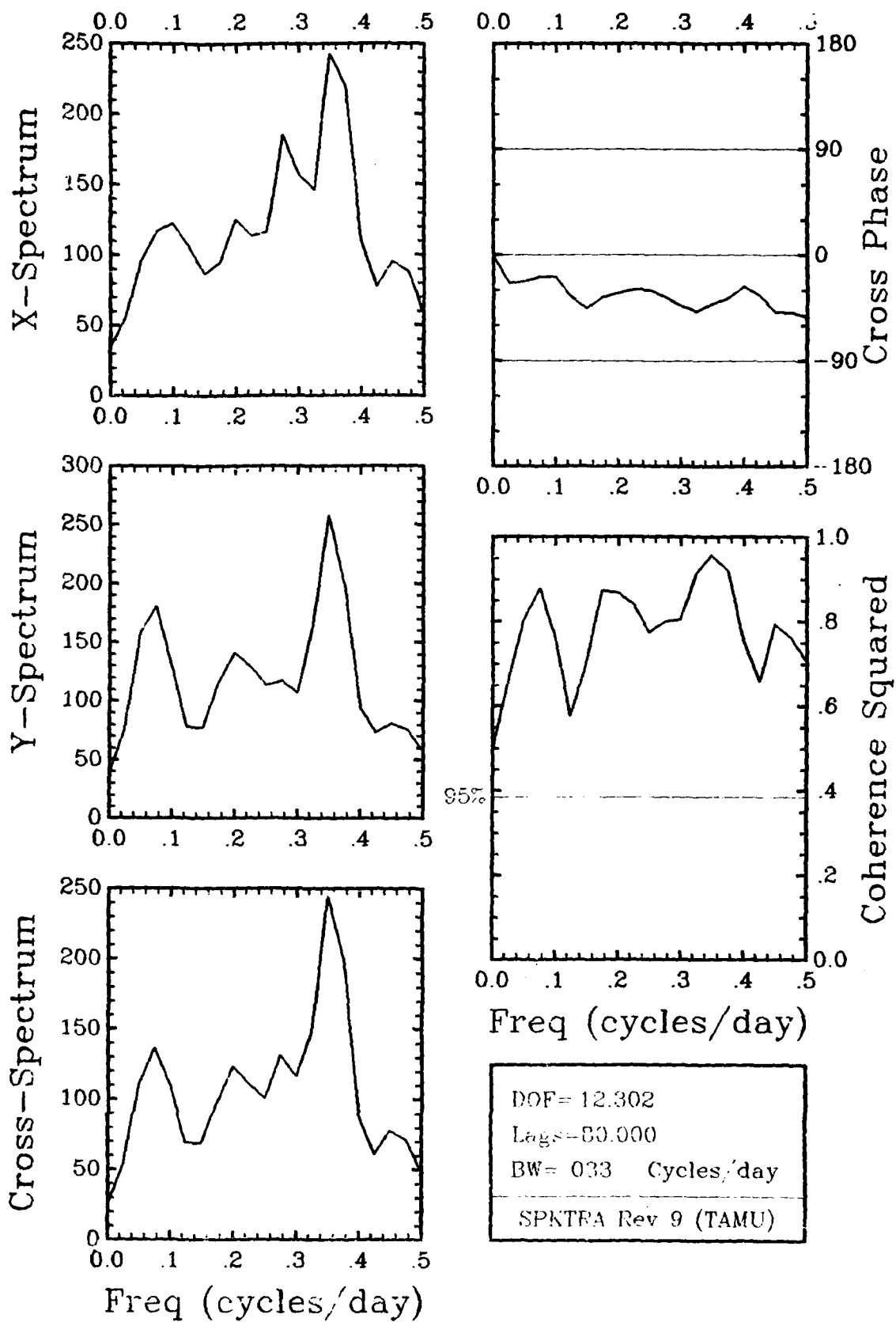


$B_T U / B_T V$ Summer 40 HR LP

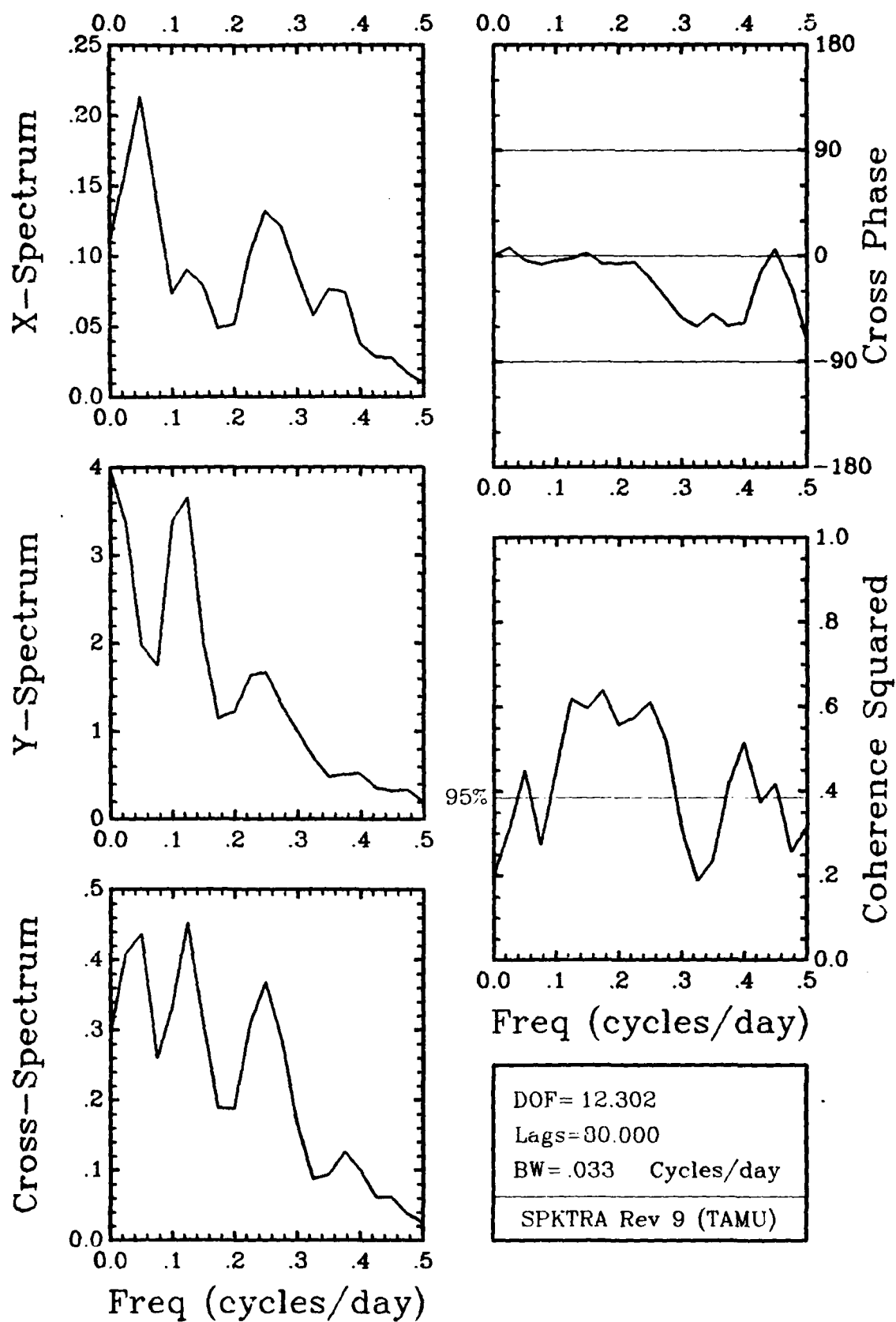


A_B U / B_B U Summer 40 HR LP


 $C_T \ V / D_T \ V$ Summer 40 HR LP



C_T U / D_T U Summer 40 HR LP



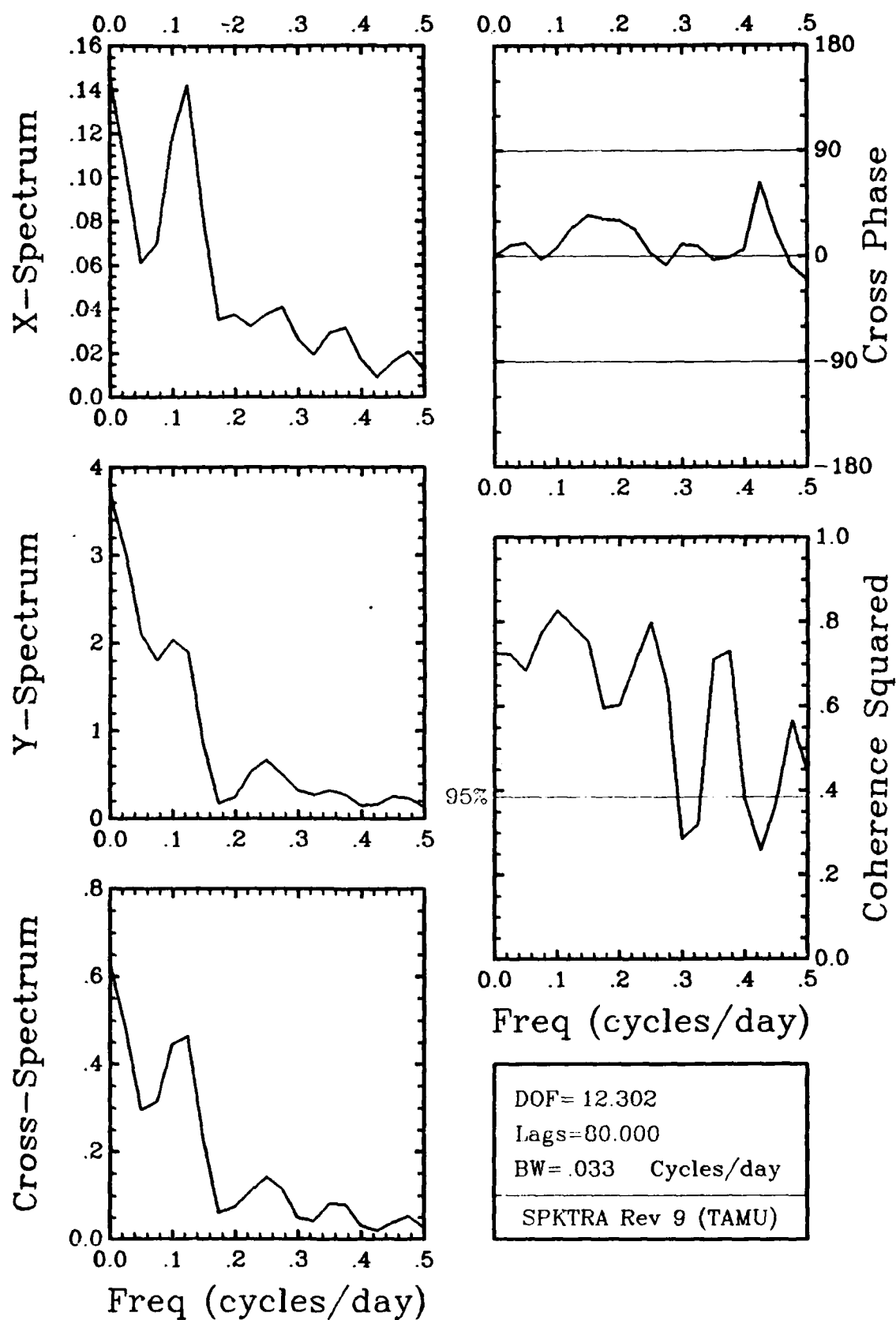
DOF= 12.302

Lags=30.000

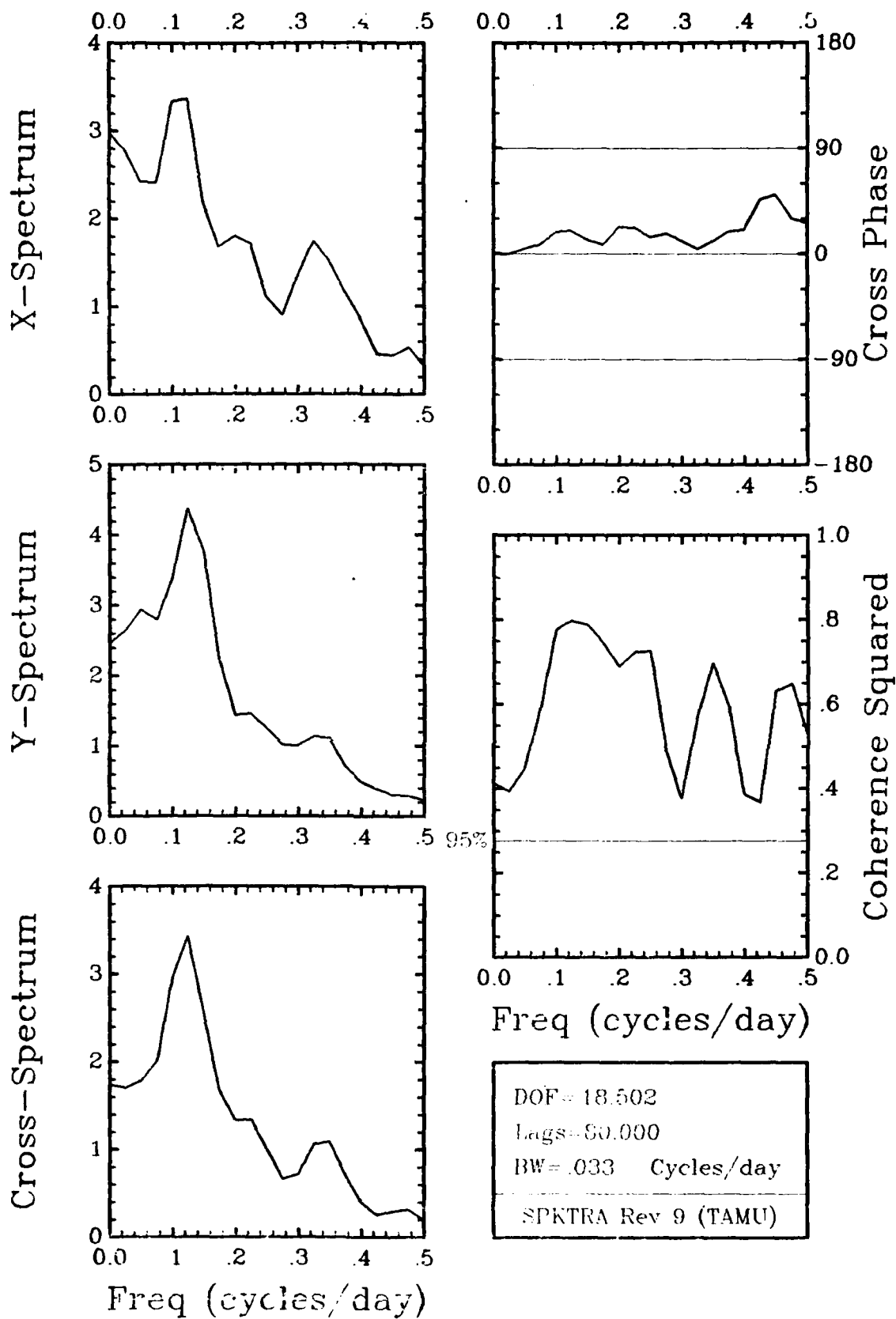
BW= .033 Cycles/day

SPKTRA Rev 9 (TAMU)

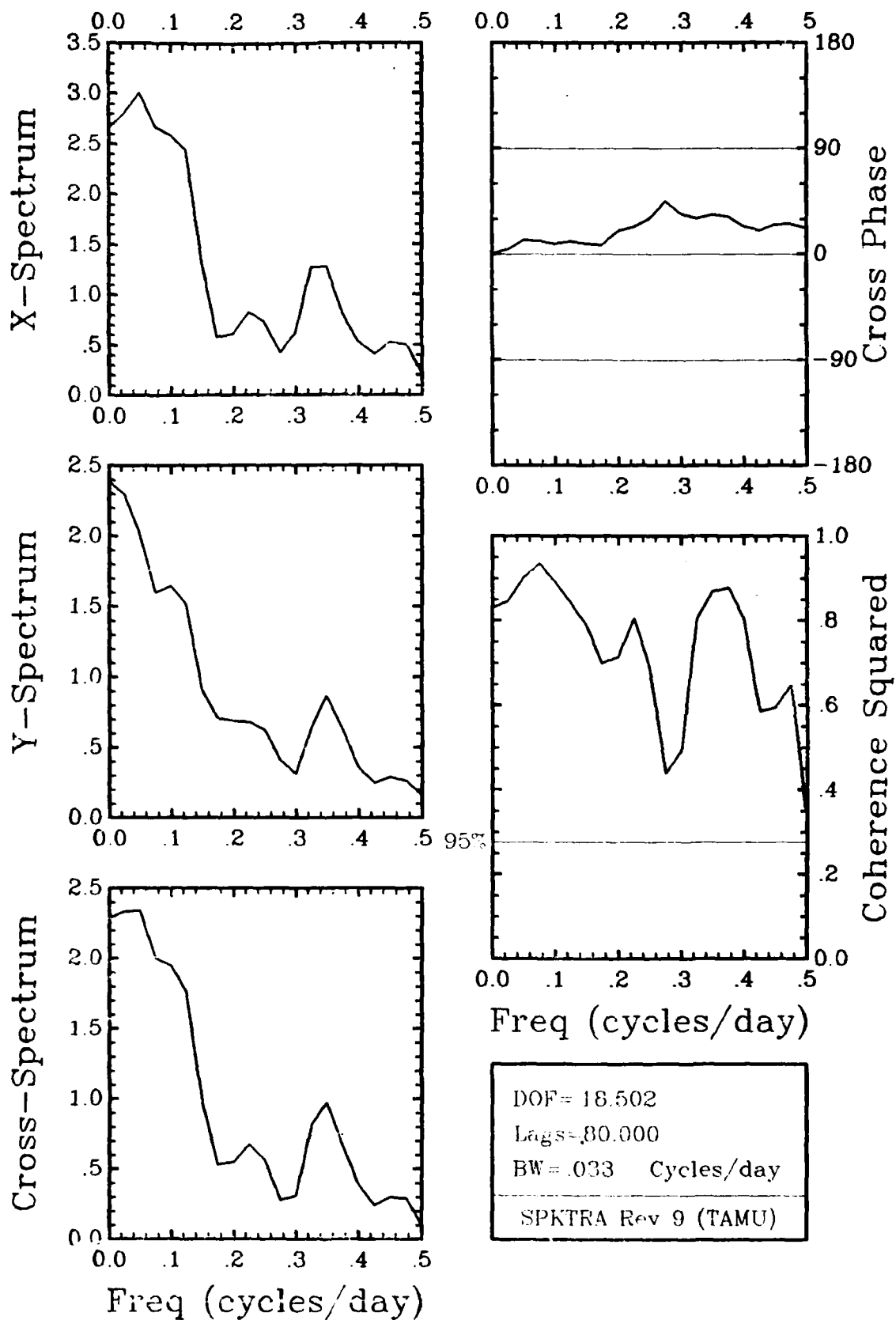
V-Stress_{HAT} / V-Stress₄₁₀₀₂ Summer 40 HR LP



U-Stress_{HAT} / U-Stress₄₁₀₀₂ Summer 40 HR LP



V-Stress₄₁₀₀₂ / V-Stress₄₁₀₀₄ Summer 40 HR LP



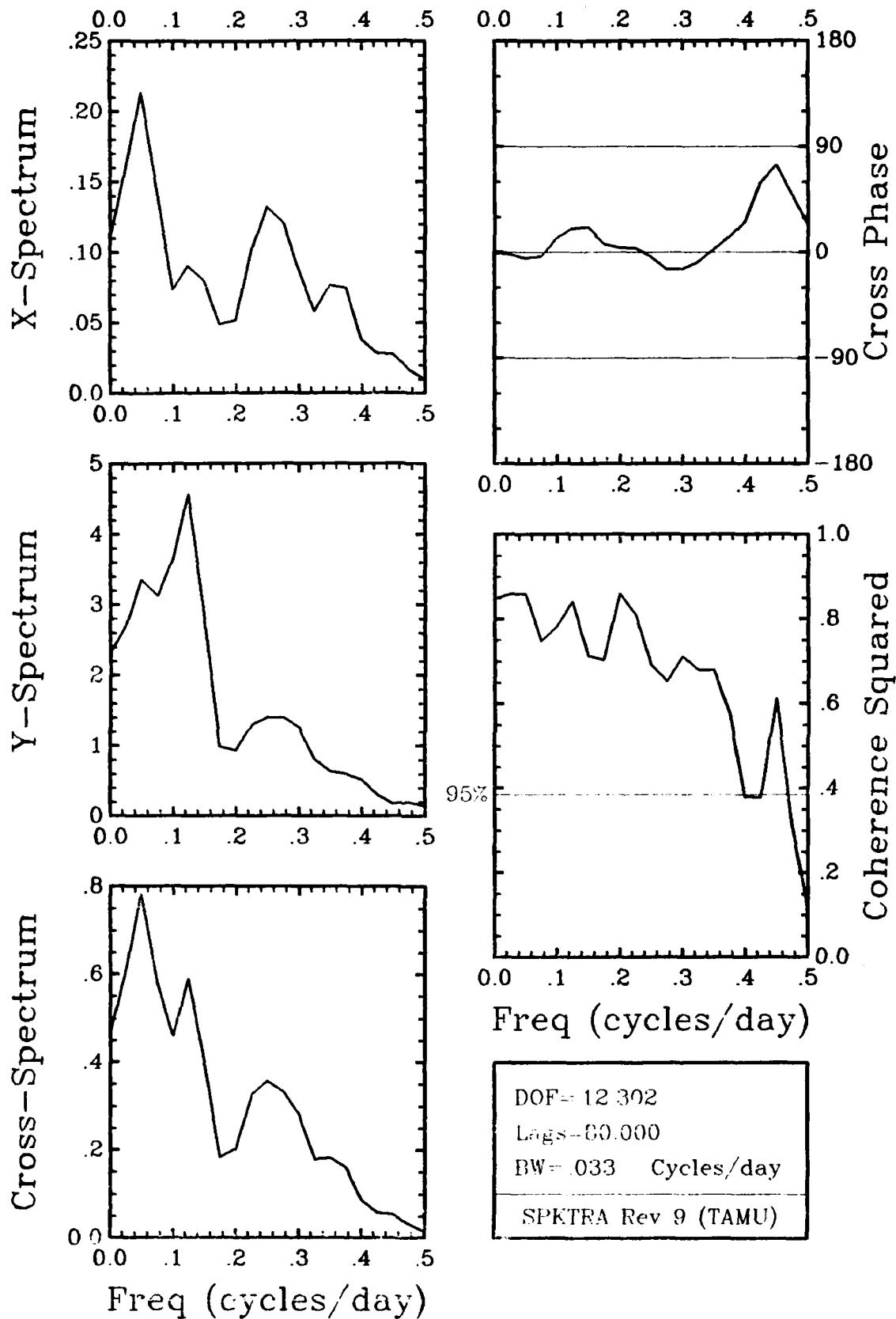
DOF= 18.502

Lags=.80.000

BW= .033 Cycles/day

SPKTRA Rev 9 (TAMU)

U-Stress₄₁₀₀₂ / U-Stress₄₁₀₀₄ Summer 40 HR I



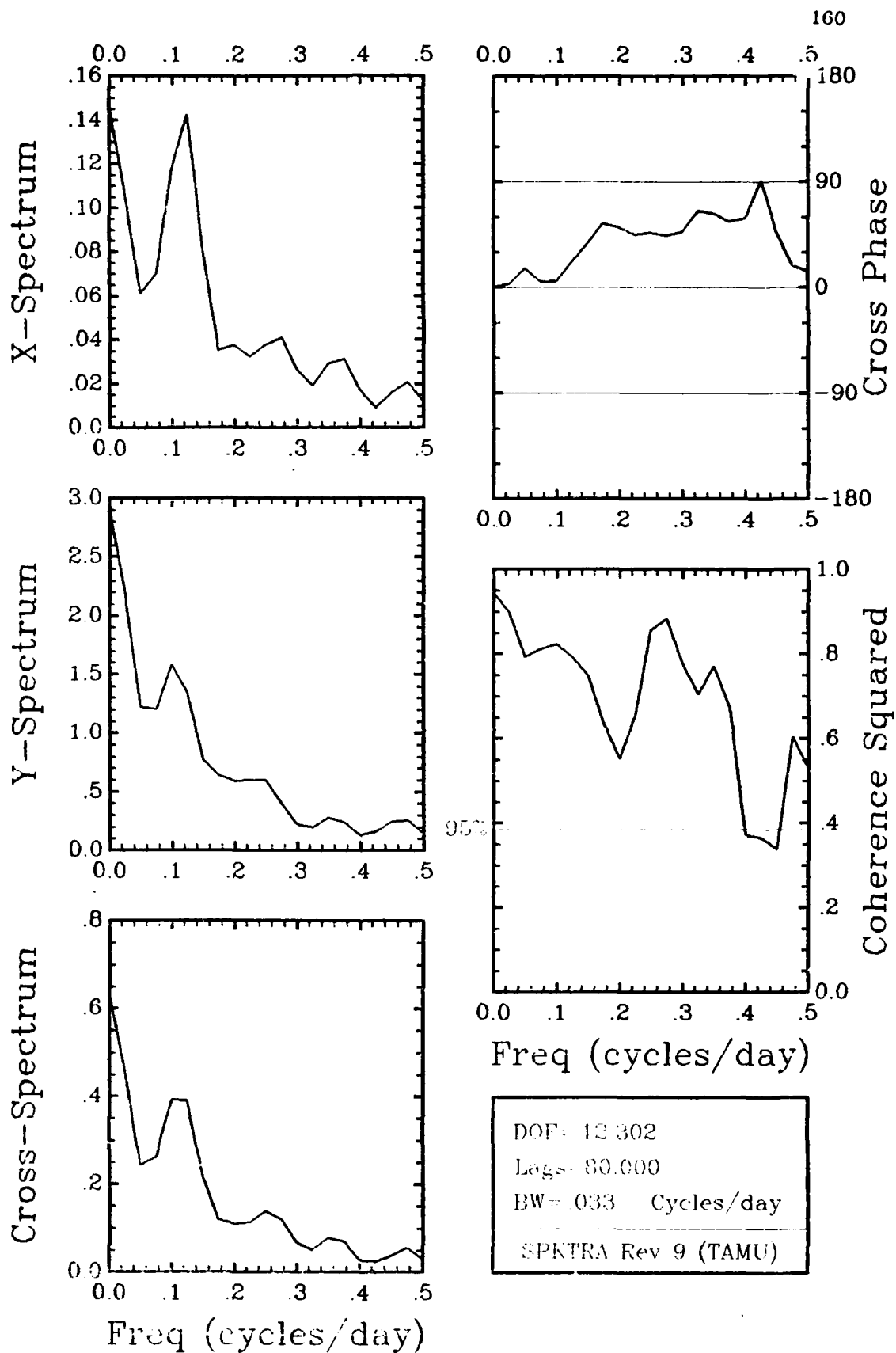
DOF= 12 302

Lags=00.000

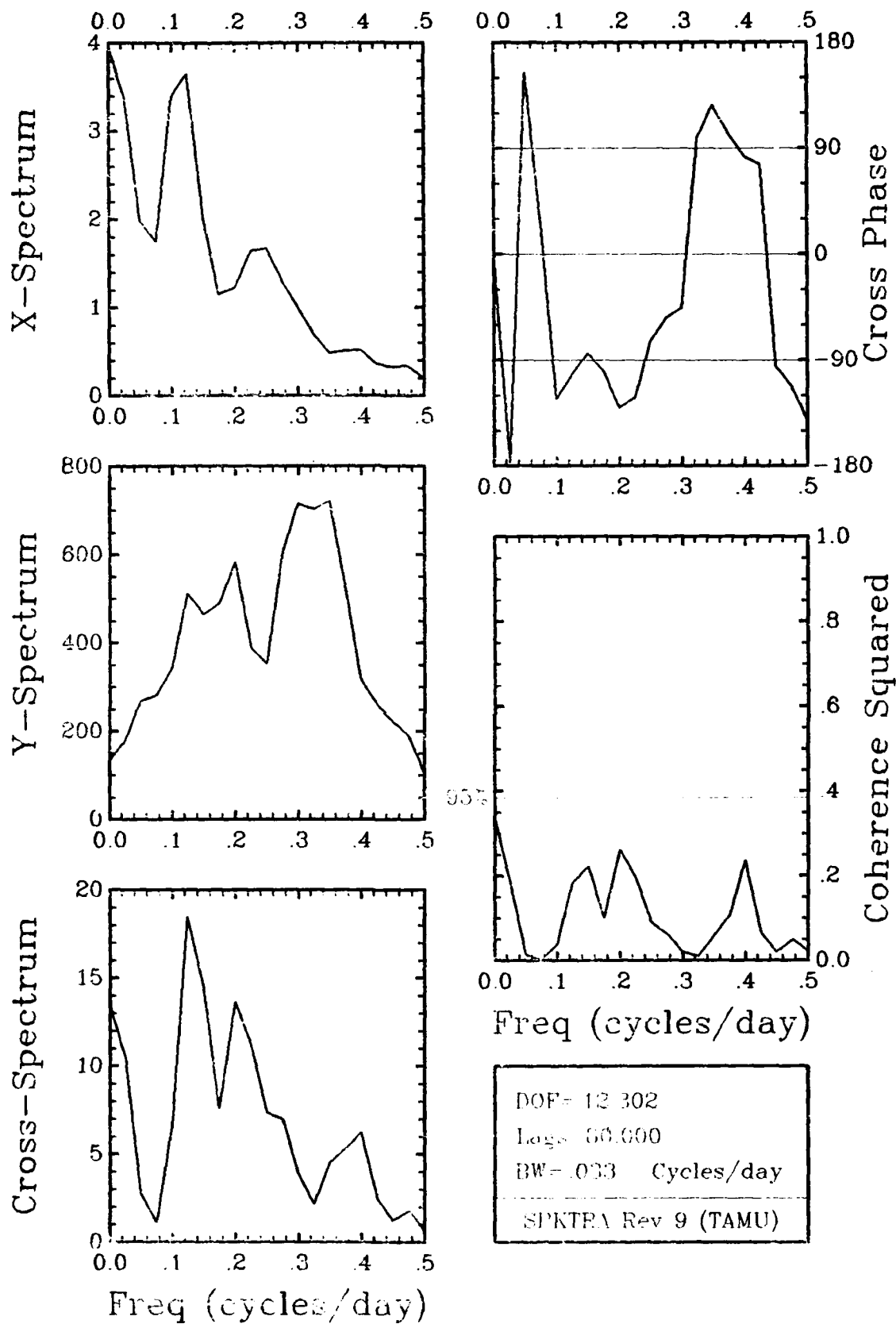
BW=.033 Cycles/day

SPKTRA Rev 9 (TAMU)

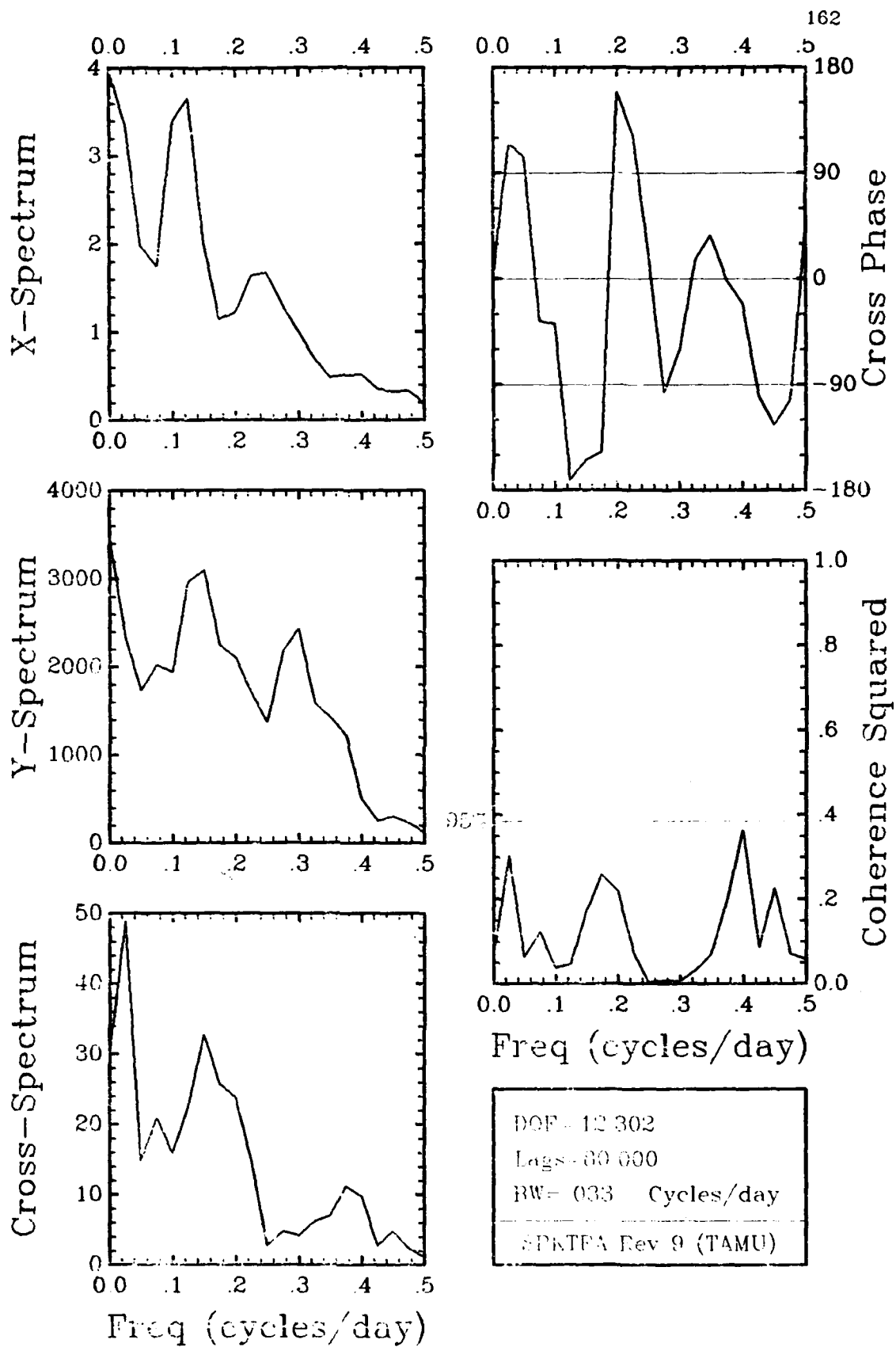
V-Stress_{HAT} / V-Stress₄₁₀₀₄ Summer 40 HR LP



U-Stress_{HAT} / U-Stress₄₁₀₀₄ Summer 40 HR LP

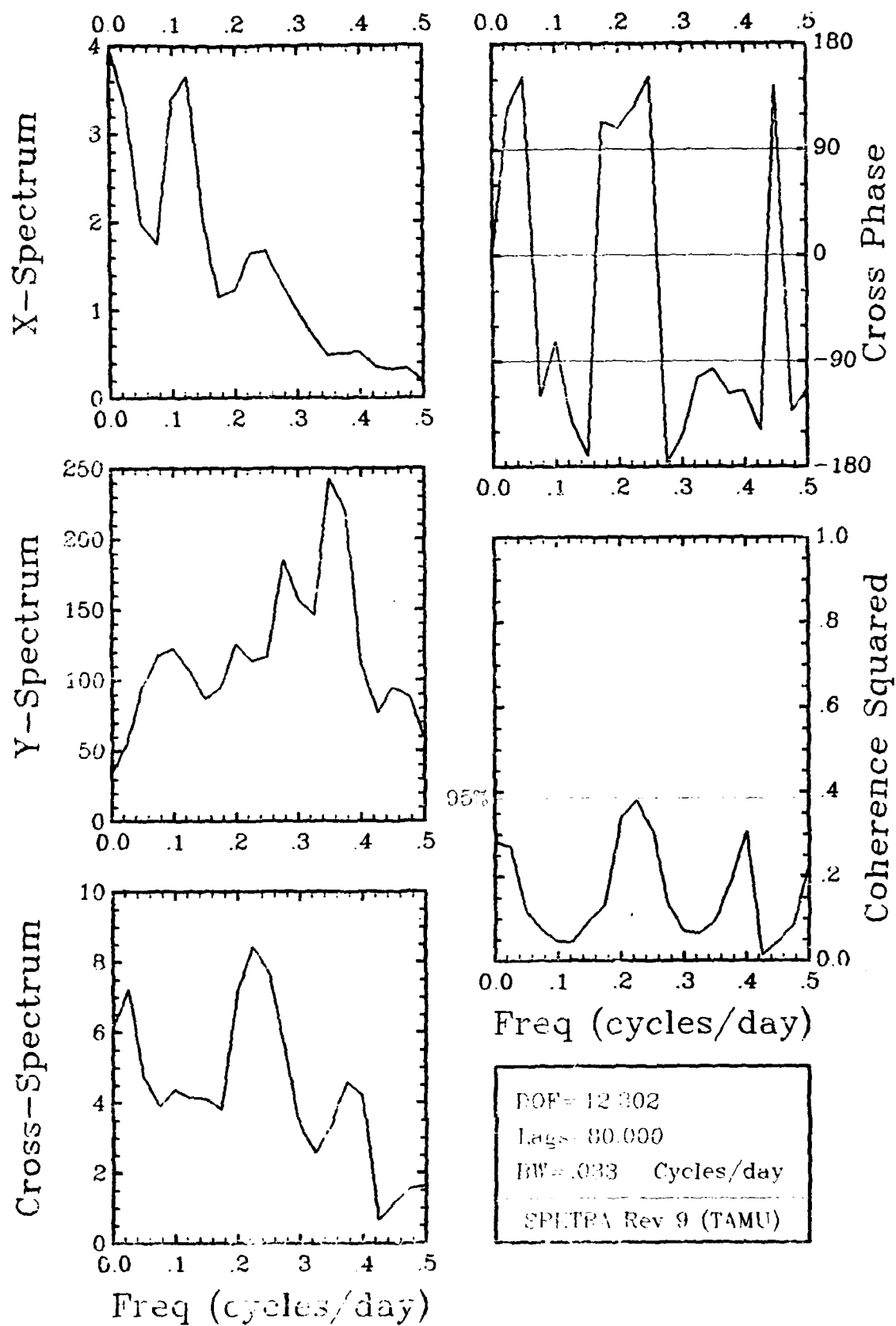


V-Stress₄₁₀₀₂ / B_TU Summer 40 HR LP



DOF = 12 302
 Logs = 60 000
 BW = 033 Cycles/day
 SPKTEA Rev 9 (TAMU)

V-Stress₄₁₀₀₂ / B_TV Summer 40 HR LP



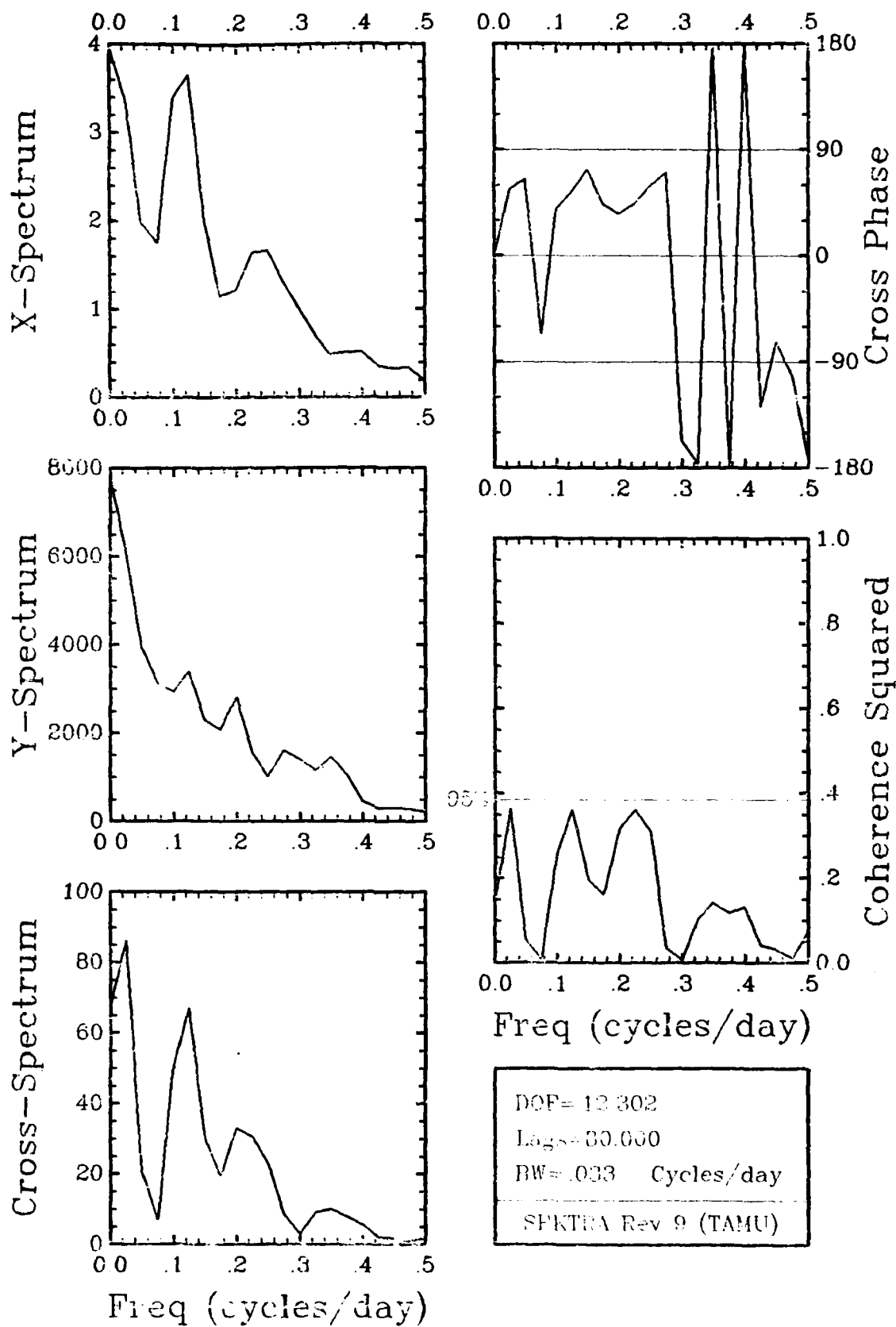
DOF= 12 302

lags= 80.000

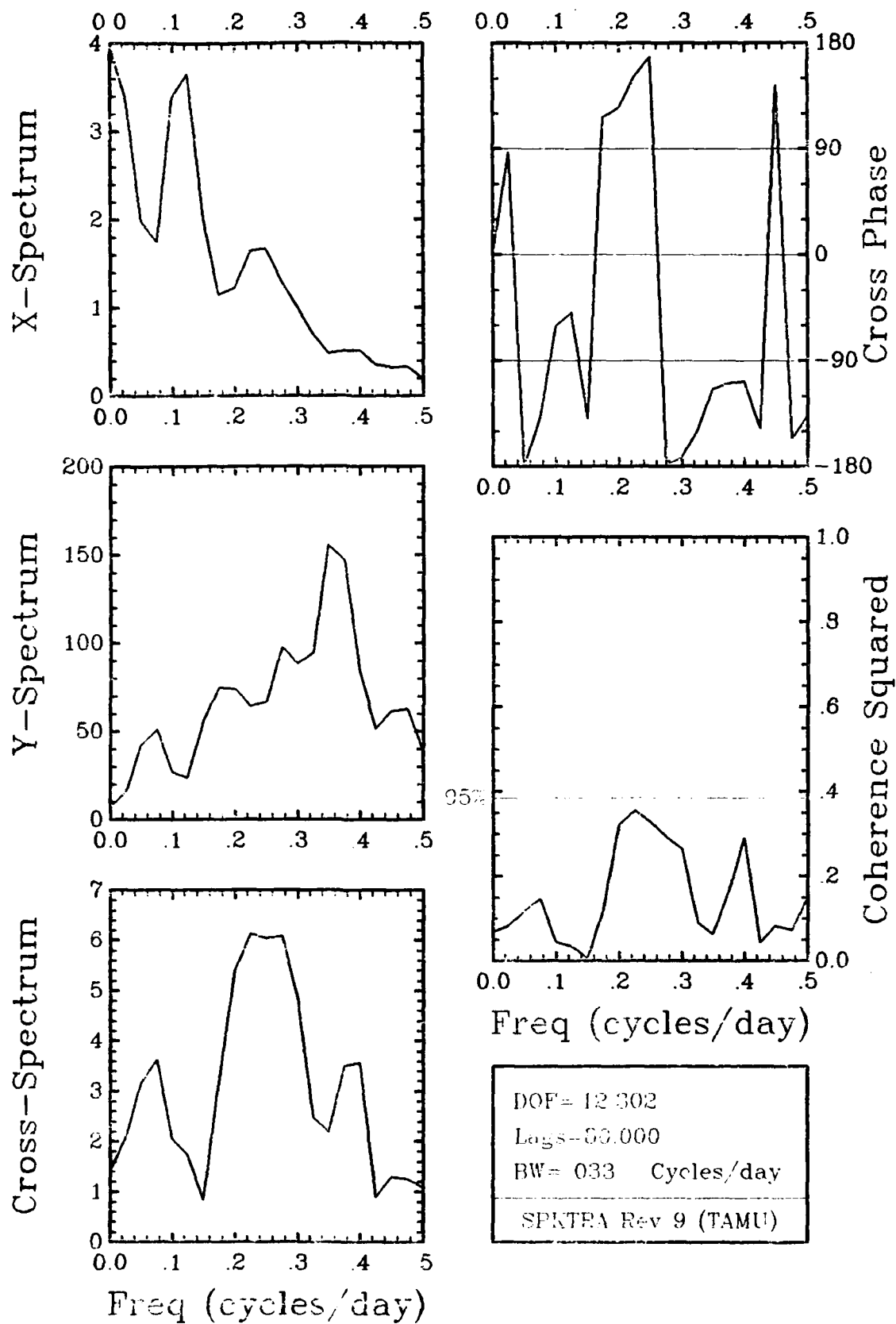
BW=.033 Cycles/day

SPETRA Rev 9 (TAMU)

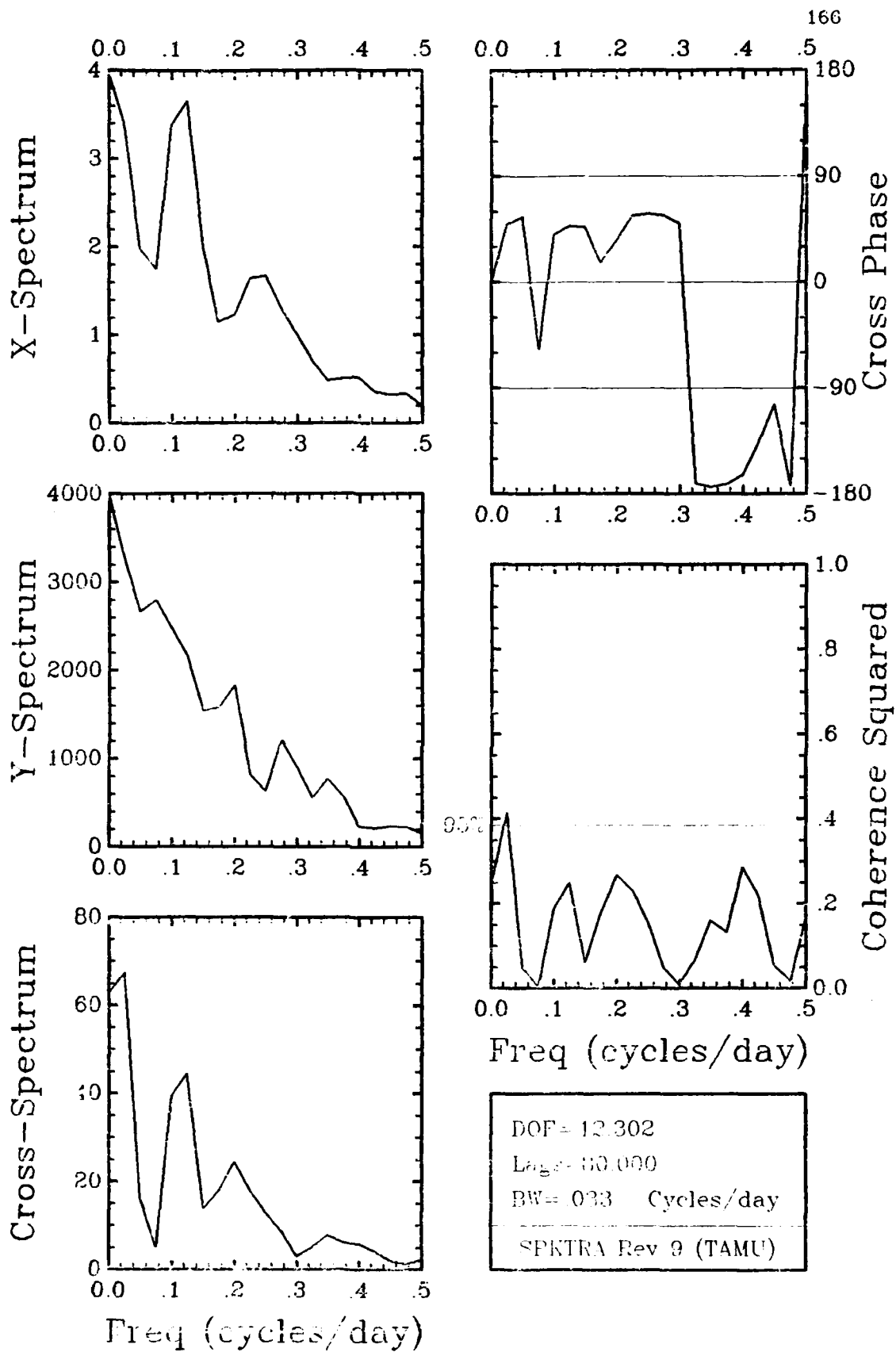
V-Stress₄₁₀₀₂ / C_TU Summer 40 HR LP



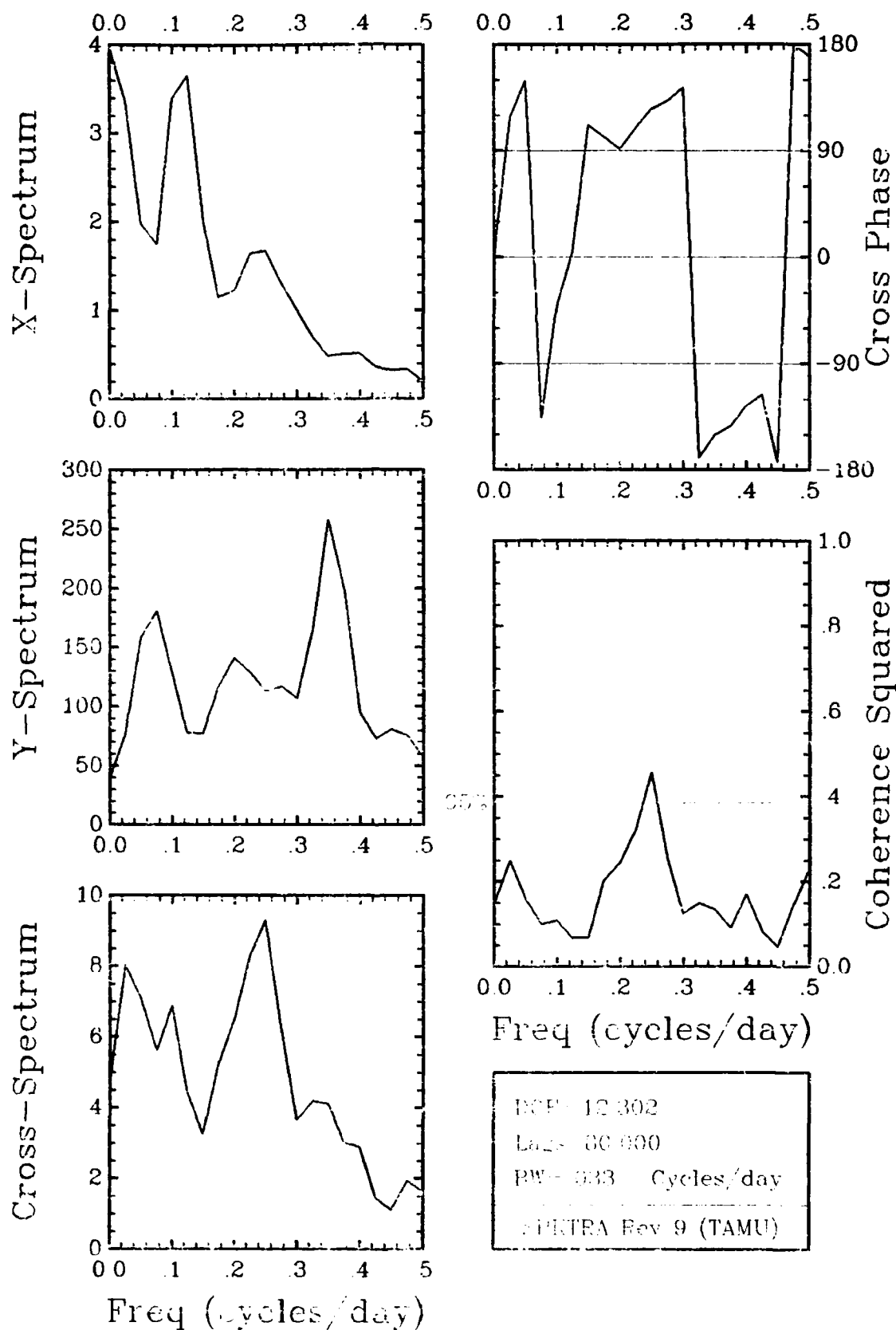
V-Stress₄₁₀₀₂ / C_TV Summer 40 HR LP



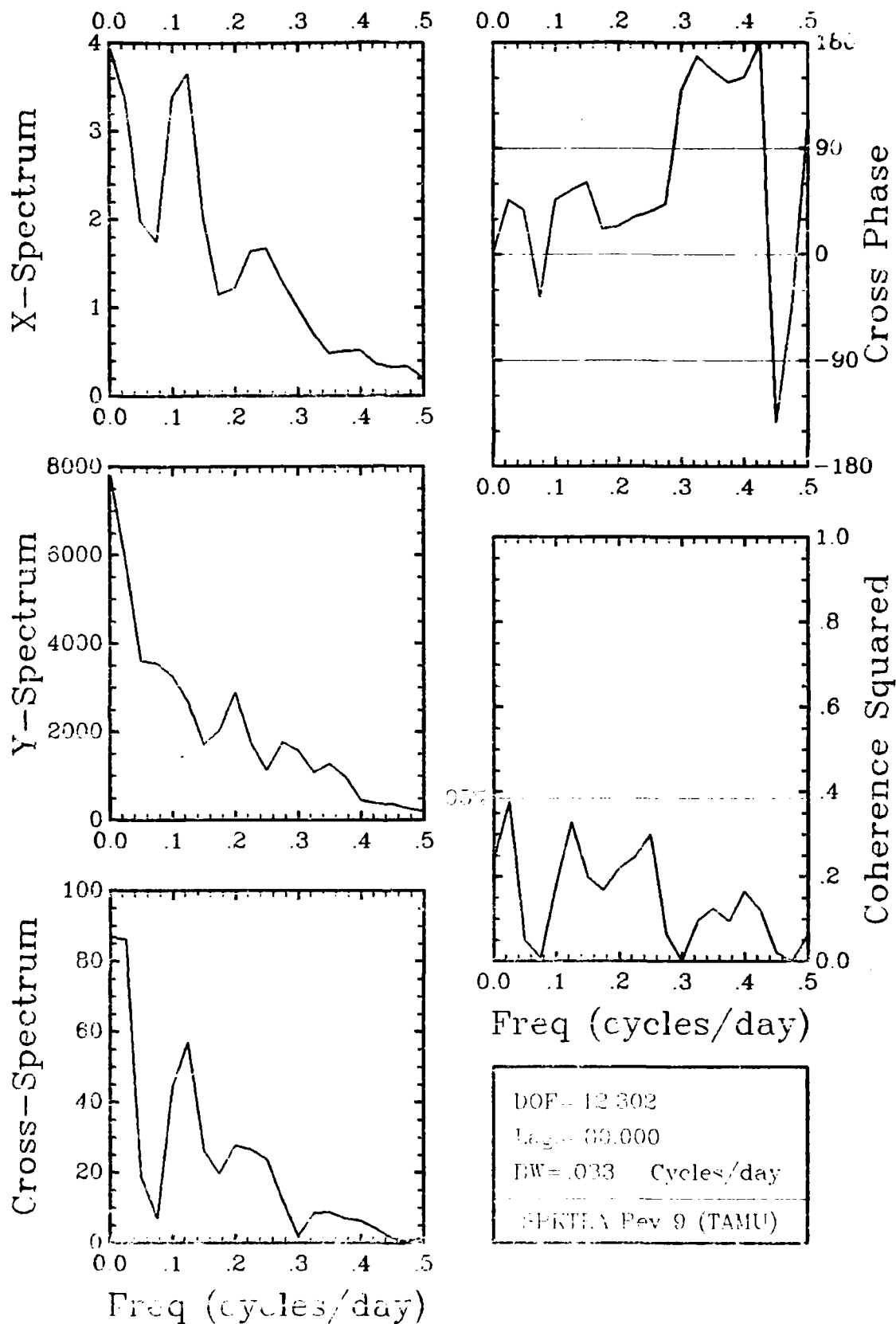
V-Stress₄₁₀₀₂ / C_MU Summer 40 HR LP



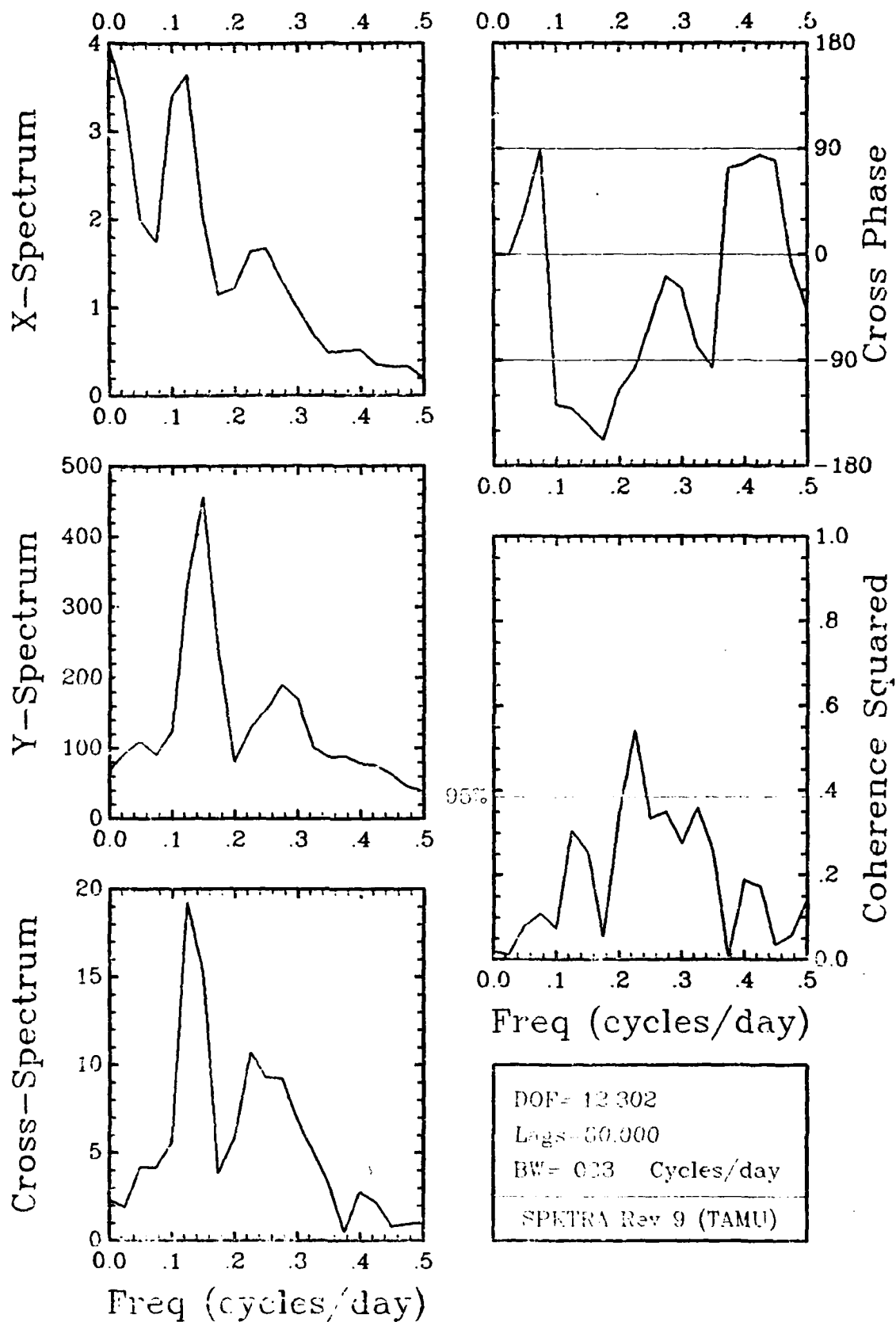
V-Stress₄₁₀₀₂ / C_MV Summer 40 HR LP



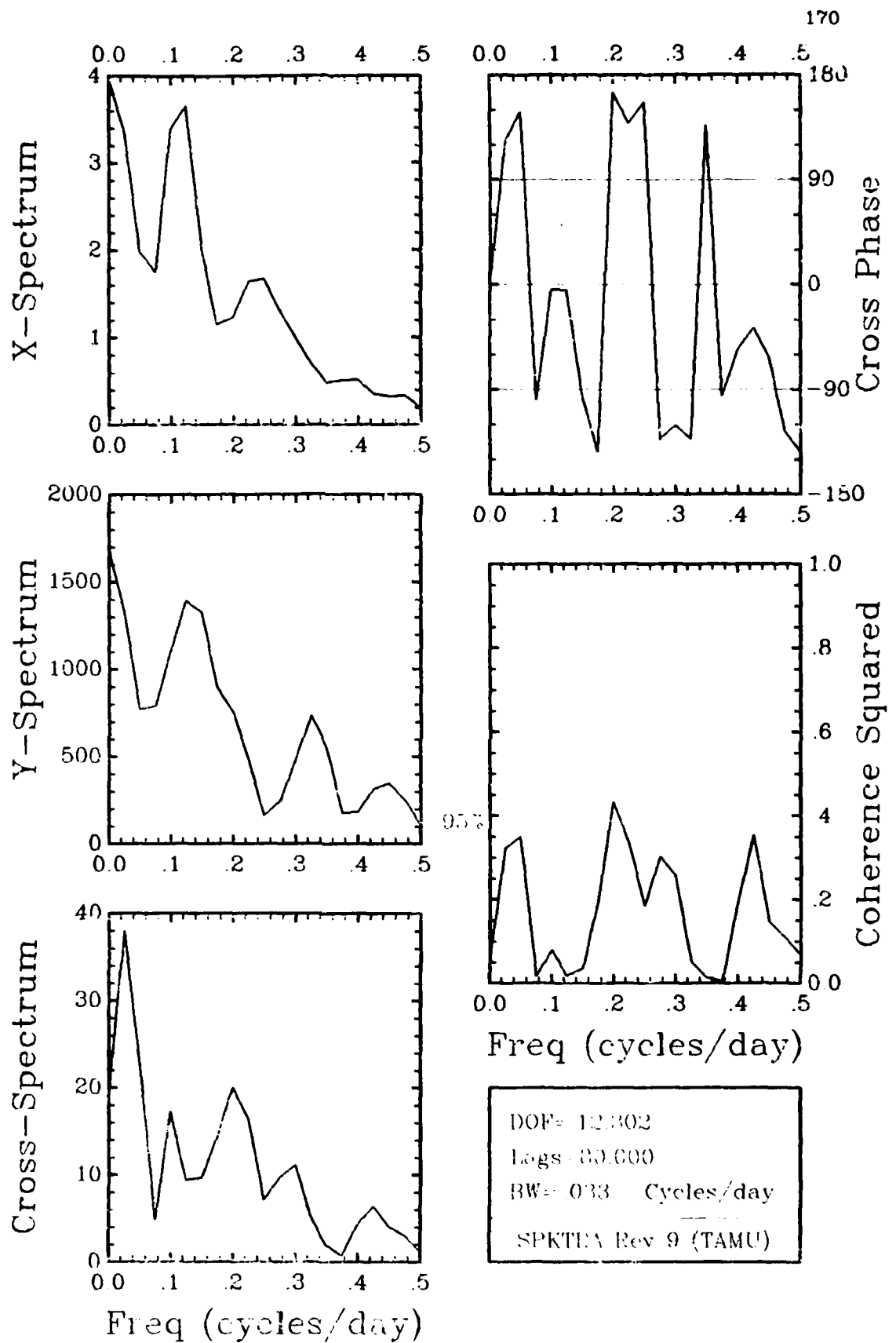
V-Stress₄₁₀₀₂ / D_TU Summer 40 HR LP



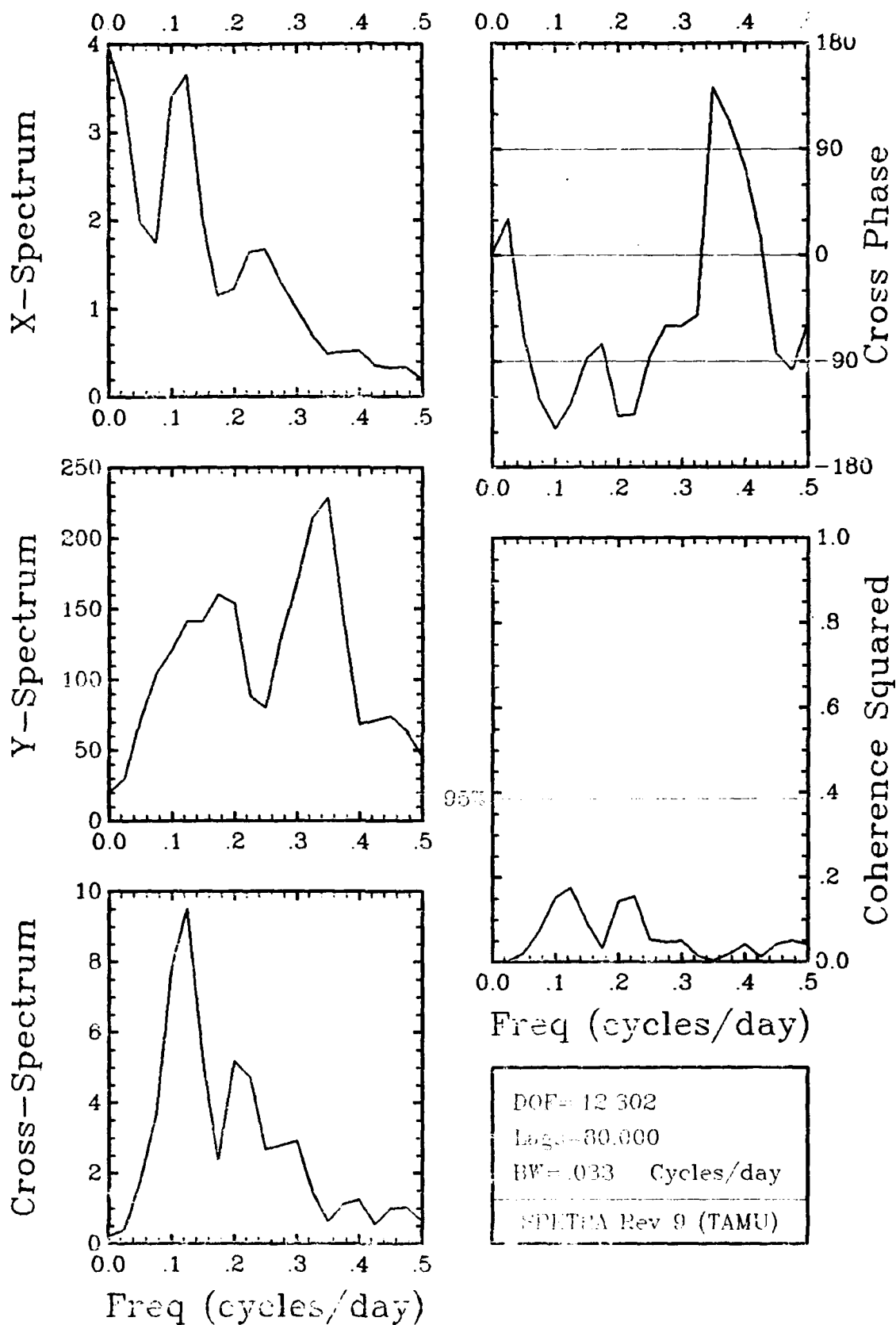
V-Stress₄₁₀₀₂ / D_TV Summer 40 HR LP



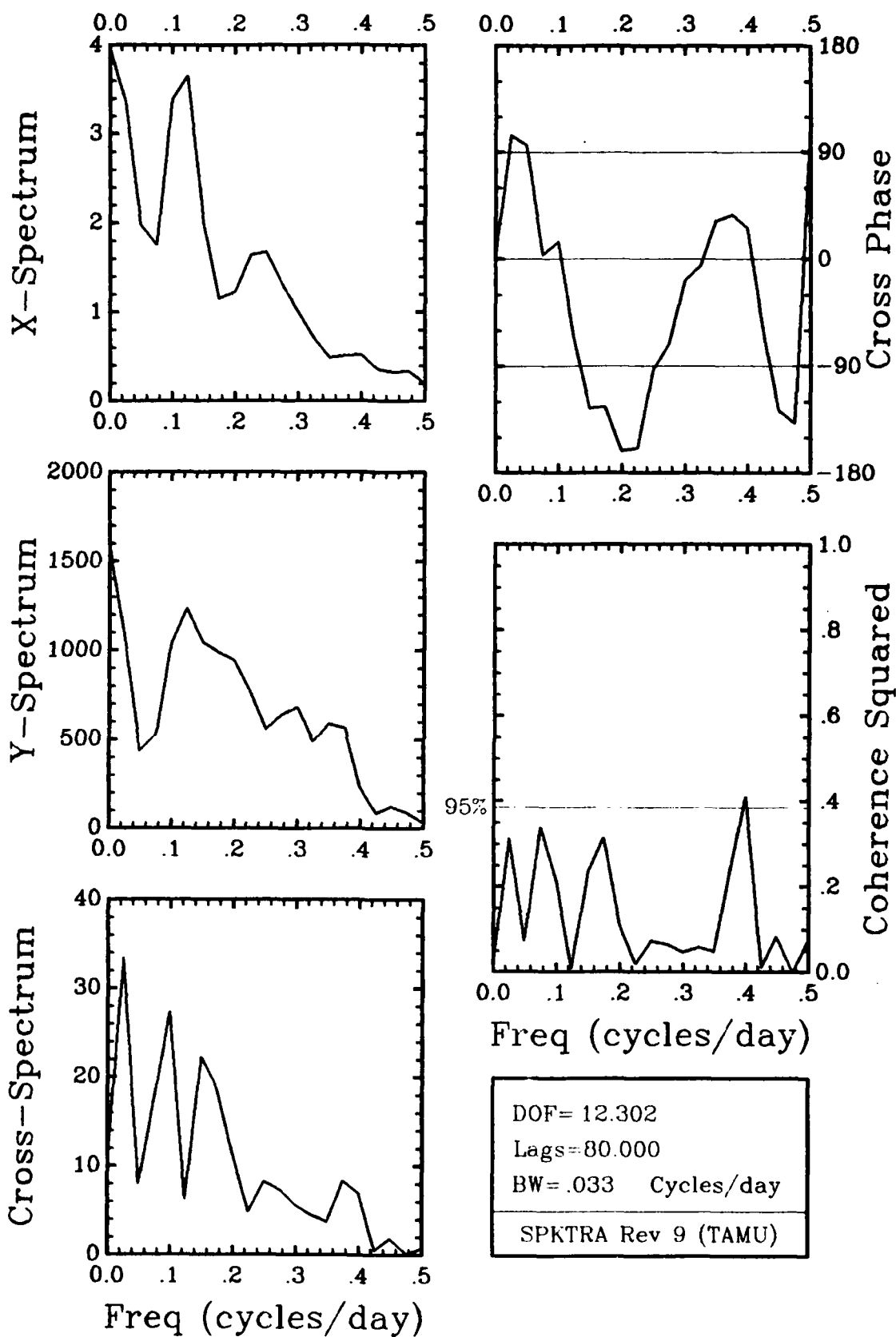
V-Stress₄₁₀₀₂ / A_BU Summer 40 HR LP



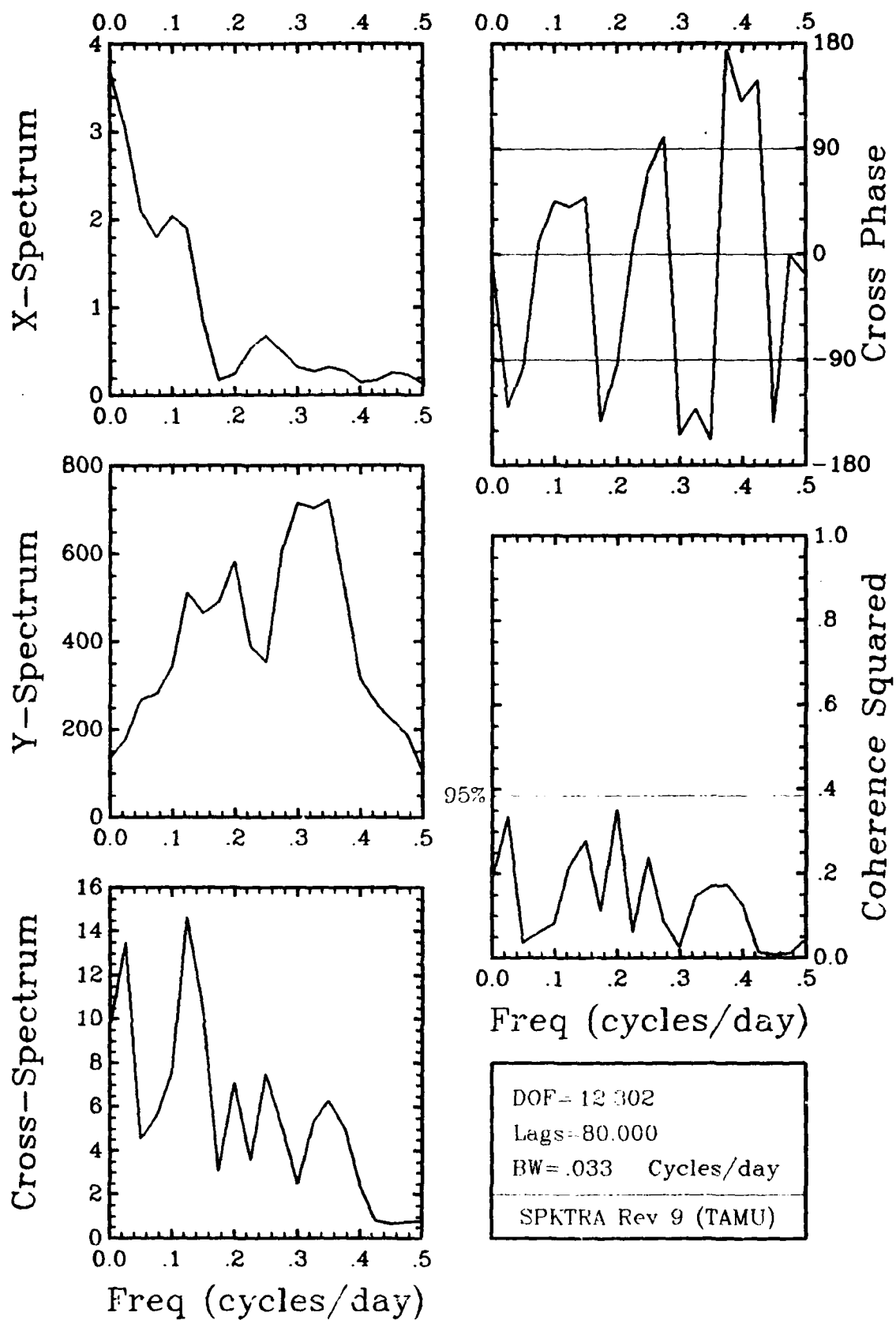
V-Stress₄₁₀₀₂ / A_BV Summer 40 HR LP



V-Stress₄₁₀₀₂ / B_BU Summer 40 HR LP



V-Stress₄₁₀₀₂ / B_BV Summer 40 HR LP



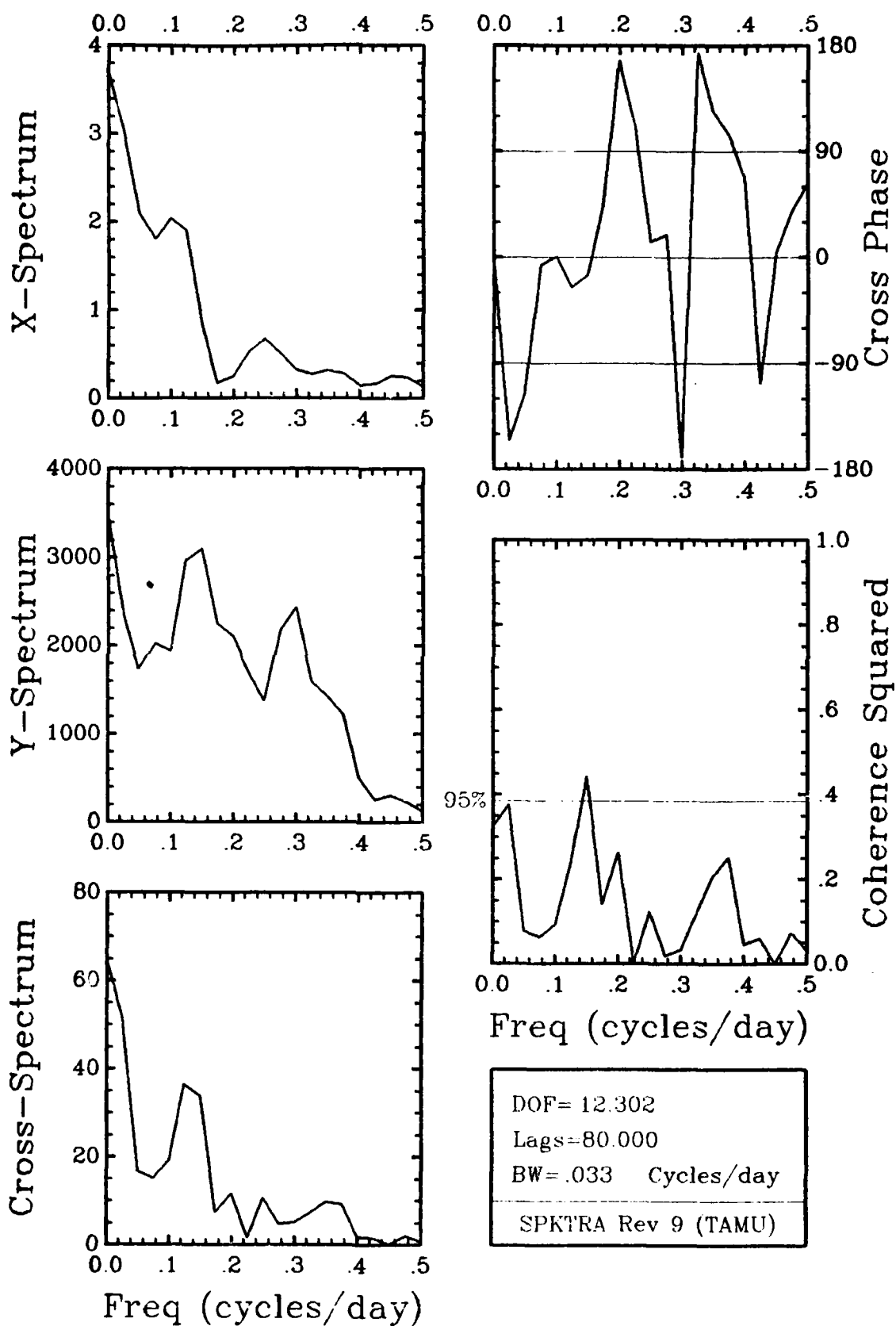
DOF = 12 302

Lags = 80.000

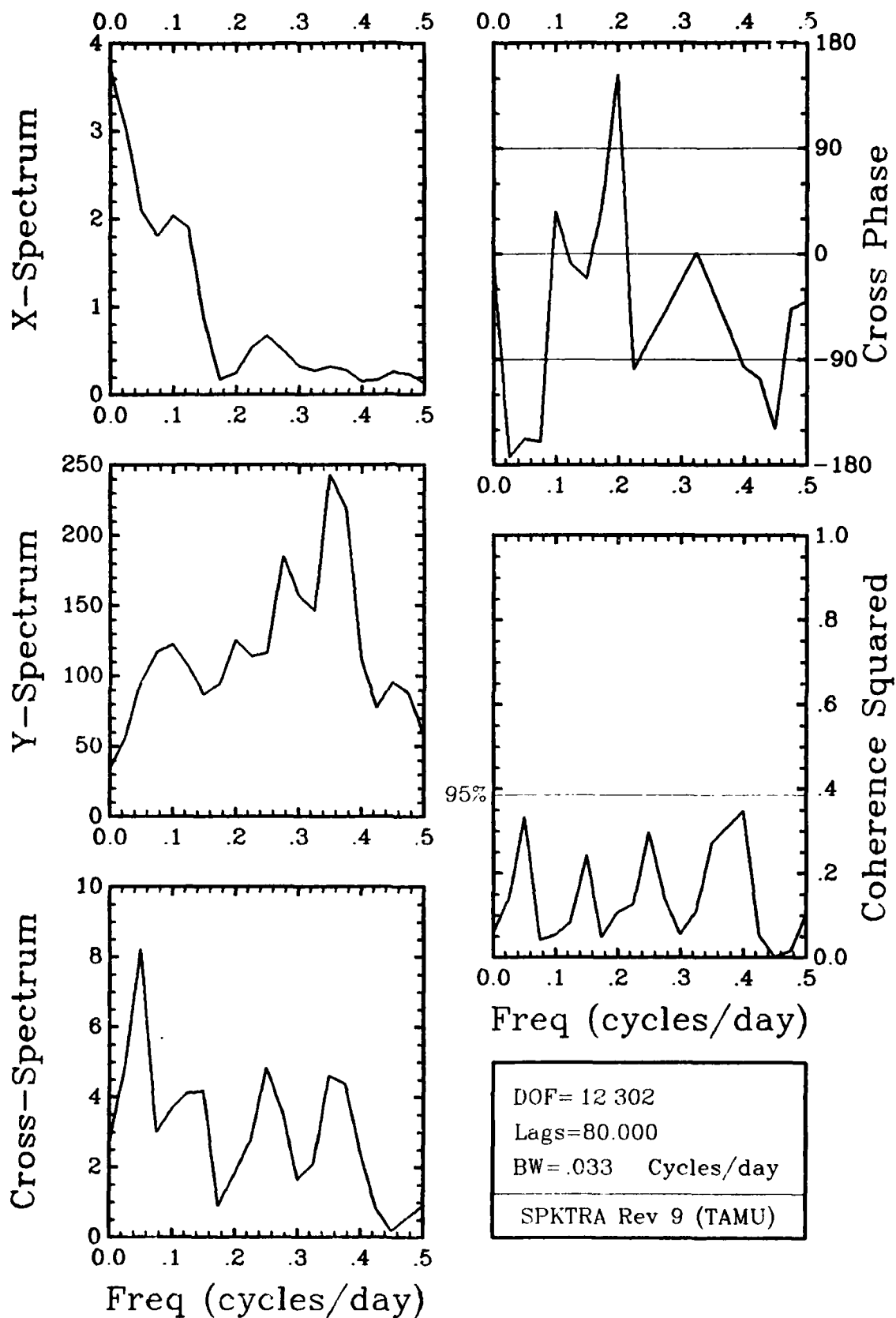
BW = .033 Cycles/day

SPKTRA Rev 9 (TAMU)

U-Stress₄₁₀₀₂ / B_TU Summer 40 HR LP



U-Stress₄₁₀₀₂ / B_TV Summer 40 HR LP



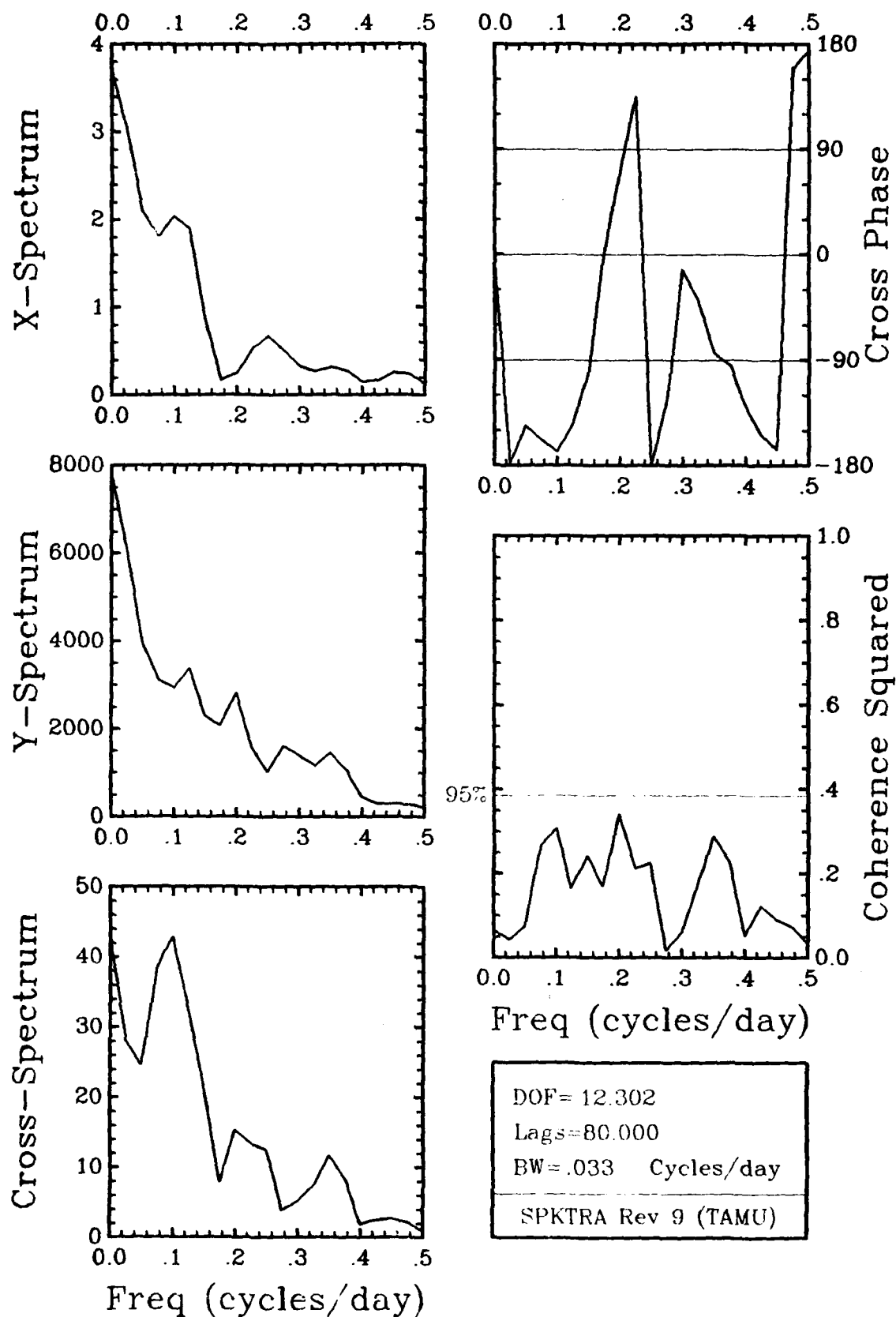
DOF= 12 302

Lags=80.000

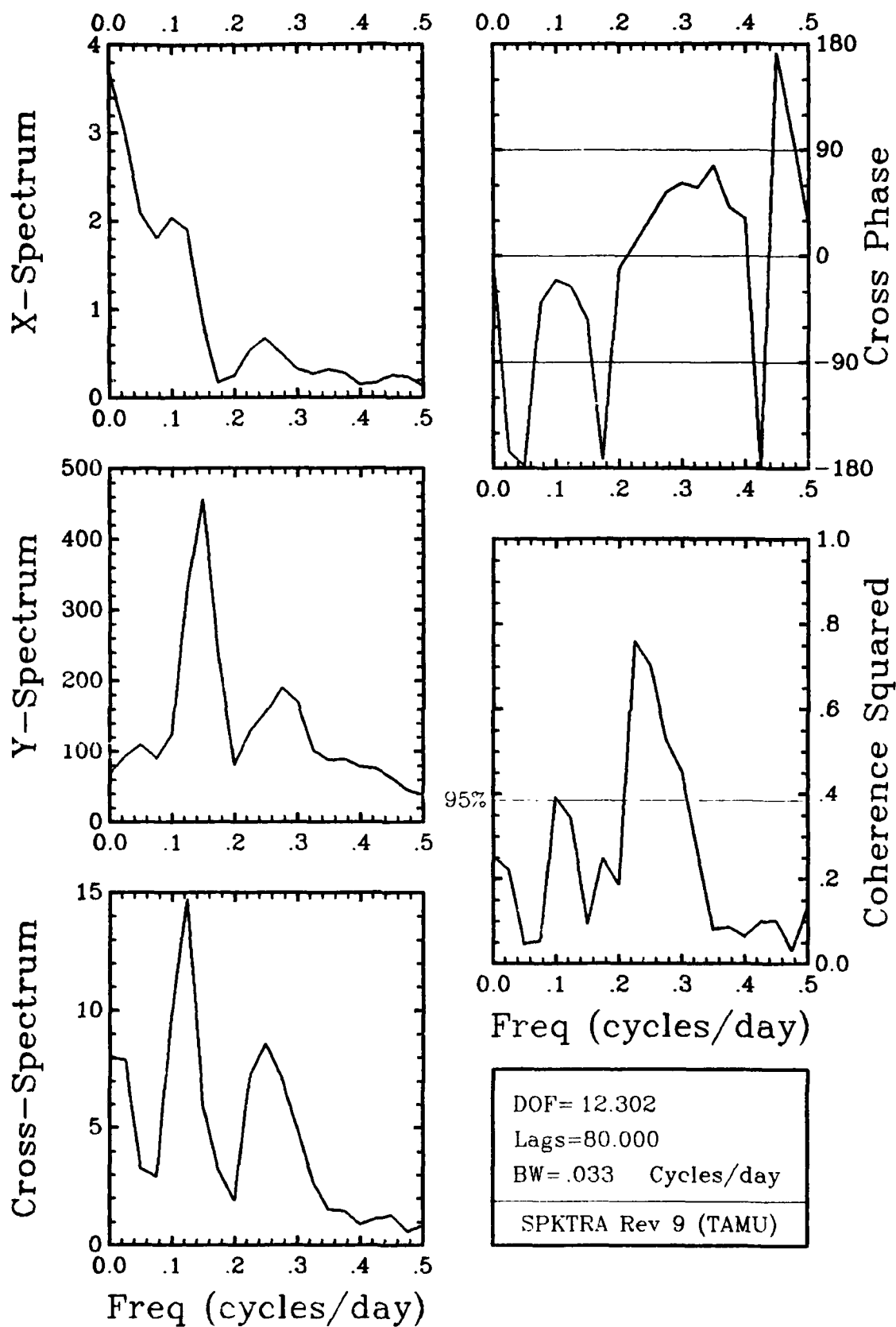
BW= .033 Cycles/day

SPKTRA Rev 9 (TAMU)

U-Stress₄₁₀₀₂ / C_TU Summer 40 HR LP



U-Stress₄₁₀₀₂ / C_TV Summer 40 HR LP



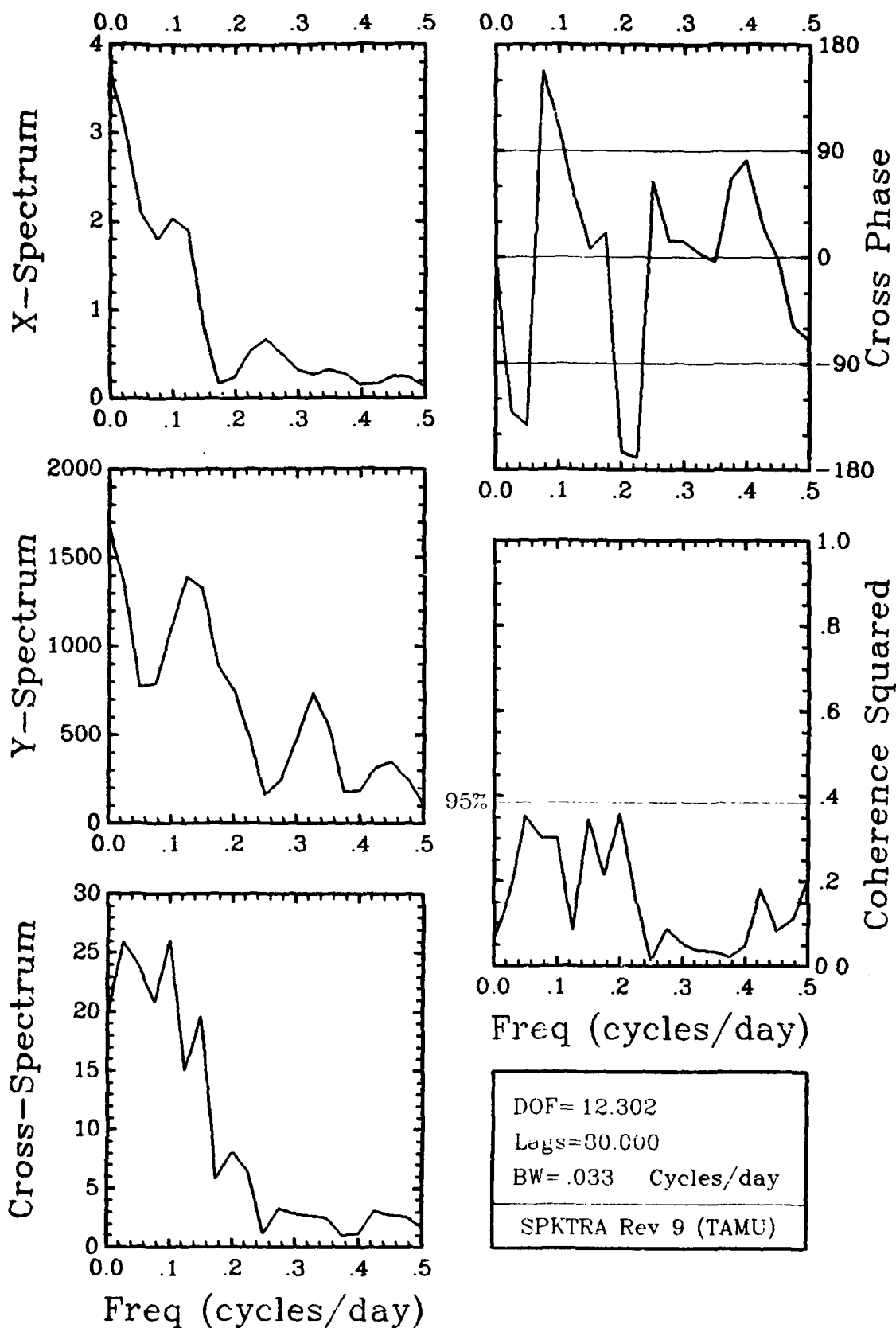
DOF= 12.302

Lags=80.000

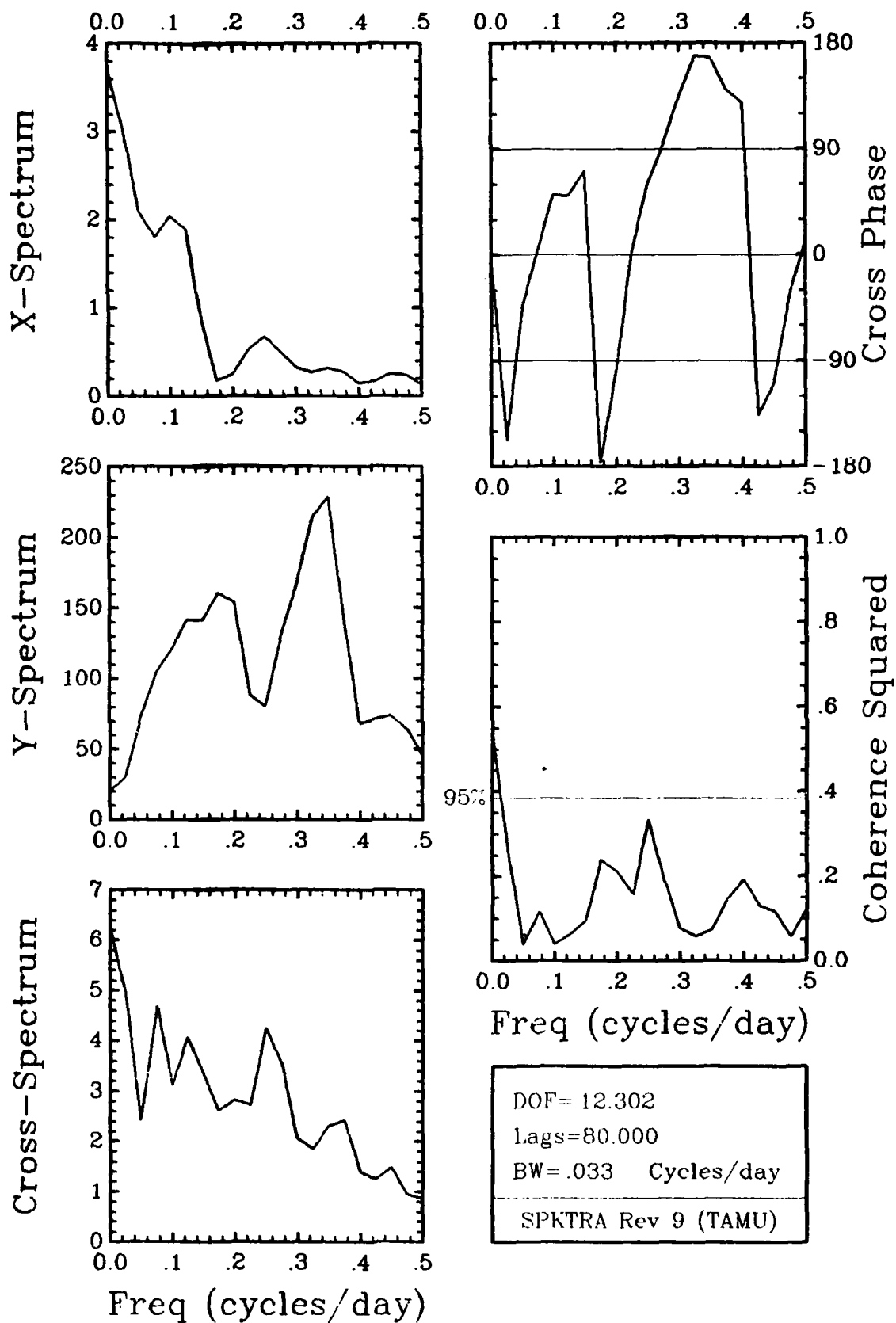
BW= .033 Cycles/day

SPKTRA Rev 9 (TAMU)

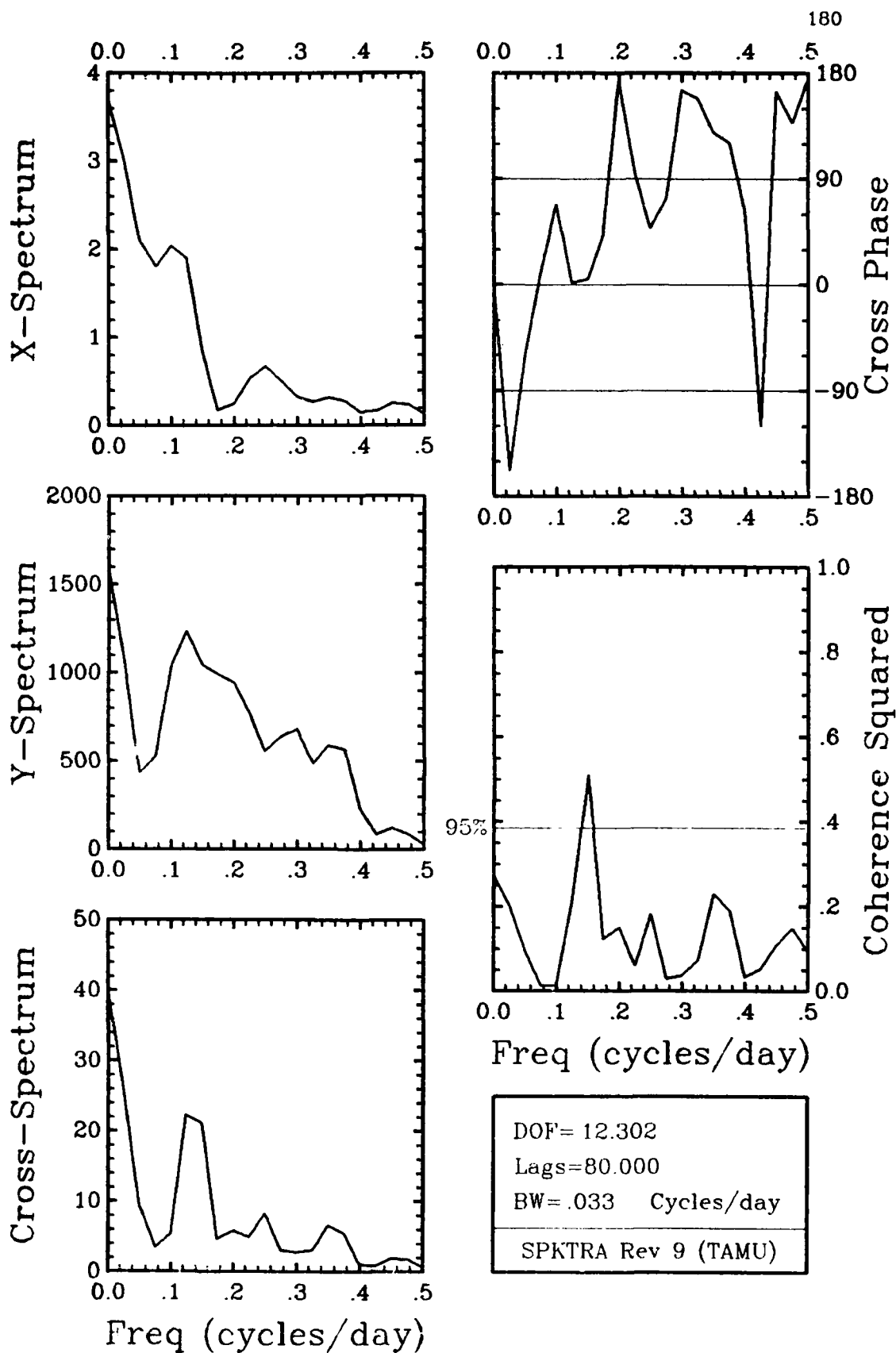
U-Stress₄₁₀₀₂ / A_BU Summer 40 HR LP



U-Stress₄₁₀₀₂ / A_BV Summer 40 HR LP



U-Stress₄₁₀₀₂ / B_BU Summer 40 HR LP



U-Stress₄₁₀₀₂ / B_BV Summer 40 HR LP

Acknowledgments

The Gulf Stream Meanders Experiment was supported by the National Science Foundation, grant numbers OCE 77-25682 and OCE 79-06710; and by the office of Naval Research, contract number N00014-77-C-0354. The successful deployment and recovery of current meter moorings was in large part due to the efforts of Mr. Paul Blankinship. We extend our appreciation to Captain Herb Bennett and the crew of the R/V *Endeavor* for expert service at sea. The delicate task of Aanderaa data tape transcription was greatly aided by Mr. Lawrence Ives, who designed and built an interface device for the purpose. Innumerable details associated with carrying out this project were attended to by graduate students at Texas A&M University, the University of North Carolina, and North Carolina State University, without whose help this experiment would not have been possible. The computer graphics and text editing software utilized in this report were implemented by Mr. Tom Reid, who also expertly directed the tedious file maintenance and data editing chores. Ms. Florace Kling painstakingly typed the tables. We thank Dr. Richard Legeckis of NOAA/NES3 for providing us with the satellite cover photo, which makes the motivation for this experiment clear in an instant.

AD-A103 487

NORTH CAROLINA UNIV AT CHAPEL HILL

F/6 8/3

THE GULF STREAM MEANDERS EXPERIMENT. CURRENT METER AND ATMOSPHE--ETC(U)

MAY 81 D A BROOKS, J M BANE, R L COHEN

N00014-77-C-0354

NL

UNCLASSIFIED

3-3
A-
4-1-10-



END

DATE

FILMED

0 81

DTIC

References

- Brooks, D. A., 1976 (Editor): Fast and EaSy Time Series Analysis at NCSU. Technical Report. Center for Marine and Coastal Studies, North Carolina State University, Raleigh.
- _____, J. M. Bane, Jr., and M. J. Ignaszewski, 1980a: The Gulf Stream Meanders Experiment: Hydrographic Data Report, R/V *Endeavor* cruises EN-031 and EN-037. Texas A&M University, Rep. 80-1-T, 145 pp.
- _____, _____, R. L. Cohen, and P. Blankinship, 1980b: The Gulf Stream Meanders Experiment: Current Meter and Atmospheric Data Report for the January to May, 1979 Mooring Period. Texas A&M University, Rep. 80-7-T, 264 pp.
- Düing, W., 1973: Observations and first results from project SYNOPS 71. Technical Report No. UM-RSMAS-73010, University of Miami, Florida, 134 pp.
- Lee, T. N. and R. L. Shutts, 1977: Technical program for Aanderaa current meter moorings on continental shelves. University of Miami, Technical Report No. TR-77-5.
- National Institute of Oceanography of Great Britain and Unesco, 1971: International Oceanographic Table, Volume 1. NIO, Wormley, England, 128 pp.

Richardson, W. S., W. J. Schmitz, Jr., and P. P. Niiler, 1969: The velocity structure of the Florida Current from the Straits of Florida to Cape Fear. *Deep-Sea Res.*, 16 (Suppl.), 225-231.

Webster, R., 1961a: A description of Gulf Stream meanders off Onslow Bay. *Deep-Sea Res.*, 9, 130-143.

_____, 1961b: The effect of meanders on the kinetic energy balance of the Gulf Stream. *Tellus*, 13, 392-401.

Weyl, P. K., 1964: On the change in electrical conductance of seawater with temperature. *Limnol. Oceanogr.*, 9, 75-78.

**DATA
FILM**